Order Number 9521279

Modeling, simulation, stability analysis and control of a modern fluidized catalytic cracker

Huang, Zupeng, Ph.D.

City University of New York, 1995

U·M·I
300 N. Zeeb Rd.
Ann Arbor, MI 48106

MODELING, SIMULATION, STABILITY ANALYSIS AND CONTROL OF A MODERN FLUIDIZED CATALYTIC CRACKER

by

ZUPENG HUANG

A Dissertation Submitted to the Graduate Faculty in Engineering in Partial Fulfillment of the Requirements for the Degree of Doctor of Philosophy, The City University of New York

1995

This manuscript has been read and accepted for the Graduate Faculty in Engineering in satisfaction of the dissertation requirement for the degree of Doctor of Philosophy.

Dec 27 1994
Date

Professor Reuel Shinnar, Chair of Examining Committee

28 DEC 1994
Date

Professor Irven H. Rinard, Co-Mentor

12/28/1994
Date

Professor Gerard G. Lowen, Executive Officer

Dr. Ajit V. Sapre

Professor Roberto Mauri

Professor Herbert Weinstein

Supervisory Committee

The City University of New York

ABSTRACT

MODELING, SIMULATION, STABILITY ANALYSIS AND CONTROL OF A MODERN FLUIDIZED CATALYTIC CRACKER

by

Zupeng Huang

Advisors: Professor Reuel Shinnar and Professor Irven H. Rinard

A detailed dynamic and steady-state model of a fluidized catalytic cracker (FCC) has been developed that allows evaluation of the impact of different designs, control configurations, catalyst and feed composition and control strategies on the control of complex system. The ten-lump kinetic model is applied for catalytic cracking reaction. A rigorous combustion kinetic model is developed in regenerator modeling. The FCC model has been validated through industrial contacts. It should be available to process control research community.

By using the model, the present work deals with the existence and stability of multiple steady states and input multiplicity. These are prerequisite conditions for the control design of a large nonlinear system. It is shown that an FCC may exhibit one, three, or even five steady states at the same input conditions. Only the hot stable steady states are needed which lie always in the region of three steady states. The unnecessary unstable and useful stable steady states will converge if close to the stability limit.

Catalyst and feed composition can strongly affect operable space. The results in

this work show that the region of hot stable steady states increases with increasing catalyst activity, heavier feed, increasing CO combustion promoter content and increasing feed temperature. CO combustion promoter can eliminate the trend toward five steady states.

The dynamic features that are captured by the model substantially represent the present-day FCC behavior. This dynamic behavior let one design a better controller that make system track the optimum point while regulating against disturbances.

The research work in this thesis should be a useful guide when one treats a complex system in which the number of process variable one would like to control substantially exceeds the number of manipulated variables that are available for the task. That is the so-called "partial control".

ACKNOWLEDGMENTS

The author wishes to express his gratitude to Professor Reuel Shinnar and Professor Irven H. Rinard for their continuous guidance, patience and contribution in directing this endeavor. He would like to thank his family for moral support and encouragement during the course of this work. He would particularly like to thank Dr. Ajit V. Sapre for his assistance. Substantial technique has been provided by Mobil Research and Development Corporation.

Financial assistance were made available by DOE, Grant #DE-FG02-91ER14221. This aid is gratefully acknowledged.

CONTENTS

LIST OF TABLES

LIST OF FIGURES

CHAPTER ONE

INTRODUCTION

The Fluidized Catalytic Cracker (FCC) is the heart of the modern refinery. Its function is to convert heavy hydrocarbon petroleum fractions into more useable products such as gasoline, middle distillates, and light olefines. As this upgrading from heavy oil is usually very profitable, the economic impact of the FCC on refinery operation is large. FCC units are one of the most complex process in an oil refinery. First commercialized over a half century ago, the FCC is still evolving. Improvements in the technology as well as changing feedstocks and product requirements continue to drive this evolution.

In recent years it has been evident that control offers an important tool to improve the profitability and competitiveness of the industry. Most of the control problems that determine the profitability of the plant concern not only dynamic control but also, and more importantly, the proper choice of the set points, i.e., steady state control or optimization. Control of the FCC has been and continues to be a challenging and important problem. As will be seen, its steady-state behavior is highly nonlinear, leading to multiple steady states, input multiplicities and all that this implies. In earlier years before the development of zeolite catalysts, the major control problem was one of stabilization, of just keeping the unit running. Now, the requirements for reformulated gasoline have shifted the focus to control of product composition.

Rational design of control systems requires both steady-state and dynamic information about the process. What is needed is a reasonably sufficiently detailed model which accounts for major process variable effects and the dominant dynamics. A

mathematical description of a process, i.e., a process model, is a prerequisite to analysis, optimization and control system design of commercial plants. In the case of complex systems like the FCC, by integrating adequate process model into on-line control there is a large potential for savings by better control. With large complex equipment, high throughput, and significant economic effects, FCC units present an opportunity and a challenge for improved operation through advanced control and optimization.

Modern digital computers provide a powerful means for process analysis, simulation, optimization and advanced control design based on the programmed process mathematical model. Computer simulation of process has been proven to be a very powerful tool for investigating process performances.

1.1 FCC Process Description

Fluidized Catalytic Crackers have operated with great success in refineries since 1940s. As a result the FCC has become the workhorse of the modern refinery throughout the world. A number of different designs have evolved but all of them share the same basic features. A schematic presentation of a typical FCC unit (FCCU) is illustrated in Figure 1-1. The process is used in converting heavy hydrocarbon oils (gas oil), generally produced by vacuum distillation of the bottom from atmospheric distillation of crude oil, into light oils, gasoline and cracked gas. It is carried out in two interconnected units: the reactor and the regenerator.

The mixture of gas oil passed through a preheater and/or a furnace is fed to the bottom of the reactor riser, where it contacts with the hot regenerated catalyst from the

regenerator. The catalytic cracking reaction occurs immediately. This reaction is endothermic, with the heat of reaction supplied by the hot regenerated catalyst. The products of reaction, gasoline, light oils, and unconverted hydrocarbons, separated from catalyst in reactor cyclones, are transferred to the main fractionator for further processing. During the reaction, coke is deposited on the catalyst surface, which consequently deactivates the catalyst, so that continuous regeneration of the spent catalyst is required.

Spent catalyst flows down through the stripper where the stripping steam is injected to remove hydrocarbons on the catalyst, to the regenerator fluidized bed where it is contacted with atmospheric air. Coke on the catalyst surface reacts with oxygen in the air to produce carbon monoxide, carbon dioxide and water in an exothermic reaction, i.e., combustion. Regenerated and hot catalyst flows back into the reactor riser through the regenerator standpipe. The combustion gases as flue or stack gas, separated from catalyst in regenerator cyclones, leave the regenerator top to carbon monoxide boiler and heat recovery exchangers.

The overhead vapor from the main fractionator is partially condensed before entering the overhead accumulator. The accumulator offgas goes to the wet gas compressor and then to the gas plant. The main fractionator bottom product is slurry. The heavier slurry and catalyst from the settling vessel are recycled back to the reactor.

1.2 The Objective of the Research Work

The goal of the present research work is to provide a more rigorous framework for designing control systems for complex processes such as the FCC process. First of all

it is required to investigate the steady-state and dynamic behavior of the FCC process. The tool for these investigations is modeling of a detailed dynamic model of the process. This model allows evaluation of the impacts of different designs, control configurations, catalyst and feed composition and control strategies on the control of an FCC process.

Based on the newly developed FCC model, the research effort includes investigation of the basic steady-state features of the system such as multiple steady states in the open loop and the input multiplicities of those control configurations currently used in the industry, determination of the operating range, and study of the dynamic behavior of the system to determine the best control scheme and control settings.

In summary the chief aims of the present study are to investigate the performance of the FCC process by means of developing a more detailed model and identifying the essential features of the process under the simulation studies. After having the knowledge of this information, a control system can be reasonably designed through the goal of this thesis.

1.3 Background

The FCC has been one of the key processes in petroleum refining. It has evolved significantly in the past 50 years but has not reached the status of a mature technology. Because of very high profit when using better operating strategy, many researchers have been studying this important process.

Before undertaking the study of the dynamics and control of any complex system, one needs an adequate model. In the case of the FCC, the literature abounds with such.

For example, one can find the integrate FCC models from Luyben and Lamb (1963), Kurihara (1967), Iscol (1970), Lee and Kugelman (1973), Seko et al. (1978, 1982), Lee and Groves (1985), McGreavy and Isles-Smith (1986), Bozicevic and Lukect (1987), Zhao and Lu (1988), Felipe (1992), Arandes and de Lasa (1992), Elnashaie and Elshishini (1979, 1990, 1993), McFarlane et al. (1993), Zheng (1994) and so on. Most are however of partial use at best. Many were developed for earlier generations of both equipment type and catalysts. Even those that have been published recently and purport to be current have severe limitations.

This is not through any shortcomings of the authors but results from the nature of the system itself. An FCC is a large, complicated system even at the experimental level. It is expensive to build and expensive to run. The only organizations that can afford to do so are the oil companies. It goes without saying that the data from such units and any models developed therefrom are proprietary. What is published, therefore, is heavily edited for one and not the latest version for another.

Because of model incompleteness, present control studies are greatly hampered by that. There is clearly the need for a model that represents the behavior of present-day FCC's. Our approach has been to start with a relatively recent model (McFarlane et al., 1993) and update and expand using other published material and then to validate the results through industrial contacts. The result is of a model which is not proprietary but which, to the best of our knowledge, reproduces the essential behavior of the FCC as it is operated today.

1.4 Outline of the Work

In Chapter 2 the importance and necessity of modeling a modern FCC are described. Three typical FCC models published are compared with our newly developed model. The results show that the published models are not suitable for predicting the performance of modern FCC's and for taking as a basis for control system design.

An FCC paper review is presented here. This previous work is a good basis for understanding the basic principles, optimal operating and control strategies of the process. It also provides the abundant information for developing a new detailed model that allows more rigorous evaluation of the impact of different designs, operating conditions and control configurations. The major features and the validation of our model are also depicted here.

In Chapter 3 a newly developed detailed modern FCC process model is described. The model includes Reactor model, Regenerator model, Catalyst Transport System model and Catalyst Management System model. The most important parts of the model are the reactor and the regenerator models. The reactor model includes the riser and the stripper models and the regenerator model includes dense and dilute phase bed models.

Ten-lumping cracking kinetic model from Jacob et al. (1976) was applied in the riser modeling, which is more detailed than three-lumping kinetics (Weekman and Nace, 1970) for describing the cracking reactions and product distribution.

In the regenerator model the kinetics of coke burning reactions was adopted from Arthur's (1951) that was modified by Weisz (1966). The homogeneous CO combustion is considered. The impact of CO promoter on combustion is also included in the model.

In Chapter 4 the behaviors of multiple steady states and input multiplicity in an FCC process are studied. This steady-state multiplicity is often a basis for understanding the overall control problem.

In this work the multiplicity of the system steady state is shown by two key inputs, the air flow rate and the catalyst circulation rate, and/or outputs, the regenerator dense bed temperature and the reactor riser top temperature. It is shown that an FCC may exhibit one, three, or even five steady states as a function of the air flow rate and catalyst circulation rate to the regenerator and the riser temperature. Furthermore, some of these can be close together in terms of the input operating space. The work also shows that conventional control structures (see Figure 1-2) can lead to input multiplicities.

The process operating maps presented in this chapter can be used to predict the proper operable range in an FCC. They also give the impacts of design and operating conditions on the existence of multiple steady states and input multiplicities. All these show that changes of input conditions may cause the system operating in an unstable steady state or winding down to a cold steady state.

The possibility of more than three steady states is also discussed here. We found that the only realistic source that lead to more than three steady states is homogeneous CO to CO_2 combustion, which is a consecutive reaction of the CO formed by catalyst surface combustion of coke. This homogeneous reaction is inhibited by the present of solid at temperature below 1300 °F. Above this temperature, the reaction will take off and five steady states are feasible. However, we show that if one uses conventional apparent activation energies to model the homogeneous combustion of CO, five steady states are not feasible because their existence requires a very high rise in the CO combustion rate

over a temperature difference of about 100 °F. If one uses data published by Upson et al. (1993) to model the homogeneous CO to CO_2 combustion in the temperature range above 1270 °F, five steady states become likely for some operating conditions. It is showed that a small amount of catalytic CO combustion promoter would eliminate the chance for the additional two steady states. However, no industrial or experimental confirmation of additional high temperature steady states has been published in the literature.

Chapter 5 gives an analysis of some FCC dynamic characteristics. The open-loop transient behaviors of the FCC in time domain and frequency domain are investigated here.

It is well known that the knowledge of dynamic features of a system is often a prerequisite for a better design of process control that keeps the process being operated effectively at optimum conditions. In this work several dynamic simulation runs in time domain are presented. They display the effects of unmeasured disturbance or manipulated variables on the FCC process.

Frequency response analysis is also studied which is based on a linearized model around some steady states. This technique yields a powerful tool both for analyzing dynamic systems and for designing feedback controllers. The FCC is a process with recycle of catalyst. The dynamics feature with recycle is investigated here.

From the work in this chapter, it is concluded that the regenerator dominates the dynamics of the whole system but the riser has an important effect which is caused by coke make in cracking reactions.

Finally in Chapter 6 the present work is summarized and the future work is suggested.

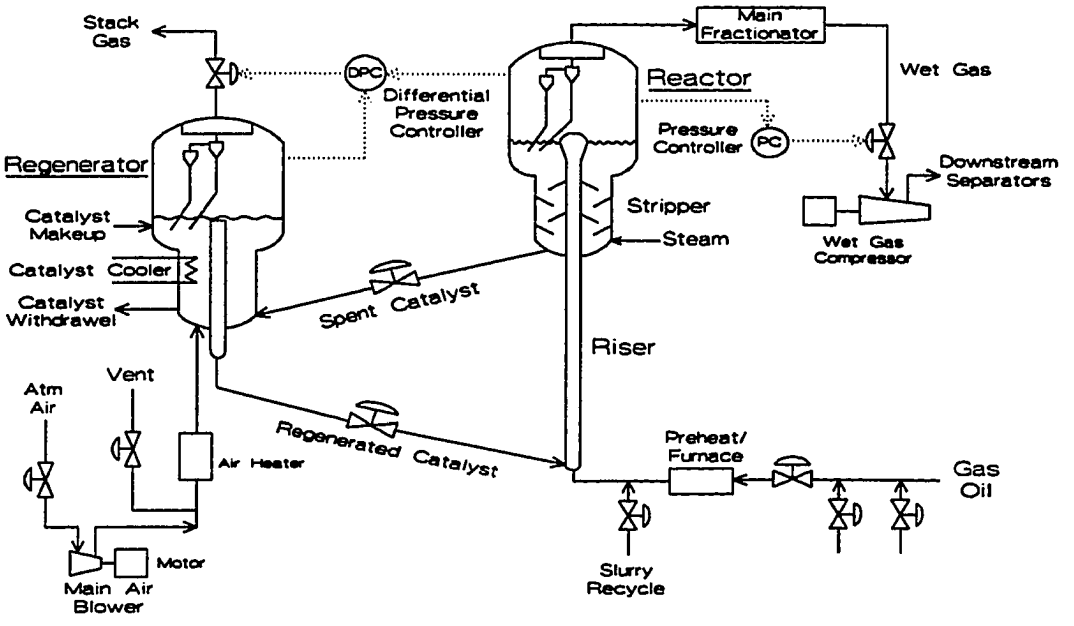

Figure 1-1. A Typical Modern Fluidized Catalytic Cracker (FCC)

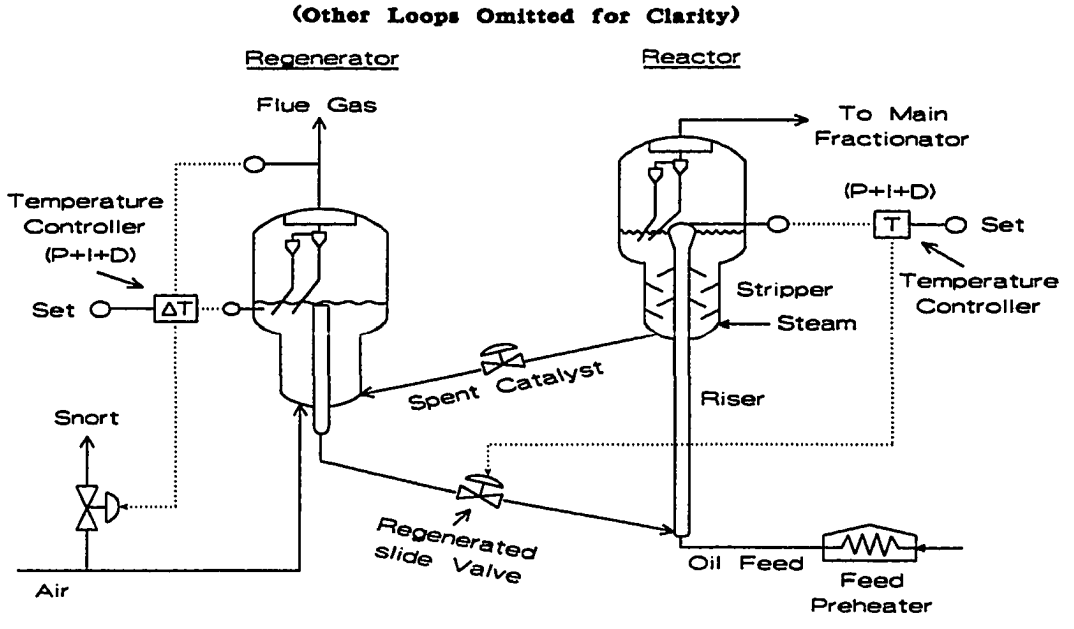

Figure 1-2. FCC Conventional Control Loops

CHAPTER TWO

EVALUATION AND DEVELOPMENT OF FCC MODEL

FCC has been one of the key processes in petroleum refining for over 50 years. It converts heavy hydrocarbon in petroleum into valuable gasoline, distillates, and light olefine. It has evolved significantly in the past 50 years but has not reached the status of a mature technology (Avidan and Shinnar, 1990).

Because of very high profit when using better operating strategy and control (Martin et al., 1985, Rhemann et al., 1988), FCC's have been an active area of control research in industry and academia alike [e.g., Luyben and Lamb (1963), Gould et al. (1970), Schuldt and Smith (1971), Arkun and Stephanopoulos (1980), Prett and Gillette (1980), Bromley and Ward (1981), Arkun and Ramakrishnan (1984), Palazoglu and Khambanonda (1987), McFarlane and Bacon (1989), Schmid and Biegler (1990), Ljungquist (1990), Balchen et al. (1992), and Hovd and Skogestad (1993) to name a few]. For better control design one need an adequate model. A lot of researchers have been trying to develop a more detailed FCC model which is capable of describing the dominant process features therefore the overall control problem can be understood. Modeling of complex chemical processes like the FCC is often an important and indispensable step for better control design and optimization to achieve a maximum profit (Lee and Weekman, 1976). Major oil companies have their sophisticated proprietary FCC models. However, in academia or research institutes the researchers who are interested in studying the control of this key oil refining process are keen to seek the published models. Fortunately the literature abounds with such.

2.1 History of FCC Modeling - A Literature Survey

Numerous papers relating to the FCC process have appeared in the published literature. They presented various aspects of mathematical modeling and simulation, stability, optimization and optimal control. A summary of them is given in Table 2-1. For a detailed description of the FCC, its historic development and the different types of units in current use, and the design philosophy underlying them, one can refer to Avidan (1991), Avidan and Shinnar (1990), Avidan, et al. (1990), Ewell and Gadmer (1978), and McDonald and Harkins (1987).

There are a lot of papers published on FCC modeling. Every model has its feature and usage. However, many were developed for earlier generations of both equipment types and catalysts. The published FCC models can be classified as the integrate models [Luyben and Lamb (1963), Kurihara (1967), Iscol (1970), Lee and Kugelman (1973), Seko et al. (1978, 1982), Lee and Groves (1985), McGreavy and Isles-Smith (1986), Bozicevic and Lukect (1987), Zhao and Lu (1988), Felipe (1992), Arandes and de Lasa (1992), Elnashaie and Elshishini (1979, 1990, 1993), McFarlane et al. (1993), and Zheng (1994)], the regenerator models [Ford et al. (1976), Errazu et al. (1979), de Lasa et al. (1981), Guigon and Large (1984), Krishna and Parkin (1985), Lee and Cheng (1989), and Wei et al. (1993)], and the reactor or cracker models [Weekman and Nace (1970), Paraskos et al. (1976), Shah et al. (1977), Takatsuka et al. (1987), Lee et al. (1989), Larocca et al. (1990), Shnaider and Shnaider (1990), Corella and Frances (1990), Farag et al. (1993), and Theologos and Markatos (1992), (1993)]. The most typical of them are Kurihara's (1967), Lee and Groves' (1985), and McFarlane's et al. (1993) models.

Table 2-1. An FCC Literature Survey

Author (year)	FCC Modeling							FCC Analysis Simulation and/or Control
	FCC Type	Main Assumptions	Kinetic Model		Equation Numbers		Model Verifi-cation	
			Cracking	Burning	ODE	Algebra		
Luyben (1963)	Typical	Adiabatic CSTR in Regenerator and in Reactor	Empirical	Empirical	6	4		Synthesis of a feed-forward control system
Kurihara (1967) (1970)	Typical	Adiabatic CSTR in Regenerator and in Reactor	Empirical	Empirical	6	12	Yes	Development of Kurihara's control scheme and study by using PI controllers
Iscol (1970)	Model IV	CSTR in Regenerator and in Reactor	Empirical	Empirical	4	2	Chevron	Analysis of basic equilibrium and stability
Schuldt (1971)	Using Kurihara's Model							Application of quadratic optimal control synthesis techniques
Lee (1973)	Typical	CSTR in Regenerator and in Reactor	Empirical	Empirical	4	6	Mobil	Studies of open-loop multiple steady states and local stability Linearized model was presented
Ford (1976)	Regenerator Model	CSTR in dense bed Adiabatic plug flow in gaseous phase		Empirical	7	4	Amoco	Amoco Ultracat regenerator model, dynamic response studies
Seko (1978) (1982)	Typical	CSTR in Regenerator and in Reactor	Week-man's 3-lump	Weisz	4			Stability analysis of FCC using Hurwitz stability criterion under a linearized model
Elnashaie (1979) (1990) (1993)	Model IV	CSTR in Regenerator and in Reactor	Week-man's 3-lump	Kunii	4	12	Yes	Digital dynamic simulation Investigation of middle unstable steady states and closed-loop behavior with FB P control
Errazu (1979)	Regenerator Model	CSTR in dense bed Plug flow in jets		Weisz	2	4	YPF Argentina	Dynamic simulation studies
Arkun (1980) (1984)	Using Kurihara's Model							Development of a structural sensitivity analysis and screening strategy. IMC was applied
Bromley (1981)	Using Kurihara's Model							Development of model-base structural control scheme
Guigon (1984)	Regenerator Model	Kunii-Levenapiel model was applied. Full CO combustion		Hano	1 (n)	15		Multistage baffled regenerator model
Chang (1985)	Pilot plant FCC							Smith predict control Analytical predict control
Groves (1985)	Typical	CSTR in Regenerator PFR in Reactor Riser	Week-man's 3-lump	Weisz	6	1		Using PI control to compare conventional control scheme with Kurihara's control scheme
Krishna (1985)	Regenerator Model	Plug flow in gaseous phase		Arthur Weisz	5	8	Gulf Co.	Steady State model of the regenerator
McPherson (1985)	Texaco dual riser unit							Application of IDCOM predictive control
Georgakis (1986)	Two heat exchangers in parallel, resembling the FCC process							Synthesis of multivariable and nonlinear control structures

Table 2-1. (Continue)

Author (year)	FCC Modeling							FCC Analysis Simulation and/or Control
	FCC Type	Main Assumptions	Kinetic Model		Equation Numbers		Model Verification	
			Cracking	Burning	ODE	Algebra		
McGreavy (1986)	Reactor Model	PFR in Riser CST in Stripper	Weekman's 3-lump		9	2		Dynamic simulation studies
Bozicevic (1987)	UOP Type	2 reactor risers CST in solid phase PF in gaseous phase	Weekman's 3-lump	Experiment	10	2	UOP	Comparison of simulated to experimental responses of process
Mauleon (1987)	Pilot plant FCC							Posed 2-stage regeneration control of feed-cat mix temp.
Palazoglu (1987)	Using Kurihara's Model							Studies of dynamic operability measure or robustness index Application of IMC
Edwards (1988)	Typical	Proprietary model of Shell Oil Company						Studies of FCC steady-state multiplicity
Rhemann (1988)	OEMV Schwechat FCCU							Application of controllers, PID, Predict and Adaptive, IDCOM
Zhao (1988)	Improved Kurihara's Model				14	22	Yes	Comparison between the model output and plant data
Lee (1989)	Regenerator Model	CSTR		Hano	0	19	Yes	3 different models were studied
McFarlane (1989)	Using Kurihara's Model							Adaptive optimizing control strategy, on-line identification and MIMC
Tomlins (1989)	Pembrake FCCU (Wales, UK)							Application of DMC
Shnaider (1990)	Reactor Model	CSTR				19		Presentation of kinetic models for cracking of oil fractions
Felipe (1992)	Typical	PFR in Riser and in Regenerator	Weekman's 3-lump	Promoter	14 PDE		Mexico	Dynamic modeling and simulation
Arandes (1992)	Typical	PFR in Riser and in Regenerator gaseous phase	Weekman's 3-lump	Hano	8	1		Simulation and analysis of steady-state multiplicity
Balchen (1992)	Lee and Groves' Model							Application of MPC technique On- and off-line identification
Grosdidier (1993)	Typical	Empirical frequency domain model						Dynamic simulation IDCOM-M controller
McFarlane (1993)	Model IV	CSTR in Regenerator bed and Reactor	No	Ford	23	95	Amoco Corp.	Dynamic simulation studies
Hovd (1993)	Lee and Groves' Model							Illustration of a methodology of control structure selection
Zheng (1994)	Typical	CSTR in Regenerator PFR in Riser	Lee's (1989) 4-lump	Krishna	7	5	Yes	Dynamic simulation including startup, shutdown and routine operation

2.2 Evaluation of Published FCC Models

Kurihara (1967) presented a widely used FCC model in which he assumed the regenerator and the reactor as two adiabatic CSTR. Based on the model he developed a new control scheme. Many papers concerning FCC process analysis and control design are based on Kurihara's model [Gould et al. (1970), Schult and Smith (1971), Arkun and Stephanopoulos (1980), Bromley and Ward (1981), Arkun and Ramakrishnan (1984), Palazoglu and Khambanonda (1987), McFarlane and Bacon (1989), and Schmid and Biegler (1990), to mention just a few]. However, in modern FCC cracking reactions occur in the reactor riser that is a vertical transport pipe and close to plug flow.

Using a stirred tank reactor model such as Kurihara's (1967), and in many old published models [Luyben and Lamb (1963), Iscol (1970), Lee and Kugelman (1973), Seko et al. (1978, 1982), Zhao and Lu (1988), and so on] will lose an important critical feature that the temperature difference across the riser has a strong impact on riser performance as the coke make at constant feed conversion is lower at higher temperatures. This feature is shown on Figure 2-1. Reactor temperature at the riser top is metallurgically limited, but at the bottom much higher temperatures are permissible. When the riser bottom temperature increases, the temperature gradient across the reactor increases. High temperatures in the bottom have advantages that previously (20 years ago) were not realized. It improves octane, olefine selectivity and gives a lower coke make at constant conversion. High temperature at the riser bottom can be achieved by lowering catalyst circulation rate which requires a higher regenerator temperature.

Figure 2-2 and 2-3 show the different performances between the PFR and CSTR

model of the riser. Although CSTR with double inventory in the riser has similar performance to PFR (Figure 2-2), the feed conversion in CSTR is always lower than in PFR even though the riser inventory increases 10 times in CSTR model (Figure 2-3).

Lee and Groves (1985) published an FCC model which included reactor riser model derived from Shah et al. (1977). Weekman's (1970) three-lump cracking kinetics was used. Their regenerator model was developed by Errazu et al. (1979). It is a two phase model. Ljungquist (1990), Balchen et al. (1992), and Hovd and Skogestad (1993) used Lee's model to design control system.

Figure 2-4 compares our case with a case based on a model published by Errazu et al. (1979) in which the CO_2/CO ratio is given as a function of temperature. The results are similar to our case up to 1250°F but obviously the Errazu's model cannot reach higher temperature. As it is a correlation over a limited temperature range, it cannot predict complete CO combustion. However, it is well known that complete CO combustion is achievable without promoters at higher temperature. Assuming CO_2/CO ratio to be a function of temperature only is fundamentally incorrect for a case in which the ratio is kinetically controlled. For this point our model contains the essential physics of the kinetic combustion processes in the regenerator.

Because of using Errazu's regenerator model, Lee's model has certainly insufficient details to be useful for understanding control or evaluation of operating strategies for modern commercial FCC's.

McFarlane et al. (1993) published a most detailed Model IV FCC model. But the model still lacked some important features. It does not include the riser cracking kinetic model which is important for the product control of the reactor. The reactor is assumed

as CSTR. Therefore it has not a temperature profile like that in PFR. The catalyst circulation rate can only be adjusted over a narrow range by the system pressure balance, the key variable being the catalyst holdup in the regenerator. While this still allows for some variation of catalyst flow, it is too slow to be useful for dynamic control. In most modern FCCUs catalyst circulation rate is adjustable by a slide valve in the pipe feeding the hot catalyst to the reactor. This allows fast and accurate control of reactor temperature. It also allows a variation of catalyst flow over a relatively wide range.

CO combustion rate given in McFarlane's model is much higher than it is normally in the absence of a CO combustion promoter. The model can always lead to full CO combustion even at a lower temperature. Obviously, it is based on using a CO combustion promoter. This limits the use of the model to the fully promoted units. Operating at full CO combustion has one significant disadvantage. In the absence of a catalyst cooler the amount of coke that can be burned, while remaining heat balanced, is less than in partial CO combustion (see Figure 2-5). This restricts the type of feeds that one can use.

The interesting dynamic effects occur mainly in the units operating in partial CO combustion. Many modern units still operate this way. They have CO boilers, which allow higher conversion with heavy oils. Figure 2-6 shows the regenerator profiles in complete CO combustion mode operation (McFarlane's model) and in partial CO combustion mode operation (our model).

2.3 Bases for Development of an FCC Model

It is clear that the current state of the art in model building of petroleum and

chemical process still has considerable room for improvement. Simplified models of complex processes are frequently inadequate in describing the true process characteristics, thus leading to erroneous control design (Lee and Weekman, 1976). From the studies mentioned, it is recognized that a complete dynamic and steady-state mathematical model with rigorous representation of modern FCC behavior has not appeared in the literature. The models presented are unsuitable for the study of current process features and more sophisticated control problems. Therefore it is necessary to develop a new FCC model which can serve as a basis for more efficient control design and optimization.

2.3.1 Modeling of Reactor

Kinetic models are the heart of the complete process models as reaction kinetics can contribute strongly to the development as well as to subsequent optimization of the process technology. For FCC reactor modeling, the establishment of a kinetic model for catalytic cracking reaction is even a key step as the feedstock contains a large number of components. Generally, predicting oil product composition is a much more difficult work than predicting the heat balance. Several thousand compounds are involved in reaction. A complete description of the system in terms of individual compounds is impractical for complex feedstocks typically processed in modern FCC's (Sapre,1991). Therefore, it is necessary to find a procedure that make the work feasible. One of the traditional approaches to modeling the reactions of the mixtures containing many components is to group molecules that react at similar rates together into compound classes. The compound classes, or kinetic lumps, are then treated as pseudo-components in the modeling (Allen

and Liguras, 1991).

The first kinetic model for cracking treated the entire gas oil feedstock as one lump (Blanding, 1953), and the overall conversion to gasoline and light products was described by a second-order reaction. Weekman and Nace (1970) refined this to a three-lump kinetic model of cracking reaction, namely, lumped oil as gas oil, gasoline, C_4-and-lighter gases plus coke. They showed that a three-lump system could adequately describe gasoline selectivity behavior in the catalytic cracking. The three-lump model is simple but has been proved to be very useful in developing optimal operating strategies, therefore improving commercial operations (Weekman, 1979).

The three-lump model could reliably predict the performance of various types of reactors such as fixed-bed, moving-bed, fixed-fluid bed, and riser reactor for a given feedstock and catalyst (Sapre, 1991). But unfortunately the rate parameters are strongly dependent on the feedstock [Nace et al. (1971), Voltz et al. (1971) and Gross, et al. (1974)]. Therefore, more lump for description of cracking reaction is necessary.

Yen et al. (1988), Lee et al. (1989), Narendra et al. (1993) and Farag et al. (1993) proposed a four-lump model which was similar to the three-lump one of Weekman's, the main difference being that coke was independently considered as a lump. Larocca et al. (1990) expanded the three-lump model into a five-lump one in which gas oil lump was split into paraffins, naphthenes, and aromatics.

Takatsuka et al. (1987) gave a six-lump model which was used to predict the cracking of residual oil. The six lumps include resid (1000°F$^+$), HFO (650 to 1000°F), LFO (430 to 650°F), gasoline (C_5 to 430°F), gas (C_1 to C_4), and coke. The six-lump model certainly gives more detailed representation of the cracking reaction of residual oil

but unfortunately, the values of kinetic parameters do not appear in their paper.

Jocob et al. (1976) published a ten-lump kinetic model of the catalytic cracking reaction. It was more detailed than three-lump kinetics for describing the cracking reactions. The rate constants in this model were invariant with respect to the original crude source of the lumps. The ten lumps include gasoline (C_5 to 430°F), C lump (H_2, H_2S, C_1 to C_4 plus coke), HFO (650°F$^+$) and LFO (430° to 650°F). Each of HFO or LFO is divided into paraffin, naphthene, aromatic substituent groups and aromatic rings. The values of kinetic parameters can be found from Gross et al. (1976), which were adopted by Coxson and Bishoff (1987).

Sha et al. (1991) expended Jocob's ten-lump kinetic model of the catalytic cracking reaction into a eleven-lump one. In their kinetic model, aromatic rings in ten-lump kinetic model was further split into mono- and bi-aromatic rings and polyaromatic rings (number of rings ≥ 3).

After reviewing all papers about FCC reactor modeling, the three-lump kinetic model turns out to be simple and fair rigorous to evaluate cracking reaction, but it is still not detailed enough for predicting product distribution and the rate parameters are strongly dependent on the feedstock. The ten-lump kinetic model is detailed enough by now to describe the cracking reactions. It has been applied to our reactor modeling.

2.3.2 Modeling of Regenerator

For the purposes of dynamic modeling, one needs very little information about the reactor because the residence time of the feed in the reactor is less than 10 seconds. All

the longer timescales of the systems relate to the regenerator. The only impact that the reactor has on dynamics is on the formation of coke. All one needs on the reactor part is an instantaneous heat balance and a relation for coke formation. Therefore if one wants to deal with stability or dynamic behavior, What he needs is a good regenerator model.

Several papers concerning FCC regenerator modeling have appeared in the literature just mentioned before. The model of coke and carbon monoxide combustion kinetics is required for regenerator modeling. Various burning kinetic model for coke and CO have been presented [Arthur (1951), Weisz and Goodwin (1966), Weisz (1966), Hano et al. (1975), Ford et al. (1976), Errazu et al. (1979), Prater et al. (1983), Krishna and Parkin (1985), Wang et al. (1982, 1986, 1989), and Morley and de Lasa (1987, 1988)].

FCC regenerator operates with or without a CO combustion promoter. Under partial combustion of CO, FCCUs have CO boiler, which allow higher conversion with heavy oils. For describing this kind of operation, Arthur's coke burning kinetics which is modified by Weisz (1966) has been adopted for our regenerator modeling. CO also burns to CO_2 as a homogeneous reaction in the gas phase but this reaction is inhibited by the presence of solids and will become fast in high temperature (> 1300 °F) (Avidan and Shinnar, 1990). Combustion of adsorbed hydrocarbons is very fast. For simplicity we lump them here with the slow burning coke. In order to investigate effects of CO promoter on combustion, the information from Chaster et al. (1981) is applied to modeling for this kind of operation.

Catalyst Cooler in the regenerator has an advantage that it allows to treat heavy oil feed no matter whether the system still operate in complete CO combustion (Shinnar, 1981). We incorporate this cooler to our model.

2.3.3 Modeling of Catalyst Management System.

The activity of FCC catalyst at typical operating condition is extremely high, with only a few seconds being required for reaction. However the coke that deposits on the catalyst during this time dramatically decreases its activity. This rapid catalyst deactivation that occurs by coke in the reactor is reversible by burning the coke deposits off the catalyst in the regenerator. However there is also a slow irreversible deactivation process that occurs as the catalyst is exposed in the regenerator to high temperature in the presence of water vapor that results from the hydrogen content of the burning coke. This permanent deactivation occurs over a period of months. Because coking, cracking, light gas formation, and product composition are strong functions of the type and activity of the catalyst, the permanent catalyst deactivation will affect optimal steady-state operation, therefore requires the addition of a fresh catalyst to the unit to maintain catalyst activity. Lee (1970), and Krambeck (1990) has discussed this kind of operation.

In addition to catalyst deactivation by steam, some metals such as sodium, nickel, and vanadium presenting in feedstock, especially in heavier feed (such as resid) can make catalyst poison, therefore accelerates catalyst deactivation (Otterstedt and Upson, 1989). Larocca et al. (1990) discussed metal poisoning effects on catalytic cracking reaction.

Catalyst makeup requirements are therefore determined by these deactivation mechanisms. Catalyst attrition and loss through the cyclones also require catalyst makeup (Wei et al., 1977). Thus catalyst management system is indispensable in FCCU operation.

Long range catalyst deactivation by steam and changes due to metal deposition are slow compared to the dynamic response in coke formation due to changes in operating

condition or feed composition. The changes in catalyst state can therefore be decoupled from the dynamic model and the state of the catalyst is used as an input. However, for steady-state control it is required a separate model describing the state of the catalyst.

All the papers relating to FCC modeling did not include this catalyst management system. We model this system to study optimal steady-state control. The information from Lee (1970), Krambeck (1990) and Johnson (1991) can be applied for modeling.

2.4 The Major Features of the New FCC Model

As mentioned before, there are many papers relating to FCC modeling, but they have various limitations. Therefore, they are unsuitable for performance and control study of modern FCC. Modeling of a modern FCC becomes essential. All the published papers provide good information for FCC modeling. Our new FCC model (see Chapter three for detailed description) is obviously very similar to other published ones, especially to that of McFarlane et al. (1993). However, ours still has own features that are different from other models as shown following:

(1) In reactor modeling the most detailed ten-lump cracking kinetic model by now from Jacob et al. (1976) is presently adopted. A PFR model is used for reactor riser modeling, which is close to modern riser operation and indicates the temperature profile across the riser.

(2) In regenerator modeling a detailed description of the combustion reaction kinetics is included, especially the combustion of CO to CO_2. A partial CO combustion kinetics is applied for agreement with a large number of FCC regenerator

operation. The effects of CO burning promoter on combustion is included in modeling. This can be used for studying complete CO combustion operation at low regenerator temperature.

2.5 Model Validation

The model developed in Chapter three has been validated through the industrial contacts. Substantial technique has been provided by Mobil Research and Development Corporation.

The model, to the best of company personnel's knowledge, is the first to describe actual behavior of commercial FCCUs which is operated today. It describes real multiple steady state phenomena and has the right properties to track dynamic response. Therefore, the model can be used for a variety of purposes, improving understanding of the complex FCC system for operators and designers, as a screening tool for predicting needed design changes in control system.

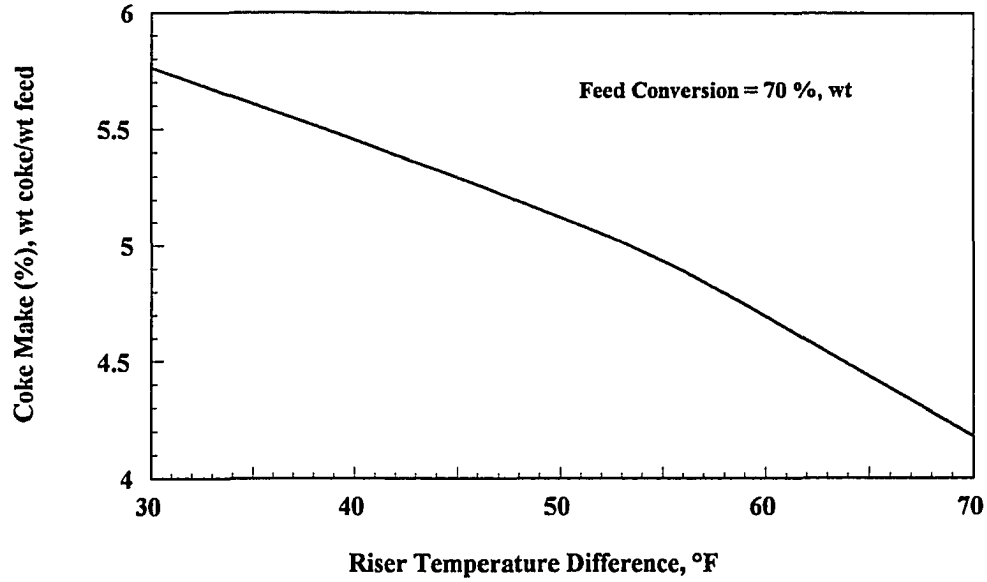

Figure 2-1. Effect of Riser Temperature Difference on Coke Make

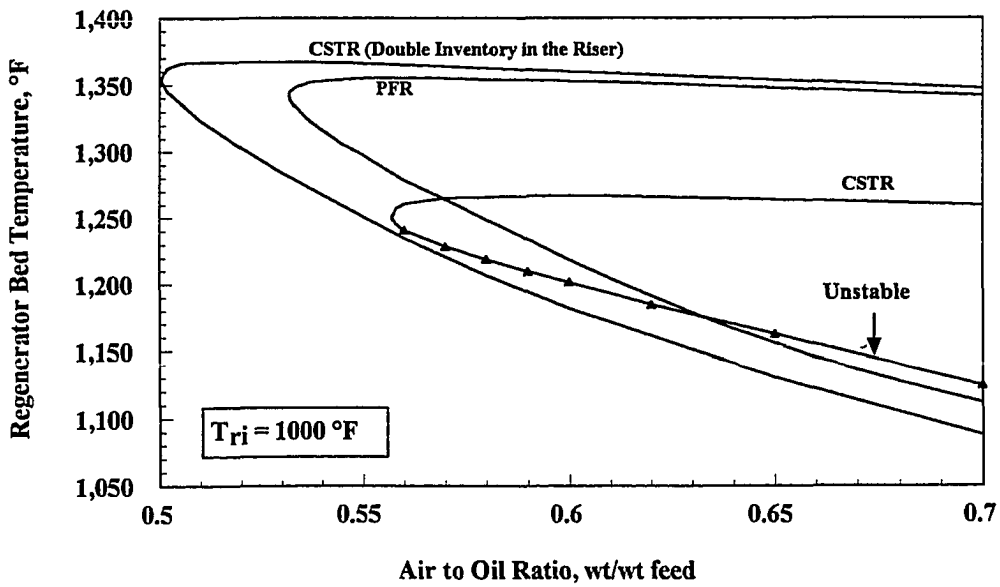

Figure 2-2. Comparison between CSTR and PFR Performances in the Riser

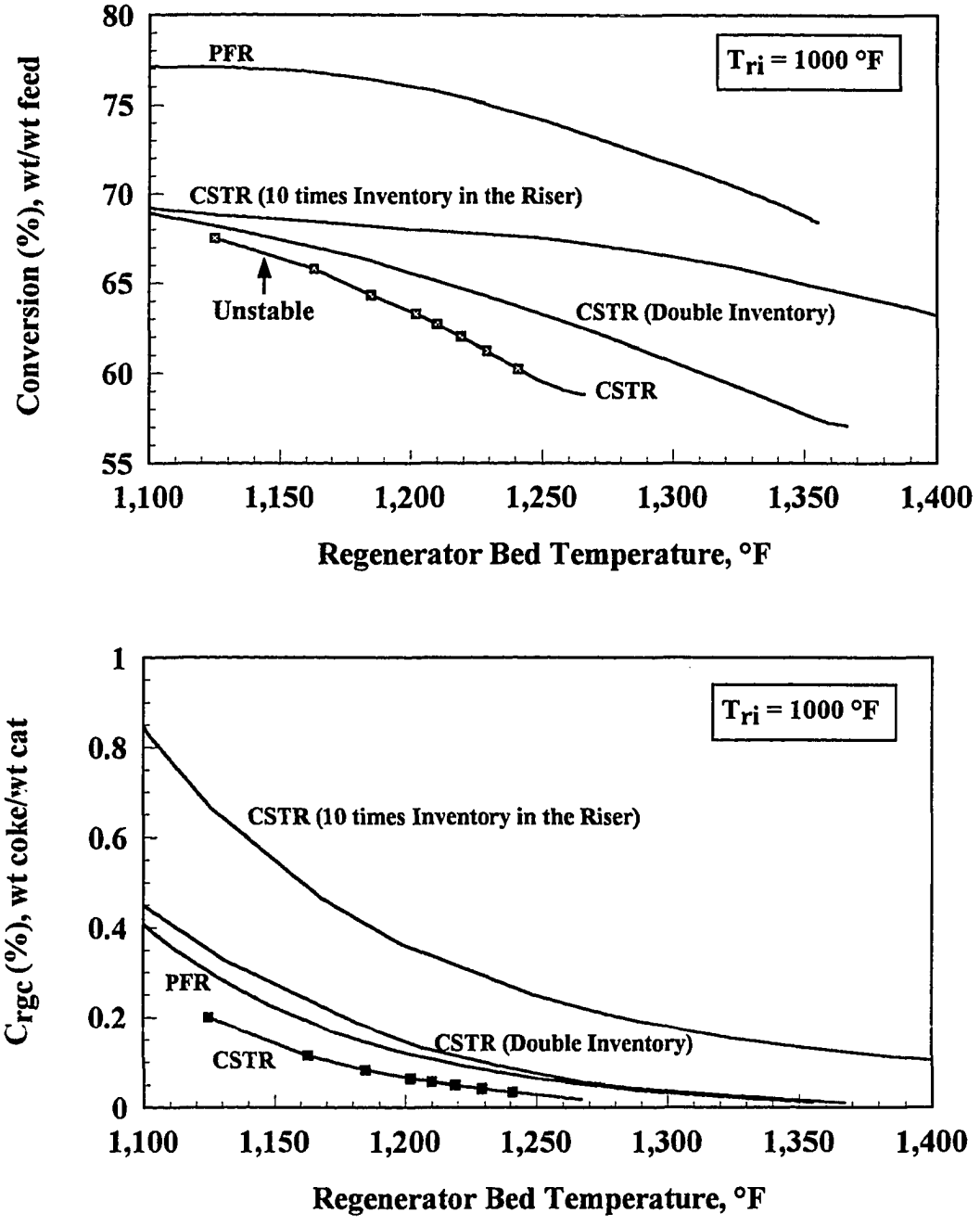

Figure 2-3. Effect of Riser Model on Conversion and C_{rgc}

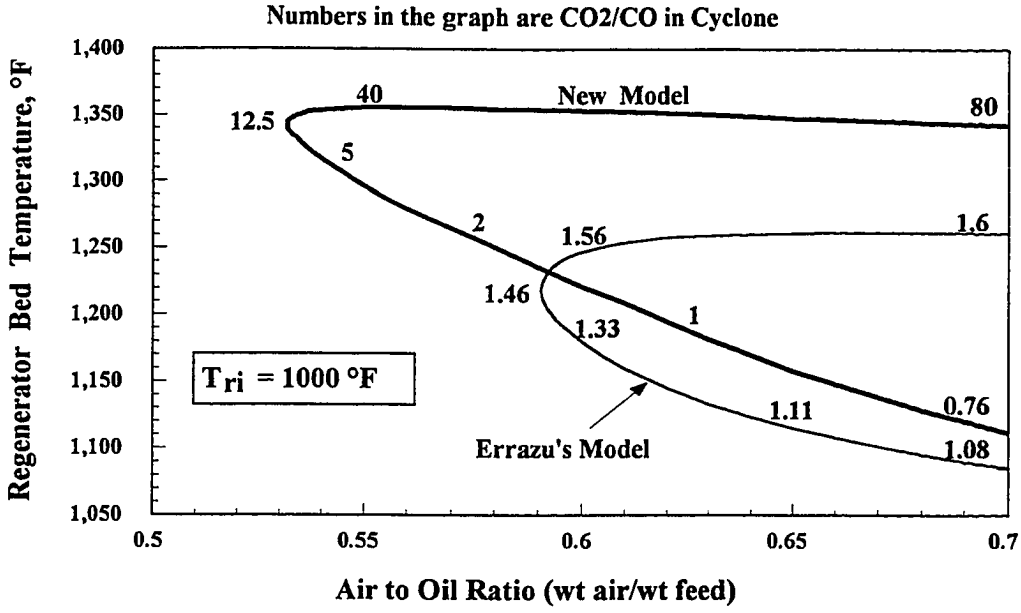

Figure 2-4. Comparison between Two Model Performances

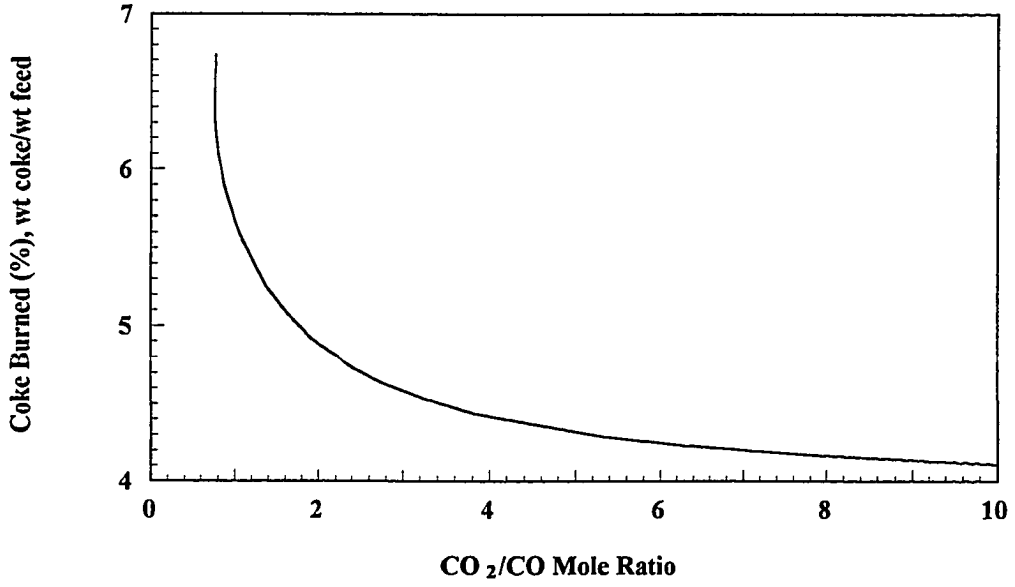

Figure 2-5. Effect of CO Combustion on Coke Burned

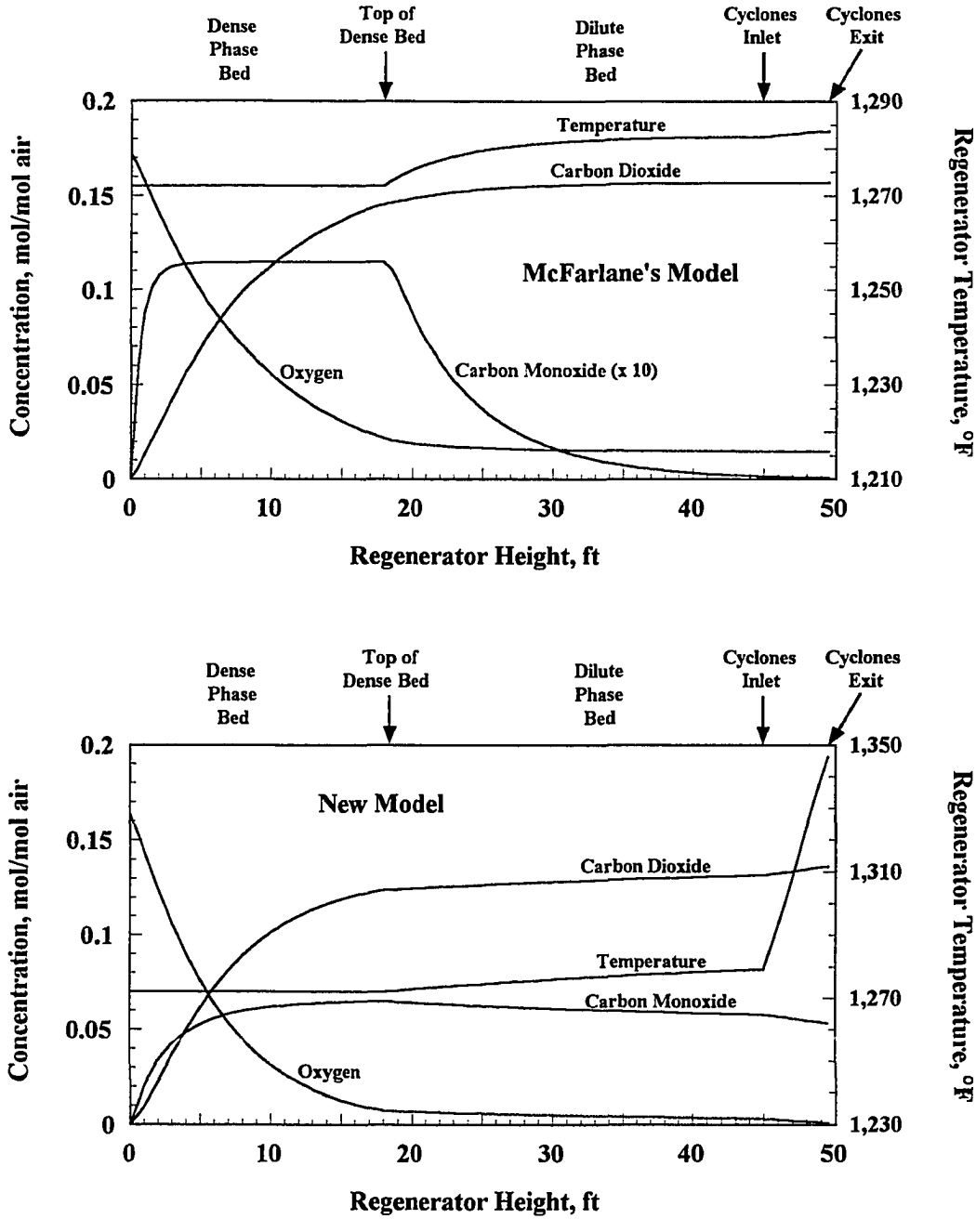

Figure 2-6. Temperature and Concentration Profile in Regenerator

CHAPTER THREE

MODELING OF A MODERN FLUIDIZED CATALYTIC CRACKER

A detailed modern FCC model has been developed which is described below. A schematic diagram of this typical FCCU is shown in Figure 1-1. The model is divided into four parts: Reactor model; Regenerator model; Catalyst Transport System model; and Catalyst Management System model. The pressure control on system is assumed to be fast enough, so the pressure of system can be considered as constant.

The reactor model consists of the riser model and the stripper model. The riser was assumed to be a plug flow reactor and the stripper stirred tank. All cracking reactions of oil were assumed to occur in the riser, therefore the stripper acts as a lumped capacitance allowing for accumulation of catalyst and coke and heat on the catalyst. The net effect in stripper is to produce a lag between the riser outlet and the regenerator.

In the riser model, the ten-lump cracking kinetics from Jocob et al. (1976) was adopted. A coke formation kinetics based on Voorhies (1945) and a catalyst deactivation function from Krambeck (1990) have been used in riser modeling.

The regenerator includes dense phase bed model and dilute phase bed model. The kinetics of coke burning reactions on catalyst surface was adopted from Arthur (1951), which was modified by Weisz (1966). The kinetics of carbon monoxide (CO) oxidation under the presence of solids from Morley and de Lasa (1988). When the catalyst solids are removed, CO will be oxidized in a fast thermal free-radical reaction (Avidan and Shinnar, 1990). For complete combustion operation of regenerator in low temperature, the model includes the impact of CO promoter

3.1 The Reactor Model

The reactor model is divided into two parts, the riser model and the stripper model. A schematic of the reactor model is given in Figure 3-3.

3.1.1 The Riser Model

The riser model is developed by applying the law of conservation of mass and energy to a differential element within the flowing fluid and solid (see Figure 3-1). The model includes coke balance on catalyst, mass balances on oil components and energy balance. Ten-lump cracking kinetic model (Jacob et al., 1976) is applied for cracking reactions. The coking kinetics comes from Krambeck (1990).

When developed the riser model, The following basic assumptions were made: i) plug flow with negligible interparticle diffusion; ii) constant void fraction; iii) same linear velocities of the catalyst and the fluid; iv) adiabatic operation; v) same temperatures of the catalyst and the fluid at any position of the riser; vi) constant heat capacity and density of oil vapor; vii) quasi-steady-state process.

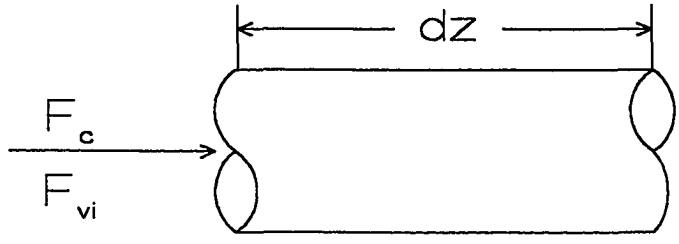

Figure 3-1. Differential Element of Riser

(1) Catalyst balance

Accumulation = $A_{ris}dz\rho_c(1-\varepsilon)$

$$\frac{\partial}{\partial t}\{A_{ris}dz\rho_c(1-\epsilon)\} = F_c - (F_c + \frac{\partial F_c}{\partial z}dz)$$

$$\therefore \quad A_{ris}\rho_c\frac{\partial \epsilon}{\partial t} = \frac{\partial F_c}{\partial z} \tag{3-1}$$

Assume ε is constant in riser, then $F_c = F_{rgc}$ throughout the riser.

(2) Coke balance on catalyst

Accumulation = $A_{ris}dz\rho_c(1-\varepsilon)C_c$

$$\frac{\partial}{\partial t}\{A_{ris}dz\rho_c(1-\epsilon)C_c\} = F_cC_c - (F_cC_c + \frac{\partial F_cC_c}{\partial z}dz) + A_{ris}dzR_{coke}(1 - \epsilon)$$

$$\therefore \quad A_{ris}\rho_c\frac{\partial[(1-\epsilon)C_c]}{\partial t} = -\frac{\partial F_cC_c}{\partial z} + A_{ris}R_{coke}(1 - \epsilon) \tag{3-2}$$

Substitute (3-1) into (3-2), we get

$$A_{ris}\rho_c(1-\epsilon)\frac{\partial C_c}{\partial t} = -F_c\frac{\partial C_c}{\partial z} + A_{ris}R_{coke}(1 - \epsilon) \tag{3-3}$$

$$or, \quad A_{ris}\rho_c(1-\epsilon)\frac{\partial C_c}{\partial t} = - F_{rgc}\frac{\partial C_c}{\partial z} + A_{ris}R_{coke}(1 - \epsilon) \tag{3-4}$$

(3) Mass balance on oil component

Accumulation = $A_{ris}dz\rho_i\epsilon$

$$\frac{\partial}{\partial t}(A_{ris}dz\rho_i\epsilon) = F_{vi} - (F_{vi} + \frac{\partial F_{vi}}{\partial z}dz) + A_{ris}dz\epsilon \sum_k a_{ik}r_k$$

$$\therefore \quad A_{ris}\epsilon\frac{\partial \rho_i}{\partial t} = - \frac{\partial F_{vi}}{\partial z} + A_{ris}\epsilon \sum_k a_{ik}r_k \tag{3-5}$$

$$F_{vi} = \rho_i A_{ris}\varepsilon u_v \tag{3-6}$$

$$\therefore \quad \frac{\partial \rho_i}{\partial t} = - (u_v\frac{\partial \rho_i}{\partial z} + \rho_i\frac{\partial u_v}{\partial z}) + \sum_k a_{ik}r_k \tag{3-7}$$

Assume $u_v = u_c$ in the riser, and

$$u_v = \frac{F_v}{A_{ris}\rho_v\epsilon} \tag{3-8}$$

$$u_c = \frac{F_c}{A_{ris}\rho_c(1-\epsilon)} = \frac{F_{rgc}}{A_{ris}\rho_c(1-\epsilon)} \tag{3-9}$$

$$\therefore \quad \frac{\partial u_v}{\partial z} = 0 \qquad and,$$

$$u_v = u_0 = \frac{F_{tf}}{A_{ris}\rho_0 \epsilon} \tag{3-10}$$

$$\rho_0 = \frac{F_{tf}\rho_c(1-\epsilon)}{F_{rgc}\epsilon} \tag{3-11}$$

$$\rho_v = \frac{F_v}{F_{tf}}\rho_0 \tag{3-12}$$

$$F_v = F_{tf} - F_c C_c - F_{tf} CCR = F_{tf} - F_{rgc} C_c - F_{tf} CCR \tag{3-13}$$

Let $y_i = \rho_i/\rho_0 = F_{vi}/F_{tf}$ and $R_k = r_k/\rho_0$, then (3-7) becomes

$$\frac{\partial y_i}{\partial t} + u_0 \frac{\partial y_i}{\partial z} = \sum_k a_{ik} R_k \tag{3-14}$$

(4) Energy balance

It is assumed that the riser is adiabatic, has same temperatures between catalyst and the fluid at any position and all heat capacities are constant.

It is also assumed that the equilibrium is achieved before a significant conversion has occurred, then the temperature of the mixture at the inlet of the riser can be shown to be (Gates et al., 1979)

$$T_0 = \frac{F_{rgc}C_{pc}T_{reg} + F_{tf}C_{pfl}T_f - F_{tf}\Delta H_{fv}}{F_{rgc}C_{pc} + F_{tf}C_{pfv}} \tag{3-15}$$

Accumulation = $A_{ris}dz[\rho_c(1-\varepsilon)(U_c + C_cU_{coke}) + \varepsilon \Sigma \rho_iU_i]$

$$A_{ris}dz\frac{\partial}{\partial t}[\rho_c(1-\epsilon)(U_c+C_cU_{coke}) + \epsilon \sum \rho_iU_i] = F_c(H_c + C_cH_{coke}) + \sum F_{vi}H_i$$

$$- \{F_c(H_c + C_cH_{coke}) + \sum F_{vi}H_i + \frac{\partial}{\partial z}[F_c(H_c+C_cH_{coke}) + \sum F_{vi}H_i]dz\}$$

$$\therefore A_{ris}\frac{\partial}{\partial t}[\rho_c(1-\epsilon)(U_c+C_cU_{coke})+\epsilon \sum \rho_iU_i] = - \frac{\partial}{\partial z}[F_c(H_c+C_cH_{coke})+\sum F_{vi}H_i] \tag{3-16}$$

because catalyst and coke are solid,

$$U_c = C_{pc}T, \quad U_{coke} = C_{pcoke}T, \quad U_i = C_{vi}T + h_{fi}, \quad H_c = C_{pc}T$$

$$H_{coke} = C_{pcoke}T, \quad H_i = C_{pi}T + h_{fi}$$

Assume $C_{vi} = C_v$, $C_{pi} = C_{pfv}$. $And\ \Sigma\rho_i = \rho_v$, $\Sigma F_{vi} = F_v$

$$A_{ris}\frac{\partial}{\partial t}\{[\rho_c(1-\epsilon)(C_{pc}+C_cC_{pcoke}) + \epsilon\rho_vC_v]T\} + A_{ris}\epsilon \sum h_{fi}\frac{\partial \rho_i}{\partial t} =$$

$$- \frac{\partial}{\partial z}\{[F_c(C_{pc}+C_cC_{pcoke}) + F_vC_{pfv}]T\} - \sum h_{fi}\frac{\partial F_{vi}}{\partial z} \tag{3-17}$$

Substitute (3-5) into (3.17) we obtain

$$A_{ris}\frac{\partial}{\partial t}\{[\rho_c(1-\epsilon)(C_{pc}+C_cC_{pcoke}) + \epsilon\rho_vC_v]T\} + \frac{\partial}{\partial z}\{[F_c(C_{pc}+C_cC_{pcoke}) + F_vC_{pfv}]T\} = -A_{ris}\epsilon\sum_k r_k\sum_i a_{ik}h_{fi} = -A_{ris}\epsilon\sum_k r_k\Delta H_{rk} \quad (3\text{-}18)$$

where

$$\Delta H_{rk} = \sum_i a_{ik}h_{fi} \quad (3\text{-}19)$$

3.1.1.1 Application of ten-lumping kinetic model

As shown by Jacob et al. (1976), the kinetics of the cracking reactions can be modeled by gasoline (G lump, C_5 to 430°F), C lump (H_2, H_2S, C_1 to C_4 plus coke), LFO (light fuel oil) (430° to 650°F) and HFO (heavy fuel oil) (650°F$^+$). Each LFO or HFO is divided into paraffin, naphthene, aromatic substituent groups and aromatic rings.

Figure 3-2 shows ten-lumping kinetic scheme. It shows that a paraffinic molecule in HFO will form paraffinic moleculars in LFO and G and C lumps. Paraffinic molecules in LFO can only crack to G and C lumps. Likewise, a naphthenic molecule in HFO can form naphthenic molecules in LFO and G and C lumps while naphthenic molecules in LFO can only crack to G and C lumps. The aromatic rings in the HFO and LFO do not form gasoline but result in the formation of the C lump. An aromatic ring with an attached substituent group reacts to give G and C lumps and this group in HFO can form aromatic rings in LFO.

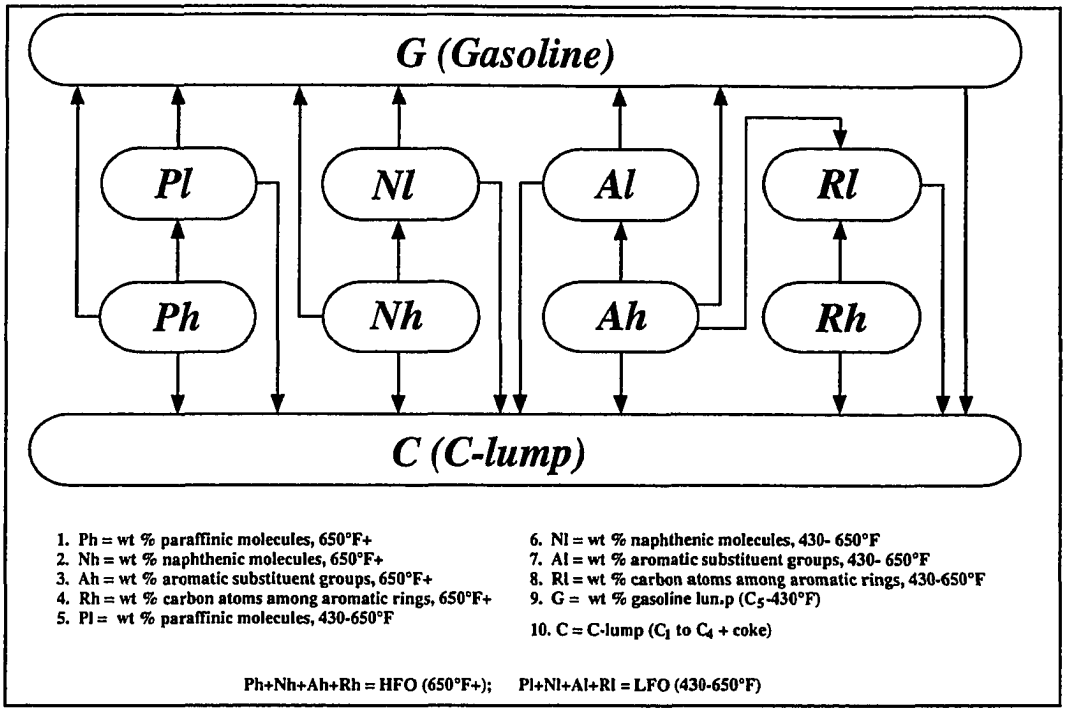

Figure 3-2. Ten-lump FCC Cracking Kinetic Scheme (From Jacob et al., 1976)

Table 3-1 shows a matrix of cracking rate constants. In ten-lumping model, all lumped components crack according to first-order kinetics and reactions are irreversible. Table 3-2 gives ten-lumping kinetic and thermodynamic parameters (Gross et al, 1976)

From Jacob, et al (1976), the rate of disappearance of a chemical species j in a single reaction of oil cracking is defined as the following formula,

$$-R_j = -k_j \Phi_j y_j \frac{\rho_c(1-\epsilon)}{\epsilon(1+K_h R_h)} = -k_{j0} e^{-\frac{E_j}{RT}} \Phi_j y_j \frac{\rho_c(1-\epsilon)}{\epsilon(1+K_h R_h)} \qquad (3\text{-}20)$$

Table 3-1. Matrix of Catalytic Cracking Reaction Rate Constants (From Jacob et al., 1976)

	P_h	N_h	A_h	R_h	P_l	N_l	A_l	R_l	G	C
P_h	$-(k_{phpl}+k_{phg}+k_{phc})$	0	0	0	0	0	0	0	0	0
N_h	0	$-(k_{nhnl}+k_{nhg}+k_{nhc})$	0	0	0	0	0	0	0	0
A_h	0	0	$-(k_{ahal}+k_{ahg}+k_{ahc}+k_{ahrl})$	0	0	0	0	0	0	0
R_h	0	0	0	$-(k_{rhrl}+k_{rhc})$	0	0	0	0	0	0
P_l	$\nu_{hl}k_{phpl}$	0	0	0	$-(k_{plg}+k_{plc})$	0	0	0	0	0
N_l	0	$\nu_{hl}k_{nhnl}$	0	0	0	$-(k_{nlg}+k_{nlc})$	0	0	0	0
A_l	0	0	$\nu_{hl}k_{ahal}$	0	0	0	$-(k_{alg}+k_{alc})$	0	0	0
R_l	0	0	$\nu_{hl}k_{ahrl}$	$\nu_{hl}k_{rhrl}$	0	0	0	$-k_{rlc}$	0	0
G	$\nu_{hg}k_{phg}$	$\nu_{hg}k_{nhg}$	$\nu_{hg}k_{ahg}$	0	$\nu_{lg}k_{plg}$	$\nu_{lg}k_{nlg}$	$\nu_{lg}k_{alg}$	0	$-k_{gc}$	0
C	$\nu_{hc}k_{phc}$	$\nu_{hc}k_{nhc}$	$\nu_{hc}k_{ahc}$	$\nu_{hc}k_{rhc}$	$\nu_{lc}k_{plc}$	$\nu_{lc}k_{nlc}$	$\nu_{lc}k_{alc}$	$\nu_{lc}k_{rlc}$	$\nu_{gc}k_{gc}$	0

where ν_{hl} = stoichiometric coefficient (MW of heavy fuel oil/MW of light fuel oil);
ν_{hg} = stoichiometric coefficient (MW of heavy fuel oil/MW of gasoline);
ν_{hc} = stoichiometric coefficient (MW of heavy fuel oil/MW of C-lump);
ν_{lg} = stoichiometric coefficient (MW of light fuel oil/MW of gasoline);
ν_{c} = stoichiometric coefficient (MW of light fuel oil/MW of C-lump);
ν_{gc} = stoichiometric coefficient (MW of gasoline/MW of C-lump) ; (MW = molecular weight).

Formation reactions	Item	E Btu/lbmol	k_0 ft^3/s.lb cat	ΔH_r Btu/lb
HFO → LFO	k_{phpl}	1.460×10^4	20.54	50
	k_{nhnl}		22.33	
	k_{ahal}		18.86	
	k_{rhrl}		5.815	
	k_{ahrl}		49.62	
HFO → G	k_{phg}	9.90×10^3	9.573	130
	k_{nhg}		14.74	
	k_{ahg}	2.610×10^4	4.424×10^3	
LFO → G	k_{plg}	9.90×10^3	4.151	80
	k_{nlg}		11.51	
	k_{alg}	2.610×10^4	1.299×10^3	
HFO → C	k_{phc}	1.530×10^4	10.10	450
	k_{nhc}		19.12	
	k_{ahc}	3.150×10^4	1.774×10^4	
	k_{rhc}		7.590×10^3	
LFO → C	k_{plc}	1.530×10^4	12.14	400
	k_{nlc}		10.52	
	k_{alc}	3.150×10^4	1.883×10^3	
	k_{rlc}		518.8	
G → C	k_{gc}	3.60×10^4	1.0×10^3	320

Table 3-2. Ten-lumping Kinetic and Thermodynamic Parameters (Gross et al, 1976)

Since the same type of catalyst site would be expected to crack both gas oil molecules and gasoline range molecules, the catalyst decay in above equation can be represented as nonselective, i.e., $\Phi_j = \Phi$. This was found to be a reasonable assumption (Weekman and Nace, 1970).

3.1.1.2 Simplification of the riser model

Since the residence time of catalyst or oil in the most of modern riser is less than 10 seconds, and the characteristic time for change in FCC reactor or regenerator dense bed is almost on the order of one hour, changes of variables in the riser with time can be neglected. The riser model can then be modeled approximately as a quasi-steady-state one.

(i) Coke formation balance on catalyst

For reactor modeling, a relation of coke formation is a key part in that coke that deposits on the catalyst during the reaction dramatically decreases catalyst activity, therefore affects product composition, and have a strong impact on dynamics of whole system.

The formation equation of catalytic coke on catalyst can be expressed from equation (3-4),

$$\frac{dC_c}{dz} = \frac{A_{ris}(1-\epsilon)}{F_{rgc}} R_{coke} \qquad (3\text{-}21)$$

$$or, \quad \frac{dC_c}{dh} = \frac{A_{ris} h_{ris} (1-\epsilon)}{F_{rgc}} R_{coke} = \frac{F_{coke}}{F_{rgc}} \tag{3-22}$$

where

$$h = \frac{z}{h_{ris}} \tag{3-23}$$

$$F_{coke} = h_{ris} A_{ris} (1 - \varepsilon) R_{coke} \tag{3-24}$$

From Krambeck (1990) and Sapre and Leib (1991), it is obtained that

$$F_{coke} = F_{tf} R_{co} \Phi C_{cr} y_{oil} \Psi \tau_r / \tau_{rr} = F_{rgc} \Phi C_{cr} y_{oil} \Psi \tau_r / \tau_{rr} \tag{3-25}$$

where

$$R_{co} = F_{rgc} / F_{tf} \tag{3-26}$$

$$y_{oil} = P_{oil} / P_r \tag{3-27}$$

Catalyst deactivation function, Φ, is given by

$$\Phi = \frac{\tau_{rr}}{C_{cr}} k_{cc} C_c^{1-\frac{1}{b}} \tag{3-28}$$

where reference parameters, τ_{rr} and C_{cr} make Φ be dimensionless, and k_{cc} is a function of

riser temperature, coke concentration in the riser inlet (see Mandal et al., 1993) and relative activity of catalyst and given by (Avidan and Shinnar, 1990),

$$k_{cc} = Ak_{cc0}e^{(\lambda_0 e^{-\lambda_1 C_{rgc}} - \frac{E_{cc}}{RT})} \tag{3-29}$$

The deactivation of the catalyst for cracking reactions essentially parallels its deactivation for coke production, so the same function, Φ, can be used to describe both (Krambeck, 1990). The value of E_{cc} varies between 0 and 5000 Btu/lbmol depending on catalyst (Wollaston et al., 1975).

Ψ is a function of feedstock quality and given by (Gross et al., 1976)

$$\Psi = 0.631P_{l0} + 0.110N_{l0} + 1.475A_{l0} + 0.0727R_{l0} + 0.631P_{h0} + 0.297N_{h0} + 0.773A_{h0} + 2.225R_{h0} \tag{3-30}$$

$$\tau_r = \frac{3600}{WHSV\ R_{co}} = \frac{3600F_{tf}}{WHSV\ F_{rgc}} = \frac{W_{ris}}{F_{rgc}} \tag{3-31}$$

$$WHSV = \frac{3600F_{tf}}{W_{ris}} \tag{3-32}$$

Therefore, equation (3-22) becomes,

$$\frac{dC_c}{dh} = \tau_r \Psi k_{cc} C_c^{1-\frac{1}{b}}\ y_{oil} \tag{3-33}$$

Above the rate equation of coke buildup is the same form as Voorhies' (1945) with,

$$t_c = \tau_r h \tag{3-34}$$

The value of b was about 1/2 for old non-zeolitic catalyst in use in the forties and fifties but modern cracking catalysts containing Y-type zeolite have values of b of approximately 1/3 ~ 1/5.

Typically less than 100% of the feed CCR goes to coke depending on the feedstock and operating conditions. However, for simplicity it is assumed that 100% of the feed CCR is deposited as coke on catalyst (Sapre and Leib, 1991) so coke concentration on catalyst at riser outlet is obtained by

$$C_{cf} = C_{rgc} + C_c \Big|_{h=1} + CCR/R_{co} \tag{3-35}$$

(ii) Mass balance on oil component

From equation (3-14),

$$\frac{dy_i}{dz} = \frac{1}{u_0} \sum_k a_{ik} R_k \tag{3-36}$$

$$or, \quad \frac{dy_i}{dh} = \frac{h_{ris}}{u_0} \sum_k a_{ik} R_k = \tau_r \sum_k a_{ik} R_k \tag{3-37}$$

where

$$\tau_r = \frac{h_{ris}}{u_0} \tag{3-38}$$

(iii) Energy balance

From equation (3-18),

$$\frac{d}{dz}\{[F_c(C_{pc}+C_cC_{pcoke}) + F_vC_{pfv}]T\} = -A_{ris}\epsilon\sum_k r_k\Delta H_{rk} \tag{3-39}$$

Since $C_c \ll 1$, C_cC_{pcoke} can be neglected and $F_v \doteq F_{tf}$ in energy equation. Equation (3-39) becomes,

$$\frac{dT}{dh} = -\frac{A_{ris}h_{ris}\epsilon\rho_0}{F_{rgc}C_{pc} + F_{tf}C_{pfv}}\sum_k R_k\Delta H_{rk} \tag{3-40}$$

$$or, \quad \frac{dT}{dh} = -\frac{F_{tf}\tau_r}{F_{rgc}C_{pc} + F_{tf}C_{pfv}}\sum_k R_k\Delta H_{rk} \tag{3-41}$$

where

$$F_{tf} = A_{ris}\,h_{ris}\,\varepsilon\,\rho_0\,/\tau_r \tag{3-42}$$

3.1.1.3 The cracking catalyst deactivation by metal contaminants

The poisoning effects of nickel and vanadium in the FCC feedstocks on the cracking reactions have been studied by Larocca et al. (1990). At regeneration conditions

vanadium migrates to the zeolite, and reacting with oxygen forms a rare earth vanadate destroying the activity site. Nickel remains randomly distributed in the matrix. Due to the undesirable effects caused by the presence of metals in the feedstocks, it is important then to acquire knowledge about how the kinetic parameters involved in the catalytic cracking reactions are modified by nickel and vanadium contaminants although modern zeolite cracking catalyst have excellent resistance to contamination by vanadium, nickel, and other heavy metals (Venuto and Habib, 1979). Therefore following Larocca et al., we obtain

$$k_i (C_m) / k_j (C_m) = k_i (C_m=0) / k_j (C_m=0) \tag{3-43}$$

and,

$$k_i (C_m) = k_i (C_m=0) f (C_m) \tag{3-44}$$

where

$$f(C_m) = e^{\sum_{i=1}^{3} b_i C_m^i + \frac{E_{base}(1-e^{-cC_m})}{RT}} \tag{3-45}$$

3.1.1.4 Wet Gas Yield model

The yield of wet gas is given by

$$Y_{wg} = X - Y_g - R_{co} (C_{sc} - C_{rgc}) \tag{3-46}$$

or, $F_{wg} = F_{lg} / M_{lg}$ (3-47)

where

$$F_{lg} = F_{of} - (1 - X + Y_g) F_{tf} \quad (3\text{-}48)$$

$$X = 1 - (P_h + N_h + A_h + R_h + P_l + N_l + A_l + R_l)\big|_{h=1} \quad (3\text{-}49)$$

$$Y_g = G\big|_{h=1} \quad (3\text{-}50)$$

$$F_{of} = F_{tf} - F_{rgc}(C_{cf} - C_{rgo}) - F_{ush} \quad (3\text{-}51)$$

$$F_{ush} = \alpha F_{rgc} C_c\big|_{h=1} \quad (3\text{-}52)$$

3.1.2 The Stripper Model

The stripper model includes catalyst inventory balance, coke balance and energy balance. The basic assumptions for developing the stripper model are: i) continuous stirred tank; ii) no cracking reactions; iii) neglecting effects of steam and catalyst entrainment.

(1) Catalyst balance

$$\frac{dW_{rs}}{dt} = F_{rgc} - F_{sc} \quad (3\text{-}53)$$

(2) Coke balance

$$\frac{d}{dt}(W_{rs}C_{sc}) = F_{rgc}C_{cf} - F_{sc}C_{sc} + F_{ush} \tag{3-54}$$

$$or, \quad \frac{dC_{sc}}{dt} = \frac{F_{rgc}}{W_{rs}}(C_{cf} - C_{sc} + \alpha C_c|_{h=1}) \tag{3-55}$$

Usually, the amount of the unstripped hydrocarbon on the catalyst is a function of the rate of stripping steam and the catalyst residence time in the stripper. This amount is about 10% of total catalytic coke production in normal operation range (Schuurmans, 1980), i.e.,

$$\alpha = \alpha\,(F_{ss},\ W_{rs} / F_{rgc}) \approx 0.1 \tag{3-56}$$

(3) Energy balance

$$\frac{d}{dt}(W_{rs}C_{pc}T_{rs}) = C_{pc}(F_{rgc}T_{ri} - F_{sc}T_{rs}) - Q_{loss} \tag{3-57}$$

It is assumed that heat loss in stripper causes a constant temperature drop,

$$Q_{loss} = F_{rgc}\,C_{pc}\,\Delta T_s \tag{3-58}$$

$$\therefore \quad \frac{dT_{rs}}{dt} = \frac{F_{rgc}}{W_{rs}}(T_{ri} - T_{rs} - \Delta T_s) \tag{3-59}$$

3.1.3 Reactor Riser Pressure

The pressure at the bottom of the reactor riser is needed in the force balance on the regenerated catalyst circulation line. It is given by

$$P_{rb} = P_r + [\epsilon\rho_v + (1-\epsilon)\rho_c]\frac{h_{ris}}{144} = P_r + \frac{\rho_{ris}h_{ris}}{144} \tag{3-60}$$

where

$$\rho_{ris} = \varepsilon\rho_v + (1 - \varepsilon)\rho_c \tag{3-61}$$

$$or, \quad \rho_{ris} = \frac{F_{tf} + F_{rgc}}{v_{ris}} \tag{3-62}$$

$$v_{ris} = \frac{F_{tf}}{\rho_v} + \frac{F_{rgc}}{\rho_c} \tag{3-63}$$

$$\epsilon = \frac{\rho_c - \rho_{ris}}{\rho_c - \rho_v} \tag{3-64}$$

The inventory of catalyst in the riser is needed in the calculation of the average catalyst residence time in the riser and is given by

$$W_{ris} = \frac{F_{rgc}A_{ris}h_{ris}}{v_{ris}} \tag{3-65}$$

3.2 The Regenerator Model

The regenerator model which is developed mainly from McFarlane et al. (1993) includes energy balance, coke balance, catalyst inventory balance (dense bed and standpipe), catalyst entrainment and mass balances on oxygen, carbon monoxide and carbon dioxide. The model derives from McFarlane et al. (1993). A schematic of the regenerator model is given in Figure 3-4. The model is divided into two parts, the fluidized dense bed and the dilute phase bed where plug flow is applied. The model assumes that the fluidized bed consists of two phase, a bubble phase of gaseous reactants and products moving up the bed in plug flow, and a perfectly mixed dense phase containing gas and solid catalyst; Mass transfer occurs between the two phases as gas moves up the bed; At typical regenerator temperature, reaction rates are controlling rather than the rate of mass transfer between the two phases. The basic assumptions for modeling are: i) adiabatic in gaseous plug flow modeling; ii) no catalyst particles at cyclone exit; iii) idea gas behavior; iv) constant heat capacities of all materials in the regenerator.

Coke combustion occurs in the regenerator. The products of the primary combustion are CO, CO_2 and H_2O. In the kinetic model of coke combustion, complete conversion of hydrogen presenting in the coke on spent catalyst to water is assumed and this reaction is much faster than others. CO reacts further with O_2 to form CO_2 in a thermal free-radical reaction, but this reaction is slowed by the presence of solids that quench free radicals. The flue gas ignited once the solid were removed from the gas in the cyclone due to the presence of CO and oxygen. The combustion of CO to CO_2 can

also be achieved by increasing combustion temperature. Temperature of above 1300 °F will result in complete CO combustion, given sufficient air (Avidan and Shinnar, 1990).

Until recently, a lot of the regenerators are still operated at partial combustion of CO in the low regenerator temperature because of consideration of processing heavy feedstocks and aggravation of catalyst deactivation by steam at high regenerator temperature. In this mode of operation concentration of oxygen at cyclone inlet should be controlled at lower level in case of high temperature to burn down cyclones. A typical profiles of temperature and compositions of gaseous components in regenerator at one steady state are shown in Figure 2-5 for this kind of operation.

Recently, more and more FCCUs have introduced the CO combustion promoter into cracking catalyst to assist CO oxidation therefore raise CO_2/CO ratio in the low regenerator temperature because of both environmental and economic factor - the need to eliminate CO emission and to make cracking processes more efficient and productive. Because additives containing precious metals, such as platinum, allow CO complete combustion to CO_2, the combustion kinetic model includes the impact of promoter on combustion reaction of CO. Some information for this kind of operation can be obtained from Chester et al. (1981).

3.2.1 Combustion Kinetic Model

Spent catalyst which contains rich coke from the reactor enters the regenerator through the spent catalyst transported line. Coke which consists of carbon and hydrogen is burnt off in the regenerator by contacting the catalyst with air in a fluidized bed. Air,

delivered directly to the bottom of the regenerator by the air blowers contribute to the fluidization and combustion reactions. Carbon in the coke reacts with oxygen to produce carbon monoxide and carbon dioxide in the following reactions:

$$2C + O_2 \xrightarrow{k_1} 2CO \qquad (I)$$

$$C + O_2 \xrightarrow{k_2} CO_2 \qquad (II)$$

Carbon monoxide reacts with oxygen to produce carbon dioxide according to:

$$2CO + O_2 \xrightarrow{k_3} 2CO_2 \qquad (III)$$

The model assumes that the conversion of hydrogen presenting in the coke on spent catalyst to water is instantaneous and complete according to the following reaction:

$$4H + O_2 \longrightarrow 2H_2O \qquad (IV)$$

Numerous investigations have been carried out on the kinetics of coke burning reactions (Arthur, 1951; Weisz and Goodwin, 1966; Hano et al., 1975; Prater et al., 1983; Wang et al., 1982, 1986; Morley and de Lasa, 1987, 1988). Based on the open literature kinetic model and data, the following coke burning kinetic model can be obtained. The carbon reaction rate equation for reaction (I) is expressed by

$$-r_{1c} = k_1 \rho_c \rho_B C_{rgc} P_{O2} / M_c \qquad (3\text{-}66)$$

The carbon reaction rate equation for reaction (II) is expressed by

$$-r_{2c} = k_2 \rho_c \rho_B C_{rgc} P_{O2} / M_c \tag{3-67}$$

where a first-order dependence on carbon-on-catalyst and oxygen partial pressure is assumed. Overall carbon reaction rate equation is obtained by combining equation (3-66) and (3-67):

$$-r_c = (k_1+k_2) \rho_c \rho_B C_{rgc} P_{O2} / M_c = k_c \rho_c \rho_B C_{rgc} P_{O2} / M_c \tag{3-68}$$

where

$$k_c = k_1 + k_2 \tag{3-69}$$

is the overall carbon reaction rate constant and is expressed by

$$k_c = k_{c0} e^{-\frac{E_c}{R(T_{reg}(z) + 459.6)}} \tag{3-70}$$

Let β represent the mole ratio of CO produced in reaction (I) to CO_2 produced in reaction (II), then

$$\beta = CO / CO_2 = (-r_{1c}) / (-r_{2c}) = k_1 / k_2 \tag{3-71}$$

Combining equations (3-68) and (3-71) gives

$$k_1 = \beta k_c \ / \ (\beta+1) \tag{3-72}$$

$$k_2 = k_c \ / \ (\beta+1) \tag{3-73}$$

It is verified that there is an intrinsic CO/CO_2 ratio at the catalyst site in the combustion of carbon (Arthur, 1951). The quantity of CO/CO_2 is a function of temperature only, and is given by

$$\beta = \beta_0 e^{-\frac{E_\beta}{R(T_{reg}(z) + 459.6)}} \tag{3-74}$$

The rate of CO conversion in reaction (III) is given by (Morley and de Lasa, 1988),

$$-r_{3CO} = 2k_3 P_{CO} P_{O_2} \tag{3-75}$$

$$k_3 = (1 - \rho_B) k_{31} + \rho_B \ k_{32} \qquad z \le z_{cyc} \tag{3-76}$$

where k_{31} is the rate constant for the homogeneous noncatalytic reaction, and is expressed as,

$$k_{31} = k_{310} e^{-\frac{E_{31}}{R(T_{reg}(z) + 459.6)}} \tag{3-77}$$

Weisz (1966) showed that the intrinsic CO_2/CO ratio, β, is modified by further oxidation

of CO to CO_2, catalyzed by the presence of transition metal oxides. Therefore k_{32} represents the rate constant for this heterogeneous catalytic reaction, and is given by,

$$k_{32} = k_{320} e^{-\frac{E_{32}}{R(T_{reg}(z) + 459.6)}} \tag{3-78}$$

When the catalyst solids are removed in the cyclones, CO will react with O_2 to form CO_2 in a fast homogeneous thermal free-radical reaction (Avidan and Shinnar, 1990).

$$k_3 = k_{33} \qquad z > z_{cyc} \tag{3-79}$$

where

$$k_{33} = k_{330} e^{-\frac{E_{33}}{R(T_{reg}(z) + 459.6)}} \tag{3-80}$$

It is assumed that this reaction is very fast and complete in a typical operating temperature range so that complete conversion of either CO or O_2 depending on their amount is applied for modeling.

Table 3-3 shows the all the values of combustion activation energies applied in our model. The references from which they come are also listed in the table.

Table 3-3. The Values of Combustion Activation Energies

Combustion Reaction Type	Activation Energy	References
Carbon Burning, k_c	37.5 kcal/mol	Prater et al., 1983
Heterogeneous CO Burning, k_{32}	28 kcal/mol	Weisz, 1966
Homogeneous CO Burning, k_{31}	70 kcal/mol	Avidan and Shinnar, 1990

3.2.2 Impact of Promoter on CO Combustion

Carbon in the coke reacts with oxygen to produce carbon monoxide and carbon dioxide according to reactions I - III. If some promoter, e.g. precious platinum, presents in the catalyst, it will promote combustion reaction of CO to CO_2, and allow complete combustion to CO_2 in lower temperature. Therefore the ratio of CO to CO_2 in regenerator stack gas can be related to the promoter content in the catalyst. From Chester et al. (1981), the following equations can be obtained,

$$\frac{1+\sigma_B}{1+\sigma} = 1 - c_{pt} X_{pt}^{\frac{1}{3}} \tag{3-81}$$

$$or, \quad \sigma = \frac{\sigma_B + c_{pt} X_{pt}^{\frac{1}{3}}}{1 - c_{pt} X_{pt}^{\frac{1}{3}}} \tag{3-82}$$

where

$$\sigma_B = \sigma (X_{pt} = 0) \tag{3-83}$$

$$\sigma = CO_2 \ / \ CO \tag{3-84}$$

From above equations and plant data, we propose the following equation for catalytic combustion of CO in our model for convenience:

$$k_{32} = k_{320} e^{\sum_{i=1}^{3} c_i X_{pt}^i - \frac{E_{32}}{R(T_{reg}(z) + 459.6)}} \tag{3-85}$$

3.2.3 Energy Balance

The catalyst phase of the fluidized bed is assumed to be perfectly mixed. The energy balance for the regenerator dense bed is given by Equations (3-86) (McFarlane et al., 1993). Heat is generated by the reactions I-IV. The amount of hydrogen burned off in the regenerator assuming total conversion is given by equation (3-95). The quantity of heat produced by reactions I-III is given by Equation (3-91).

$$[(W_{reg} + W_{sp})C_{pc} + M_I]\frac{dT_{reg}}{dt} = Q_{in} - Q_{out} \tag{3-86}$$

where

$$Q_{in} = Q_{air} + Q_H + Q_c + Q_{sc} \tag{3-87}$$

$$Q_{out} = Q_{fg} + Q_{rgc} + Q_e + Q_{rm} \tag{3-88}$$

$$Q_{air} = F_{air} C_{pair} (T_{air} - T_{base}) \tag{3-89}$$

$$Q_H = F_H \ \Delta H_H \tag{3-90}$$

$$Q_c = F_{air} (X_{CO,sg} \ \Delta H_1 + X_{CO2,sg} \ \Delta H_2) \tag{3-91}$$

$$Q_{sc} = F_{sc} C_{pc} (T_{rs} - T_{base}) \tag{3-92}$$

$$Q_{fg} = [F_{air} (X_{O2,sg} C_{pO2} + X_{CO,sg} C_{pCO} + X_{CO2,sg} C_{pCO2} + 0.79 C_{pN2}) + 0.5 F_H \ C_{pH2O}] (T_{sg} - T_{base}) \tag{3-93}$$

$$Q_{rgc} = F_{rgc} C_{pc} (T_{reg} - T_{base}) \tag{3-94}$$

$$F_H = F_{sc} (C_{sc} - C_{rgc}) C_H \tag{3-95}$$

A catalyst cooler or steam generator in the regenerator allows heat removal and permits one to operate with heavy feeds but forms excess coke. This increases the

operating space of the unit (Shinnar, 1981). The following equation can represent the cooler model.

$$Q_{rm} = F_s \, \Delta H_s \tag{3-96}$$

Equation (3-97) gives the temperature profile above the bed. As described below, catalyst is present above the bed due to entrainment. Temperature increases above the bed due to heat generated by reactions I - III. The heat balance between the top of the bed and the inlet of the cyclones is affected by the presence of catalyst in this zone, as given in the last term of Equation (3-98).

$$\begin{aligned} \frac{dT_{reg}(z)}{dz} &= 0 \qquad 0 \le z \le z_{bed} \\ &= (\Delta H_1 \frac{dX_{CO}(z)}{dz} + \Delta H_2 \frac{dX_{CO_2}(z)}{dz}) \frac{1}{C_p(z)} \qquad z_{bed} < z < z_{top} \end{aligned} \tag{3-97}$$

$$\begin{aligned} C_p(z) &= 0.79 C_{pN_2} + X_{CO}(z) C_{pCO} + X_{CO_2}(z) C_{pCO_2} + X_{O_2}(z) C_{pO_2} \\ &\quad + [0.5 C_{pH_2O} F_H + \delta_z C_{pc} M_e] \frac{1}{F_{air}} \end{aligned} \tag{3-98}$$

where

$$\delta_z = 0 \qquad z \geq z_{cyc}$$
$$= 1 \qquad z < z_{cyc} \tag{3-99}$$

3.2.4 Carbon Balance on Catalyst

The first term in the parenthesis in the regenerator carbon balance, Equation (3 - 101), represents the quantity of carbon entering the regenerator with the spent catalyst (the quantity $F_{sc}C_{sc}$ is the quantity of coke while F_H is the amount of hydrogen). The remaining terms describe the amount of carbon leaving the regenerator on catalyst flowing over the weir into the standpipe and the carbon in the flue gas (carbon monoxide and carbon dioxide).

$$\frac{dW_{reg}}{dt} = F_{sc} - F_{sp} \tag{3-100}$$

$$\frac{d}{dt}(W_{reg}C_{rgc}) = (F_{sc}C_{sc} - F_H) - [F_{sp}C_{rgc} + M_c F_{air}(X_{CO,sg} + X_{CO_2,sg})] \tag{3-101}$$

Therefore,

$$\frac{dC_{rgc}}{dt} = [F_{sc}(C_{sc} - C_{rgc}) - F_H - M_c F_{air}(X_{CO,sg} + X_{CO_2,sg})]\frac{1}{W_{reg}} \tag{3-102}$$

3.2.5 Standpipe Inventory Balance

$$\frac{dW_{sp}}{dt} = F_{sp} - F_{rgc} \tag{3-103}$$

3.2.6 Mass Balance

Similar as reactor riser model, from (3-5) or (3-7) with neglecting time derivative term, mass balances on oxygen, carbon monoxide and carbon dioxide are given by Equations (3-104), (3-105), and (3-106), respectively. The concentrations of carbon monoxide and carbon dioxide in the air entering the regenerator are assumed to be zero. The amount of oxygen available for reaction I - III is that available in the air flow entering the regenerator minus the oxygen consumed in the combustion of hydrogen [Equation (3-108)].

$$\frac{dX_{O_2}(z)}{dz} = -[(0.5k_1 + k_2)\rho_c \rho_B(z)\frac{C_{rgc}(z)}{M_c}X_{O_2}(z) + k_3 X_{CO}(z) P_{rg} X_{O_2}(z)]\frac{R(T_{reg} + 459.6)}{v_s} \tag{3-104}$$

$$\frac{dX_{CO}(z)}{dz} = [k_1 \rho_c \rho_B(z)\frac{C_{rgc}(z)}{M_c}X_{O_2}(z) - 2k_3 X_{CO}(z) P_{rg} X_{O_2}(z)]\frac{R(T_{reg}+459.6)}{v_s} \tag{3-105}$$

$$\frac{dX_{CO_2}(z)}{dz} = -\frac{dX_{O_2}(z)}{dz} - 0.5\frac{dX_{CO}(z)}{dz} \tag{3-106}$$

$$X_{CO_2}(z) = X_{O_2}(z=0) - X_{O_2}(z) - 0.5X_{CO}(z) \tag{3-107}$$

$$X_{O_2}(z=0) = \frac{1}{F_{air}}\{0.21F_{air} - 0.25F_H\} \tag{3-108}$$

$$\frac{dC_{rgc}(z)}{dz} = 0; \qquad 0 \le z \le z_{bed}$$

$$= -k_c P_{rg} C_{rgc}(z) X_{O_2}(z)/v_s \qquad z_{bed} < z \le z_{cyc} \tag{3-109}$$

Generally, $C_{rgc}(z)$ does not change too much, therefore $C_{rgc}(z) \doteq C_{rgc}$.

The output concentrations are converted to the appropriate units as given below:

$$C_{O_2,sg} = \frac{100F_{air}X_{O_2,sg}}{F_{sg}} \tag{3-110}$$

$$C_{CO,sg} = \frac{100F_{air}X_{CO,sg}}{F_{sg}} \tag{3-111}$$

$$C_{CO_2,sg} = \frac{100F_{air}X_{CO_2,sg}}{F_{sg}} \tag{3-112}$$

where

$$F_{sg} = 0.5F_H + F_{air}(0.79 + X_{O_2,sg} + X_{CO,sg} + X_{CO_2,sg}) \quad (3\text{-}113)$$

3.2.7 Volume Fraction of Catalyst

Void fraction in the regenerator bed (ε_f) is assumed to be constant and is given empirically by Equation (3-116). Volume fraction of catalyst ($\rho_B(z)$) is given by (3-114). It is assumed that any entrained catalyst entering the cyclones is removed and returned to the bed so that $\rho_B(z)$ is zero above the cyclones. The following empirical equations are from McFarlane et al. (1993).

$$\begin{aligned} \rho_B(z) &= 1 - \varepsilon_e & 0 \le z \le z_{bed} \\ &= \rho_{c,dilute} / \rho_c & z_{bed} < z \le z_{cyc} \\ &= 0 & z_{cyc} < z \end{aligned} \quad (3\text{-}114)$$

$$\epsilon_e = min[1,\ max(\epsilon_f,\ \epsilon_f + \frac{1.904 + 0.363v_s - 0.048v_s^2}{z_{bed}})] \quad (3\text{-}115)$$

$$\varepsilon_f = 0.332 + 0.06v_s \quad (3\text{-}116)$$

3.2.8 Catalyst Entrainment

The mass flowrate of entrained catalyst leaving the bed is described empirically by Equations (3-117) and (3-118) (McFarlane et al., 1993).

$$M_e = A_{reg}\, v_s\, \rho_{c,dilute} \tag{3-117}$$

$$\rho_{c,dilute} = Max(0,\ -0.878 + 0.582 v_s) \tag{3-118}$$

Superficial velocity is given by Equation (3-119),

$$v_s = \frac{F_{air}}{\rho_g A_{reg}} \tag{3-119}$$

where

$$\rho_g = \frac{0.0933 P_{rg}}{T_{reg} + 459.6} \tag{3-120}$$

here ideal gas behavior is assumed.

3.2.9 Regenerator Pressure

The pressure at the bottom of the regenerator, P_{rgb}, is required in the calculation

of force balance on the spent catalyst circulation line.

$$P_{rgb} = P_{rg} + \frac{W_{reg}}{144A_{reg}} \tag{3-121}$$

$$\Delta P_{RR} = P_{rg} - P_r \tag{3-122}$$

3.2.10 Bed Height

The regenerator bed height is given empirically by Equation (3-123) (McFarlane et al., 1993).,

$$z_{bed} = min\{z_{cyc},\ (2.85 + 0.8v_s + \frac{W_{reg} - \rho_{c,dilute}A_{reg}z_{cyc}}{A_{reg}\rho_{c,dense}})\frac{1}{1-\frac{\rho_{c,dilute}}{\rho_{c,dense}}}\} \tag{3-123}$$

where

$$\rho_{c,dense} = \rho_c\,(1 - \varepsilon_f) \tag{3-124}$$

3.3 Catalyst Transport System Model

Circulation of spent and regenerated catalyst is modeled as single phase flow governed by simple force balances. Factors which affect catalyst circulation in a real

FCCU, such as concentration of carbon on regenerated catalyst and aeration steam at various point in the catalyst transported line, have been ignored in this model. Because the dynamics of the catalyst circulation lines are orders of magnitude faster than other dynamic elements in FCCU system (notably the regenerator thermal dynamics), a pseudo-steady state assumption is applied to the force balances on the spent and regenerated catalyst circulation lines. The model of catalyst circulation for slide valve type is developed according to Bulsara et al. (1964).

3.3.1 Regenerated Catalyst Circulation Line

$$F_{rgc} = 96 A_{prgc} C_{sv} \sqrt{\rho_{cs} \Delta P_{rgc}} \tag{3-125}$$

where

$$\Delta P_{rgc} = P_{rg} - P_{rb} + \left(\frac{W_{sp}}{A_{sp}} + \rho_{cs} h_{rgc}\right)\frac{1}{144} \tag{3-126}$$

3.3.2 Spent Catalyst Circulation Line

$$F_{sc} = 96 A_{psc} C_{sv} \sqrt{\rho_{cs} \Delta P_{sc}} \tag{3-127}$$

where

$$\Delta P_{sc} = P_{r} - P_{rgb} + \left(\frac{W_{rs}}{A_{stripper}} + \rho_{cs} h_{sc}\right)\frac{1}{144} \tag{3-128}$$

3.4 The Catalyst Management System Model

Catalyst management in FCC process is concerned with the understanding and control of catalyst properties and movement to optimize FCC performance, therefore it is necessary to model it. As described before, all the papers relating to FCC modeling exclude this catalyst management system. Here a catalyst management system model is presented. It can be used for steady-state simulation.

3.4.1 Catalyst Deactivation Rate

The permanent deactivation of catalyst is caused by dealumination and metal poisoning. This component of deactivation cannot be recovered in the cracking reactor-regenerator system. The metal poisoning has been discussed in section 3.1.1.3. Dealumination is caused by steaming in the regenerator. The steam produces from combustion of hydrogen in coke. Zeolite catalyst deactivation can be represented by a power-law function as shown below (Johnson, 1990):

$$\frac{dA_d}{dt} = - k_d A_d^n \qquad (3\text{-}129)$$

where k_d and n vary for different catalysts. n changes between 1 and 5, depending on the type of catalyst. k_d varies with regenerator temperature and steam partial pressure according to,

$$k_d = k_{d0} P_{H_2O} e^{-\frac{E_d}{R(T_{reg}+459.6)}} \tag{3-130}$$

where

$$P_{H_2O} = P_{rg} X_{H_2O} \tag{3-131}$$

$$X_{H_2O} = \frac{0.5 F_H}{F_{air}} \tag{3-132}$$

3.4.2 Catalyst Average Activity Model

With the assumption that relative activity is directly proportional to the number of active sites on the catalyst surface and that the catalyst within the FCC system is perfectly mixed, we obtain (Lee, 1970):

$$\frac{d[A_m W]}{dt} = F_n A_n - (F_w + F_l) A_m - k_d A_m^n W \tag{3-133}$$

The catalyst mass balance for the system is:

$$\frac{dW}{dt} = F_n - (F_w + F_l) \tag{3-134}$$

Combining Equation (3-133) and (3-134), and letting

$$s = F_n / W \tag{3-135}$$

the catalyst activity equation, (3-136) is obtained:

$$\frac{dA_m}{dt} = sA_n - sA_m - k_d A_m^n \tag{3-136}$$

with the initial condition:

$$A_0 = A_m \ (t = t_0) \tag{3-137}$$

Equation (3-136) can be solved by numerical method. For constant s and A_n, and time-invariant k_d we have:

$$\int_{A_0}^{A_m} \frac{dA}{sA + k_d A^n - sA_n} = -\int_{t_0}^{t} d\theta \tag{3-138}$$

Solution of above equation for n=1 is:

$$A_m = A_0 e^{-(s+k_d)(t-t_0)} + \frac{sA_n}{s+k_d}[1 - e^{-(s+k_d)(t-t_0)}] \tag{3-139}$$

for n=2:

$$A_m = \frac{1}{2k_d}\left[\frac{1 + \beta_d e^{-\alpha_d(t-t_0)}}{1 - \beta_d e^{-\alpha_d(t-t_0)}}\alpha_d - s\right] \tag{3-140}$$

where

$$\beta_d = \frac{2k_d A_0 + s - \alpha_d}{2k_d A_0 + s + \alpha_d} \tag{3-141}$$

$$\alpha_d = \sqrt{s^2 + 4k_d s A_n} \tag{3-142}$$

As time goes to infinity, the steady-state or equilibrium catalyst activity can be obtained just for setting differential term of equation (3-136) to zero and solving the equation to get A_e. From equation (3-139) and (3-140), we have:

$$\lim_{t\to\infty} A_m = A_e = \begin{cases} \dfrac{sA_n}{s + k_d} & n=1 \\ \dfrac{\alpha_d - s}{2k_d} & n=2 \end{cases} \tag{3-143}$$

$$k_{i1} = A_{e1}\, k_{i2} \,/\, A_{e2} \tag{3-144}$$

Above two equations implies that as catalyst makeup rate, s, increases, the equilibrium activity increases, which is always less than the fresh activity of the makeup catalyst. As the activity increases, the cracking reaction rate increases, which may result in a higher conversion. However, at a high activity level overcracking may occur, producing more gases at the expense of the more valuable gasoline fraction. On the other hand the cost of makeup catalyst increases at a high activity level. Therefore, an optimal equilibrium activity level must be found. Generally, the optimal equilibrium activity level strongly depends on the quality of the feed.

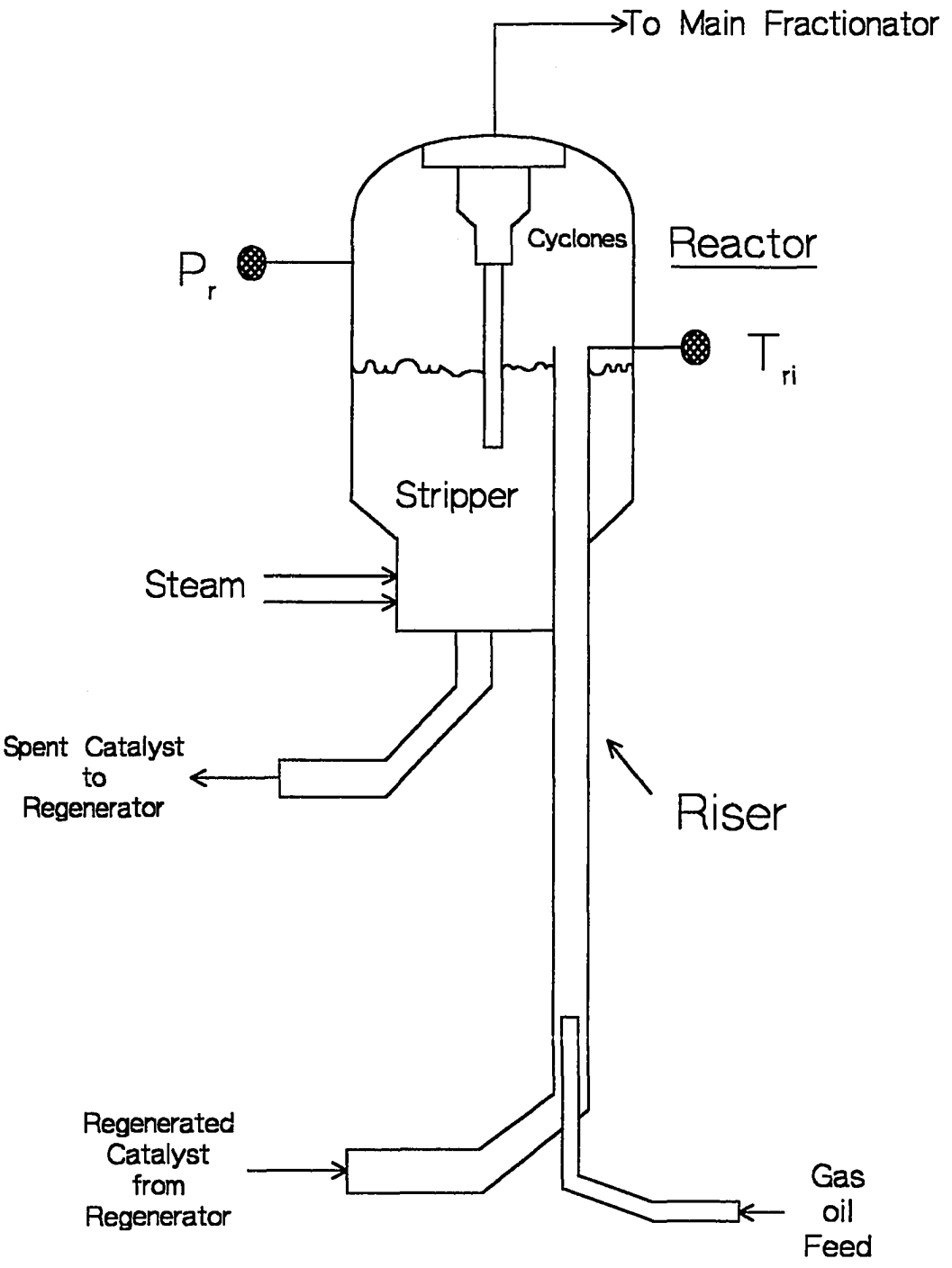

Figure 3-3. FCC Modeling - Reactor Model

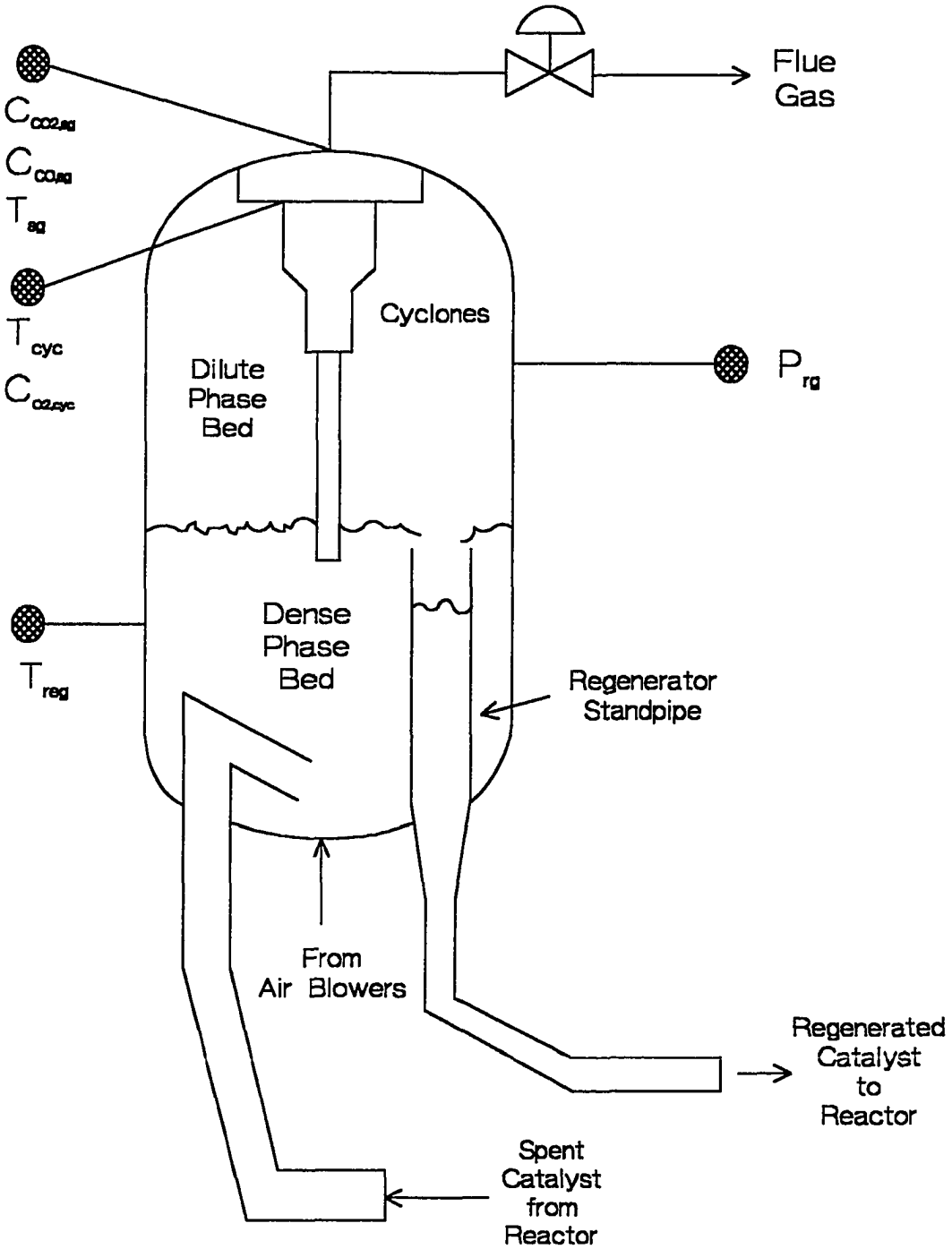

Figure 3-4. FCC Modeling - Regenerator Model

CHAPTER FOUR

MULTIPLE STEADY STATES AND INPUT MULTIPLICITIES IN FCC

For the control of a large nonlinear system, the main problems that one has to concern are stability and the potential existence of multiple steady states in the system. FCC is such a complex nonlinear system that allows one to investigate most of the problems in the control of complex process.

Knowledge of the existence of multiple steady states and other instability is essential if one wants to design a control system for any nonlinear system. It is the objective of this chapter to do so in a way that should be useful to the practitioner. In the chapter we will show that there is still a chance of five steady states in the FCC. But for acceptable operation, we need at least three. In the case of only one steady state, this state is trivial (a cold system with no conversion).

Several papers have addressed the issue of stability and the possibility of multiple steady states [Iscol (1970), Lee and Kugelman (1973), Elnashaie and El-Hennawi (1979), Seko (1982), Edwards and Kim (1988), Elshishini and Elnashaie (1990), Arandes and de Lasa (1992), and Hovd and Skogestad (1993)]. None, however, have addressed these issues in a thorough theoretical way or investigated the impact of design, operating conditions, and catalysts on the existence of multiple steady states and instabilities.

Before going to a quantitative evaluation of multiple steady states and a discussion of the effects of various operating conditions and control designs on the system stabilities, we will depict briefly the steady-state simulation for finding the operating map. This should be a useful guide for using our model.

4.1 Steady-State Simulation

The FCC model in Chapter three was used to find the steady-state points in the typical input conditions just setting the dynamic terms, i.e., the terms of time derivative in dynamic equations to zero. Some operating conditions were kept constant in this simulation. Among them were pressures of reactor and regenerator, catalyst holdups in reactor and regenerator, air inlet temperature, feed rate, feed composition and so on. Catalyst cooler are not active in the simulation.

FCC operates about atmospheric pressure which does not allow to vary too much. Furthermore, the pressure control on both the regenerator and the reactor is assumed to be fast enough, so the pressure in both can be taken as constant.

In steady-state operation, the circulation rates of the spent and the regenerated catalysts are the same each other. Therefore, the catalyst holdups in both the reactor and the regenerator are invariable. we assumed that the catalyst holdups were kept at the same level throughout the steady-state simulation.

Table 4-1 shows some typical operating conditions for this steady-state simulation. Table 4-2 gives a feed composition in the simulation which was adopted from Jocob et al. (1976). Some feed compositions can also be obtained from Nace et al. (1971).

The model has been translated into the FORTRAN code. This becomes easy for computer simulation. For numerical reasons, plug flow riser and gas flowing in regenerator were approximated by four different CSTRs in series. Adding more CSTRs did not almost change the results.

Table 4-1. Typical Operating Conditions for Steady-State Simulation

Feed Flowrate F_{tf} = 131 lb/s	Base Case: Feed Temperature T_f = 670 °F
Oil Gas in the Riser y_{oil} = 1	Air Inlet Temperature T_{air} = 270 °F
Regenerator Pressure P_{rg} = 29.6 psia	Regenerator Holdup W_{reg} = 2.74×10^5 lb

Table 4-2. Feed Composition (From Jocob et al. 1976)

Lumping Component	wt % (wt/wt feed)	Lumping Component	wt % (wt/wt feed)
Ph	17	Pl	14
Nh	20	Nl	8.5
Ah	24	Al	2
Rh	12.5	Rl	2
G	0	CCR	0

4.2 Steady-State Multiplicity

The steady-state multiplicities and stabilities of the FCC system have been studied here under the certain conditions of fixed feed rate, feed temperature, feed composition, catalyst activity, and/or air flow rate and catalyst circulation rate. All these

conditions can be independently manipulated. The mechanisms that make multiple steady states in the FCC are also discussed in this section.

4.2.1 Outline of the Problem

Although there are quite a number of different designs, The FCC's still share the same features. The simplest FCC (see Figure 4-1 for a schematic description) has a reactor in which hot catalyst is contacted with cold oil leading to the formation of cracked liquid products, gases and oil. The catalyst will coke and it is then burnt with air in a second reactor, known as a regenerator. The regenerated and now hotter catalyst is then recycled again to the reactor. This is a totally adiabatic system.

Most of modern FCC's are equipped with a feed preheater that allows to set feed temperature either at a fixed set point or, coupled by a feedback controller, to maintain reactor temperature. However, the feed temperature must be kept below 800°F to prevent coking in the tubes of the preheater (Avidan and Shinnar, 1990).

All the FCC's are autothermic and require heating during startup. As a result all FCC reactors have multiple steady states in the classical sense just like any combustor. There is always the possibility that, by improper operation, the FCC will wind down to a "cold" steady state, which is always unconditionally stable regardless of the degree of preheat. In current design, as the feed can not be preheated high enough to achieve self-ignition, a start-up burner is required. Therefore, if there is only one stable steady state, it has to be the cold one which is a trivial case. Whenever there is a useful nontrivial or, in other words, hot steady state, there are always at least three steady states, one of which

is open loop unstable. It is therefore important to know at which operating conditions the hot steady state is stable and how changes in process conditions affect stability. It is quite possible for an operator to change operating conditions in such a way that the upper steady state is lost and the unit winds down.

In many cases, there are not sufficiently accurate models to quantify the stability boundaries exactly, but most operators know from experience how to choose the operating conditions and how to reverse a wind-down. However, for design of control systems we need a more thorough understanding of these stability limits, which we will try to provide here.

Steady-state multiplicity in the FCC operation has been discussed in the literature. However many papers could not define the meaning of multiple steady states clearly. For example, Lee and Kugelman (1973) discussed the stability of FCC reactors showing that for their operating conditions the system was linearly stable. They gave an example for one unstable steady state without pointing out that this was simply the intermediate unstable steady state that existed for all FCC operation. Their unstable case had a conventional stable steady state at a higher temperature. Our results in steady-state simulation show that operation at an open-loop unstable steady state could occur at reasonable operating conditions. Furthermore, close to the stability limits the unstable and the stable steady states converge. In this chapter we will discuss both the conditions needed for three steady states and the potential for more than three ones.

Before going into a quantitative formulation of the problem let us rephrase the stability problem from the view of the operation. If the FCC has only one steady state, it is in low temperature and therefore trivial. The first question and maybe the most

difficult one is therefore that can the operating conditions chosen lead to a high temperature steady state? In other words, are the control settings chosen permissible in the sense that they lead to an upper steady state? If not, the system will wind down. The control settings which are permissible can easily become non-permissible if the catalyst deactivates or the feed composition changes. An unstable steady state is less of a problem as one can in principle stabilize it by feedback control. However, the controller tuning might not be suitable to that task. It is therefore essential that understanding the probability of choosing controller settings that lead to an unstable steady state.

For the operator it is also essential to know if one of the high temperature steady states is economically useful in terms of conversion and product qualities. Furthermore, it cannot violate system constraints such as maximum temperatures or gas make. Excessively high temperatures in the cyclones or in the riser will violate metallurgical constraints, and high gas make could cause the wet gas compressor to trip. A detailed discussion of these problem is outside the scope of this work, but it will be shown how one takes this into account.

4.2.2 Definition of Steady-State Multiplicity

Steady-state multiplicities include output multiplicities and input multiplicities. The so-called output multiplicity means that when the system is under open-loop operation, i.e., fixed inputs, multiple equilibrium points can be obtained.

The FCC process always operates with at least some variables in dynamic feedback. For this case, depending on the control scheme used, there is a potential for

input multiplicities, in which several steady states are consistent with controller settings. In brief, input multiplicity means that more than one input values give an identical output.

4.3 Steady-State Operating Map

This section will present the quantitative results of steady-state simulation. The stability of the system is studied by varying air flow rate and catalyst circulation rate at different catalyst properties, feed rate and composition and temperature. The steady-state performances under partially closed-loop operation are also studied here.

4.3.1 Output Multiplicity

To understand the output multiplicity of the system, let us now look at a typical example (Figure 4-2, Case a). Here all input conditions are fixed. Three heat equilibrium points are definitely seen from the figure*. The conditions for this case are summarized in Table 4-3.

When the catalyst circulation rate increases or decreases to some extent, the stable and unstable points converge (see Figure 4-2, Case b and c). These points are obviously stability limits. Beyond these points the system will wind down to the cold steady states. Because the cold steady state is meaningless for operation, we have to prevent it happens in normal operation.

**The lower stable steady state, i.e., "cold" steady state, SS1 is at too low a temperature for the model to predict, and therefore missing.*

Table 4-3. Simulation Conditions for Case a in Figure 4-2

Simulation Condition	Stable Steady State (SS3)	Unstable Steady State (SS2)
Air/Oil, wt/wt	0.55	
Cat/Oil, wt/wt	5.6	
Feed Temperature, °F	670	
Regenerator T_{reg} , °F	1274	1173
Reactor Riser T_{ri} , °F	993	953

FCC is a more complex system. There s an interaction between the regenerator and the reactor since the amount of coke gen ated depends on the reactor temperature and therefore on the regenerator temperature.] ius, it requires investigating the stability of each steady state. Table 4-4 gives the eige values of the different steady states in Figure 4-2 Case a (a linearized FCC model for determining the eigenvalues is given in Appendix A). It is noted that the behavior is ide tical to the case described in the figure.

Table 4-4. Eigenvalues of the Steady States in igure 4-2 Case a

Stable SS3	-2.566×10^{-4}	-7.821×10^{-3}	-9.797×10^{-3} $+6.138\times10^{-3}i$	-9.797×10^{-3} $-6.138\times10^{-3}i$
Unstable SS2	1.383×10^{-4}	-9.079×10^{-3} $+5.909\times10^{-3}i$	-9.079×10^{-3} $-5.909\times10^{-3}i$	-7.785×10^{-3}

4.3.1.1 Stability of the base case

In this case, feed temperature is kept at 670°F, and feed and catalyst properties are in normal operating state. As we will show, in a nonlinear system like an FCC only certain combinations of inputs are permissible. Now we have to define what permissible means. Obviously, any physically reachable combinations of inputs, F_{air} and F_c are permissible. However as Figure 4-3 shows, only a limited range will lead to a stable hot steady state (One can see from the figure that there are a maximum and a minimum catalyst circulation rates for which hot steady states exits). Beyond the range, the system can only stay in cold steady state. Therefore the range in which the stable hot steady states exist is permissible for operation. In fact the catalyst circulation rate is not directly adjusted as an input but via a control circuit in which riser top temperature adjusts the position of the slide valve in regenerated transported line (see Chapter three, section 3.3 and Figure 1-2). However for simplicity, one can still take it for an input.

Figure 4-3 also shows some important regenerator and riser top temperature isoclines. From these lines, one can easily find the normal operating range in the FCC.

The region of multiple steady states in Figure 4-3 was plotted as a function of manipulated inputs, air rate and catalyst circulation rate. While this is the conventional way to represent stability maps (fixed inputs) in the chemical reaction engineering literature, the operator thinks more in terms of the set points he uses for control. Figure 4-4 shows a permissible operating range using two key process variables, T_{reg} and T_{ri}. This answers the question what combination of setting for T_{reg} and T_{ri} will give a unique hot stable steady state. One may also use other controller settings such as the temperature

difference across the regenerator cyclones but we here suffice ourselves to give the limit of operability in terms of T_{reg} and T_{ri}. The figure also shows the unstable steady-state range but the open-loop unstable steady states are less desirable in operation while they are permissible and can be stabilized.

There are other limitations, e.g., air rate, catalyst circulation rate, wet gas compressor and so on, on permissibility in real plant operation. Figure 4-4 also gives some air/oil and cat/oil isoclines for easy determination of these operating limitations.

With present catalyst and operating conditions one is more likely to deal with constraints than inherent instability. Units mostly operate close to maximum air rate. Therefore, for a given steady state [T_{ri}, T_{reg}] if the air rate required becomes higher than existent maximum one due to perturbations, there is no operable stable high temperature steady state. Similarly, the permissible steady state cannot exceed wet gas compressor limits or otherwise the compressor will trip. So the constraint protection or a sufficient safety limit is needed. Figure 4-5 gives the wet gas yield (C_4^-) as a function of regenerator and reactor riser temperatures for one to know how to release the constraint by changing riser temperature. One could plot all these constraints in Figure 4-4 but this is strongly unit dependent. Again, Figure 4-6 should be a useful guide for one to see how he can use riser temperature to remove constraints. Figure 4-7 shows the lines of constant conversion to indicate the useful range. The outer bounds in the figure are identical to Figure 4-3.

Constraints like F_{air}, F_c, and wet gas compressor are strong function of the feed rate. Therefore, we can move them by either increasing or decreasing feed rate. The catalyst activity and the coking rate are also controllable inputs, and affect these constraints.

4.3.1.2 Impact of catalyst activity on stability

The catalyst activity can change intentionally or unintentionally due to catalyst management. It can affect the steady-state operation although its changes are slow compared to dynamic responses of the unit due to changes in air rate or catalyst circulation rate. Figure 4-8 shows the effect of the catalyst activity on permissible stability limit. As one can see from the figure, the three-steady-state range becomes narrower if the catalyst activity decreases. Conversely, it will become wider. This happens because catalyst activity changes cracking reactions thus coking rate which strongly affects the heat balance in regenerator.

The changes on stability caused by catalyst activity remind us that we have to change input conditions lest the system winds down when the catalyst deactivate during the operation. But the question is that can the controller settings, e.g., [T_{ri}, T_{reg}], keep the same level no matter how changes in catalyst activity? Figure 4-9 describes that if the catalyst activity decreases 30%, some stable settings in base case still stay in stable region [980°F, 1240°F] but some will fall into unstable region [980°F, 1150°F], some are even unfeasible [980°F, 1280°F]. Therefore, it is important that the catalyst makeup rate should be adjusted with its deactivation rate.

4.3.1.3 Impact of coking rate on stability

For the operator, another problem, i.e., feed property, relating to stability is more important than the catalyst activity because feed changes can be fast. The changes in feed

property can alter the coking rate in two ways: i) the intrinsic coking rate; ii) addition of resid which can introduce a different type of coking (Conradson carbon), where the amount of additional coke formed is independent of catalyst activity or Cat-to-Oil ratio (see Edward and Kim, 1988). Furthermore as mentioned before, the catalyst activity could also change coking rate. Here we only discuss the effects of intrinsic coking rate on stability map.

Figure 4-10 shows the change of permissible stability range with 30% increase in coking rate. As we expect, the three-steady-state range becomes wider. Figure 4-11 gives the permissible operating map using two key process settings, T_{ri} and T_{reg}. Again, we see the wider stable range. Therefore, we note that lowering the coking rate may cause the system wind down as no high temperature steady state is feasible at this operating temperature.

Figure 4-12 shows the impacts of coking rate and catalyst activity on feed conversion and regenerated coke content on catalyst respectively, in order to let one understand thoroughly how these two perturbations affect the system performance.

4.3.1.4 Impact of feed temperature on stability

One of very important variables is feed preheat temperature. Most units today are equipped with feed preheaters. In fact the feed temperature is not really an input, but a setpoint for the feed furnace control. The inputs to that furnace are oil feed rate, fuel rate and air rate to this furnace. However, we can still take the feed temperature as an input because the response in preheater is relatively fast compared to the FCC.

Figure 4-13 shows the effects of feed preheat temperature on operating stability map. It is noted that feed preheat temperature strongly reduces air requirements at the expense of conversion. It is therefore a prime tool in optimization strategies. From Figure 4-14 we can see that at T_f = 500 °F (one may consider this temperature as no preheat furnace) most of relevant operating temperature range fall into unstable region.

Figure 4-15 shows the impacts of feed temperature on feed conversion and regenerated coke content. we find that there is a big effect on conversion but almost no change on regenerated coke content when feed temperature changes from 670 to 500°F.

4.3.1.5 Impact of CO combustion promoter on stability

In complete CO combustion, one could use promoter. One also often uses them in partial CO combustion at high values of regenerator temperature. Promoters were initially introduced to eliminate the need for CO boilers. Although there are a disadvantage just mentioned in Chapter two, using the promoter has still some advantages. Even in limited promotion, the promoters reduce or eliminate the chance of five steady states and therefore guarantee that the operating points are stable (this will be described in section 4.4). They also improve operability as they eliminate or reduce the problem of hot cyclones due to local maldistribution.

To understand the effects of CO promoter on operating stability map, Figure 4-16 was plotted. Here we gives two levels of promoter defined by the rate of heterogeneous catalytic CO combustion relative to the unpromoted case. Unpromoted FCC catalyst also promotes the CO combustion (Weisz, 1966) but at a low level. The promoter containing

small levels (ppm) of platinum can increase this base rate by a factor of up to 100. It is noted that three-steady-state range increases as the level of promoter increases. Therefore when someone operates an FCC in lighter feed or lower catalyst activity, he can consider using a promoter to ensure the operation in hot stable steady state. Figure 4-17 gives the permissible operating range. Again, we see that the stable range becomes wider but the maximum regenerator temperatures are unchanged.

There is a penalty one pays for the use of promoter in partial combustion. Conversion is reduced. This can be seen from Figure 4-18, where conversion and C_{rgc} versus T_{reg} are plotted.

4.3.2 Input Multiplicity

This section discusses the existence of input multiplicity in the FCC. Nonlinear system like the FCC besides multiple steady states can also have input multiplicities. As the system has many state variables, keeping a limited number constant by control does not mean that the system has a unique steady state. Furthermore if one chooses two measured variables for a 2×2 dynamic matrix, there may be different combinations of the two manipulated inputs that give the same results in two controlled variables. Koppel (1982, 1985) called this an input multiplicity and Morari et al. (1982, 1985, 1988) investigated their properties.

The problems of input multiplicity always appear in the closed-loop system. The potential for input multiplicities is an important factor when considering the choice of the dynamic control matrix. Therefore, input multiplicities is really a problem of the design

of control matrix while some of them have properties and implications similar to multiple steady states.

4.3.2.1 Input multiplicity in two typical cases

In the cases, catalyst and feed properties, feed rate and temperature, etc. are fixed in a normal status just the same as those mentioned in 4.3.1.1. Figure 4-19 gives the possible steady states at the case of fixed air rate but varying catalyst circulation rate. This is a practical control case (fixed T_{ri} and F_{air}) today since many units try to operate at maximum air. In the figure, open-loop stability is indicated. There is a range of T_{ri} and T_{reg} for which a steady state exists. In the range, we can always find two catalyst circulation rates giving the same T_{ri} but with different T_{reg} (for example, point A and B). While both are open loop stable, one cannot find a linear controller with integral action controlling T_{ri} by changing F_c because the steady state gains of the controllers have opposite signs. One would normally design a controller for point A which is in partial CO combustion, but would not operate with that controller at point B which is in full CO combustion.

Edwards and Kim (1988) described such a case that a system operating in partial combustion drifted to another steady state when the controller controlling T_{reg} by manipulating F_{air} was put on manual temporarily. The reason for the drift is that when both loops are closed, the gain used for tuning the controller in riser is positive under constant T_{reg} (see Table 4-5). When air control is put on manual the gain becomes negative and the control loop with integral action becomes unstable at point A, and thus

either drifts to point B or leads to wind down.

Let us look at the reverse case where T_{reg} is controlled by air rate and catalyst circulation rate is fixed, i.e., fixed T_{reg} and F_c. This happens in the old Model IV FCC units in which the catalyst circulation rate is fixed or can only be dynamically varied over a narrow range. A wider variation requires change in the catalyst inventory and is therefore only part of the slow control.

A plot of multiple steady states for the similar conditions as in Figure 4-19 is given in Figure 4-20 for constant F_c. Again for a given pair [T_{reg}, F_c] there are two possible values of F_{air} and T_{ri} (point A and B). Therefore for both cases, specifying [T_{ri}, F_{air}] or [T_{reg}, F_c] does not specify a unique steady state.

Table 4-5. Open and Close Loop Performances with Perturbation

Base Case Condition		T_{ri} = 1000 °F; T_{reg} = 1250 °F; Cat/Oil = 6.47; Air/Oil = 0.58					
Perturbation		Relative Coking Rate		Relative Cat Activity		Feed Temp. Change	
Variable Change		0.8	1.3	0.7	1.3	-30 °F	30 °F
Open-loop Output Change	ΔT_{ri}, °F	-23	9	5	-6	-39	25
	ΔT_{reg}, °F	-33	7	5	-8	-52	23
Close-loop Input Change	ΔCat/Oil	0.13	-0.20	-0.09	0.03	0.35	-0.37
	ΔAir/Oil	0.014	-0.015	-0.005	0.007	0.032	-0.033

4.3.2.2 Impact of catalyst activity and coking rate on input multiplicity

Figure 4-21 shows a wider range with increasing coking rate or catalyst activity, or a narrower range with decreasing them at constant F_{air}. But input multiplicity still exists. It also shows that for fixed catalyst circulation rate one can lose the upper stable steady state by either losing the catalyst activity due to insufficient catalyst addition and withdrawal or by getting a feed with a lower coke making tendency.

4.3.2.3 Impact of feed temperature on input multiplicity

Figure 4-22 gives a plot of the effect of feed temperature on steady states at constant F_c. It shows a wider range with increasing feed temperature. Input multiplicity certainly exists.

4.3.2.4 Impact of CO combustion promoter on input multiplicity

Figure 4-23 shows the effect of CO promoter on steady states at constant F_{air}. Again, the wider ranges are obtained as the amount of promoter rises in addition to existing input multiplicity.

4.3.3 Multiplicity under Partially Closed-loop Operation

When people discussed the local controllability for one of the useful steady state,

they could start with [T_{reg}, T_{ri}] and do this by giving a plot of T_{reg} and T_{ri} as a function of air rate and catalyst circulation rate keeping the other input constant. This is hard to do as it requires a four dimensional plot. In most cases the priority is given to reactor temperature control. Therefore from the isocline of constant T_{ri}, it is sufficient for a two dimensional plot using air rate as the abscissa and T_{reg} as ordinate. The question now appears to us that does the system still have steady-state multiplicity at totally or partially closed-loop operation (fixing T_{ri} by F_c and/or T_{reg} by F_{air})? In general, this is one of the most important questions one has to ask when controlling the complex systems. The question will be answered by the Figure 4-24. When multiplicity is discussed under partially closed-loop FCC operation, the input multiplicity definitely exists in the close-loop side. Therefore, the multiplicity under partially closed-loop belongs to the scopes of input multiplicity in a sense.

4.3.3.1 Multiplicity in base case

Figure 4-24 gives a plot of T_{reg} versus air rate for three isoclines of T_{ri}. The open-loop stability of each steady state is indicated in the plot. From the plot it can be seen that there is a unique steady state for a given consistent set [T_{ri}, F_c, T_{reg}, F_{air}]. If Air rate is fixed and T_{ri} is kept constant by manipulating F_c, two regenerator temperatures can reach this goal. Two or one of them are stable hot steady states. If T_{ri} and T_{reg} are fixed (by feedback control), there is a region of input multiplicities close to maximum T_{reg}. Two pairs of [F_{air}, F_c] give the same [T_{reg}, T_{ri}] which is stable high temperature steady state. However as the steady-state gains have opposite signs, a linear controller with integral

action is only stable for one of these states depending on how one choose to set it.

In maximum T_{reg} region or close to complete CO combustion, T_{reg} is not a suitable control variable as the gains are close to zero. One can use excess oxygen control. Actually, the region of multiplicities is theoretically larger than plotted. At very high air rates, large values of excess air can make a T_{reg} at a stable steady state significantly lower than maximum T_{reg}. As one always operates FCC close to maximum air rate, these are unreachable steady states and can be disregarded in a real system. Therefore for most of region, a set value of [T_{ri}, T_{reg}] will completely determine the system.

For control system design, it is noted that there are two regions in Figure 4-24 where the system is locally uncontrollable. One is maximum regenerator temperature at which the slope is zero. The other is minimum air rate at which the slope is infinity. At the zero slope point, the system is controllable by measuring excess oxygen while close to the region of infinite gain the system is not controllable locally with the air rate and the catalyst circulation rate. We need here another manipulated variable such as the feed temperature. Luckily there is no special advantage to operating in that area.

T_{reg} as a function of air rate has one interesting property which is counter intuitive. In the partial combustion region (lower T_{reg}), T_{reg} decreases with increasing the air rate under close loop of T_{ri}. But the opposite is true under open loop of T_{ri}, or fixed the catalyst circulation rate (see Figure 4-20). Both T_{reg} and T_{ri} increase with increasing the air rate. This difference in response is caused by the fact that T_{ri} is controlled closely. If T_{reg} decreases, F_c has to increases at constant T_{ri}. Increasing F_c will generate more coke. The only way that more coke is burnt is to increase air rate. Conversely, if T_{reg} increases, F_c decreases and therefore coke make decreases requiring less air for combustion. At

higher T_{reg} the CO_2/CO ratio increases supplying the required heat with less air and coke. If F_c is constant, higher T_{ri} will generate more coke.

Figure 4-24 also shows that there is an open-loop unstable steady state at T_{reg} below 1180°F with T_{ri} = 950°F. The stability will therefore strongly depend on controller tuning. Maximum regenerator temperature becomes lower as riser top temperature lower.

4.3.3.2 Impact of catalyst activity and coking rate on multiplicity

Figure 4-25 gives a plot of air rate versus T_{reg} for different levels of coking rate and activity at constant T_{ri}. It indicates how catalyst activity and coking rate can be modified to move T_{reg} in the desired direction. Output and input multiplicities are still maintained. It is noted that the maximum T_{reg} moves strongly when either activity or coking rate change. This has implications when one operates in full CO combustion or close to the maximum value of T_{reg} in partial combustion. Close to maximum T_{reg}, the controller is not robust and this has to avoid.

For a 30% increase in either catalyst activity or coking rate, the system remains stable. Air rates at constant T_{reg} and T_{ri} were almost constant for the increase in activity and decreased for an increase in coking rate. But if the catalyst activity decreases by 50%, the changes are dramatic. As expected, maximum T_{reg} decreases but the air rate increases significantly. More importantly, all steady states are open loop unstable. Reducing coking rate has even a stronger effect. There is therefore a range of activity and coking rate for which the control is not robust at this riser temperature. Increasing riser temperature would allow some stable steady states.

4.3.3.3 Impact of feed temperature on multiplicity

The effect of feed preheat temperature is given in Figure 4-26. Again, we can see that it strongly reduces air requirements but output and input multiplicities are still maintained. At 500°F of T_f, the system becomes open loop unstable at T_{reg} below 1230°F while T_{ri} is kept at 1000°F. The maximum regenerator temperature is the same in both feed temperatures.

4.3.3.4 Impact of CO combustion promoter on multiplicity

As mentioned before, one uses promoters for complete CO combustion. To understand their effects, Figure 4-27 was plotted. Here, two levels of promotion was given. It is noted that for both levels of promotion, output and input multiplicities are still maintained. However, the steep region of T_{reg} with air rate increases. It is concluded that when one wants to use full promotion at lower T_{reg}, he can use a lower activity catalyst to reduce maximum T_{reg}.

4.3.3.5 Impact of CCR on multiplicity

Until now we only investigate the stability performances in the FCC under absence of Conradson Carbon Residue in feedstock. However, in present operation the resid is often directly added to the FCC. The CCR on the resid to a great part deposits directly on the catalyst almost independent of activity. As the CCR can affect the heat balance of

whole system, we have to investigate how it change the operable space.

CCR on resid can go up to over 20% of feed. If its amount deposited on the catalyst exceeds about 5 to 6%, one cannot balance heat of the unit in the range of air rates given in our plot because there are not enough air to burn it. However much before that, the conversion would become so low that operation is not economically practical.

One can always find the operating conditions where one can get a stable hot steady state with any level of CCR, but this is not of interest. However as low levels of CCR are common, we give a plot in Figure 4-28 for the cases with up to 2% CCR at constant T_{ri}. From the Figure, it can be seen that T_{reg} increases with increasing CCR at complete CO combustion region and decreases at partial CO combustion region. This happens because C_{rgc} increases with increasing CCR at the same air rate. There is one point that all levels of CCR give the same T_{ri}, T_{reg} at the same air rate. However, CO_2/CO and conversion decrease definitely with increasing CCR, and C_{rgc} increases.

4.4 Possibility of Existence of Five Steady States in FCC

Till now, we have discussed the three steady states existed in the FCC. The question now is if the FCC has more than three steady states. To answer this question, we have to investigate thoroughly the mechanisms for which multiple steady states occur.

4.4.1 Sources of Five Steady States

Let us first look at the reactor side. Cracking with simultaneous formation of coke

is an endothermic reaction. Most modern crackers use a riser reactor, in which the catalyst is mixed with gas oil at the bottom and the cracked products lift it through the reactor at high velocity. In modeling, such a riser reactor is often approximated as plug flow. In reality, there is a backmixing at the bottom and also some backmixing in the riser itself due to catalyst slip. Viitanen (1993) had studied the performances of an FCC riser reactor.

While there are endothermic catalytic reactions that lead to multiple steady state in stirred tank, these have more complex kinetics than those occurring in catalytic cracking. As cracking has a Langmuir type of kinetics, the reactions are close to pseudo first order which should not give rise to multiplicities. All we can say is that we are not aware of any experimentally observed multiplicities for cracking reactions with current cracking catalysts.

The other reaction occurring in the reactor is coke formation. Coke formation is actually the only reaction in the reactor important to the stability of the overall system as it ties the reactor and regenerator together.

Coke formation could in theory give rise to more than three steady states in two ways. One results from the interaction between coke formation in the reactor and coke combustion in the regenerator and the other could occur if the kinetics of coke formation is such that multiple steady states can exist in the reactor at constant inlet composition. There is no evidence for the latter. The kinetics of coke formation are normally described adequately by a relation first suggested by Voorhies [1945] (see Equation 3-33). However, this kinetic expression does not lead to multiple steady states in an endothermic reactor. We therefore have to focus our attention on the two remaining possibilities, high temperature multiplicities caused by the kinetics in the regenerator and those caused by

the interaction of coke combustion and formation via temperature and catalyst properties.

There are two potential reasons for multiplicities in the regenerator itself. One is due to mass transfer and the other is due to heat transfer. Any simple heterogeneous exothermic reaction can have more than three steady states due to mass transfer and heat transfer limitations. This happens in single catalyst particles or in different temperatures for the mixed solid phase and the gas phase. Elnashaie and Yates (1973) have published a paper showing such a possibility using a two phase model for the fluid bed reactor.

Two phase models (see Figure 4-29) have been extensively discussed in the literature [Kunii and Levenspiel (1969), Errazu et al. (1979), Elnashaie and El-Hennawi (1979), Lee et al. (1989), Arandas and de Lasa (1992)]. They describe well certain aspects of reactions in the fluidized beds at low gas velocities which leads to a regime of well established bubbles. But there are several problems of using such a model for our case.

First, the two phase model only describes some overall steady-state properties. In the bubble regime a fluidized bed reactor is a highly stochastic system, and the classical two phase model does not describe this dynamic behavior. Using it for computing instabilities is therefore quite meaningless.

Second, there is a more fundamental problem that makes multiple steady states due to transport limitations highly unlikely in an FCC. For such states to exist mass and heat transfer resistance have to be of the same order of magnitude. In fact Elnashaie (1977) assumed that they are equal. In an FCC heat transfer is much more rapid between the two phases than mass transfer. On the surface of catalyst particles heat and mass transfer occur by similar mechanism (Schmidt number close to unity). Even in a bubbling fluid bed far from incipient fluidization, the heat transfer is much larger than mass transfer as the

mechanisms are totally different. Solids showering through the bubble have sufficient heat capacity to give a large effective coefficient of heat transfer between the bubble phase and the so-called emulsion phase. What has been reported (Ross et al., 1981, 1982) is excess temperature for single burning particles. Furthermore, Ross et al. show that this requires a high oxygen concentration which only exists in the bottom of the bed.

While some fluid beds with fast reactions have excess temperatures near the bottom, there has never been a report of an industrial fluid bed with a temperature difference between the bed and the gas just above it. The excellent temperature uniformity of fluid beds is the main attraction for exothermic chemical reactors. FCC regenerators are always in the turbulent flow regime (Sapre et al., 1990), where mass transfer rates to the emulsion phase are also high. Therefore, the so-called emulsion phase is unlikely to lead to multiplicities.

The only mechanism that we are aware of that could lead to five steady states in a regenerator are consecutive exothermic reactions. In this reactions five steady states are feasible if the second reaction requires a significantly higher temperature, as can be seen from Figure 4-30 (UOP data from Upson et al., 1993). The combustion reactions in the regenerator are known to have consecutive feature. When coke burns at the surface of catalyst, the reaction leads to a mixture of CO and CO_2, the ratio of which is a function of temperature only (see Equation 3-74 from Arthur, 1951). However, CO will react with oxygen further to give CO_2 at the operating temperature range of regenerator. In partial CO combustion operation of the regenerator, the ratio of CO_2 to CO in flue gas is close to unity (see Figure 4-31).

This secondary reaction has a strong impact on the dynamic behavior and stability.

We therefore need understand it. It is the only kinetic process that, so far as we know, with present catalyst five steady states could occur. The word "could" is stressed as there is no evidence of their existence, and our imperfect knowledge about the kinetic processes does not allow reliable predictions. This can be done in the future but now only the kinetic nature of the processes is being discussed. In many processes the accurate kinetic information is lacked but we have enough laboratory data and approximate qualitative understanding of the process to judge if multiple steady states are feasible and what their nature would be. This is important for designing and controlling complex processes with limited model information.

The CO to CO_2 reaction occurs in two parallel kinetic pathways: one by heterogeneous catalysis, the other by homogeneous combustion. One or two of the reactions can make five steady states theoretically in FCC operation.

Regular FCC catalyst has a limited catalytic activity (Weisz, 1966) which has been included in our model. Metals deposited from feed (such as nickel and vanadium) are also catalytically active though the effect is normally small. Addition of CO combustion promotor in catalyst can lead to full CO to CO_2 combustion even at temperatures of 1200°F below. This subject has been discussed before. However, as the catalytic CO combustion rate and activation energy of catalytic CO combustion are low (about the order of 20 kcal/mol, Prater et al., 1983), this should not give rise to five steady states.

CO combustion to CO_2 also occurs as a homogenous reaction in the gas phase. Truly homogeneous CO combustion has an activation energy around 70 kcal/mol and is fast at temperatures of 1200°F. However, almost any surface has a strong inhibitory effect on the homogeneous CO combustion. This has definitely a strong impact on the FCC

operation. In partial CO combustion if there is any O_2 left in the gas, the flue gas will ignite after first cyclone the moment the catalyst is removed from the gas. To ensure complete solid removal two or three cyclones are used in series. This ignition occurs despite the fact that the adiabatic temperature rise after the cyclones is often small (< 100 °F) and the residence time very short (< 0.5 second) compared to the residence time in the dilute phase of the regenerator of 20 to 30 seconds.

At lower temperature (< 1050°F) afterburn does not occur, but this is below the temperature range of the FCC. This afterburn has to be paid attention to the FCC operation in partial CO combustion as one has to ensure that excess oxygen is low to prevent damage to the cyclones.

The existent of inhibition surfaces of the homogeneous CO to CO_2 reaction is due to interception of the free radicals that promote the homogeneous combustion rate. With increasing temperature the mean free pathway of a free radical decreases, and the inhibition becomes less effective. Above 1400°F, homogeneous CO combustion is quite fast even in the presence of catalyst particles. In the past even without CO promoters some units were working at full CO combustion between 1300°F and 1350°F (Avidan and Shinnar, 1990).

The problem is however that it is extremely difficult in small laboratory units to get detailed kinetic data on homogeneous CO combustion in the presence of solids. The wall itself can inhibit the homogeneous reaction and like the FCC catalyst simultaneously catalyze the reaction by heterogeneous catalysis. Even the data for the heterogeneous combustion of CO promoted by the regular FCC catalysts such as Weisz (1966), are affected by the simultaneously occurring homogeneous reaction. Furthermore, inhibition

also depends on the amount of catalyst present or in the case of an empty tubular reactor, the diameter of the tube and the material of the tube wall.

Due to the difficulty of such experiments under laboratory conditions, there is a lack of reliable detailed data to get an exact kinetic description of the takeoff phenomenon. The most relevant data published from UOP (Upson et al., 1993) are given in Figure 4-32. To see the temperature dependence better we give the rate as a function of temperature (ln r versus 1/T) in Figure 4-33. We note the change of the slope in this type of reactor. The apparent activation energy could reach 500 kcal/mol.

Figure 4-32 gives the homogeneous rate in both the presence and the absence of the catalyst. Both plots show a similar form the only difference being that the curve for the catalyst is transposed to a higher temperature. What is called the homogeneous combustion in Figure 4-32 by the authors is really combustion inhibited by the wall of the reactor as the rates have a magnitude lower than observed for homogeneous combustion in afterburn. But the data clearly show that the reactor even in the presence of the catalyst has the potential of a strong increase in the rate over a narrow temperature range giving the feature that could lead to multiple high temperature steady states. What we lack are reliable data for the exact temperature of the takeoff under different conditions, and oxygen and catalyst concentration. Such takeoffs are hard to model by using apparent activation energies.

The takeoff occurs under condition of fast homogeneous CO combustion rate and higher reaction heat of CO to CO_2. The reaction heat for burning CO to CO_2 is 2.6 times as large as the reaction heat of formation of CO for burning coke (see Table 4-6) so it could give rise to five steady states.

Table 4-6. Formation Heat of Carbon Monoxide and Carbon Dioxide

Combustion Reaction	Carbon to CO	Carbon to CO_2	CO to CO_2
ΔH_f (Btu/lbmol carbon)	46,368	169,080	122,712
ΔH_f (Btu/lbmol oxygen)	92,736	169,080	245,424

Before a quantitative evaluation of the five steady states, we would like to discuss what happens if there is a chance for five steady states. Here, the limits of the region for no hot steady state is not changed. Only change is that a given setting at higher temperatures may now suddenly become an open-loop unstable intermediate steady state (the fourth out of five). As the FCC's are very seldom operated in complete open loop, there are no data that prove the existence of five steady states. Edwards and Kim (1988) claimed that they had observed two stable hot steady states in an industrial FCC. They found that a stable steady state in partial combustion of CO at a given setting of T_{ri} and T_{reg} could drift to a new stable steady state with complete CO combustion when air flow rate was put on manual. However, this is not open-loop multiplicity but rather an input multiplicity just mentioned before as the reactor temperature was controlled by the catalyst circulation rate.

4.4.2 A Quantitative Evaluation for the Potential Five Steady States

For the quantitative evaluation of five steady states, the model described in the Chapter three is used. As said before, we have no exact data for the homogeneous CO

reaction and in section 4.3 we applied a value of homogeneous activation energy, 70 kcal/mol from Avidan and Shinnar (1990) which described the data well up to 1270°F. As the model has the detailed kinetics of both heterogeneous and homogeneous CO combustion, the dependence of the rate on temperature can be varied in any desired way. Therefore we look at the sensitivity of the results to the rate expression for CO combustion. But before presenting our model results let us quantify the conditions for the existence of five steady states in more general way using the heat balance.

While the incremental heat of burning CO to CO_2 is large, the CO_2/CO ratio in partial combustion between 1100-1230°F normally keeps around unity as shown by Errazu et al. (1979) and increases at higher temperatures (see Figure 4-31). It is however not solely a function of the regenerator temperature as stated by Errazu et al. (1979). The ratio at the surface is a function of temperature but the CO to CO_2 combustion competes for oxygen with the combustion of coke and is therefore a function of coke on regenerated catalyst. In complete CO combustion with an excess of oxygen (Between 0.5 to 2% in the flue gas), coke on regenerated catalyst is very low as at high temperature coke combustion is too fast to allow excess oxygen to reach the cyclones at a significant value of C_{rgc}.

For five steady states to exist, the two stable steady states in high temperature have to be separated by a reasonable temperature difference. Sufficient heat release is required in this temperature range. In Figure 4-34, we plot the incremental heat release per mole of oxygen consumed, going from potential to full CO combustion as a function of the ratio of CO_2 to CO. As we deal in open loop with fixed cat/oil and fixed air rate, this incremental heat will raise both reactor and regenerator temperatures or in other

words it raises the feed temperature and supply the heat for the additional cracking that occurs. Coke formation will also increase with increasing reactor temperature. As the air rate is constant, increasing the CO_2/CO ratio consumes less coke. C_{rgc} would have to therefore increase at the upper steady state.

Figure 4-35 gives the potential incremental temperature rise for the regenerator due to full CO combustion for two catalyst to oil ratios as a function of the air rate in the base case. It is noted that the maximum temperature rise in the range of stable steady states is around 100°F if complete CO combustion reaches.

Now at a base temperature of 1200°F the CO_2 to CO ratio is plotted in Figure 4-36 as a function of the CO combustion rate. This ratio also depends on the changes in C_{rgc} but to simplify matters, it is computed for a fixed level of coke on regenerated catalyst. We note in Figure 4-36 that if the ratio of CO_2 to CO increases 30 times, the CO combustion rate must increase 50 times.

Figure 4-37 gives the rate of CO combustion as a function of CO homogeneous activation energy. We note that the activation energies of about 200 kcal/mol are needed to give the necessary increase of the CO_2/CO if temperature rise is 100°F from base temperature of 1200°F. By modeling we could never find a case for five steady states when using an activation energy of 70 kcal/mol for the homogeneous CO combustion. An apparent activation energy around 200 kcal/mol is therefore needed for obtaining five steady states.

If we use the relation given in Figure 4-32 then we can find five steady states as shown in Figure 4-30. However, the actual rate of homogeneous CO combustion in the absence of a catalyst is not well-known. To find five steady states we need the take-off

to occur between 1250-1320°F. This is plausible but we have no real accurate data to prove that.

The data in Figure 4-32 also illustrate why it is no difficult to get reliable data on inhibited CO combustion. The data were taken under isothermal conditions, which requires good heat exchanges and therefore a small tube, or a large heat exchange surface to volume ratio. This heat exchange surface will introduce either a significant inhibitory effect or depending on the wall a catalytic effect. Kinetic data on combustion kinetics are therefore mostly taken in adiabatic gas phase stirred tank reactors (see Krambeck et al., 1972, Evangelista et al., 1969, and Longwell and Weiss,1955), adjusting the temperature of the inlet conditions.

One cannot do that in the presence of catalyst. What one needs is a controlled fluid bed reactor as well as a riser reactor in which the catalyst density can be controlled. To give reliable kinetic measurements, such a reactor has to be quite large to reduce wall effects. No such data have been published. It would be an interesting albeit expensive research project.

Regrettably, it is also not reasible to estimate this rate from actual operating data on an FCC. Modern FCC in partial combustion are operated below 1270°F. At higher temperatures combustion promoters are often added even operating in full combustion with excess oxygen.

In the past some units were reported to have operated with full CO combustion at temperature of 1350°F or even at 1300°F (Avidan and Shinnar, 1990). However, no detailed data are available. This in itself is not conclusive evidence. In complete CO combustion there is excess oxygen and the coke on regenerated catalyst is very low. Our

model describes such an operation reasonably well with an activation energy of 70 kcal/mol. On the other hand, in our case with five steady states excess oxygen has to be low in full CO combustion. At the lower stable steady state less air is required to burn the coke, and therefore the air rate will be lower than required for operating at full CO combustion with excess oxygen if F_c is kept constant. Furthermore, going to full CO combustion at constant oxygen will as said before lead to an increase in coke on regenerated catalyst.

To predict steady state in full CO combustion with excess oxygen better data on the take-off of the inhibited CO to CO_2 reaction are not needed. What would be needed is to predict the possibility and existence of five steady states, or the stability of steady states above 1250°F. In the absence of such data it makes sense to take into account that a steady state above 1250°F could be an unstable steady state and add a moderate amount of CO combustion promoter. In Figure 4-38 we regive Figure 4-30 with a moderate amount of promoter added (an increase by a factor of 4 of the heterogeneous CO combustion rate constant). The excess high temperature steady states (4 and 5) disappear.

To better illustrate this we give in Figure 4-39 a map of multiple steady states for a specific base case. The existence of 1, 3 or 5 steady states is plotted as a function of air to oil and catalyst to oil ratios. The map is based on our model with one modification. Above 1270°F, we modify the reaction rate for homogeneous CO combustion using the temperature dependence given in Figure 4-32. From the data in Figure 4-32 the following equation is obtained:

$$k_{31} = 3.6323\times10^{-6} e^{50.18 e^{100-\frac{1.827\times10^5}{T_{reg}+459.6}}} \qquad (4\text{-}1)$$

As one normally thinks of an FCC operating in terms of the regenerator and riser temperatures, we regive the map in Figure 4-40 in terms of these two temperatures, giving the borders for temperature settings for which there is a steady state as well as the borders of the temperature settings for which the open-loop conditions correspond to five steady states and a fourth unstable steady state.

We emphasize here that while the boundaries for three steady states are based on model properties backed by sound data, the boundaries for five steady states are schematic and speculative. The only data that we have would indicate that below regenerator temperatures of 1270°F it is unlikely that a given controller setting leads to an unstable fourth steady state. However, the system could have a higher steady state in open-loop operation (both F_c and F_{air} fixed). Also an operation at $T_{reg} > 1300°F$ cannot be a fourth unstable steady state if there is significant excess oxygen, as used in complete CO combustion.

If we take these fact into consideration, we should be able to design a satisfactory FCC control despite the uncertainty of the potential for additional high temperature steady states. The results also show the advantage of using CO combustion promoter at high regenerator temperatures in complete CO combustion.

4.5 Results and Discussions

To understand control of a complex system, one has to understand its dynamic behavior and stability. Of primary importance is clarification of the existence of multiple steady states and their stability. In this chapter we have tried to present a systematic

approach for understanding this issue.

If an FCC has only one stable steady state, it is inoperable as this state is trivial. Present FCC's have no input conditions in which the hot steady state is the only stable one. There are at least three steady states, two of which are stable. For a wide range of operating conditions, three steady states are feasible but only one is practical. The intermediate unstable steady state is of no interest even if it is stabilized by control. The problem here is to understand the conditions at which the useful steady state disappears and therefore the units will wind down. Five steady states are possible in theory because the secondary homogeneous combustion rate of CO becomes much faster at regenerator temperature above 1270°F and heat release from CO to CO_2 is much larger than from carbon to CO. However, we have no data to prove its existence but we can still take this into account in control design.

Figure 4-2 shows the classical multiple steady state behavior existed in the FCC. It is called output multiplicity of a system. Figure 4-3 gives the region of multiple steady states in terms of two input variables, F_c and F_{air}. Figure 4-4 gives the stability range in terms of two process variables, T_{ri} and T_{reg}. Figure 4-8 to 4-18 depict the effects of various input perturbations on stability limits. we note that the unstable region becomes smaller for higher feed temperature, higher catalyst activities, higher coking rate and for adding a promoter. All the figures are essential for steady-state control design and optimization. As the FCC has nonlinear instabilities, operation close to a bifurcation point is undesirable.

Input multiplicity is really a problem of the control matrix design although it has strong similarities to the open-loop steady states. Figure 4-19 to Figure 4-23 describe

clearly the input multiplicities existed in FCC operation. Two different inputs can make an identical output. However, the control tuning is different for these two input points. We note that for example, point A and B in Figure 4-19 have opposite slope in the controller gain. If we use a linear controller with an integral function only one of these points can be stable for a given tuning. We can design a linear controller with integral action such that either point A or B is stable but we cannot design it such that both are stable.

The plots given in Figure 4-24 to 4-28 show the multiple steady states at partially closed-loop operation. We conclude that fixing F_{air}, F_c, T_{reg} and T_{ri} leads to a unique steady state but fixing T_{reg} and T_{ri} alone does not do so. There is a region of input multiplicities. For reasonable values of Fair this region exists at high regenerator temperatures close to or in complete CO combustion. However for most of region, a set value of T_{reg} and T_{ri} will completely determine the system. The two regions have to be noted because the system is locally uncontrollable. One is maximum regenerator temperature at which the slope is zero. The other is minimum air rate at which the slope is infinity. This is a bifurcation point. The former problem can be solved by controlling oxygen concentration. The latter by feed temperature.

Figure 4-39 and 4-40 show the maps of five steady states for a specific base case in terms of two input, F_c and F_{air}, and T_{ri} and T_{reg} respectively. the boundaries in the figures are only schematic and speculative. However, the figures are still a useful guide to a satisfactory FCC control design.

In all these figures we do not consider the unit constraints, such as wet gas compress, metallurgical temperature limit, valve limit, air blower capacity and so on.

What we concerned here is the chance of cause a unit wind-down due to the changes of operating conditions and input conditions such as feed temperature, feed composition or catalyst activity. The plots provide only useful bounds for operability.

There is a caveat in our results. While the results are plotted over a slightly wider range, the model is limited as to the riser and regenerator temperatures. When describing cracking and coking reactions one approximates complex relation by an overall activation energy. Such relations do not hold over a wide range of temperatures. Our model for the reactor holds for temperatures between 900 and 1050°F. At higher temperatures thermal cracking becomes important (Avidan and Shinnar, 1990). The model for the regenerator is valid for temperatures above 1000°F. The prediction of the unstable steady state is therefore unreliable if it occurs at temperatures below that given. However, normal operating range is at T_{reg} above 1150°F and T_{ri} between 950 and 1030°F. This definitely does not limit the applicability of our results.

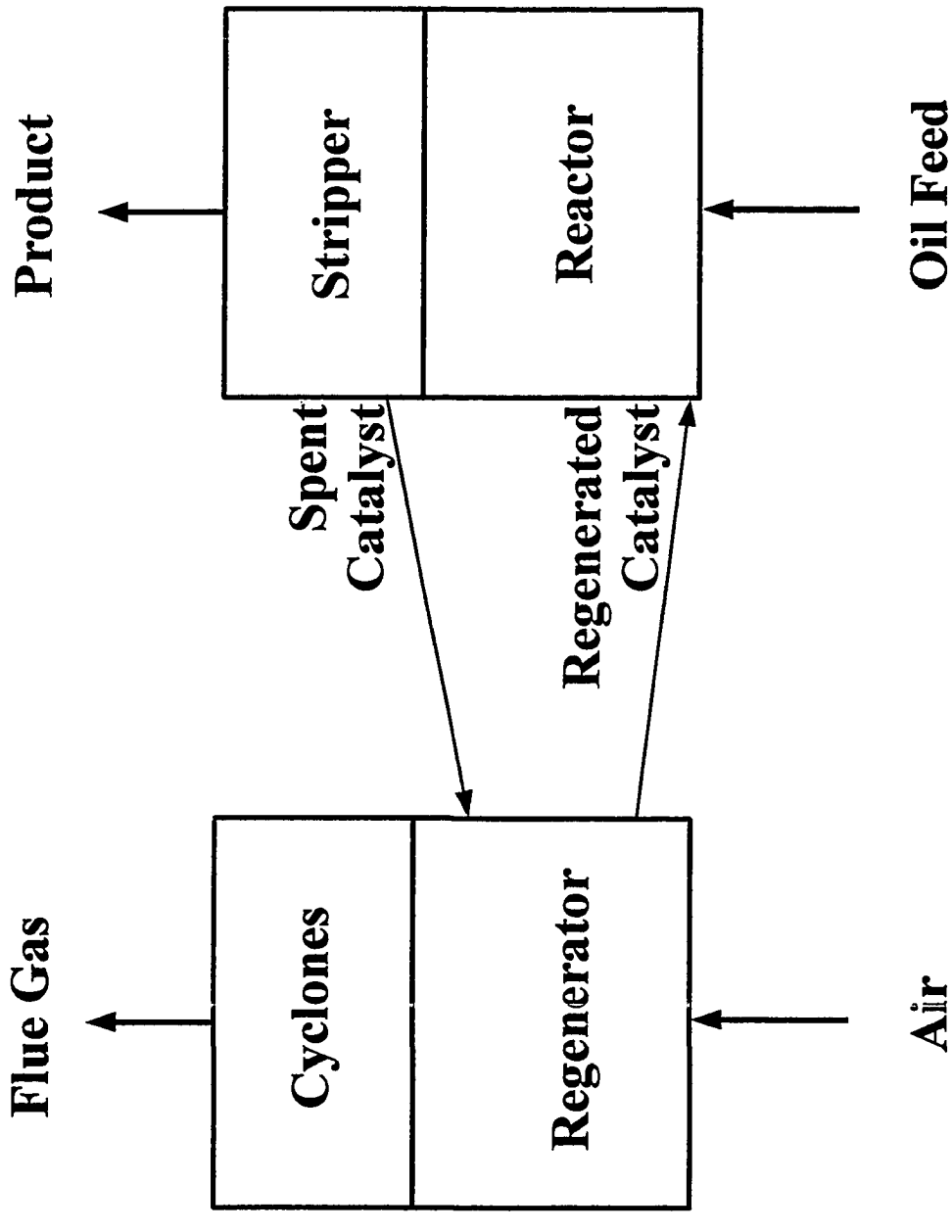

Figure 4-1. Schematic Features of FCC

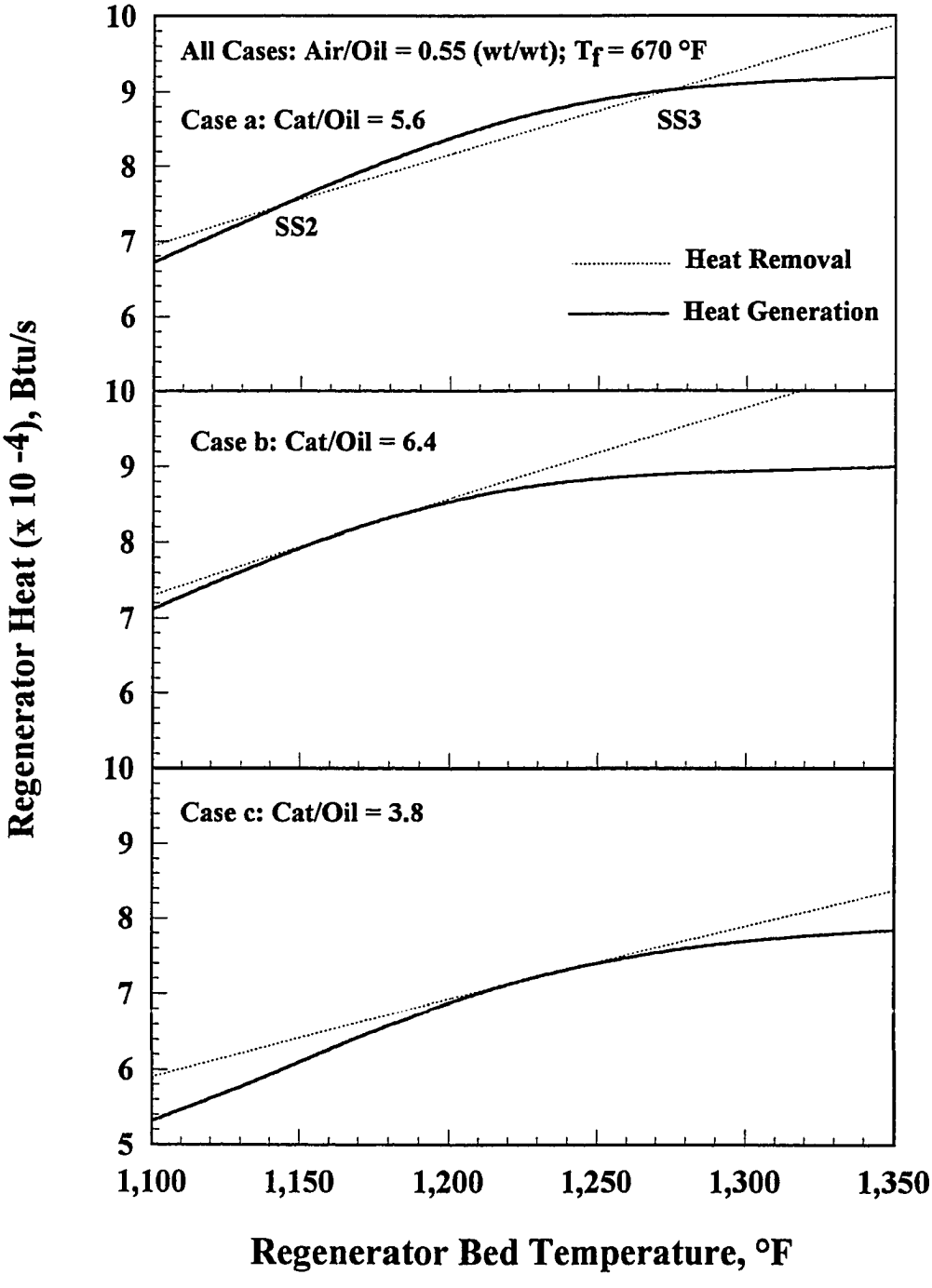

Figure 4-2. Heat Balance Curves of FCC

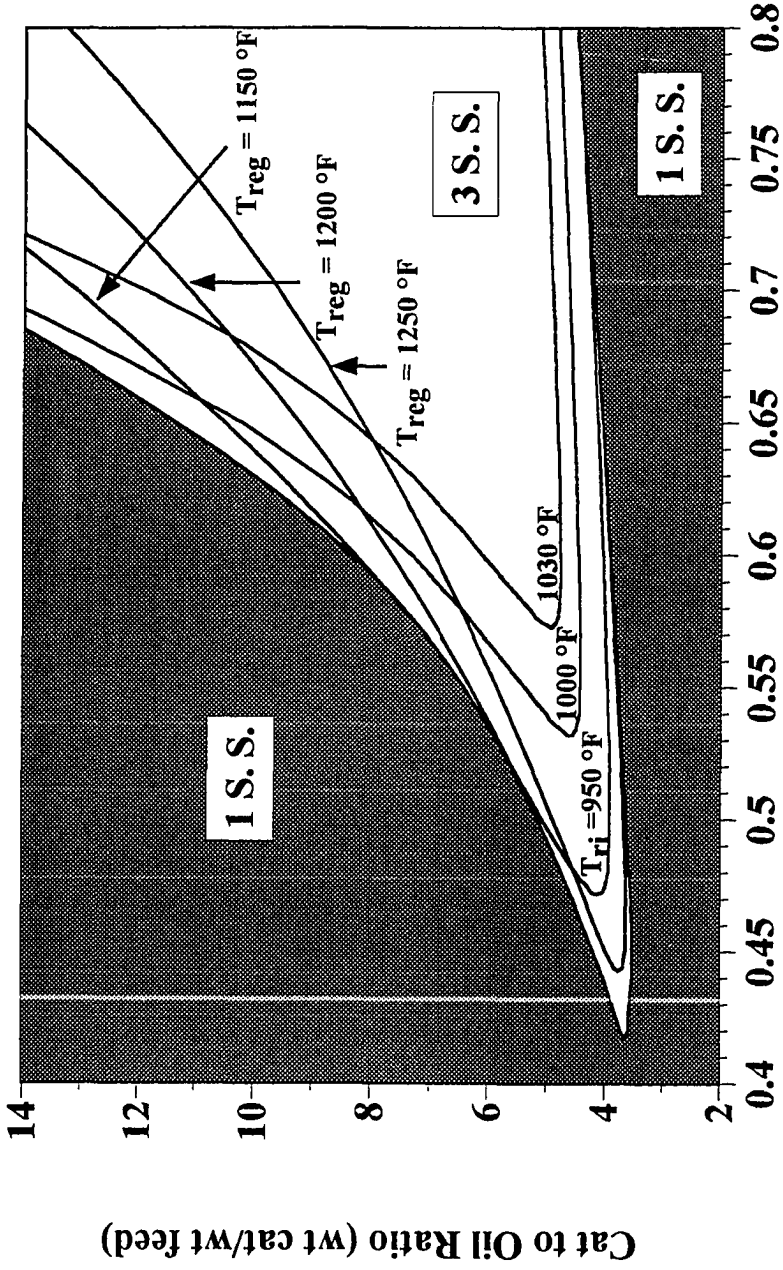

Figure 4-3. Multiple Steady-State Map of Basic Case

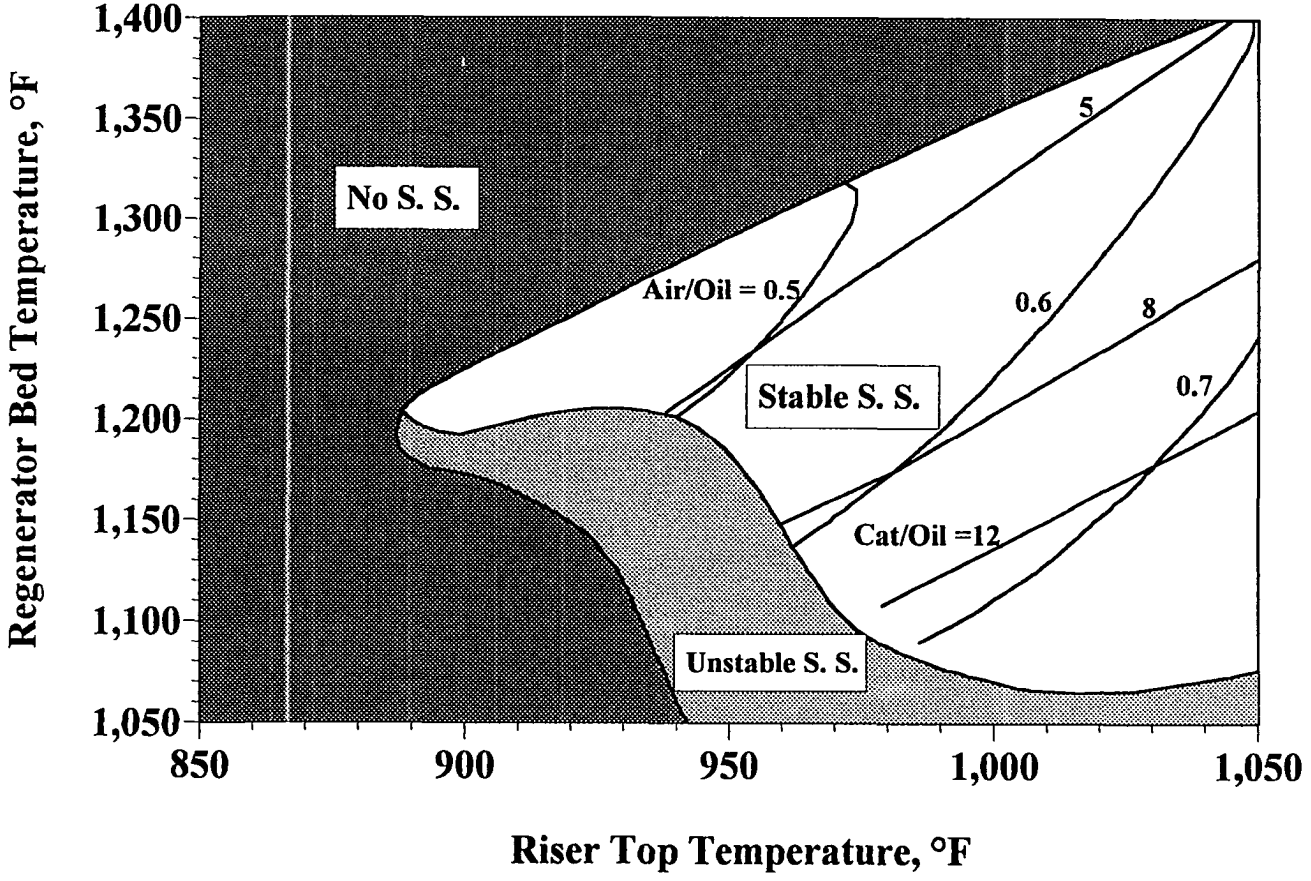

Figure 4-4. Permissible Steady-State Operating Map of Basic Case

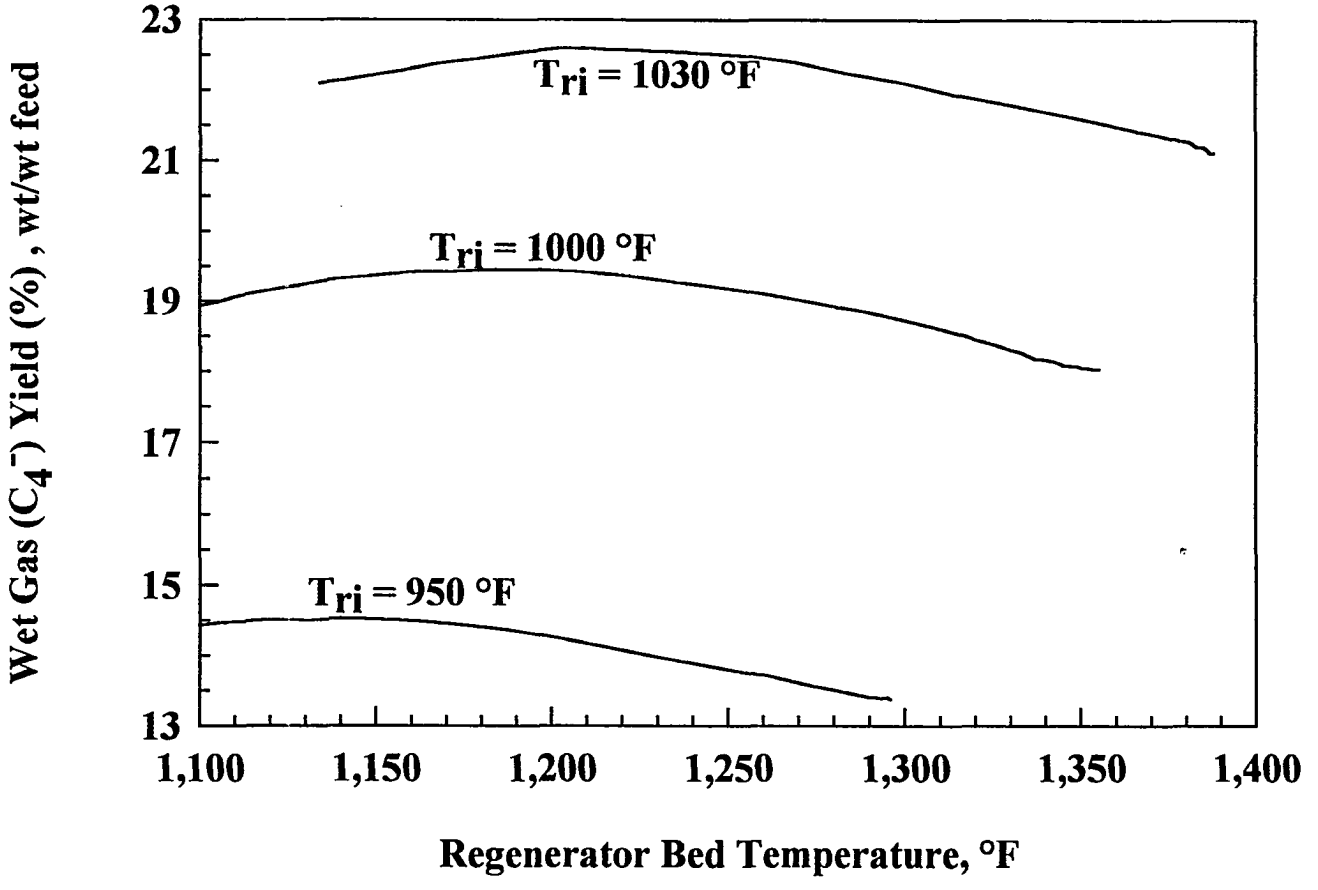

Figure 4-5. Effect of Temperatures on Wet Gas Yield

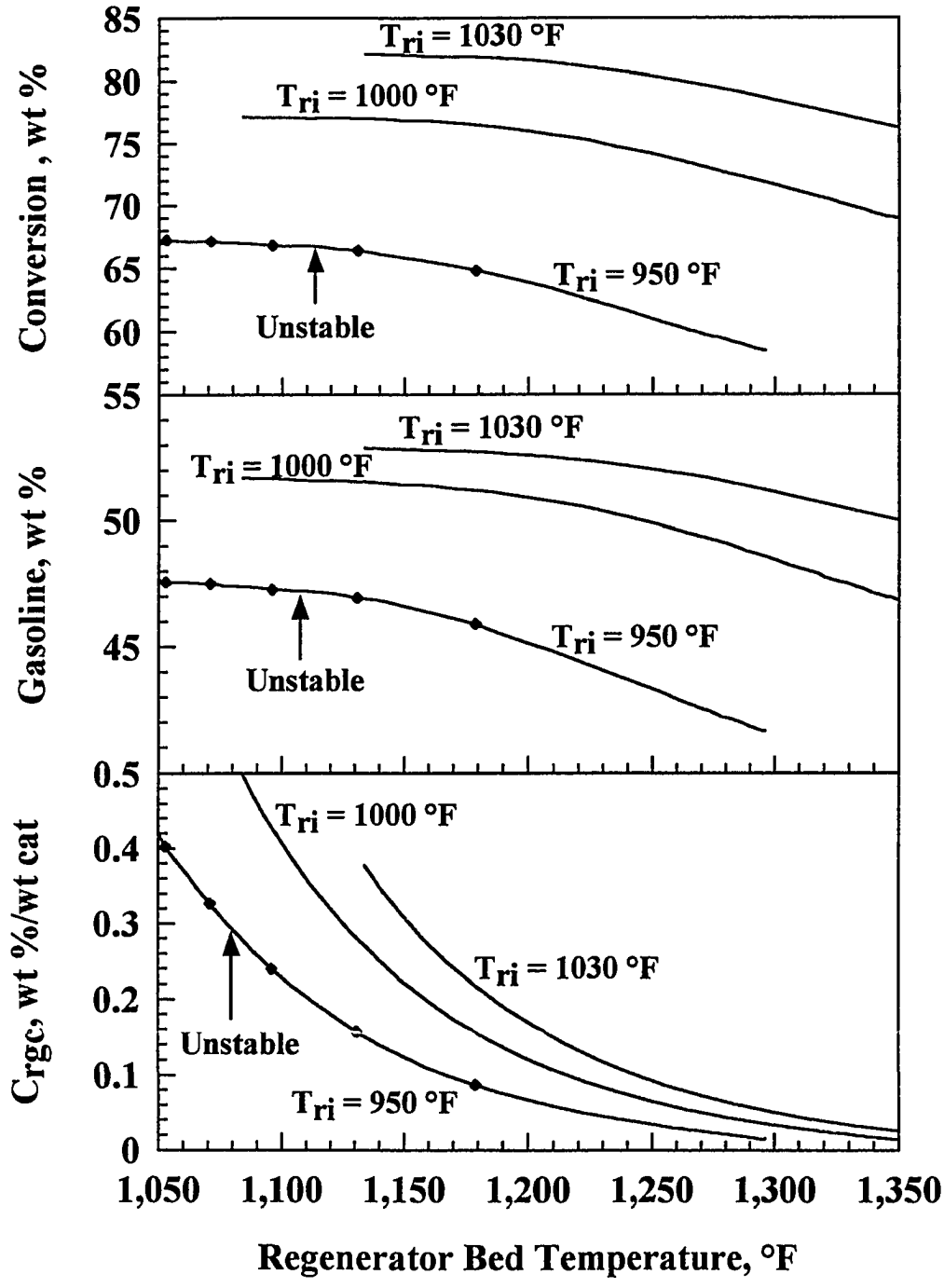

Figure 4-6. Effect of Temperatures on Conversion, Gasoline Yield and C_{rgc}

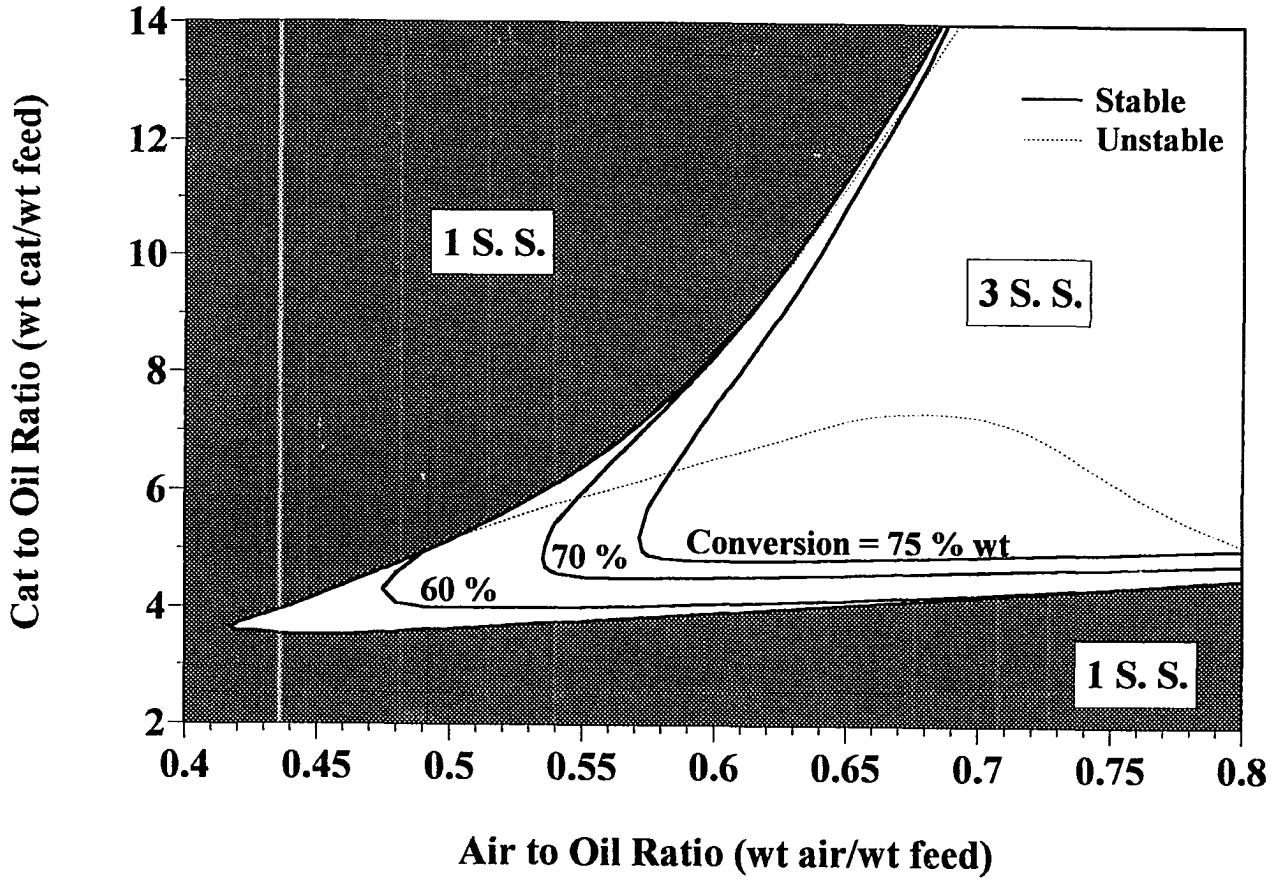

Figure 4-7. Conversion Isoclines in Steady-State Map

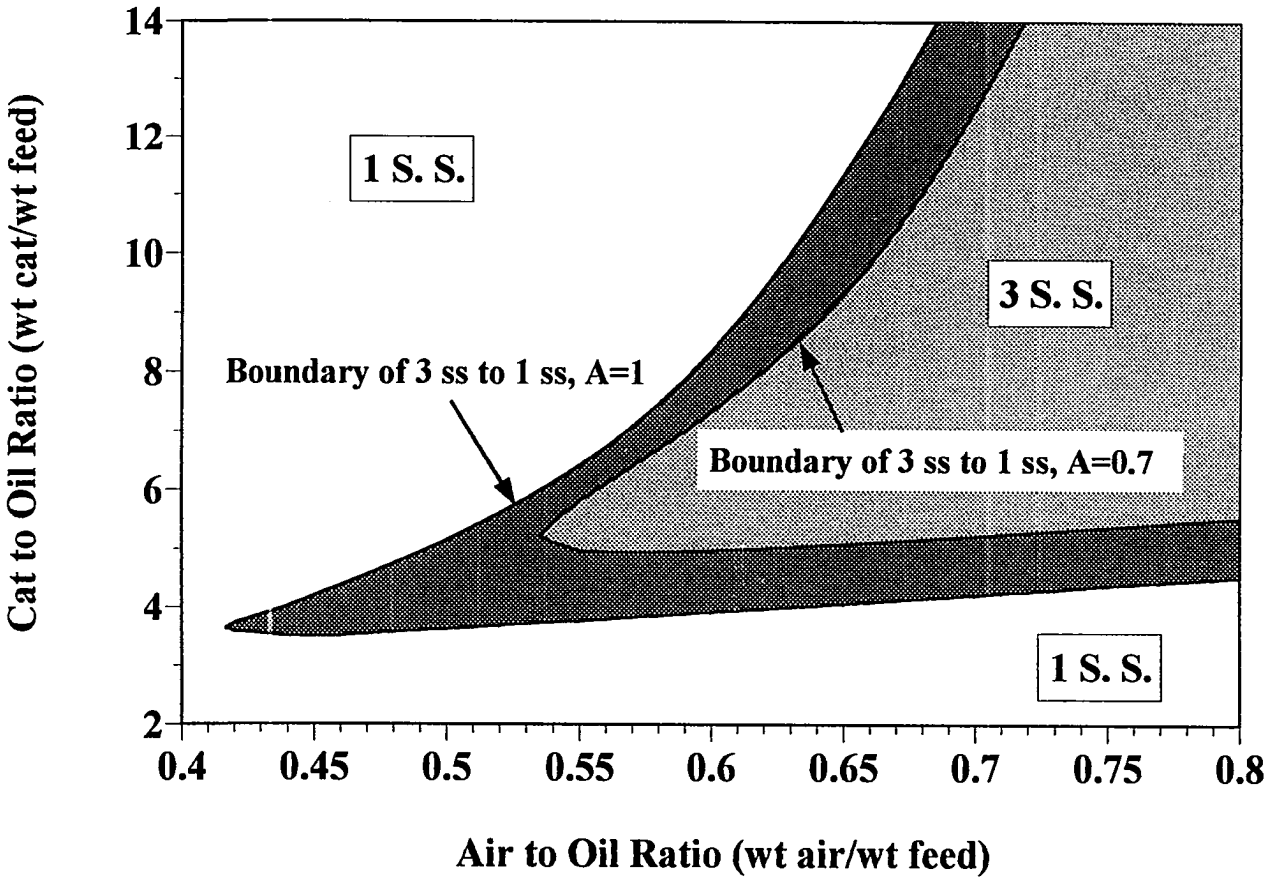

Figure 4-8. Impact of Catalyst Activity on Multiple Steady-State Map

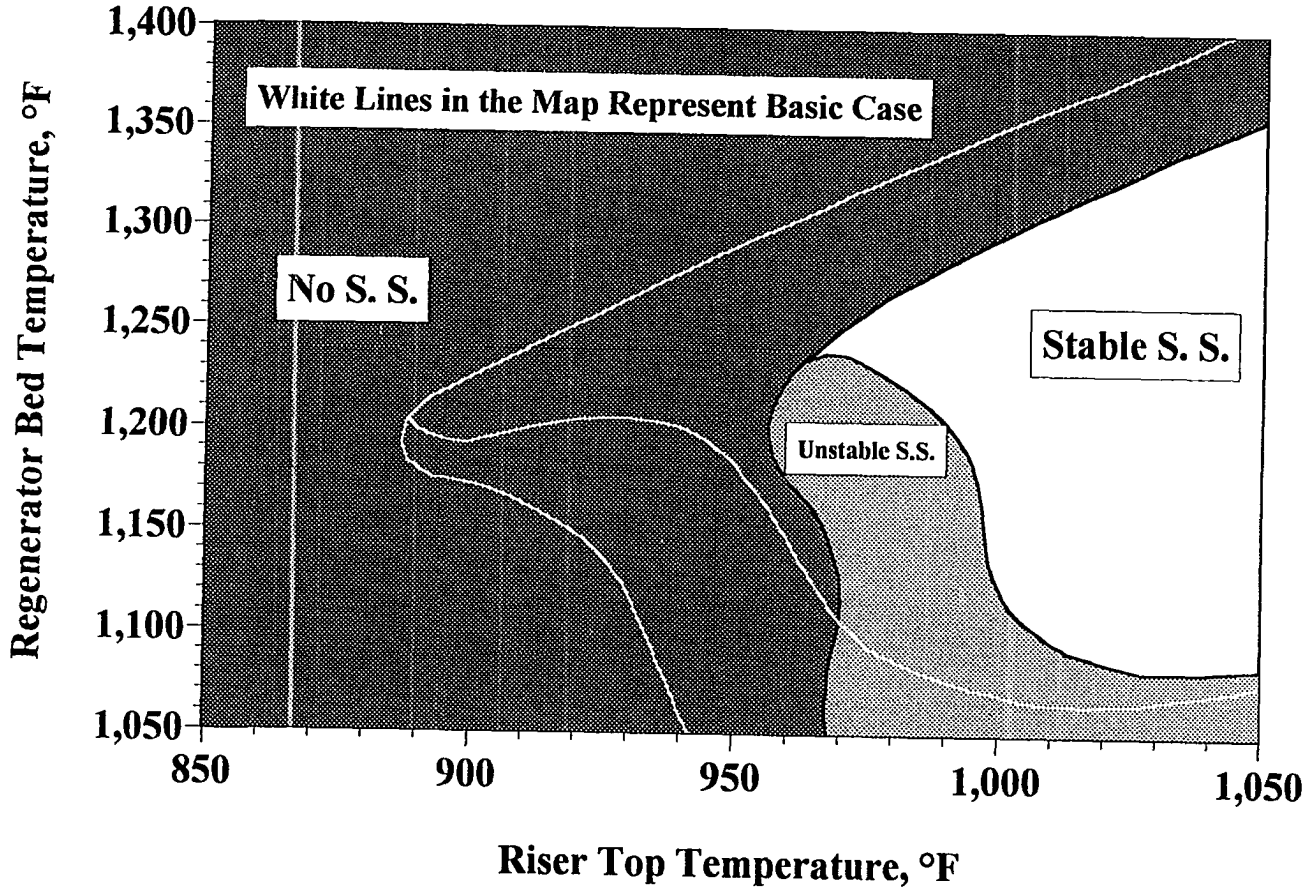

Figure 4-9. Permissible Steady-State Operating Map When A=0.7

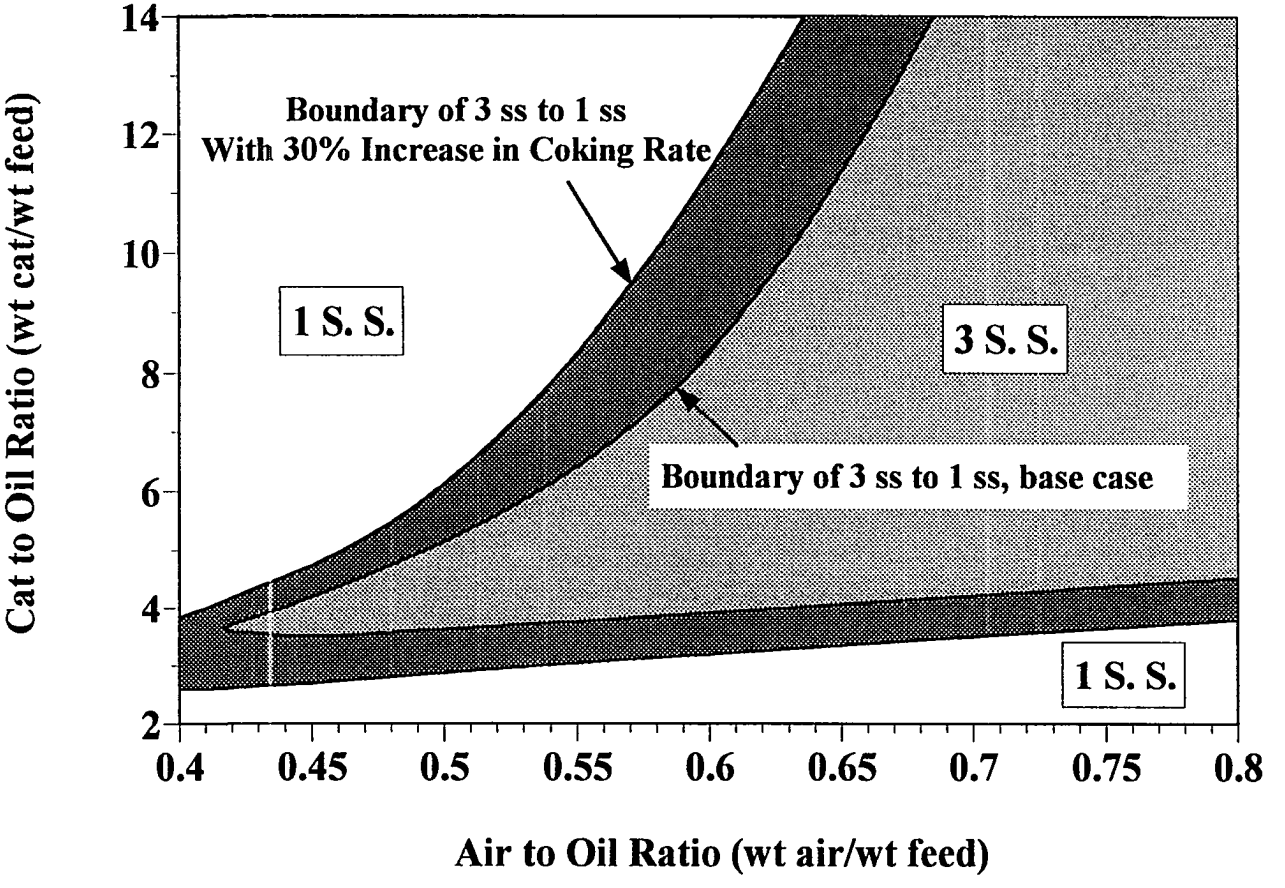

Figure 4-10. Impact of Coking Rate on Multiple Steady-State Map

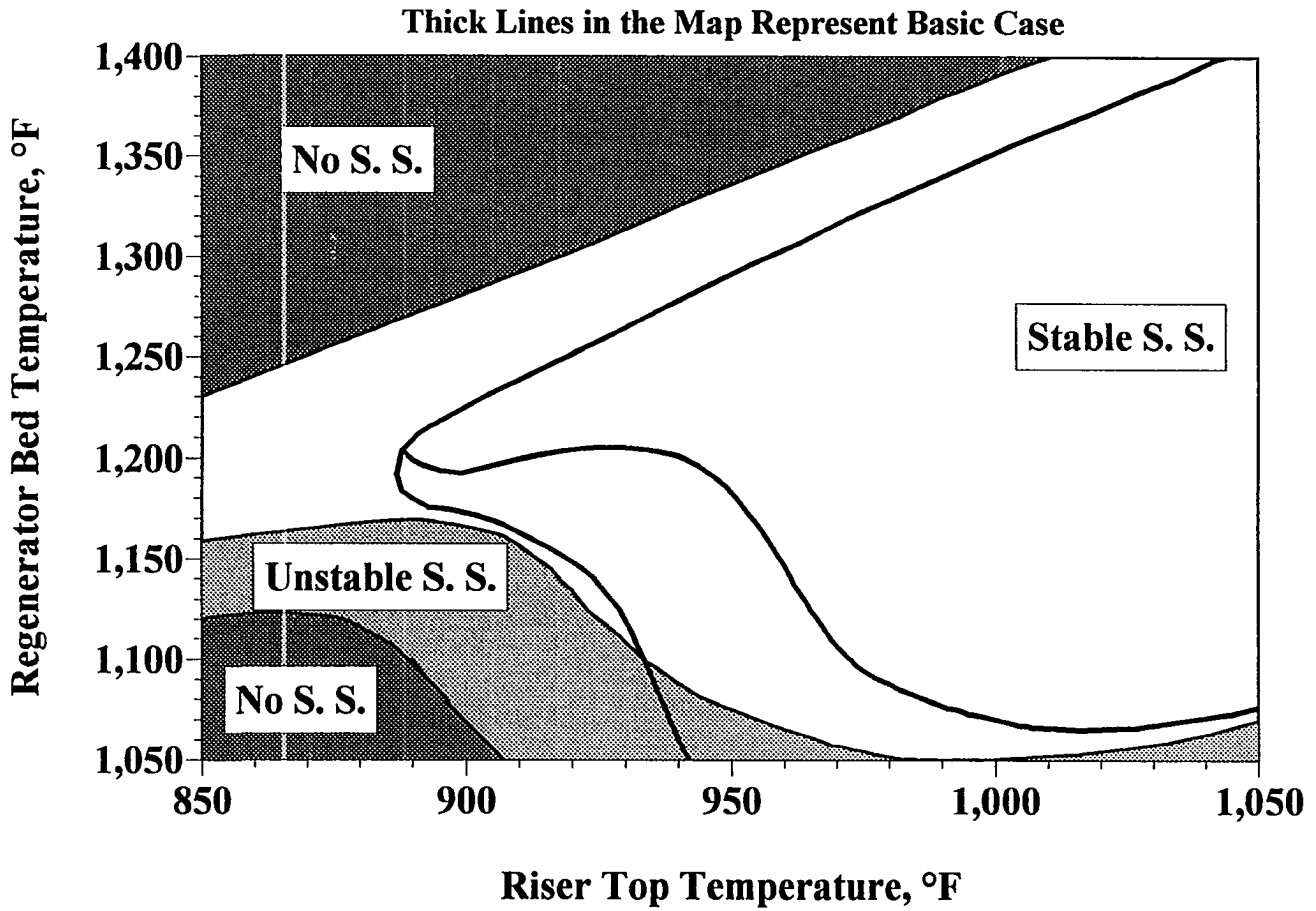

Figure 4-11. Permissible Steady-State Operating Map with Coking Rate 30% Rise

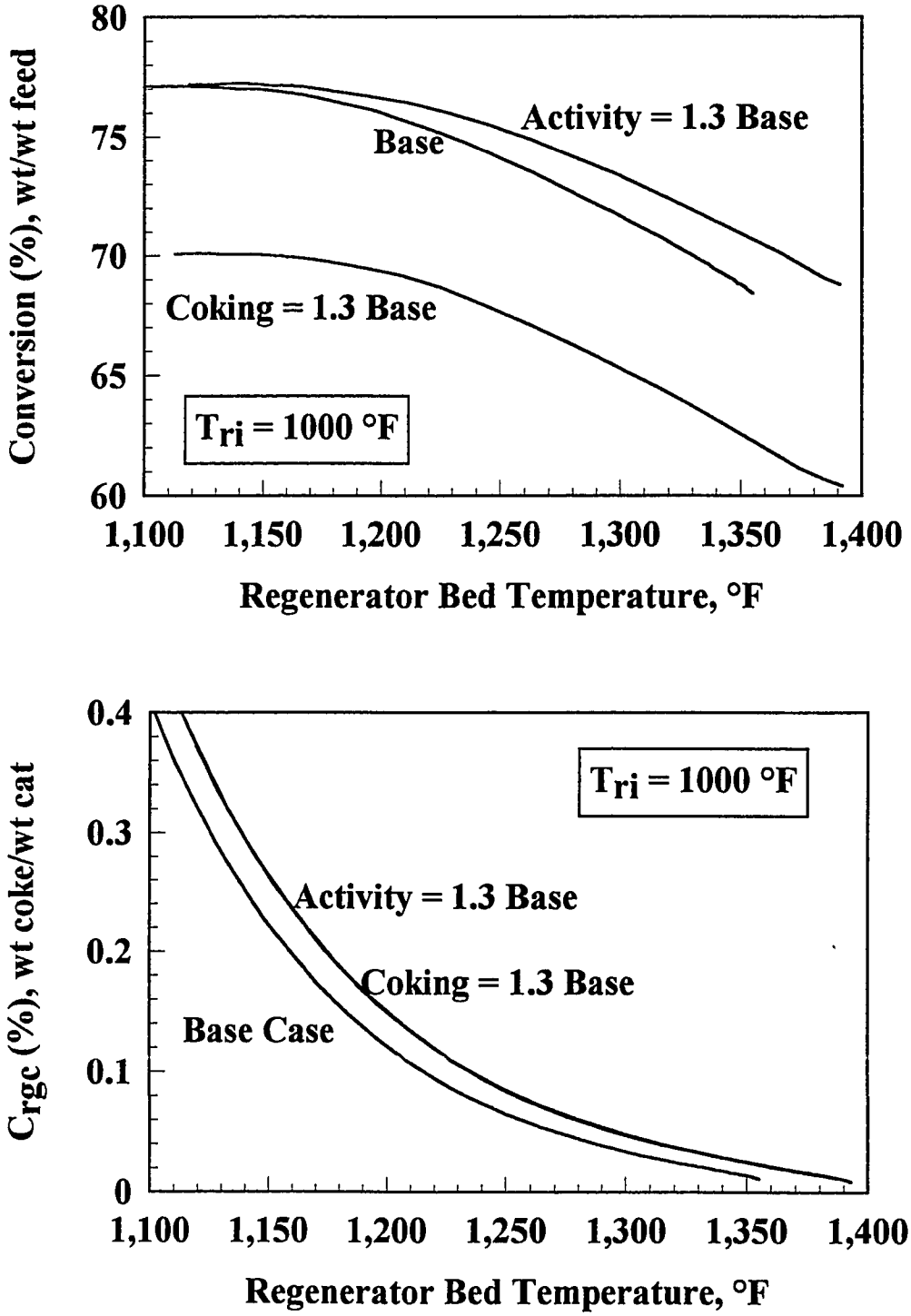

Figure 4-12. Impact of Activity and Coking Rate on Conversion and C_{rgc}

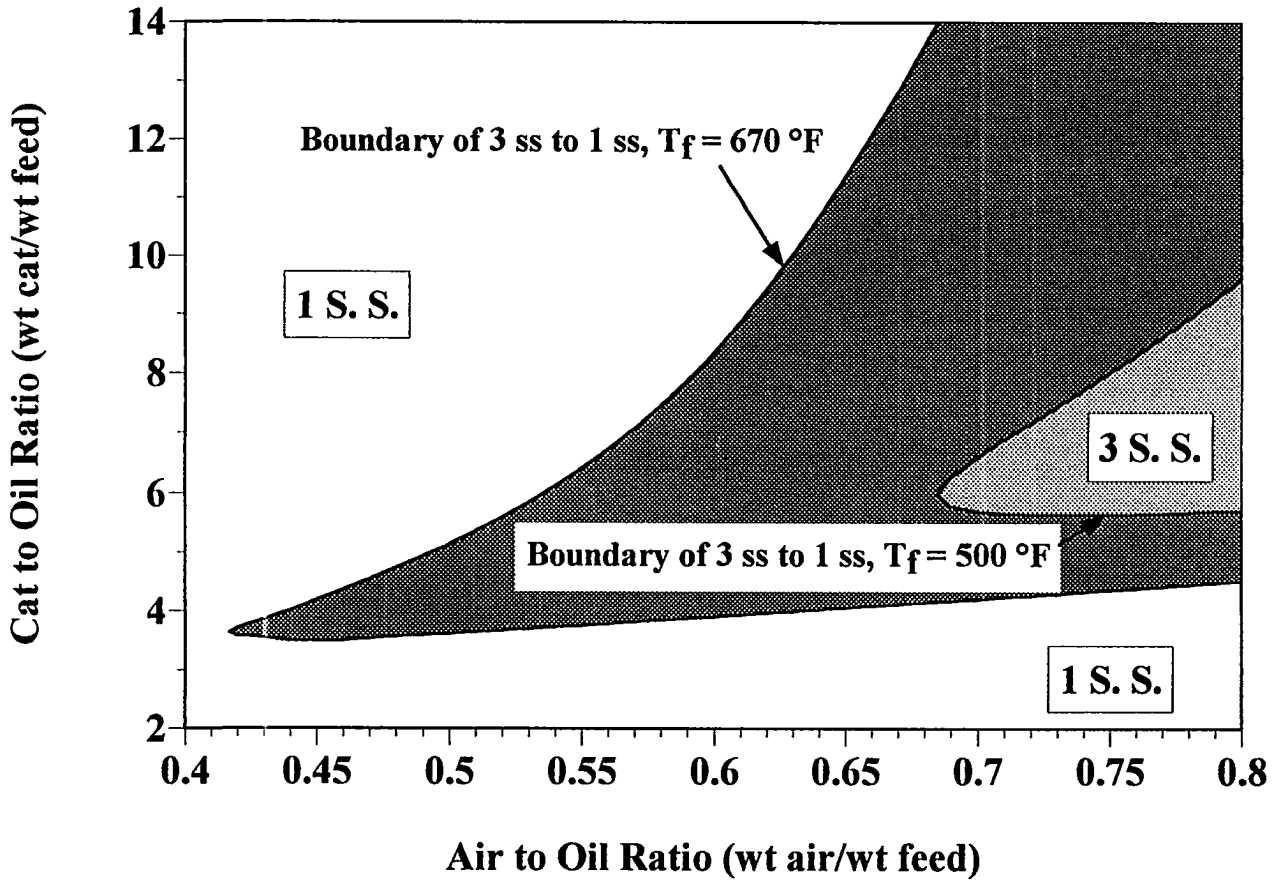

Figure 4-13. Impact of Feed Temperature on Multiple Steady-State Map

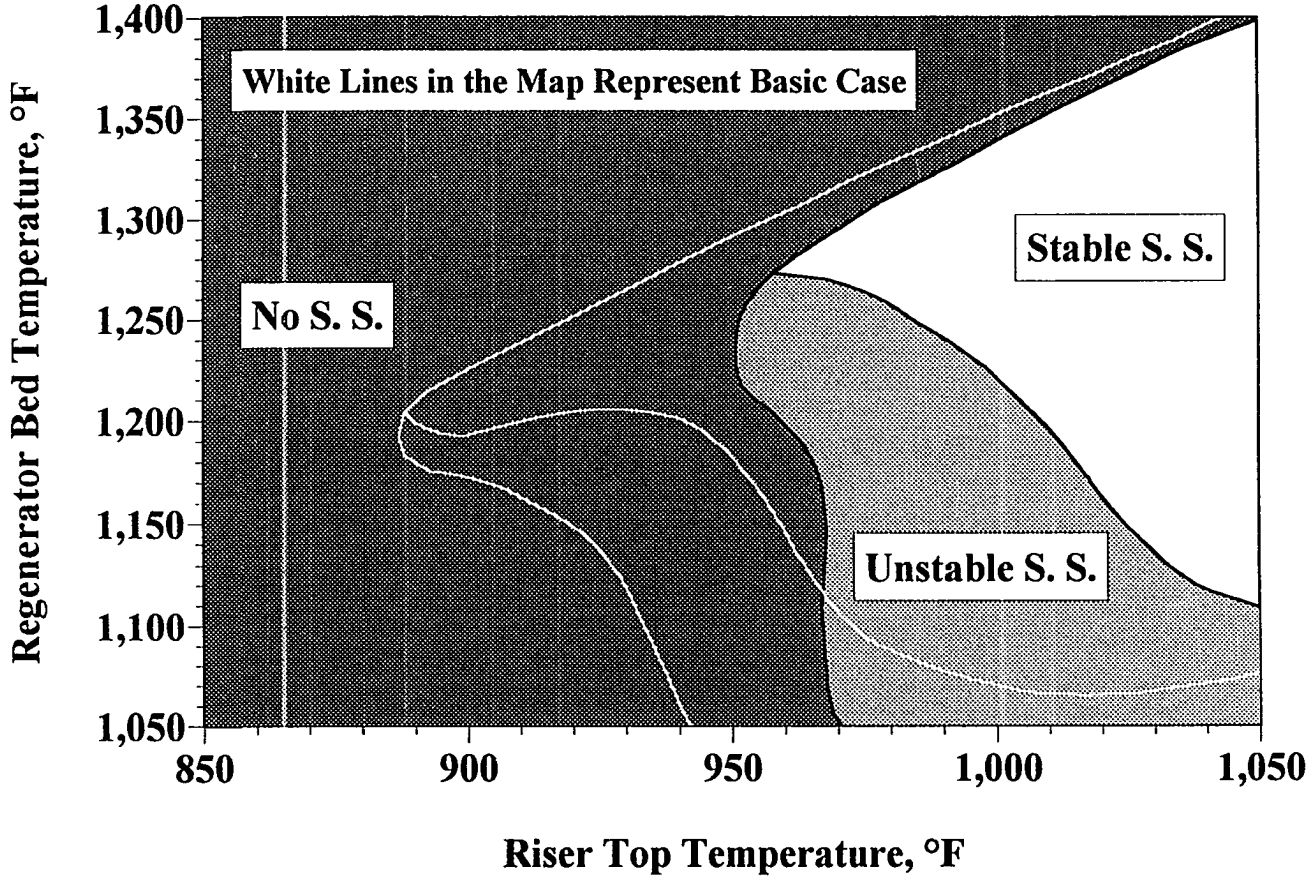

Figure 4-14. Permissible Steady-State Operating MapWhen T_f = 500 °F

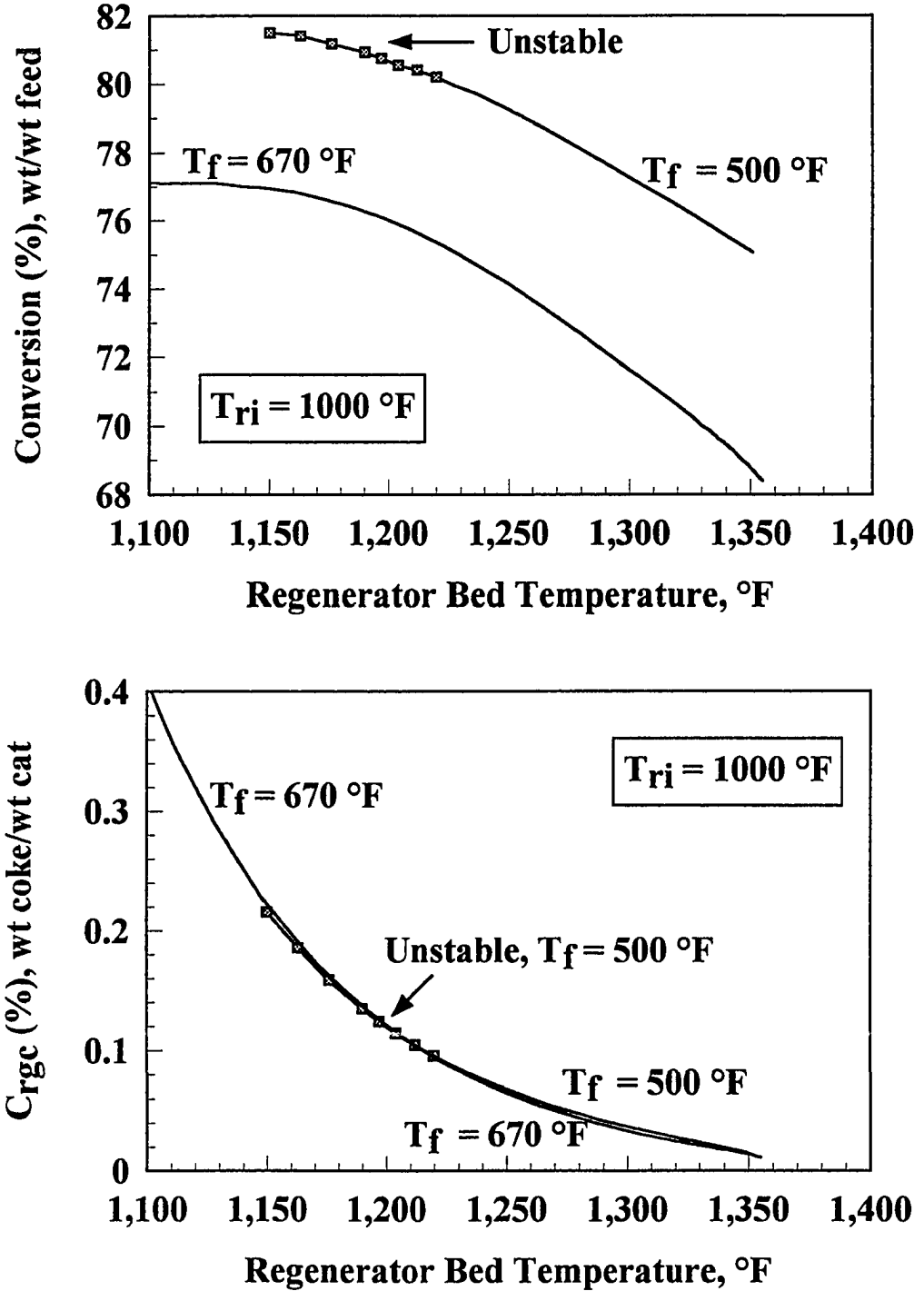

Figure 4-15. Impact of Feed Temperature on Conversion and C_{rgc}

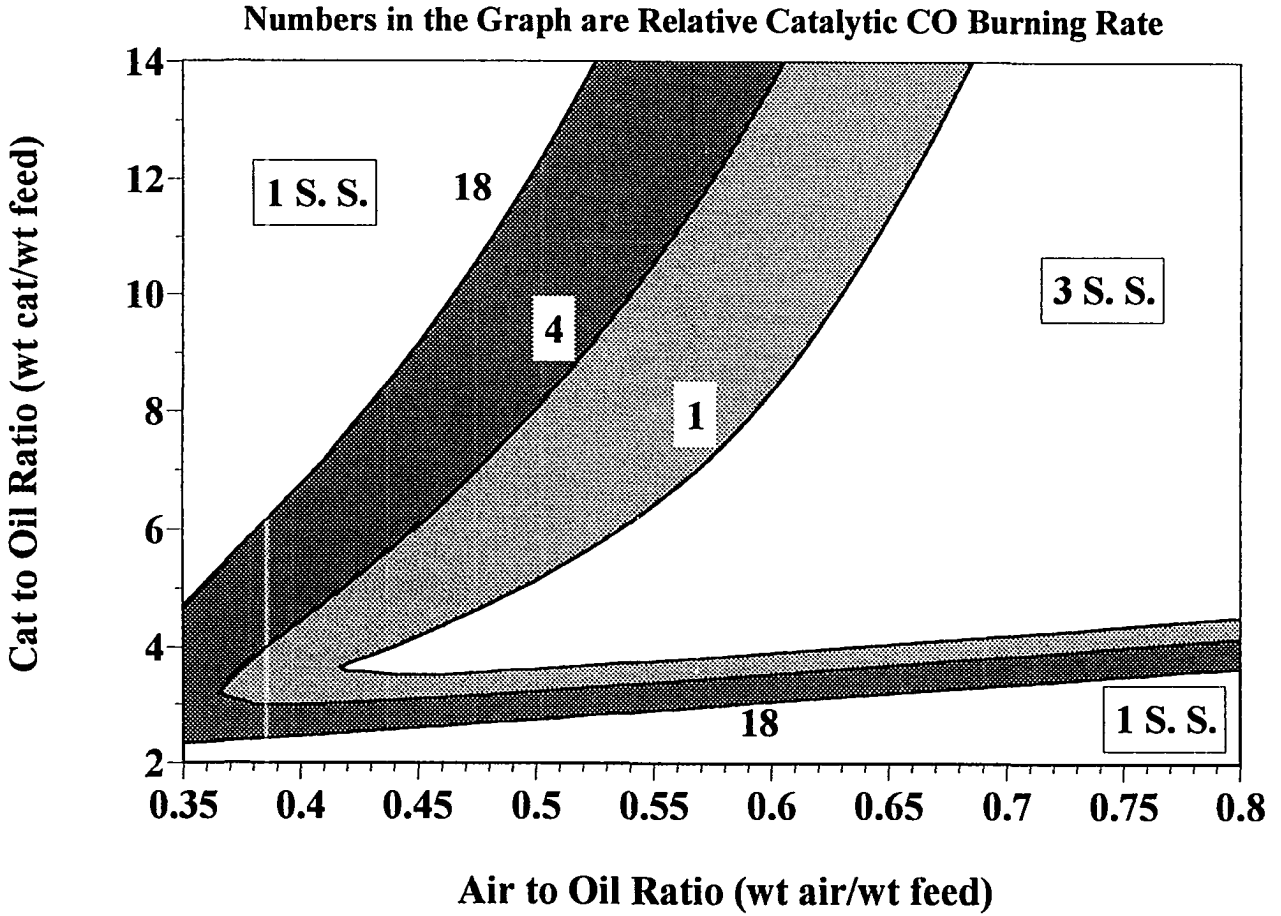

Figure 4-16. Impact of CO Combustion Promoter on Multiple Steady-State Map

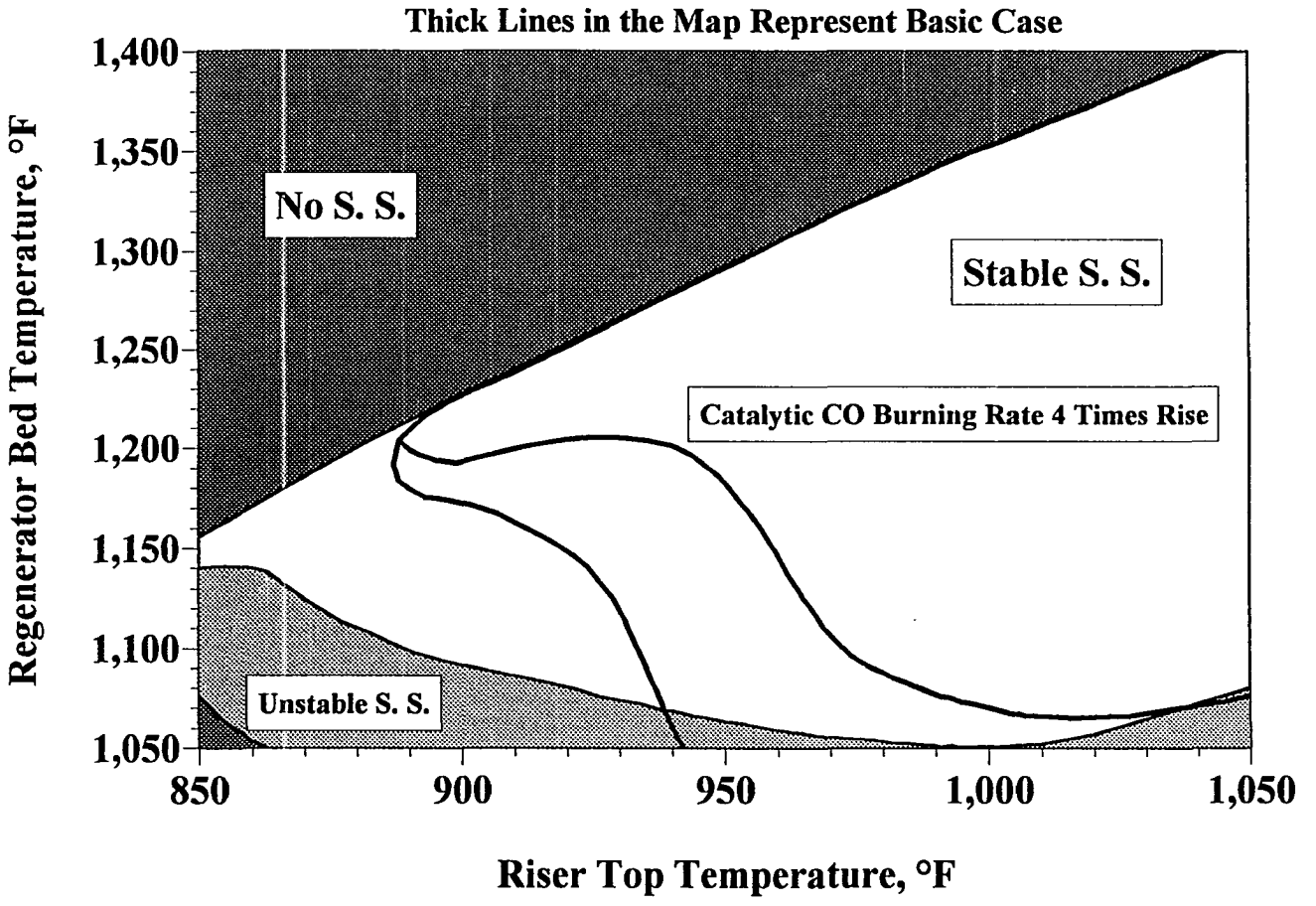

Figure 4-17. Permissible Steady-State Operating Map with CO Combustion Promoter

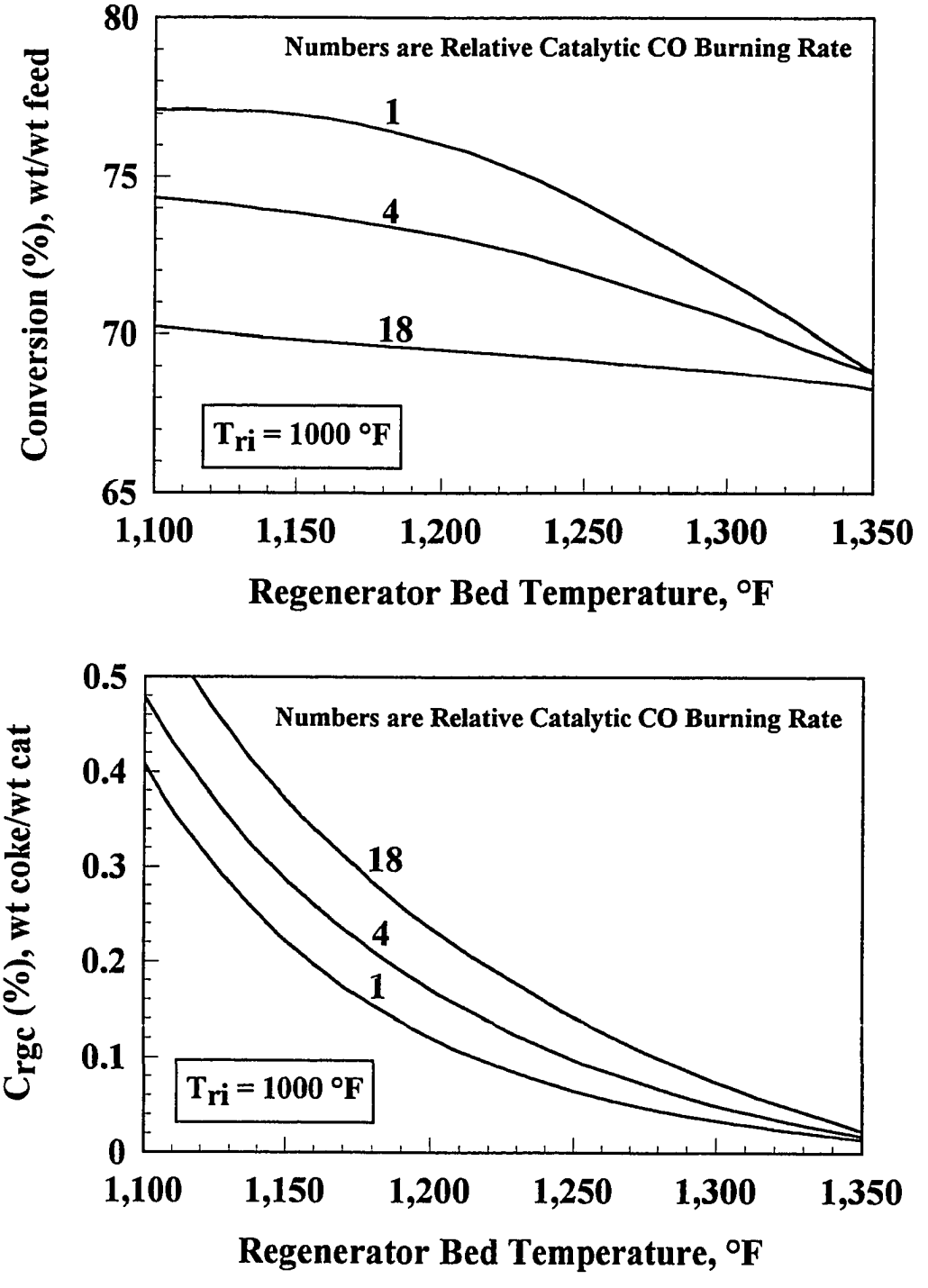

Figure 4-18. Impact of CO Combustion Promoter on Conversion and C_{rgc}

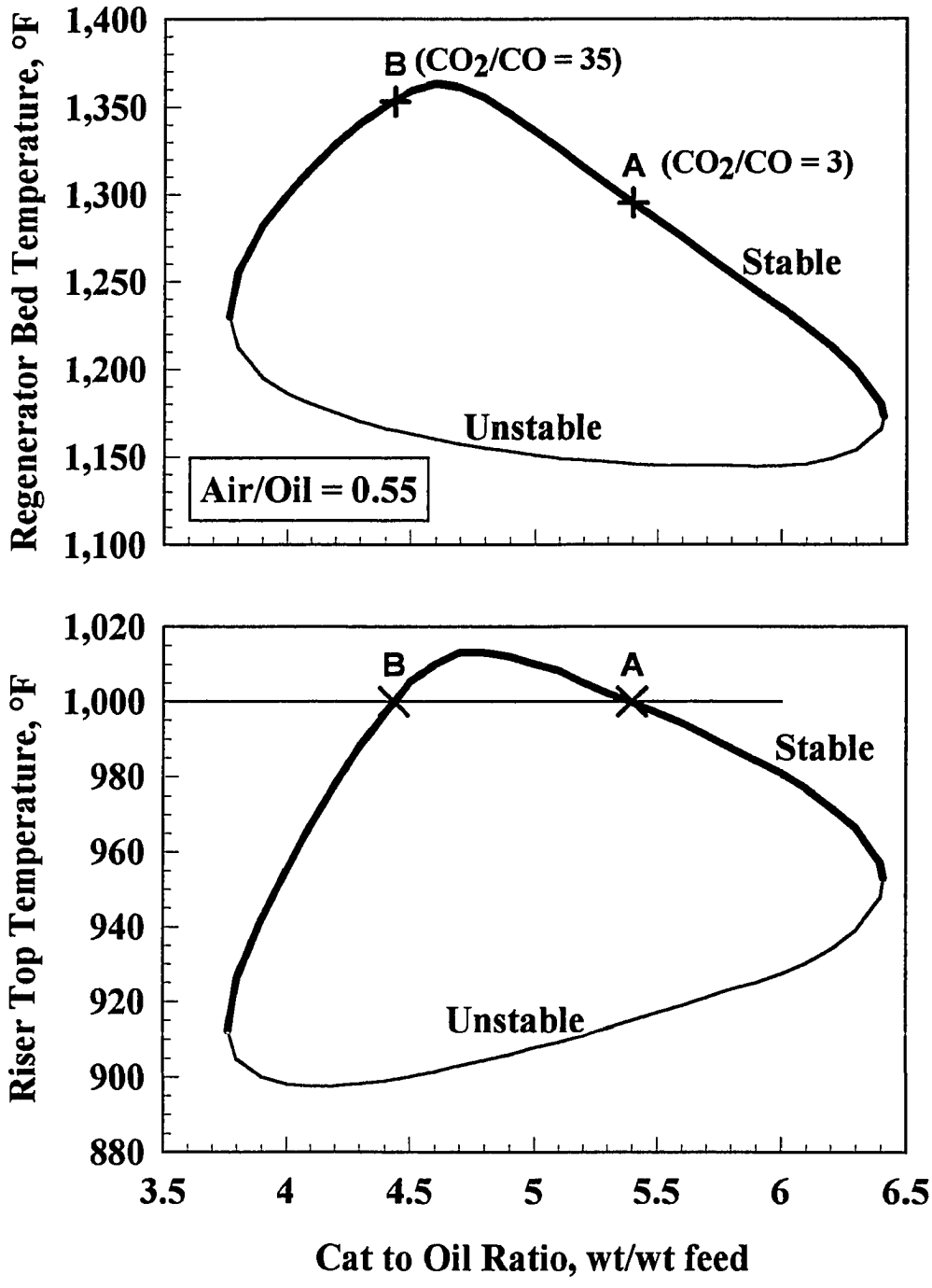

Figure 4-19. Multiple Steady States at Constant Air/Oil

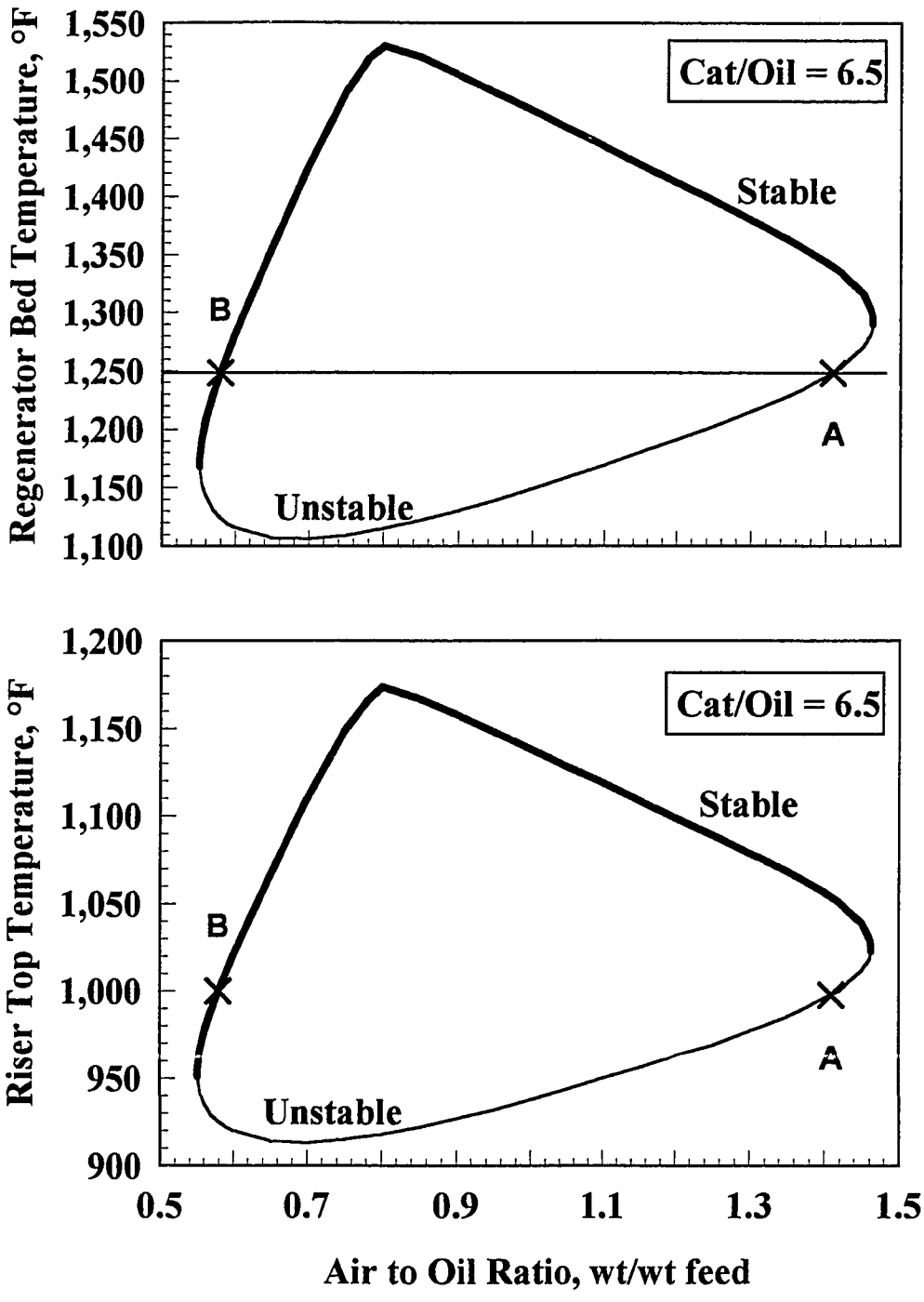

Figure 4-20. Multiple Steady States at Constant Cat/Oil

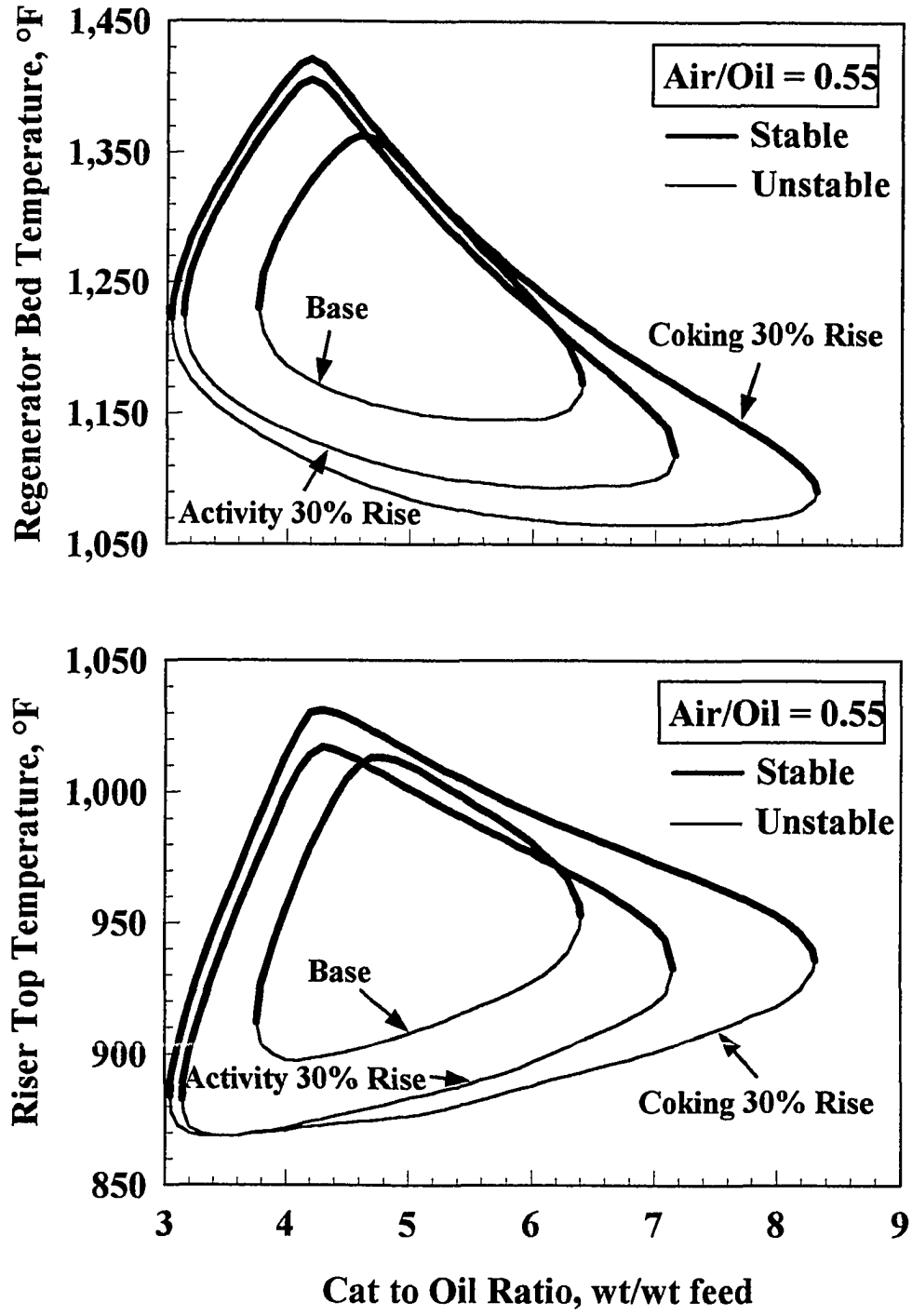

Figure 4-21. Impact of Activity and Coking Rate at Constant Air/Oil

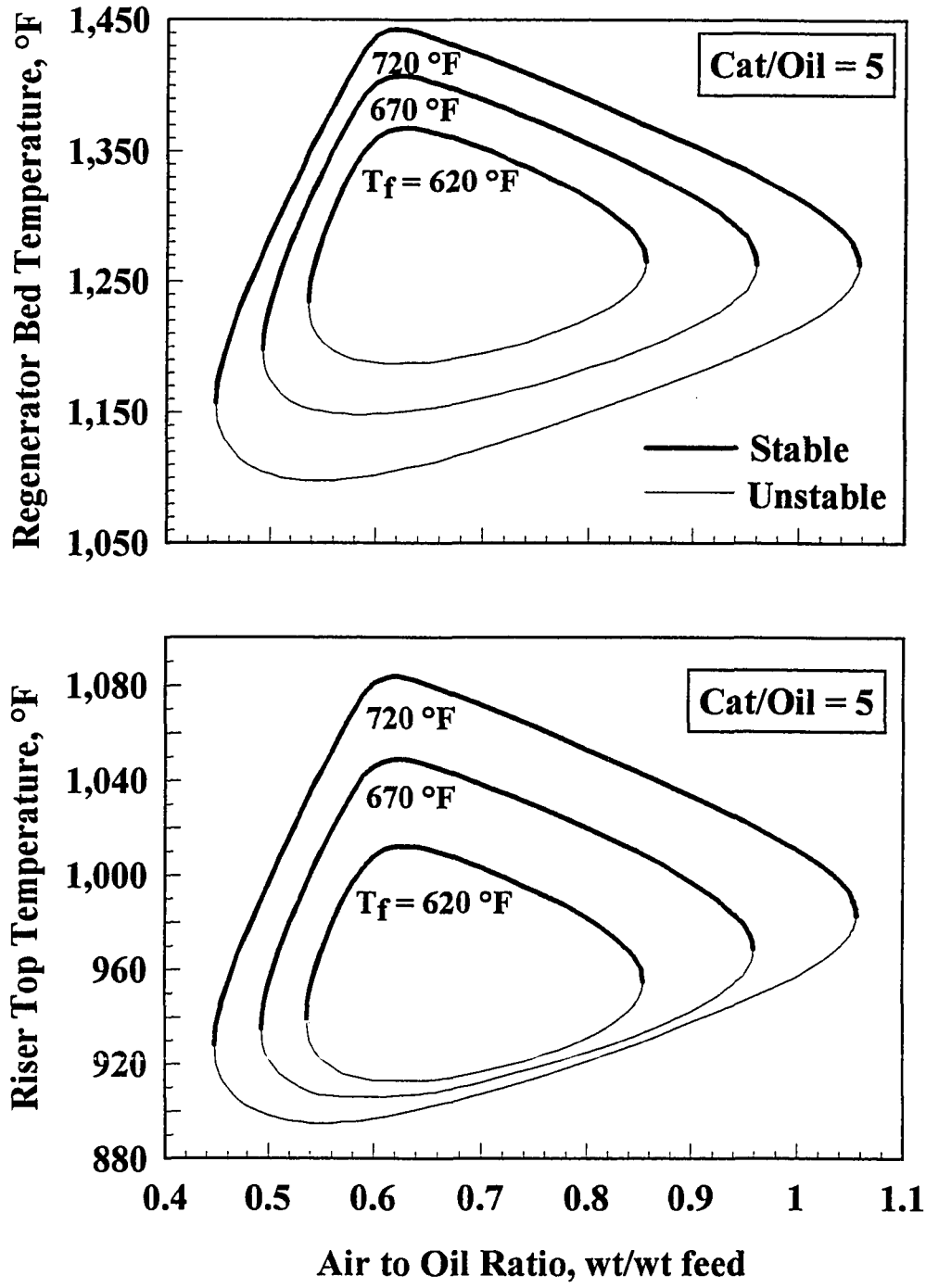

Figure 4-22. Impact of Feed Temperature at Constant Cat/Oil

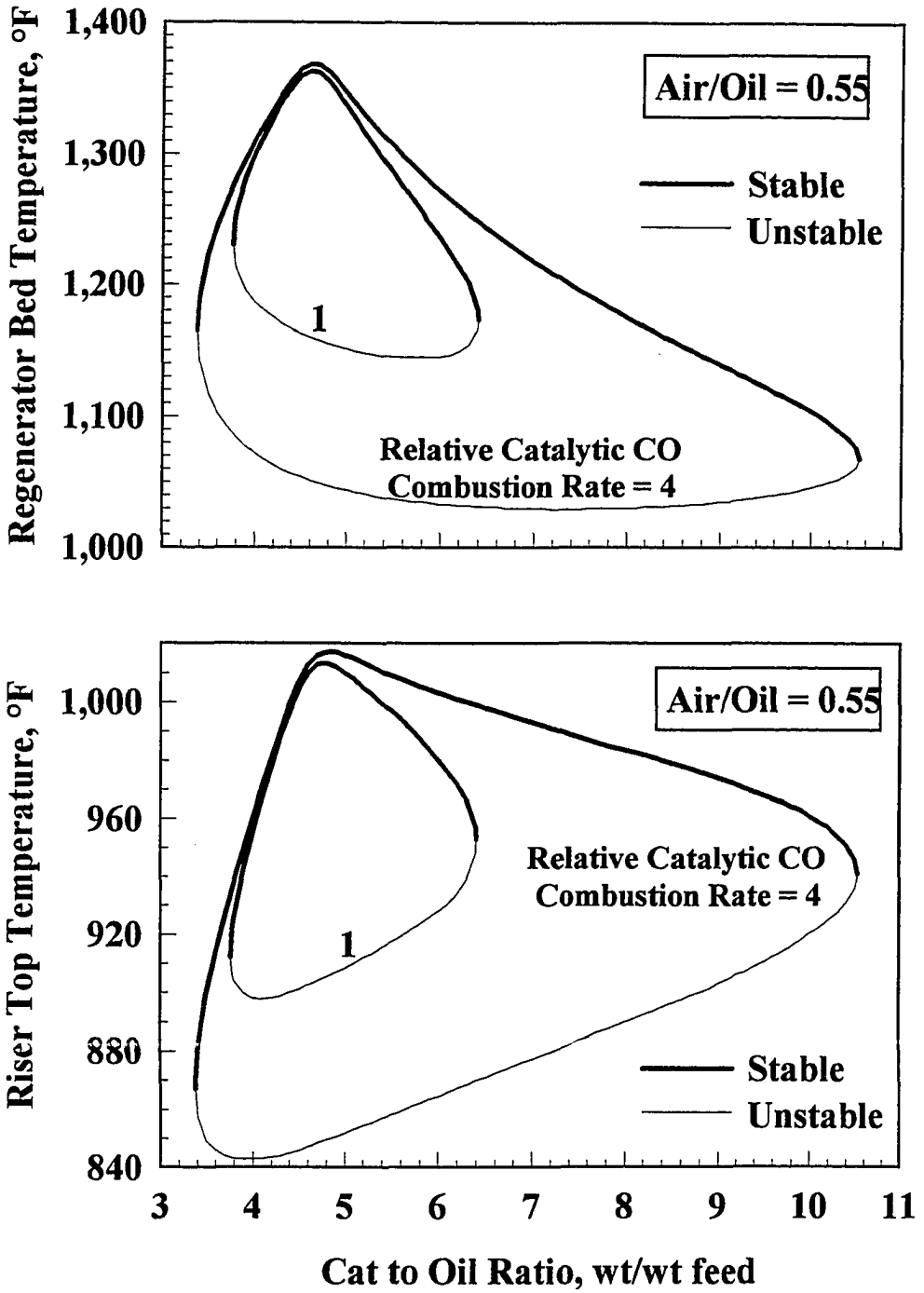

Figure 4-23. Impact of CO Combustion Promoter at Constant Cat/Oil

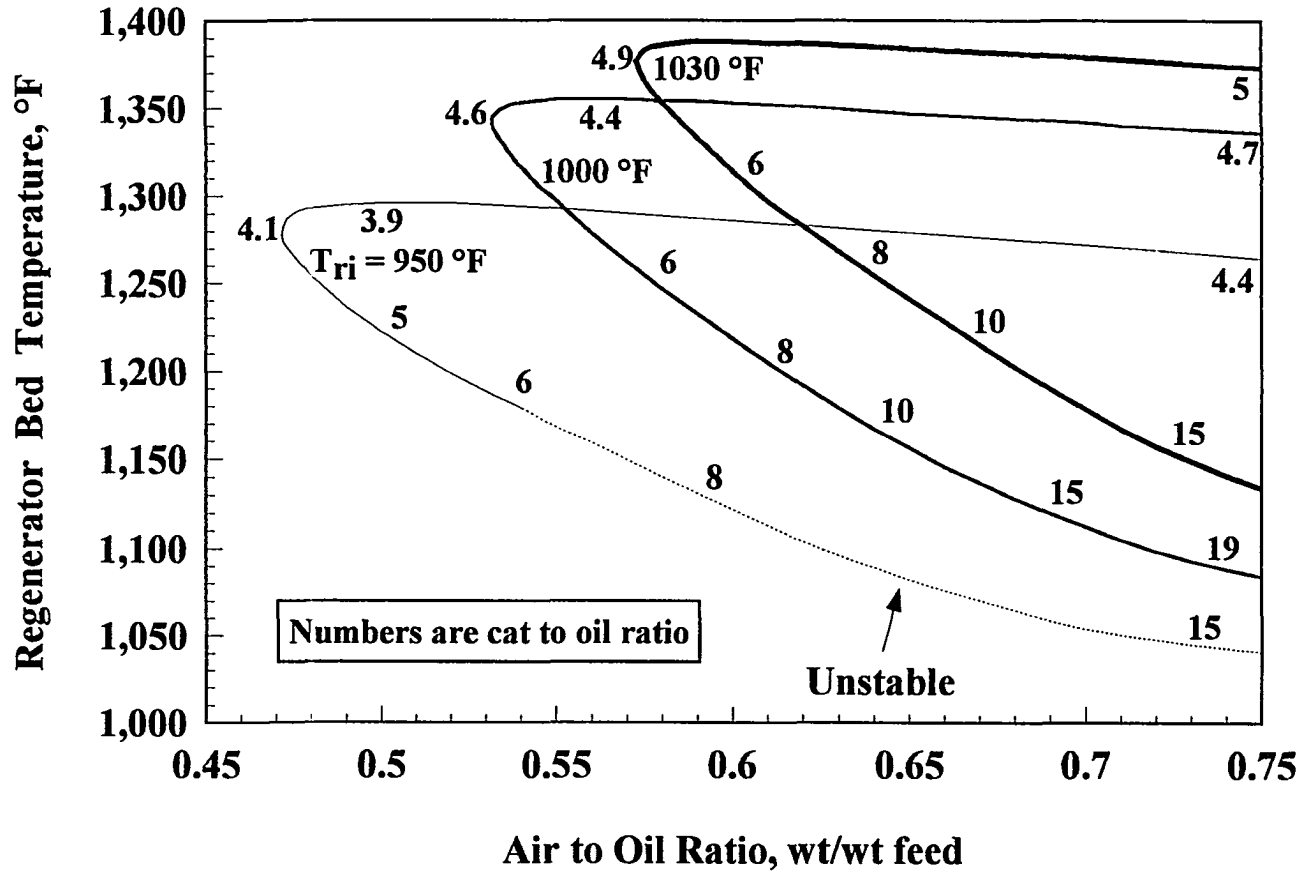

Figure 4-24. Steady-State Performance at Constant Riser Top Temperature

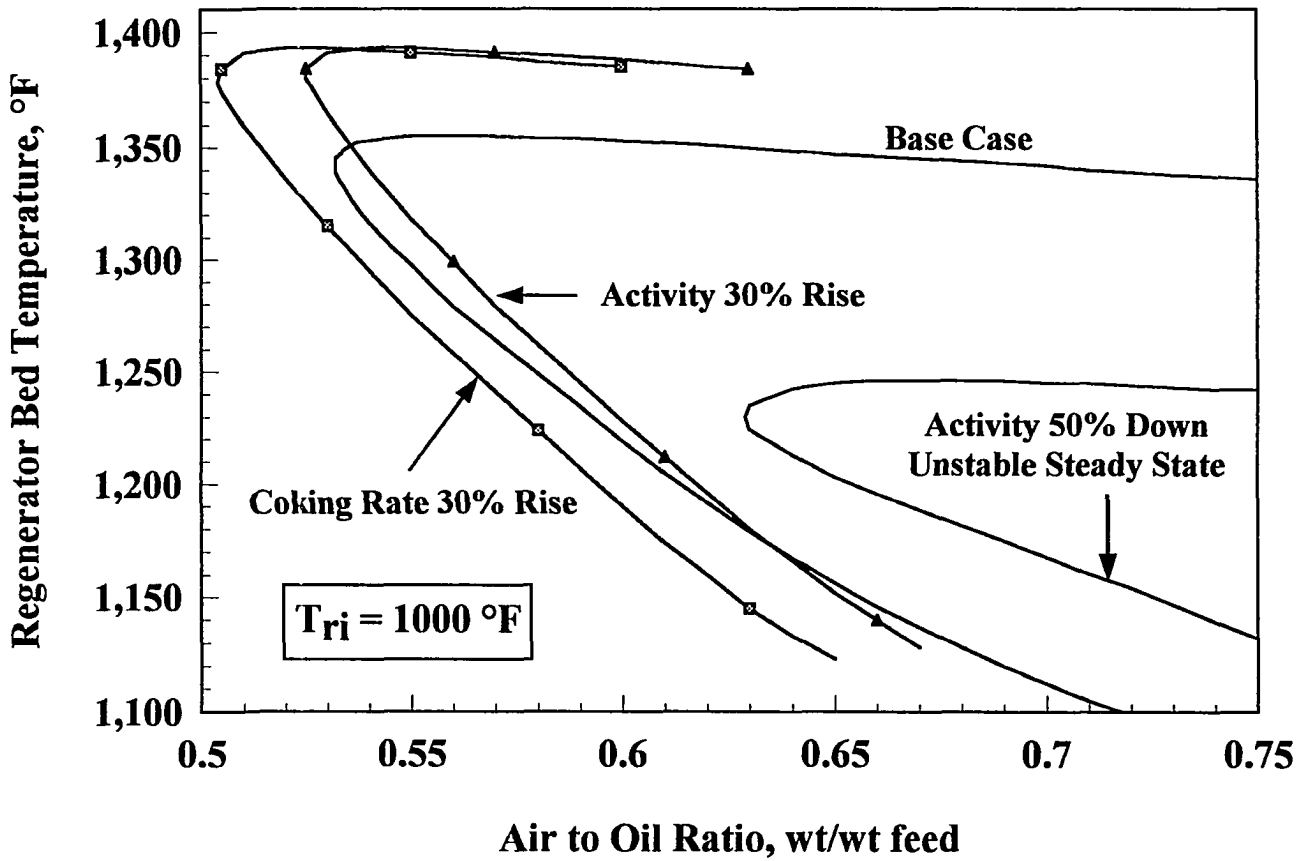

Figure 4-25. Impact of Activity and Coking Rate at Constant Riser Top Temperature

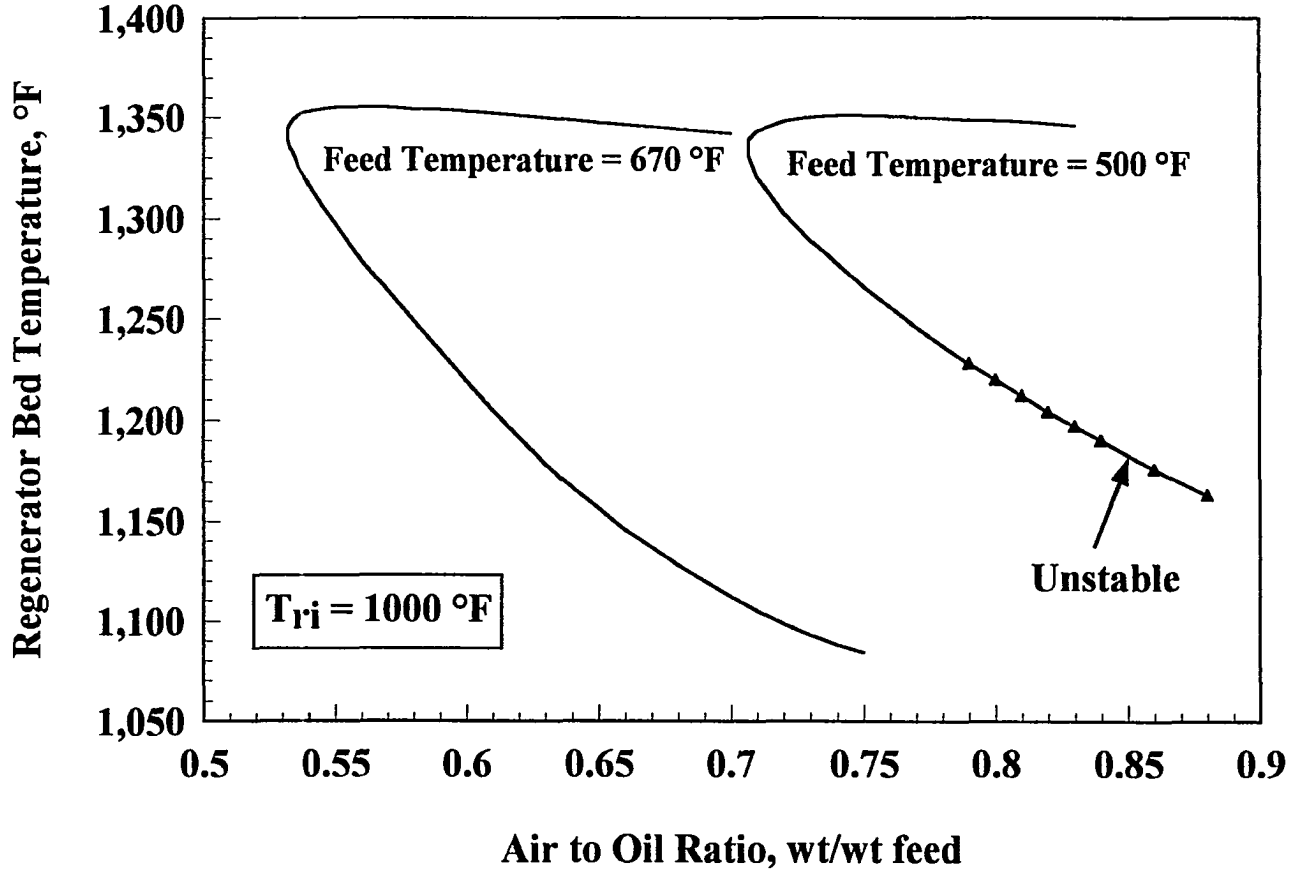

Figure 4-26. Impact of Feed Temperature at Constant Riser Top Temperature

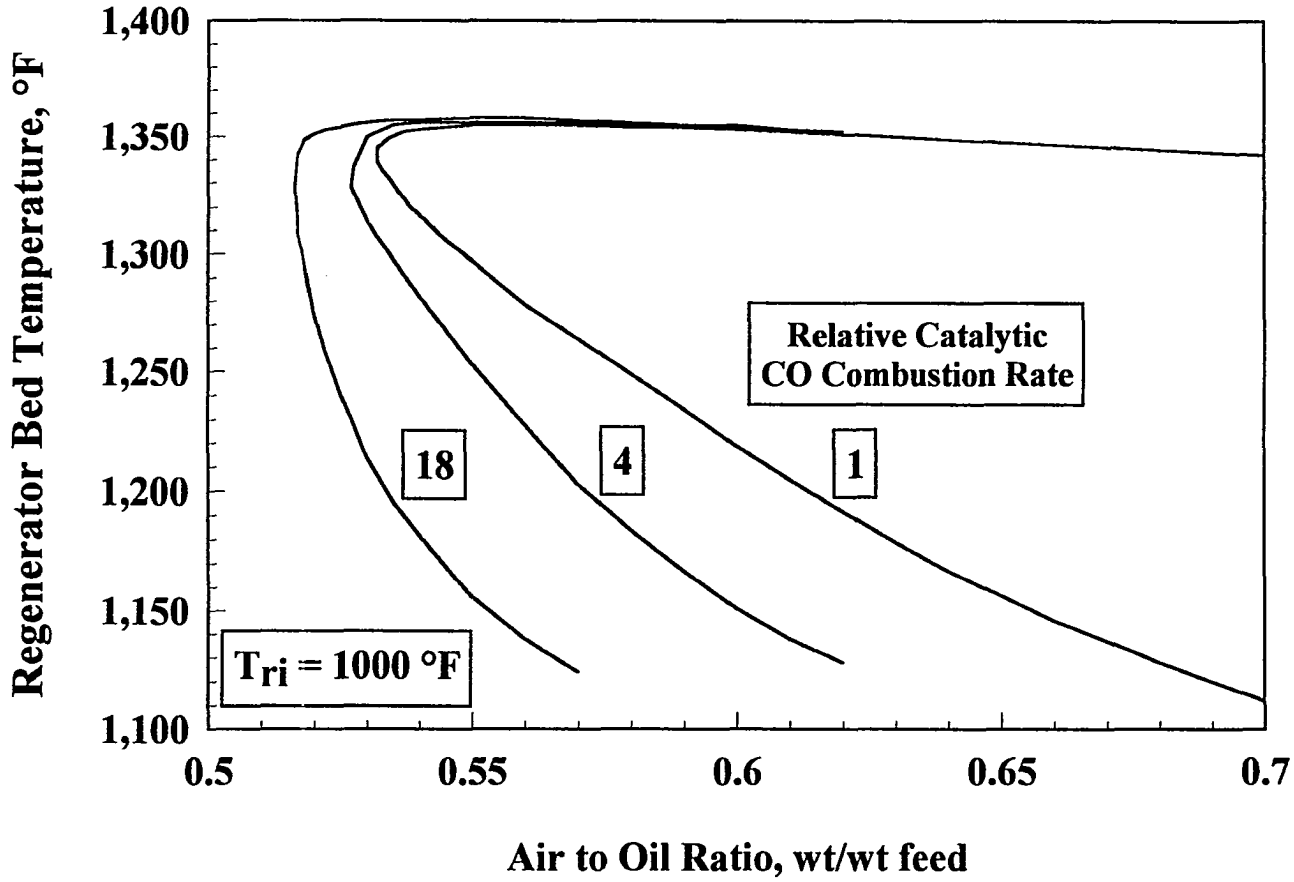

Figure 4-27. Impact of CO Combustion Promoter at Constant Riser Top Temperature

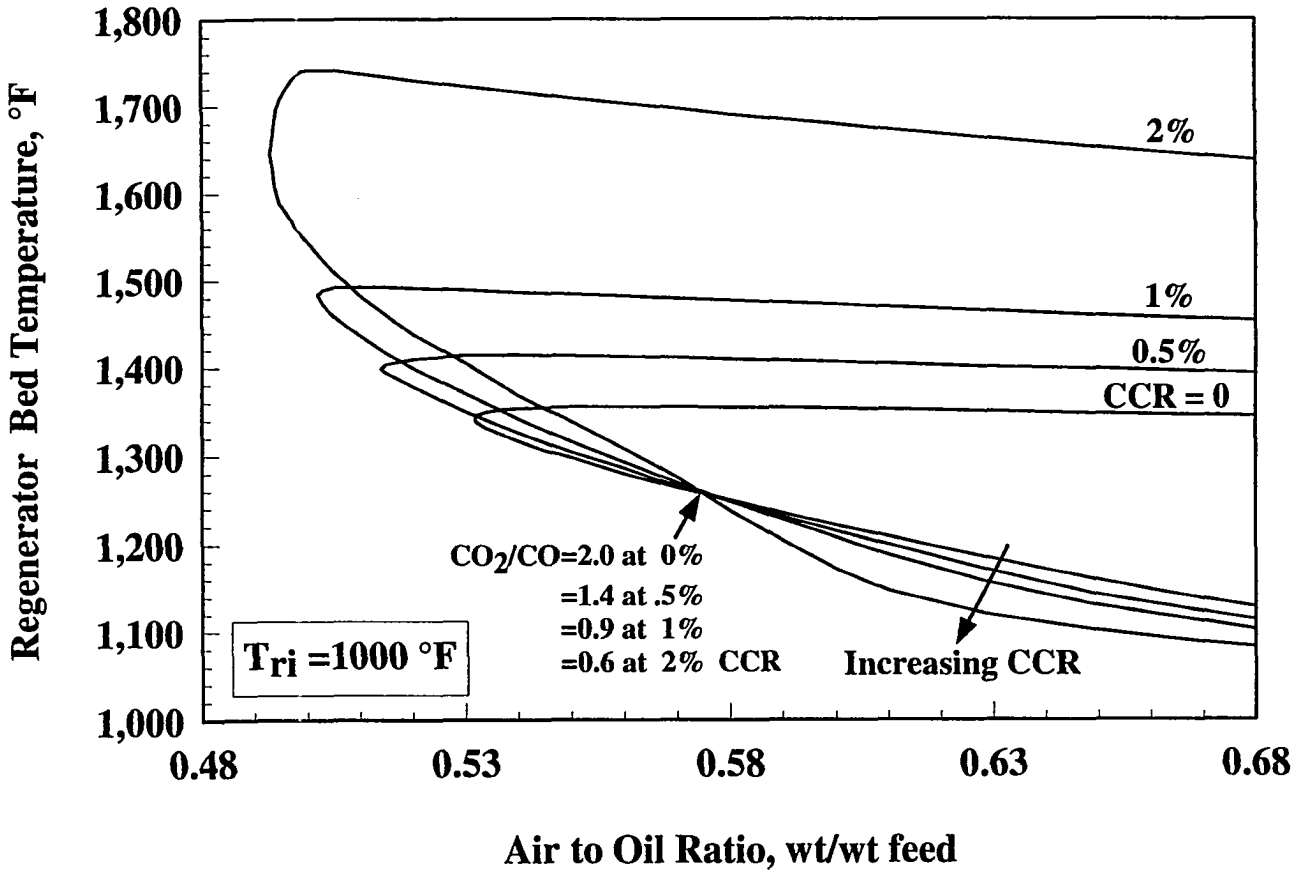

Figure 4-28. Impact of CCR at Constant Riser Top Temperature

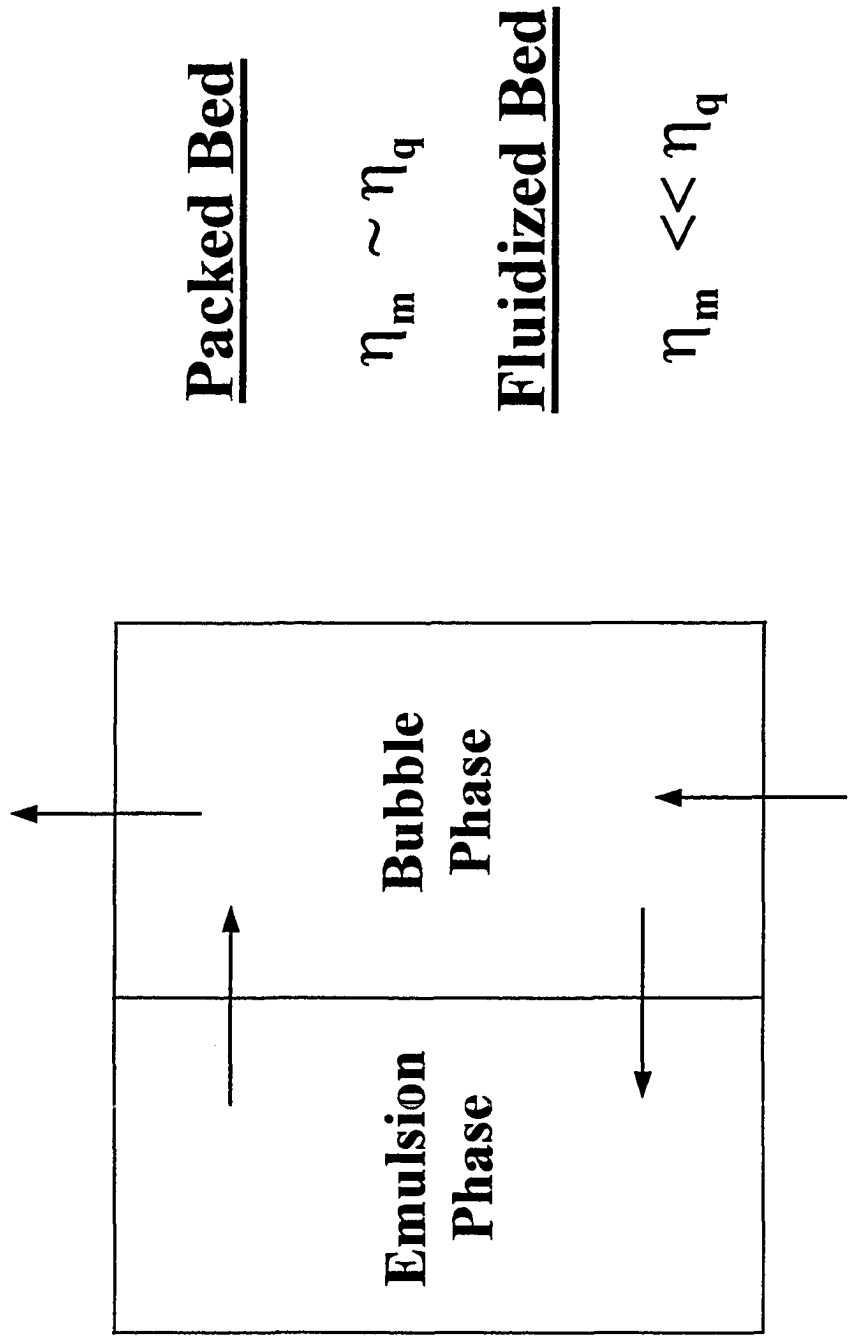

Figure 4-29. Two Phase Fluidized Bed Model

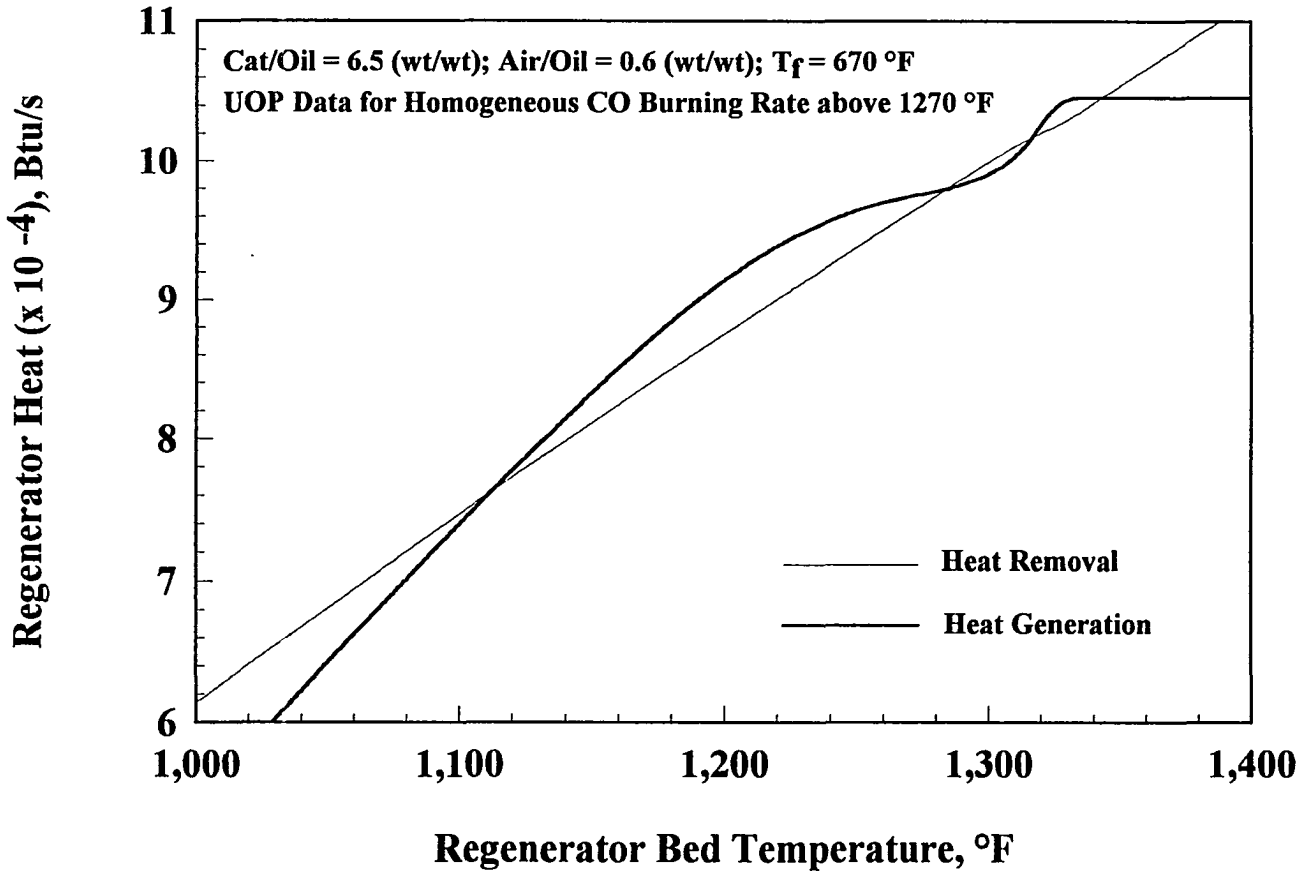

Figure 4-30. Five Steady States in FCC

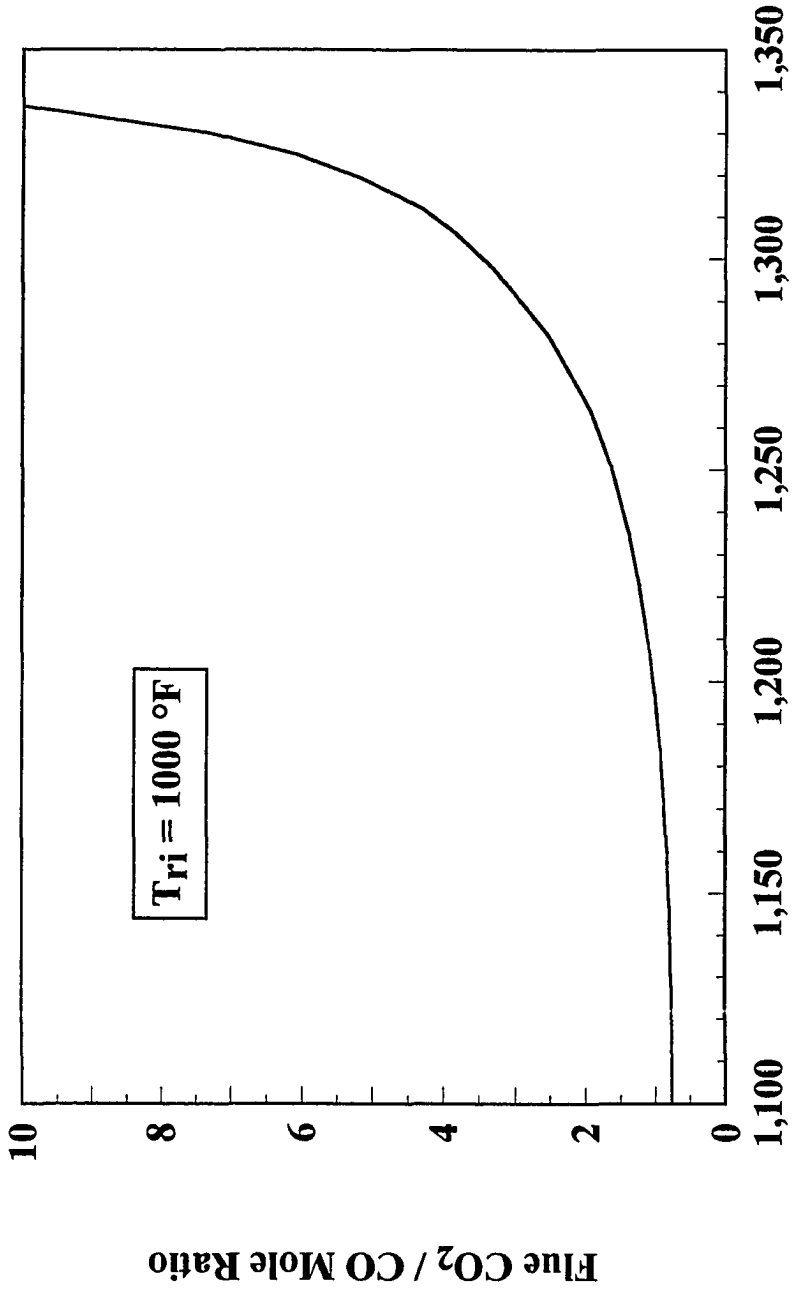

Figure 4-31. Typical CO_2/CO Ratio as Function of T_{reg}

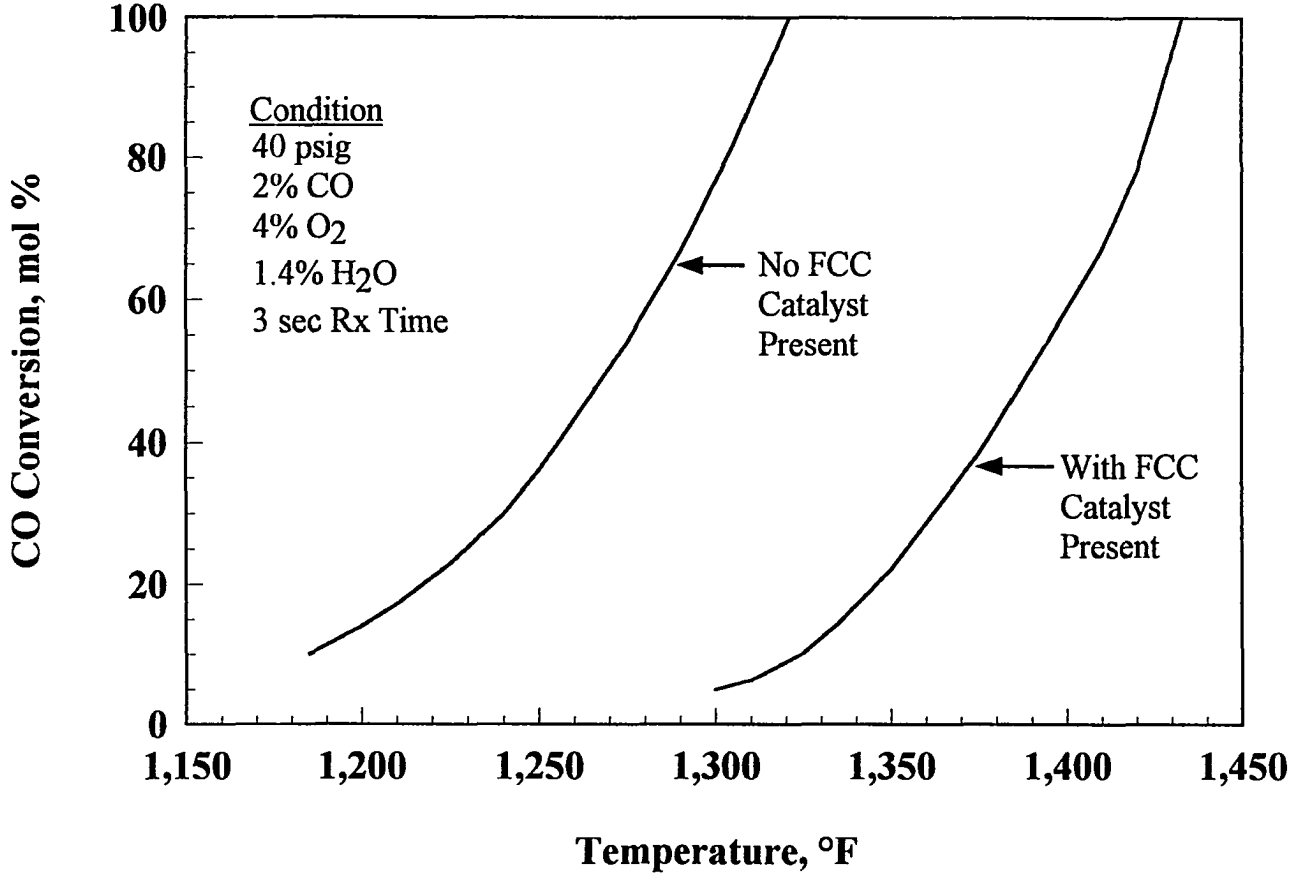

Figure 4-32. Effect of Catalyst on CO Burning Rate, from UOP Data (Upson et al., 1993)

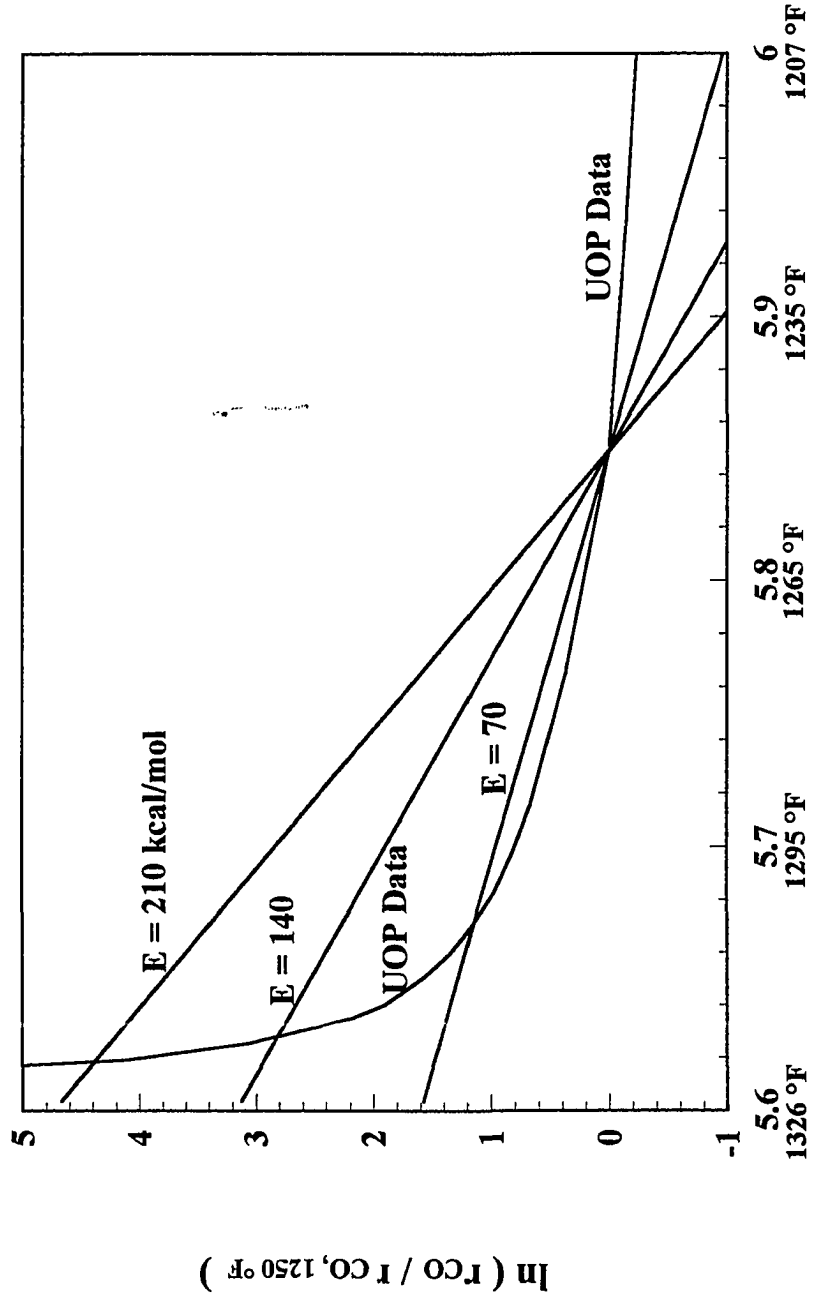

Figure 4-33. Effect of Homogeneous Activation Energy on CO Reaction Rate

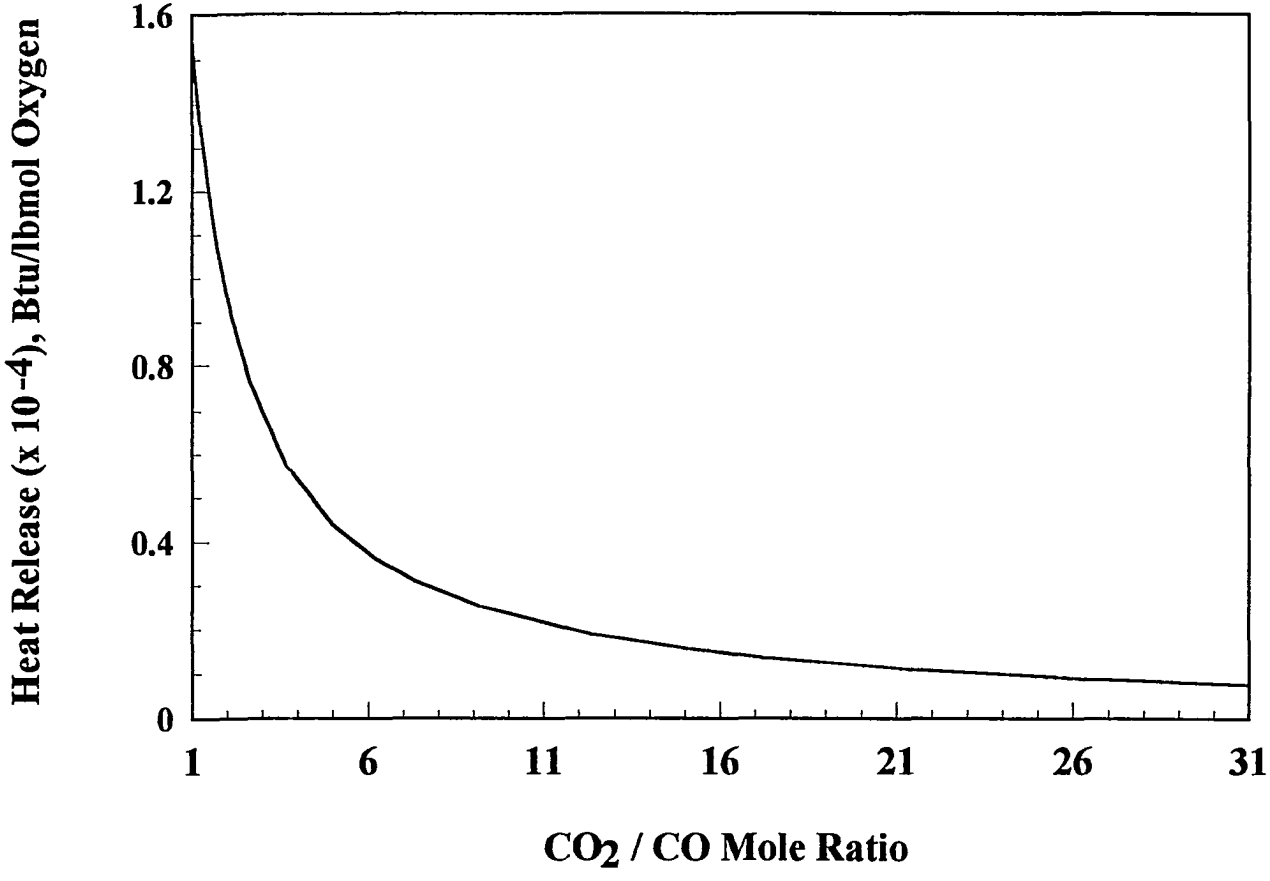

Figure 4-34. Incremental Heat Release from Potential to Full CO Combustion

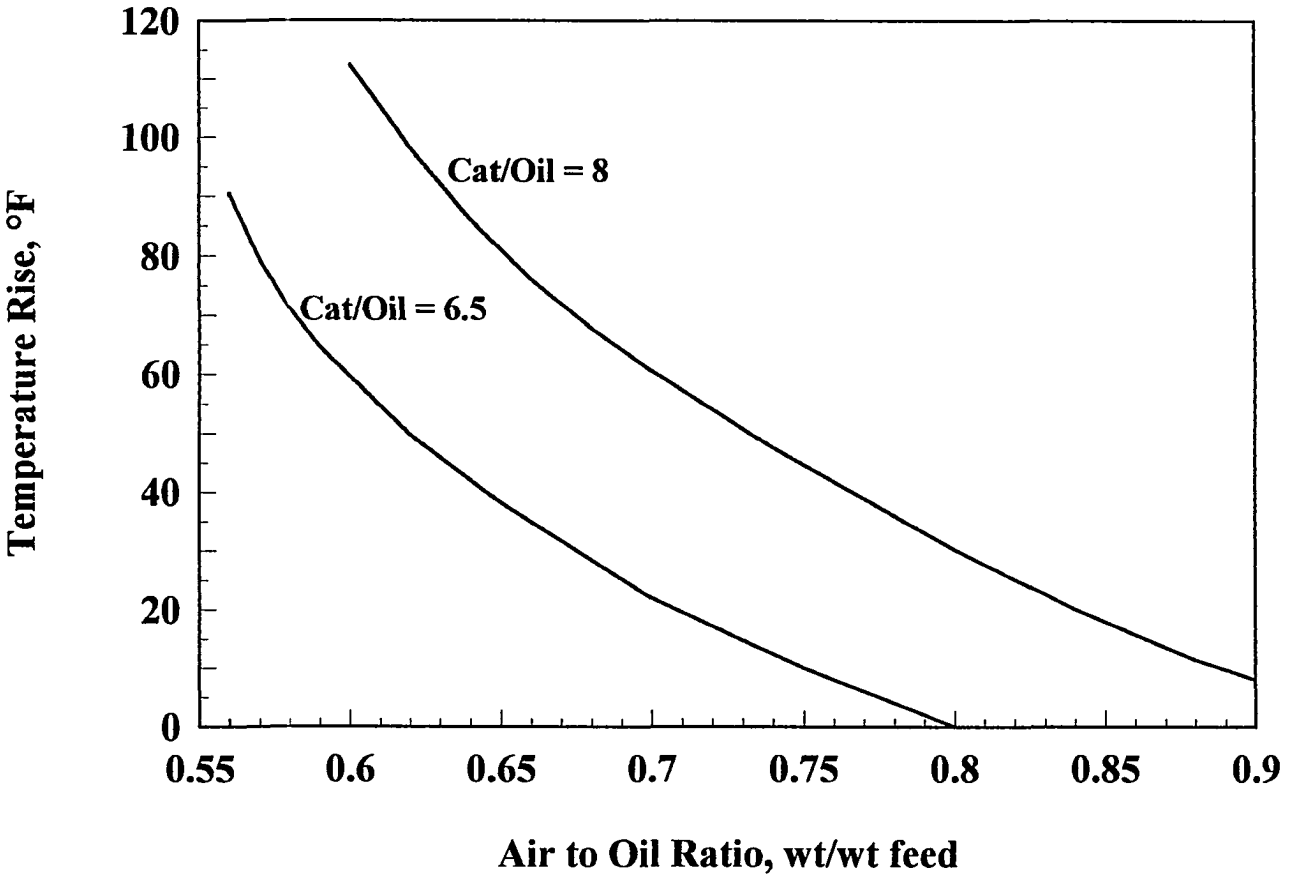

Figure 4-35. Temperature Rise in Regenerator due to Complete CO Combustion

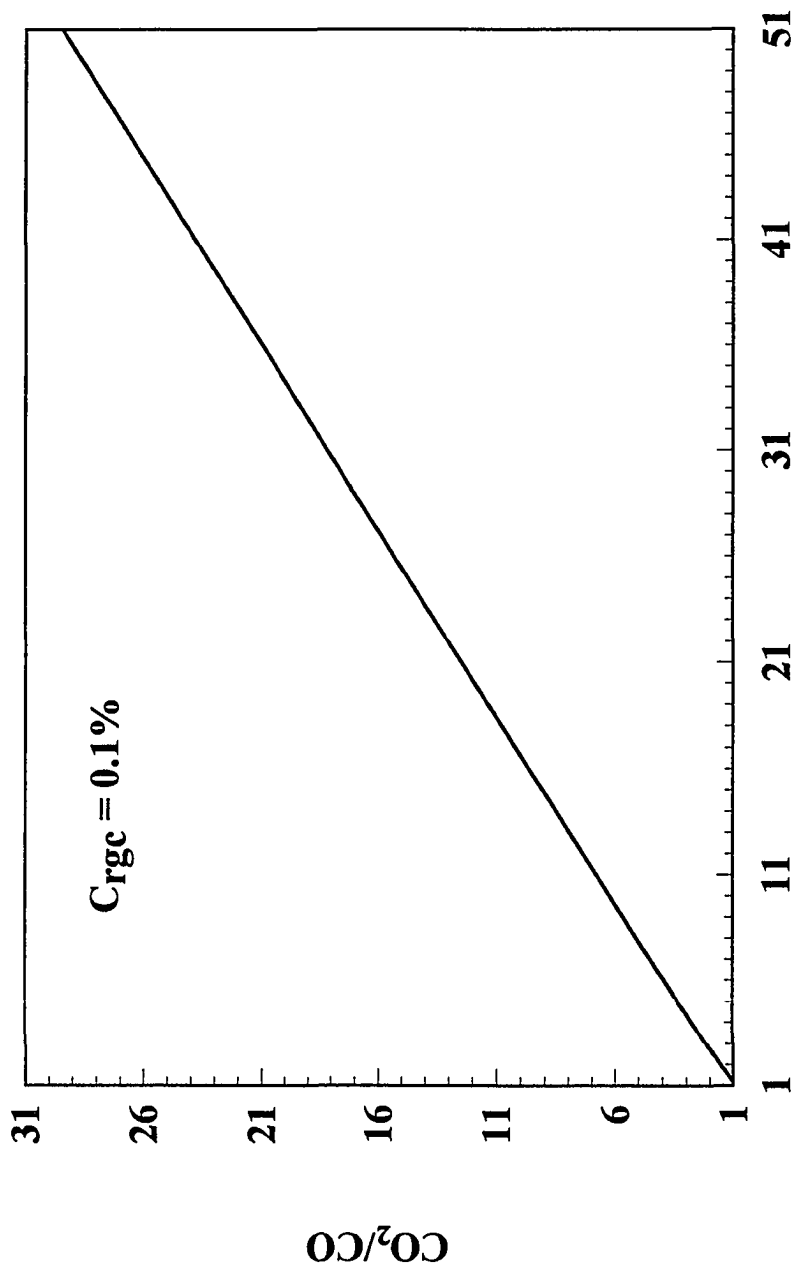

Figure 4-36. Effect of CO Combustion Rate on Ratio of CO_2 to CO

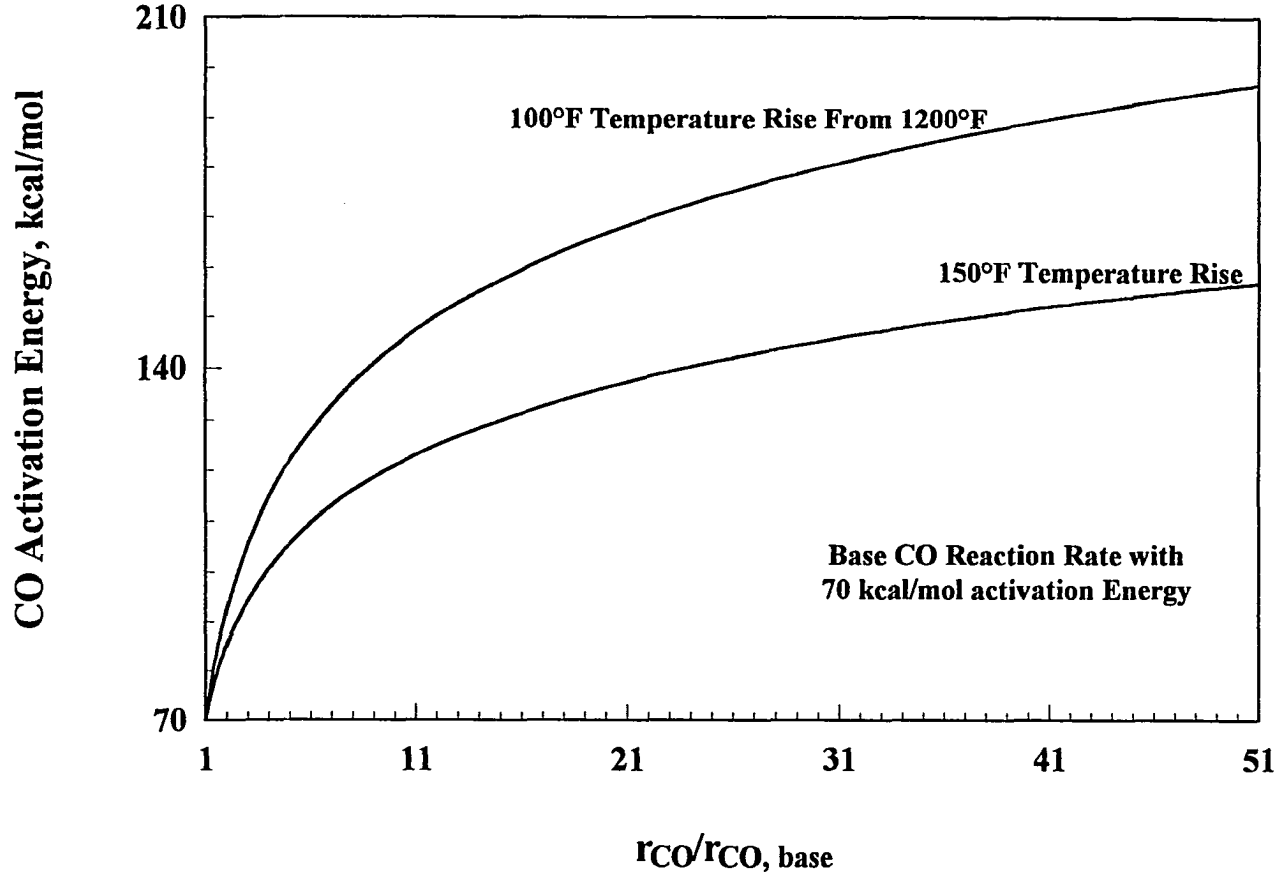

Figure 4-37. Effect of CO Combustion Activation Energy on CO Reaction Rate

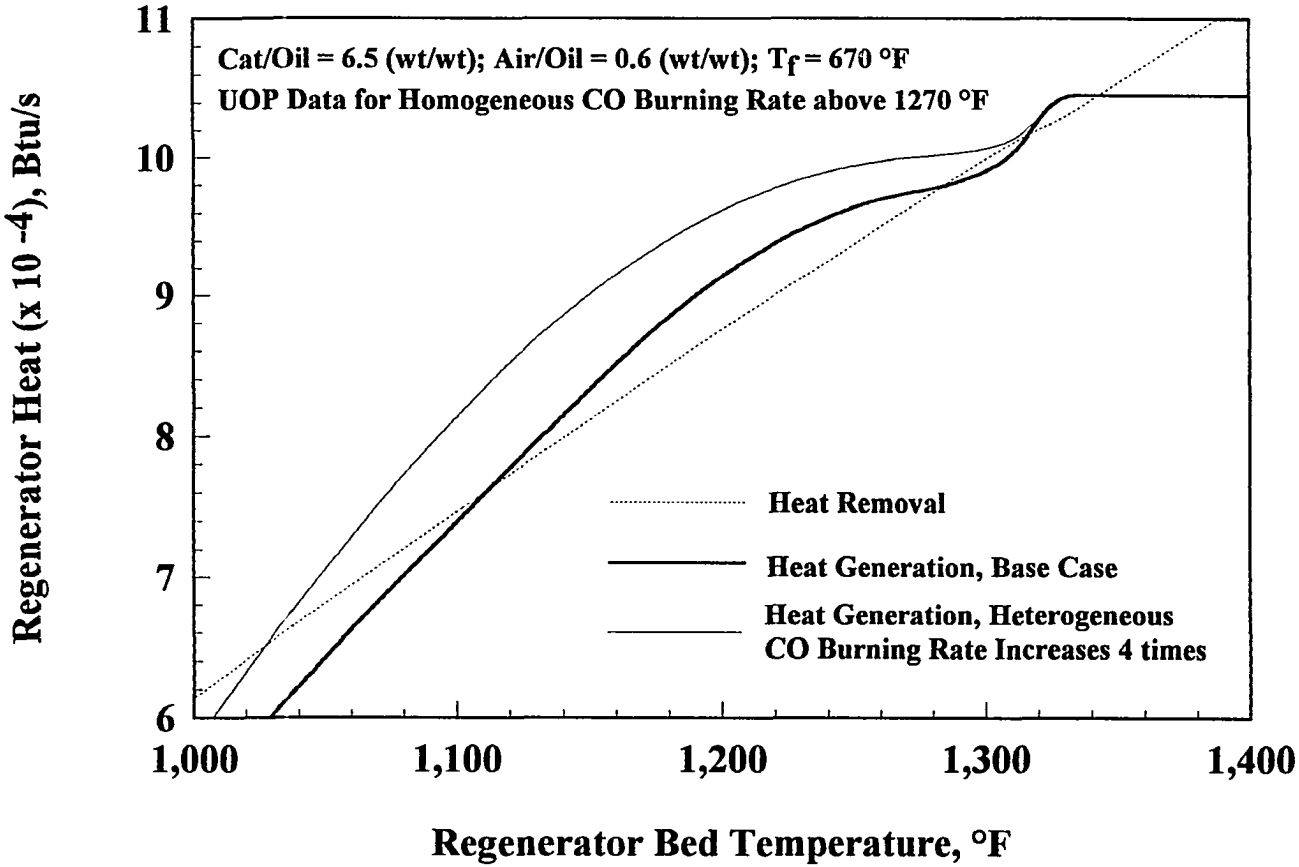

Figure 4-38. Effect of CO Combustion Promoter on Multiple Steady States

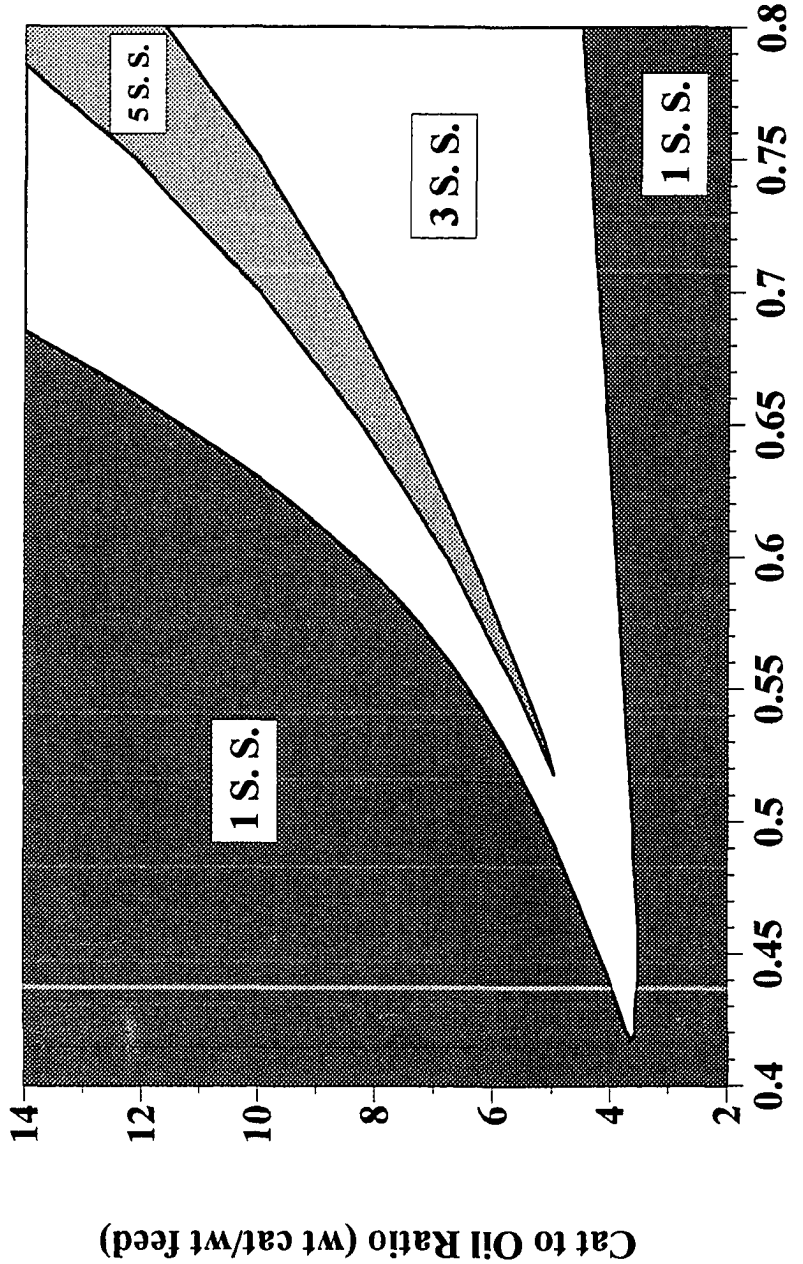

Figure 4-39. Five Steady-State Map with UOP Data

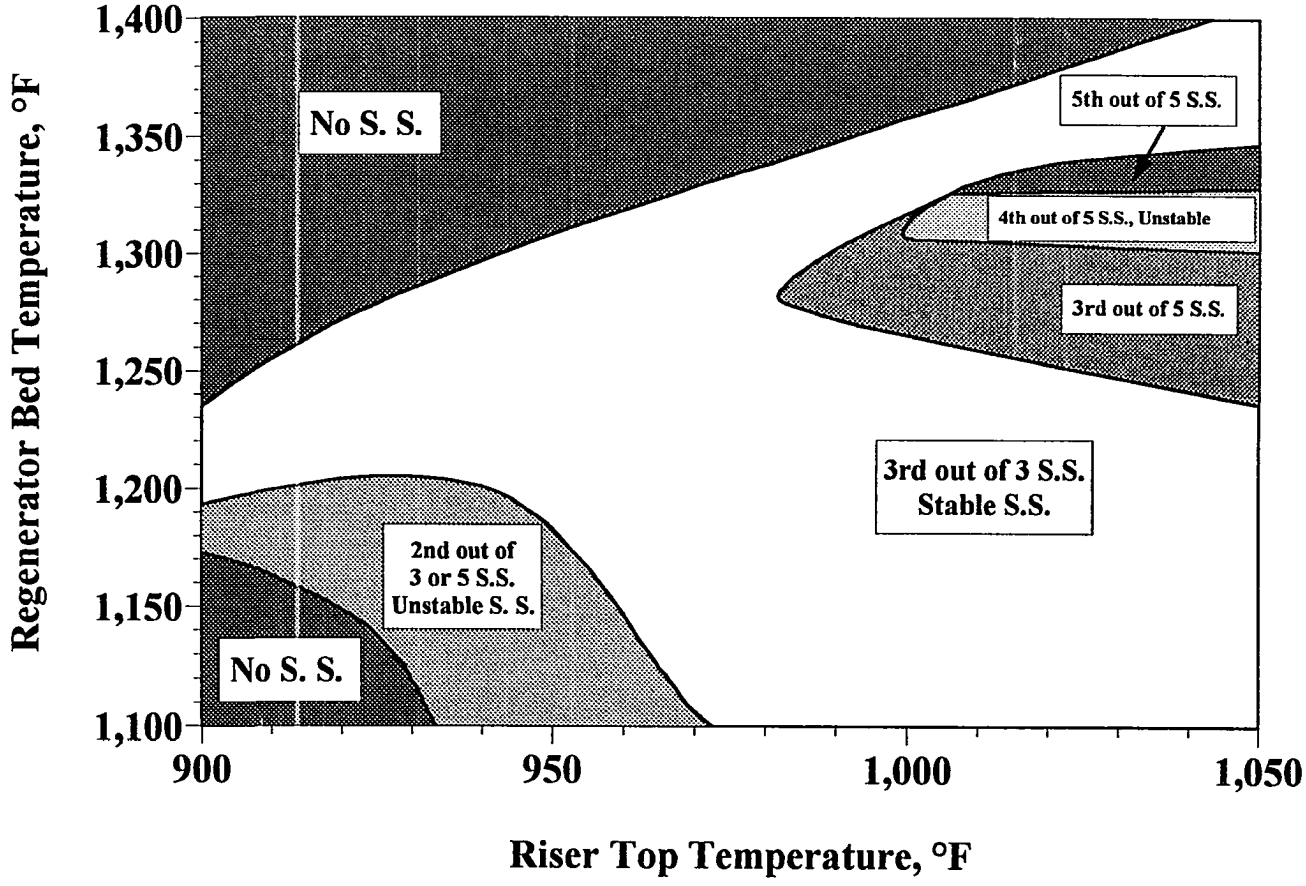

Figure 4-40. Permissible Five Steady-State Operating Map with UOP Data

CHAPTER FIVE

FCC TRANSIENT PERFORMANCE STUDIES

In considering how to devise the control scheme and controller, a priori knowledge of the dynamic response features of the system is highly desirable and very important. Knowing the dynamic features of a system is also a prerequisite for a better design of process control that keeps the process being operated effectually at optimum conditions. Using FCC dynamic model, which has been developed in Chapter three, we could study its dynamic features. Therefore, a good dynamic control design could be made very well.

5.1 FCC Dynamic Features in Time Domain

To demonstrate some dynamic features of the FCC system, several dynamic runs are presented here which include open or close loop operation. The FCC dynamic model developed in Chapter three was used to simulate these features at some typical steady state.

The dynamic model has been translated into the FORTRAN code for simulating the FCC process. LSODE software package was used for solving ordinary differential equations in dynamic simulation. For a closed-loop simulation conventional control scheme was applied (see Figure 1-2). Discrete digital PI feedback controllers were used for the simulation. Because their sampling interval was set to two second, compared with FCC system response time, this sampling time was so short that the controllers could be considered as continuous ones.

5.1.1 Basic Operating Conditions for Dynamic Simulation

In dynamic simulation, some basic operating conditions were assumed to keep constant which is the same as those in steady state simulation. Among them were pressures of reactor and regenerator, catalyst holdups in reactor and regenerator which means one catalyst circulation rate throughout the dynamic process, air inlet temperature, feed rate, and so on. Catalyst cooler are also not active in the simulation. Because changes in catalyst activity are much slower than dynamic responses, it can be considered as constant.

In normal operation, the feed temperature and feed composition are invariable. The feed composition is the same as that shown in Table 4-2. Table 5-1 shows some typical operating conditions for the dynamic simulation.

Table 5-1. Typical Operating Conditions for Dynamic Simulation

Air Inlet Temperature T_{air} = 270 °F	Regenerator Pressure P_{rg} = 29.6 psia
Regenerator Holdup $W_{reg} = 2.74\times10^5$ lb	Standpipe Holdup W_{sp} = 3565 lb
Feed Temperature T_f = 670 °F	Feed Flowrate F_{tf} = 131 lb/s
Reactor Holdup $W_{rs} = 1.0\times10^5$ lb	Oil Gas in the Riser y_{oil} = 1

5.1.2 FCC Dynamic Features

This section will show some dynamic features of simulated FCC under open or close loop. The initial steady-state values of process variables are given in Table 5-2.

Table 5-2. Values of Process Variables for a Nominal Steady State

T_{ri} = 1000 °F	C_{sc} = 0.85 % wt/wt cat	Cat/Oil = 6.47 wt/wt feed
T_{reg} = 1250 °F	C_{rgc} = 0.065% wt/wt cat	Air/Oil = 0.58 wt/wt feed

5.1.2.1 Open-loop response to a 10% step rise in coking rate

This run simulates an unmeasured disturbance to feed composition. Figure 5-1 shows the open-loop dynamic time responses of the system to a 10% step increase change in feed coking factor, Ψ, at time after five minutes, where R_{h0} changes from 12.5% to 16.5% and N_{h0} changes from 20% to 16%. The performance in Figure 5-1 is analyzed as following.

The increase in coking rate results in a rapid increase in coke deposition on the catalyst in the riser. Therefore spent coke content, C_{sc}, increases rapidly. The conversion of feed, gasoline yield and wet gas decrease because of more rapid deactivation of catalyst caused by more coke deposition on the catalyst. The riser top temperature, T_{ri}, increases rapidly because of lower conversion with endothermic reaction. However, all these changes are short lived.

The additional coke is transported to the regenerator on the spent catalyst resulting in higher combustion rate of coke in the regenerator and thus an increase in regenerator temperature, T_{reg}. However, this increase in combustion rates is insufficient to burn off all additional coke arriving from the reactor, and so regenerated coke concentration on the catalyst, C_{rgc}, increases. Consumption of oxygen increases, therefore oxygen concentration,

$C_{O2,cyc}$, decreases because of additional amount of coke. As a direct function of oxygen concentration, Temperature rise across the regenerator cyclones, T_d, also declines. This make the stack gas temperature, T_{sg} decrease. Stack CO concentration, $C_{CO,sg}$ increases because of no enough oxygen to make CO oxidize further. So stack CO_2 decreases with the increase of CO. As T_{reg} increases, combustion rate increases and more of the coke transported from the reactor are consumed. The C_{rgc} peaks and then declines slightly.

Increasingly hotter regenerated catalyst is transported back to the riser, affecting its energy balance. As riser temperature increases, conversion of gas oil, yield of gasoline and wet gas increase due to higher cracking rates.

From the figure, it can be seen that the response time of regenerator temperature dominates that of most output variables. Thus, it is a slow dominant variable. The moderately slow response is sometimes beneficial for one has sufficient time to correct mistakes and prevent the unit from wind-down.

5.1.2.2 Open-loop response to drop in intrinsic coking rate

In this simulation run, only intrinsic coking rate (see equation 3-33) is altered rather than feed property. Figure 5-2 gives the time responses to 20% and 30% step decrease changes in intrinsic coking rate. It shows that the system goes to a new steady state with a lower temperature at 20% drop in coking rate, but winds down to a cold steady state at 30% drop in coking rate. This depicts that the FCC system may become unstable if lighter feed is treated in operation. This situation might be avoided if suitable feedback control was used.

5.1.2.3 Time response to a 2% step rise in air flow rate

Figure 5-3 describes the time responses to a 2% step increase change in air flow rate without and with reactor control where T_{ri} is controlled by F_c to keep constant. Two kinds of PI controller are used (controller A and B). The control action of the controller A is represented by following formula:

$$F_c = F_{c,ss} + K_c(-\Delta T_{ri}) + \frac{K_c}{\tau_I}\int_0^t(-\Delta T_{ri})dt \tag{5-1}$$

where

$$\Delta T_{ri} = T_{ri,sp} - T_{ri} \tag{5-2}$$

And the control action of the controller B is,

$$F_c = F_{c,ss} + K_c\Delta T_{ri} + \frac{K_c}{\tau_I}\int_0^t \Delta T_{ri}dt \tag{5-3}$$

K_c and τ_I can be determined by using Ziegler-Nichols (1942) tuning method. For the regenerator and reactor closed-loop operation, controller B is suitable (see Table 4-5). But when regenerator leaves open, it will cause the system going to complete CO combustion.

If controller A is applied, the system can still operate in partial CO combustion. Obviously, the sign of steady-state gains changes. This has been explained in Chapter four (see Figure 4-24 and 4-19).

5.1.2.4 Open-loop response to a 20°F step drop in feed temperature

This simulation run which is shown in Figure 5-4 demonstrates the big effect of feed temperature on the FCC. Therefore, the feed temperature is a useful manipulated variable in a control system design.

As seen from the figure, As T_f decreases, T_{ri} decreases rapidly due to heat balance in the riser. The conversion of feed, gasoline yield and wet gas also decrease because of lower cracking rates at lower riser temperature. The coke deposited on catalyst declines as feed conversion drop.

Lower reactor temperature makes the regenerator temperature go down through catalyst circulation because whole FCC system must be under heat balance. Lower T_{reg} results in lower coke combustion rate and therefore higher C_{rgc}. Because less coke is transported to the regenerator on the spent catalyst resulting in excessive oxygen, the oxygen concentration goes up. T_d and T_{sg} therefore rise. More oxygen results in higher CO combustion rate in the regenerator. This make CO concentration decrease and CO_2 increase.

When the regenerated catalyst at lower temperature is transported back to the riser, the riser temperature goes to a lower level, and make conversion of gas oil, yield of gasoline and wet gas decrease further due to lower cracking rates.

5.1.3 Process Linearity Analysis

Some variables in FCC have linear features. In partial CO combustion operation, the system responses under the conventional control scheme (see Figure 1-2) display the approximated linear behavior. Figure 5-5, 5-6 and 5-7 show this property.

The open-loop dynamic responses based on the linearized model which is given in Appendix A are also plotted in the figures for comparison between the linear and nonlinear models. One can see that the linear model has the same tendency as the nonlinear one.

After analysis of system behavior in the figures and Table 5-3 we conclude that the FCC has output linear characteristics at this steady-states point. All the control design methods for the linear system can be applied for the FCC at this case.

Table 5-3. Process Gains at Steady-State Point in Table 5-2

Input Variable	$\frac{\Delta \text{Input}}{\text{Input,ss}}$	Process Gain		
		$\Delta T_{reg}/\Delta$Input	$\Delta T_d/\Delta$Input	$\Delta T_{ri}/\Delta$Input
F_{air}	2%	373.1	-660.9	225.6
	4%	363.5	-551.6	220.3
	Linear	354.6	-818.1	215.6
F_c	3%	-0.607	1.159	-0.205
	6%	-0.601	1.298	-0.207
	Linear	-0.565	1.167	-0.173
T_f	-1.5%	1.000	-3.407	0.865
	-3%	1.096	-4.215	0.924
	Linear	0.816	-2.577	0.755

5.2 FCC Dynamic Features in Frequency Domain

When a linear system is subjected to a sinusoidal input, its ultimate response is also a sustained sinusoidal wave. This characteristic constitutes the basic of frequency response analysis. It is another tool for studying the dynamic features of the system.

Frequency response analysis is also a useful tool for designing feedback controller. It helps designer to study the stability characteristics of a closed-loop system, using Bode or Nyquist diagrams of the open-loop transfer function and to select the most appropriate values for the adjustable parameters of a controller.

Generally, the Bode diagrams provide a convenient way to evaluate the frequency response characteristics of a system. Before analyzing the frequency response using Bode plot, a process transfer function is required which is obtained from a linearized model. Therefore, the nonlinear state equations should be linearized.

In FCC process, the major controlled or output variables of interest include regenerator temperature, temperature difference across regenerator cyclones or oxygen concentration in stack gas, riser top temperature and product composition. The manipulated variables include air flow rate, catalyst circulation rate and feed temperature. Many control scheme have been proposed for improving control effects, for instance, Kurihara's (1967) scheme, Lee-Weekman's (1976) scheme in addition to so-called conventional control scheme (see Figure 1-2).

In this work, the FCC frequency response characteristics are studied by using the conventional control scheme. A linearized FCC model given in Appendix A has been used to find the process transfer function, $G_p(s)$ which is determined by the following formula,

$$G_p(s) = C(sI - A)^{-1}B + D \tag{5-4}$$

where **A**, **B**, **C**, and **D** are state-space matrixes. By means of Bode plots of $\mathbf{G}_p$, the FCC frequency response features in a designative steady state can be understood and therefore, let one design a more effective controller.

5.2.1 Frequency Responses in Some Steady-State Points

Frequency responses of simulated FCC are shown here at four different steady states (see Table 5-4). The steady states are open loop stable. This is proven from Table 5-5 as the eigenvalues of their process matrix, **A** have negative real parts. Steady state i and ii are in partial CO combustion operation, and iii and iv in complete CO combustion.

Figure 5-8 shows the frequency responses at steady state i by using Bode plots. In this mode operation, the controlled variable in regenerator can be either T_{reg} or T_d depending on the controlled goal. When T_d is output and F_{air} input, from the figure the process gain is found to be larger than 1 at the crossover frequency where the phase lag is equal to 180°. According to Bode stability criterion a feedback control system may become unstable for the process gain. Therefore, it is worth notice when design this feedback controller. T_f as manipulated variable is feasible in addition to F_{air}. Control set [T_{reg}, F_{air}] looks like first-order system and [T_{reg}, T_f] second-order system.

Figure 5-9 shows the frequency responses at steady state ii. Because this steady state is also in partial CO combustion mode, the frequency responses are similar to those in Figure 5-8.

Table 5-4. Steady-State Points for Simulation

Process Variables	Steady-State Operating Points			
	i	ii	iii	iv
T_f, °F	670	670	670	670
Air/Oil, wt/wt	0.618	0.58	0.56	0.531
Cat/Oil, wt/wt	8.15	6.47	4.43	4.59
T_{ri}, °F	1000	1000	1000	1000
T_{reg}, °F	1200	1250	1355	1342
T_d, °F	191	108	46	112
$X_{O2,sg}$, mol%	0	0	1.23	0
Stack CO_2/CO	1.34	1.91	∞	30
C_{rgc}, wt%	0.1204	0.0648	0.0101	0.0168
C_{sc},wt%	0.8118	0.8508	0.9093	0.9012

Table 5-5. Eigenvalues of the Steady-State Points in Table 5-4

SS	Eigenvalues of Process Matrix, A			
i	-2.341×10^{-4}	-1.148×10^{-2}	$-9.642\times10^{-3}+8.488\times10^{-3}i$	$-9.642\times10^{-3}-8.488\times10^{-3}i$
ii	-2.632×10^{-4}	-9.066×10^{-3}	$-9.364\times10^{-3}+7.345\times10^{-3}i$	$-9.364\times10^{-3}-7.345\times10^{-3}i$
iii	-4.025×10^{-2}	-2.099×10^{-4}	-6.112×10^{-3}	-6.779×10^{-3}
iv	-2.351×10^{-4}	-6.382×10^{-3}	-1.780×10^{-2}	-8.750×10^{-3}

The steady state iii used in Figure 5-10 is in complete CO combustion operation. As mentioned in Figure 4-24, F_{air} cannot be used to control T_{reg} as the control gain is close to zero if reactor is in closed-loop operation. One can use oxygen content in stack gas as controlled variable instead of T_{reg}.

The frequency responses in Figure 5-10 show that the choice of control set [$X_{O2,sg}$, F_{air}] or [T_d, F_{air}] seems to be better than that of [T_{reg}, F_{air}]. In modern FCC's which operate in full CO combustion, CO combustion promoters are always added to the system. T_d therefore close to zero. At this case choice of oxygen content in stack gas as controlled variable is more suitable than T_d. T_f as manipulated variable is still reasonable.

Figure 5-11 shows the frequency responses at steady state iv. The steady state is in full CO combustion operation. Choice of the control set [T_d, F_{air}] is obviously unsuitable at this steady state. We can choose [T_{reg}, F_{air}] or [T_{reg}, T_f]. However, If T_{ri} is in control, we know from Figure 4-24 that control set [T_{reg}, F_{air}] has infinity control gain. Therefore, only the choice of [T_{reg}, T_f] is feasible for regenerator control at steady-state point iv.

5.3 Dynamic Feature of Recycle System

Recycle operation is commonplace in the process industries. The overall dynamics of a process with recycle can be very different from the dynamical responses of the individual units. Because the recycle process is topologically equivalent to a closed loop feedback control system with a negative gain (i.e., positive feedback), it can greatly increase the process response time and often leads to considerable deterioration of plant

dynamics. The previous studies on dynamics and control of recycle system have appeared in the literature [Rinard and Benjamin (1982), Denn (1982), Kapoor et al. (1986), and Taiwo (1986)].

FCC is such a process with a recycle of the catalyst. Therefore, it has a feature that any recycle process behaves. To investigate recycle characteristics in the FCC, a typical input and output set (T_f, T_{ri}) was chosen. A block diagram of the FCC for this set is given in Figure 5-12, From which the process transfer function is easily determined as follows,

$$\frac{\Delta T_{ri}(s)}{\Delta T_f(s)} = \frac{\dfrac{G_{p1}}{1+R_{co}}}{1 - \dfrac{R_{co}}{1+R_{co}} G_{p1}G_{p3}G_{p2}} \tag{5-5}$$

Figure 5-13 gives the Bode plots to show the different responses of recycle and non-recycle system at steady-state point ii in Table 5-4. Here we define "non-recycle" as that T_{reg} is constant, i.e., not a function of T_{ri}. and the transfer function for this system is,

$$\frac{\Delta T_{ri}(s)}{\Delta T_f(s)} = \frac{G_{p1}}{1+R_{co}} \tag{5-6}$$

If non-recycle means that R_{co} is equal to zero, then the riser becomes a plug-flow pipe and we have,

$$\frac{\Delta T_{ri}(s)}{\Delta T_f(s)} = G_{pl} = e^{-\frac{A_{ris}H_{ris}\rho}{F_{tf}}s} \tag{5-7}$$

In Figure 5-13, we neglect the dead time in the riser. This is reasonable because in this case the residence time in the riser is about 3 seconds and results in less effects on dynamics among the interested frequency range.

The effect of catalyst recycle on the FCC dynamics can be examined from the figure. We find that the response in the recycle case has a higher steady-state gain and longer characteristic time than that in the non-recycle case. Therefore, control design for the reactor riser in the FCC is greatly different from that in the tubular reactors.

5.4 Results and Discussion

In this chapter we are concerned with two specific aspects of FCC dynamics. One is time response, the other is frequency response.

Open or partially closed loop time responses are studied. It is found that some disturbances, e.g., feed property, may make system be unstable and wind down at certain condition. Open-loop response is different from partially closed-loop response. This is due to the tight interaction between the regenerator and the reactor. All these features have to be considered in control design.

Figure 5-5 to 5-7 demonstrate that the FCC has output linear property at some partial CO combustion operating point. One can use linear control theory to design controller.

Frequency response is also a powerful tool for dynamic feature analysis and for feedback control design. In this work Bode diagrams of Figure 5-8 to 5-11 are used to represent the frequency response characteristics of the FCC system at four different steady states.

We conclude that at different steady state different controller has to be design for satisfying the control goal. Closed-loop stability of the system is also understood from the plots. We find that a feedback control system may be unstable for the process gain if T_d is a controlled variable and F_{air} is a manipulated variable.

The dynamics of the FCC with recycle of catalyst are equivalent to those of a system with a positive (negative gain) feedback controller. The general effect of recycle as shown in Figure 5-13 is to increase the steady-state gain and the dominant system time constant.

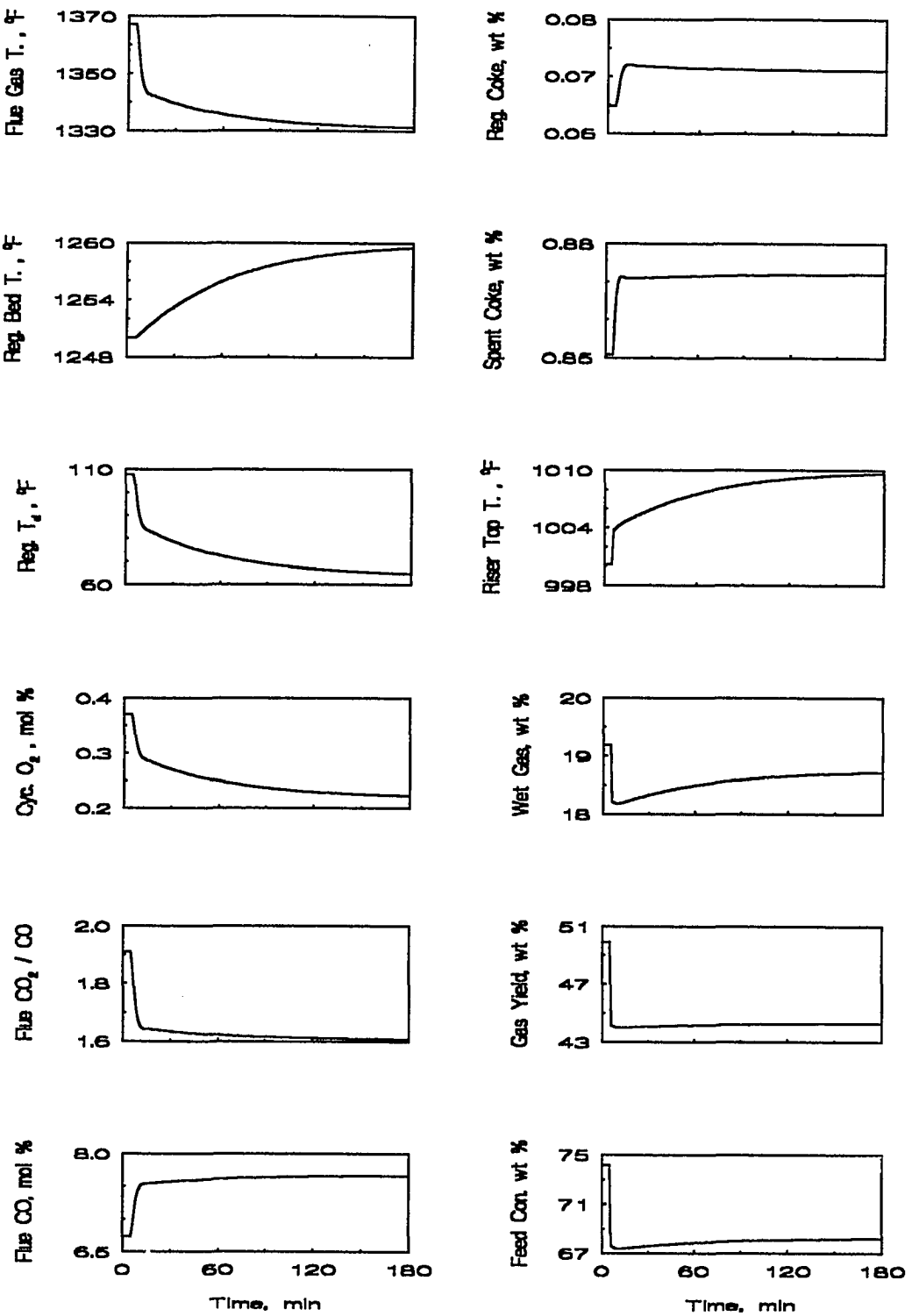

Figure 5-1. Open-loop Responses to 10% Step Rise in Coking Rate

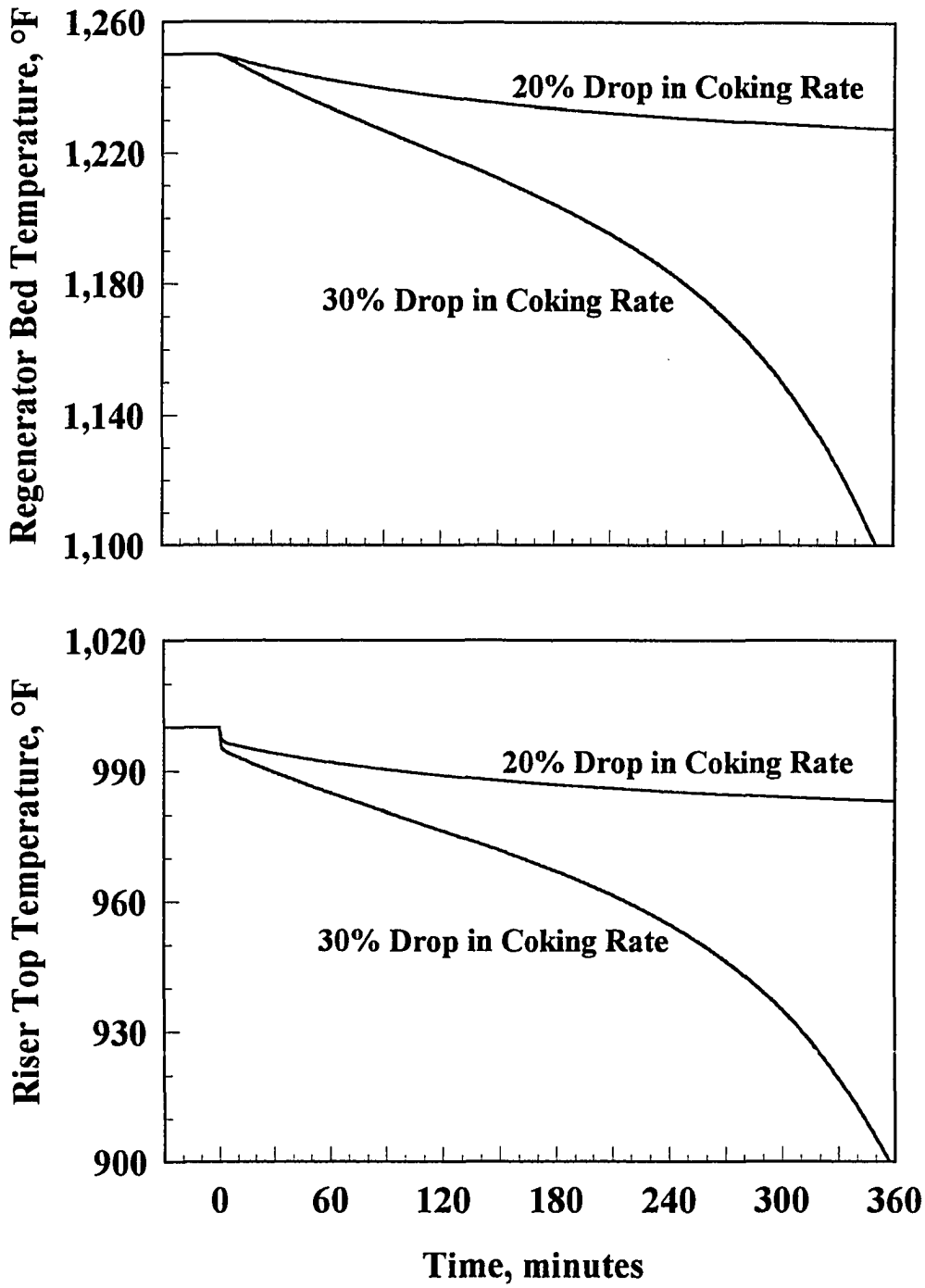

Figure 5-2. Open-loop Time Responses to Decreases in Relative Coking Rate

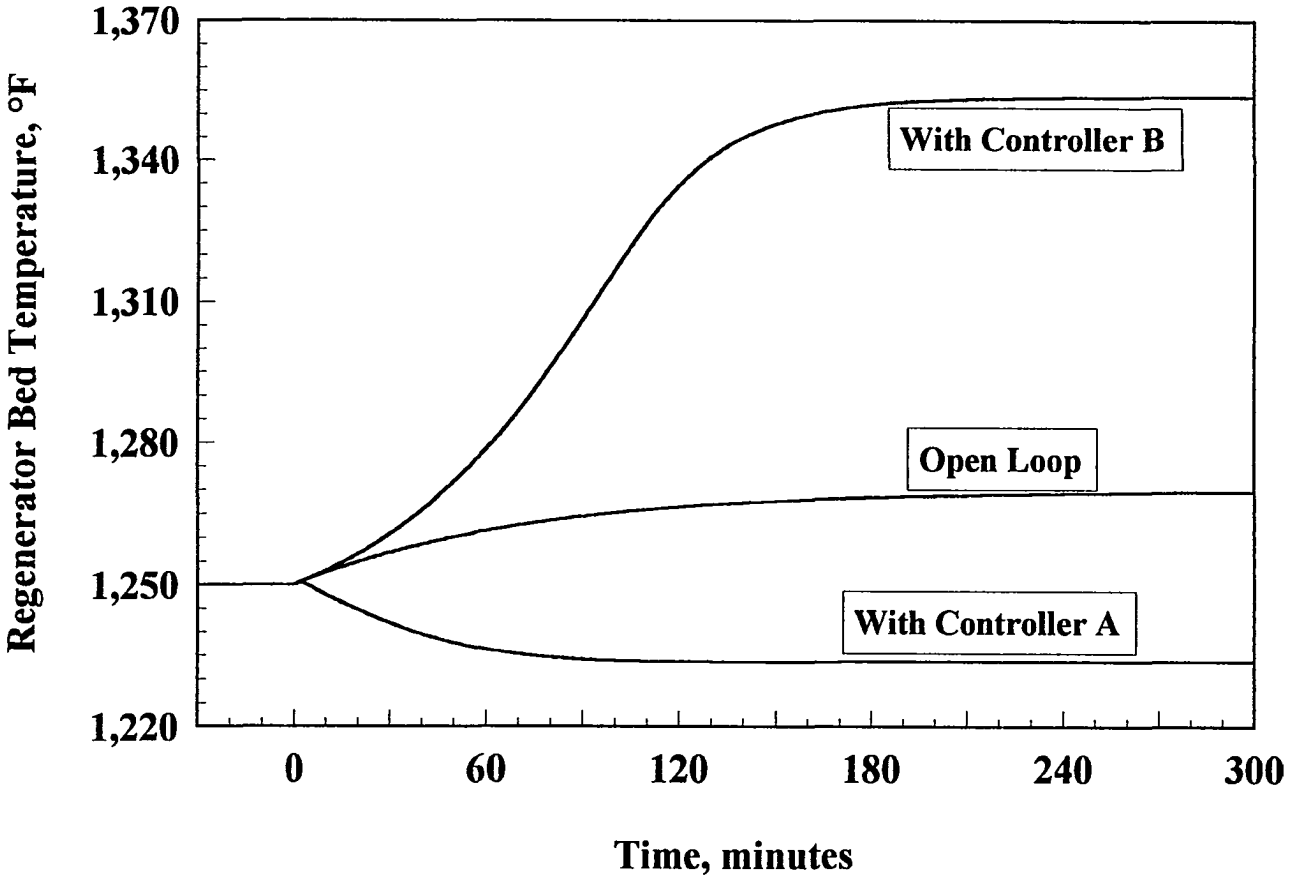

Figure 5-3. Time Responses to 2% Step Increase in Air Flow Rate

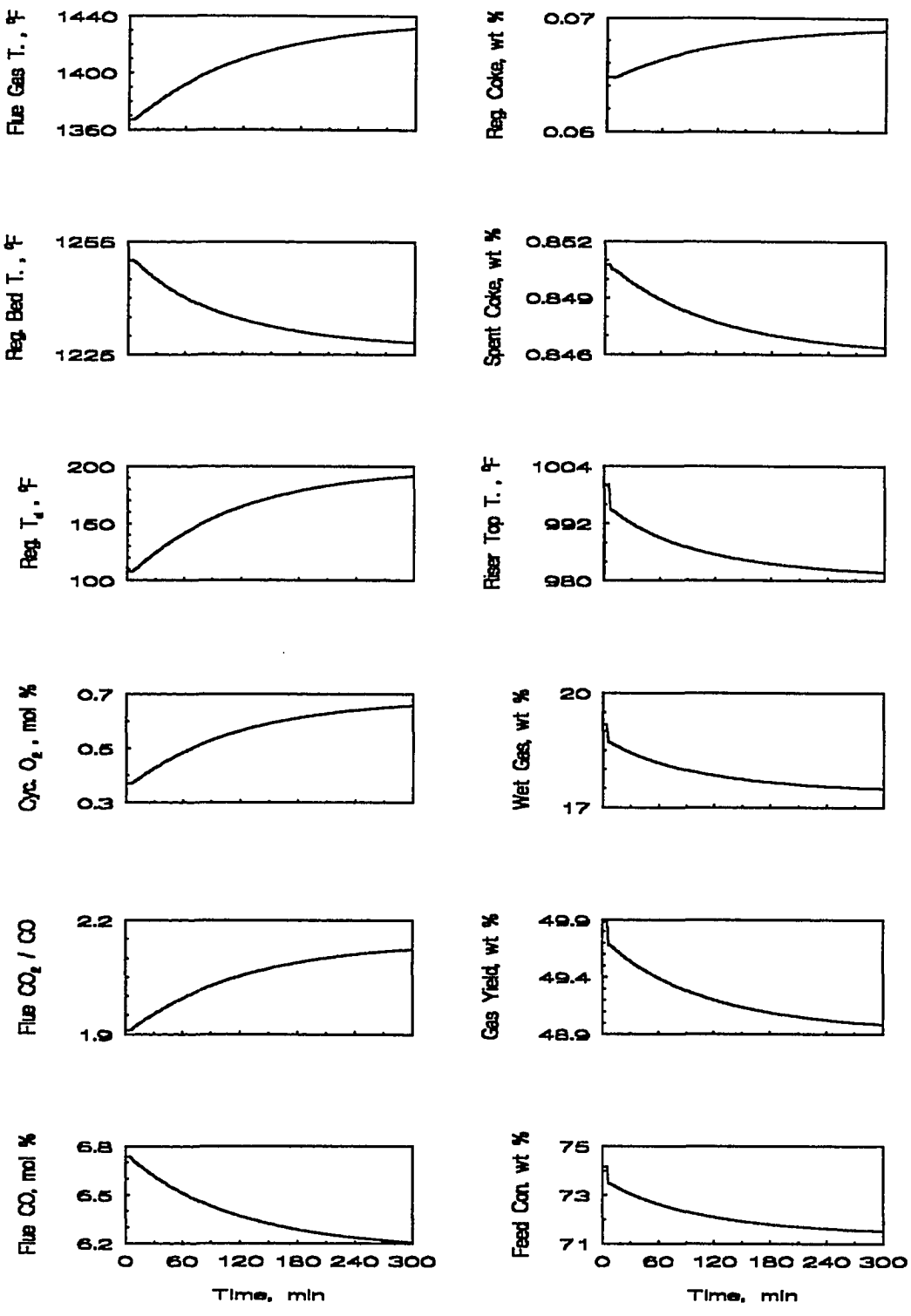

Figure 5-4. Open-loop Responses to 20°F Step Drop in Feed Temperature

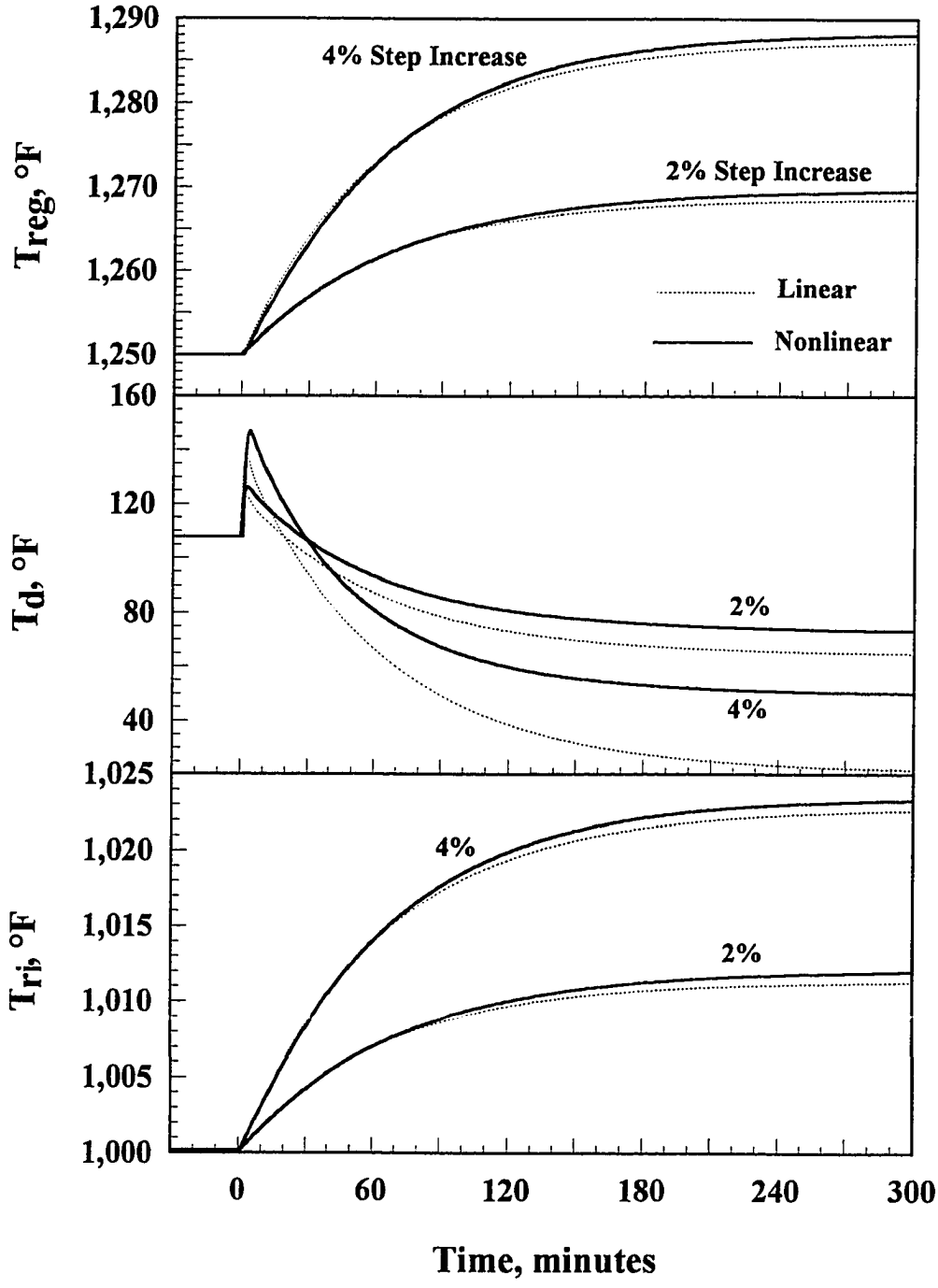

Figure 5-5. Dynamic Responses to Step Increases in Air Flow Rate

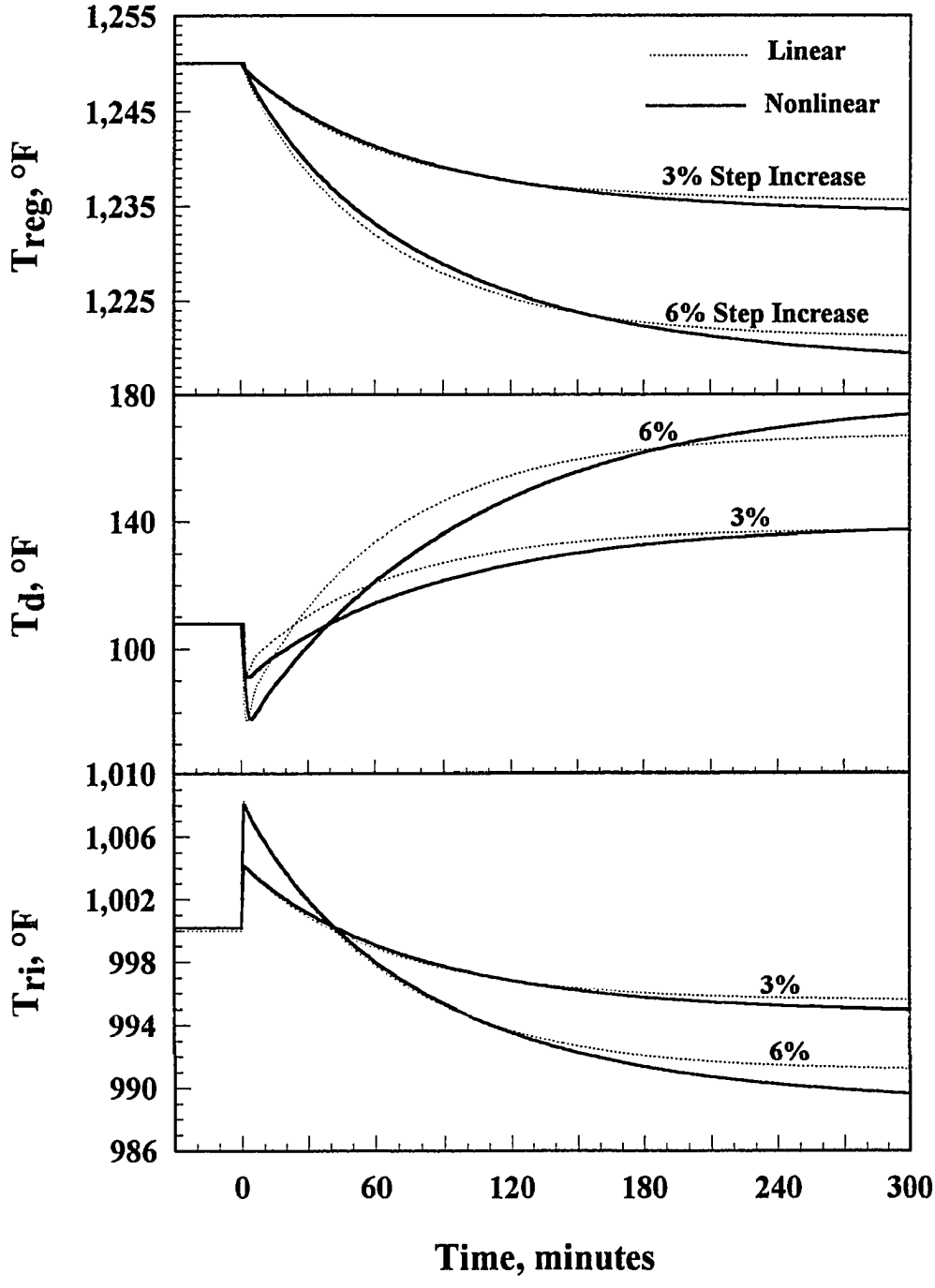

Figure 5-6. Dynamic Responses to Step Increases in F_c

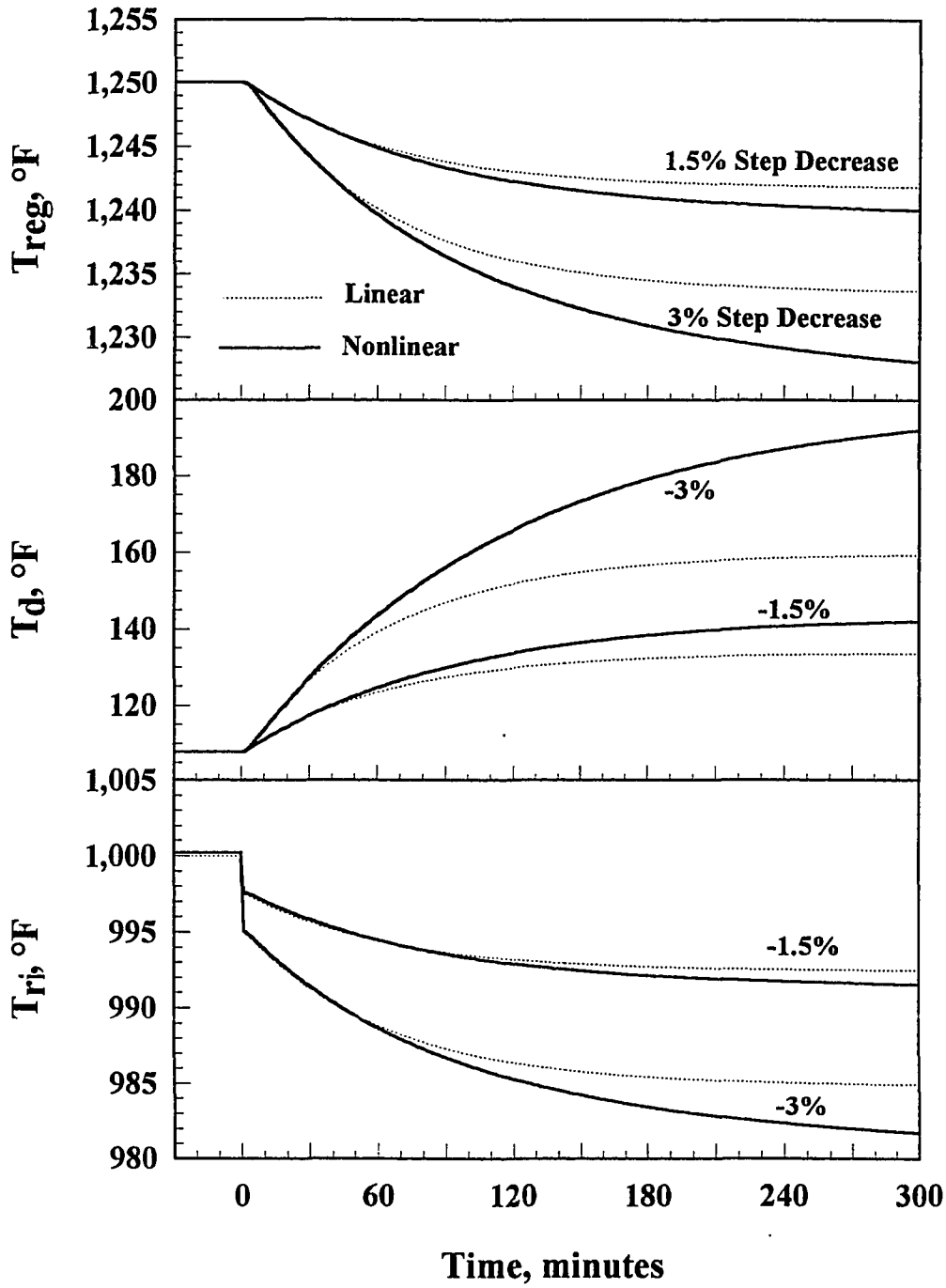

Figure 5-7. Dynamic Responses to Step Decreases in Feed Temperature

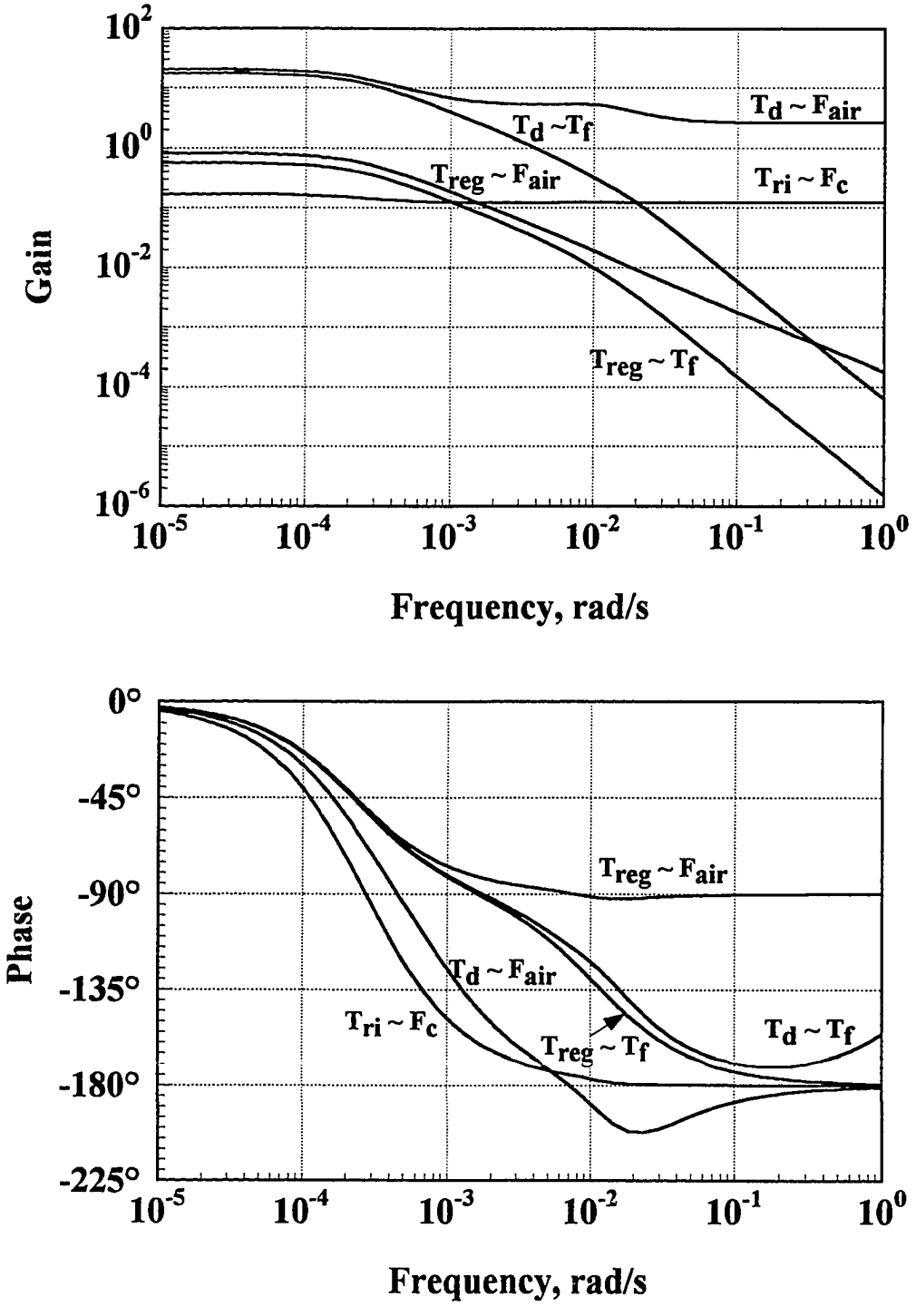

Figure 5-8. Frequency Responses at Steady-State Point i

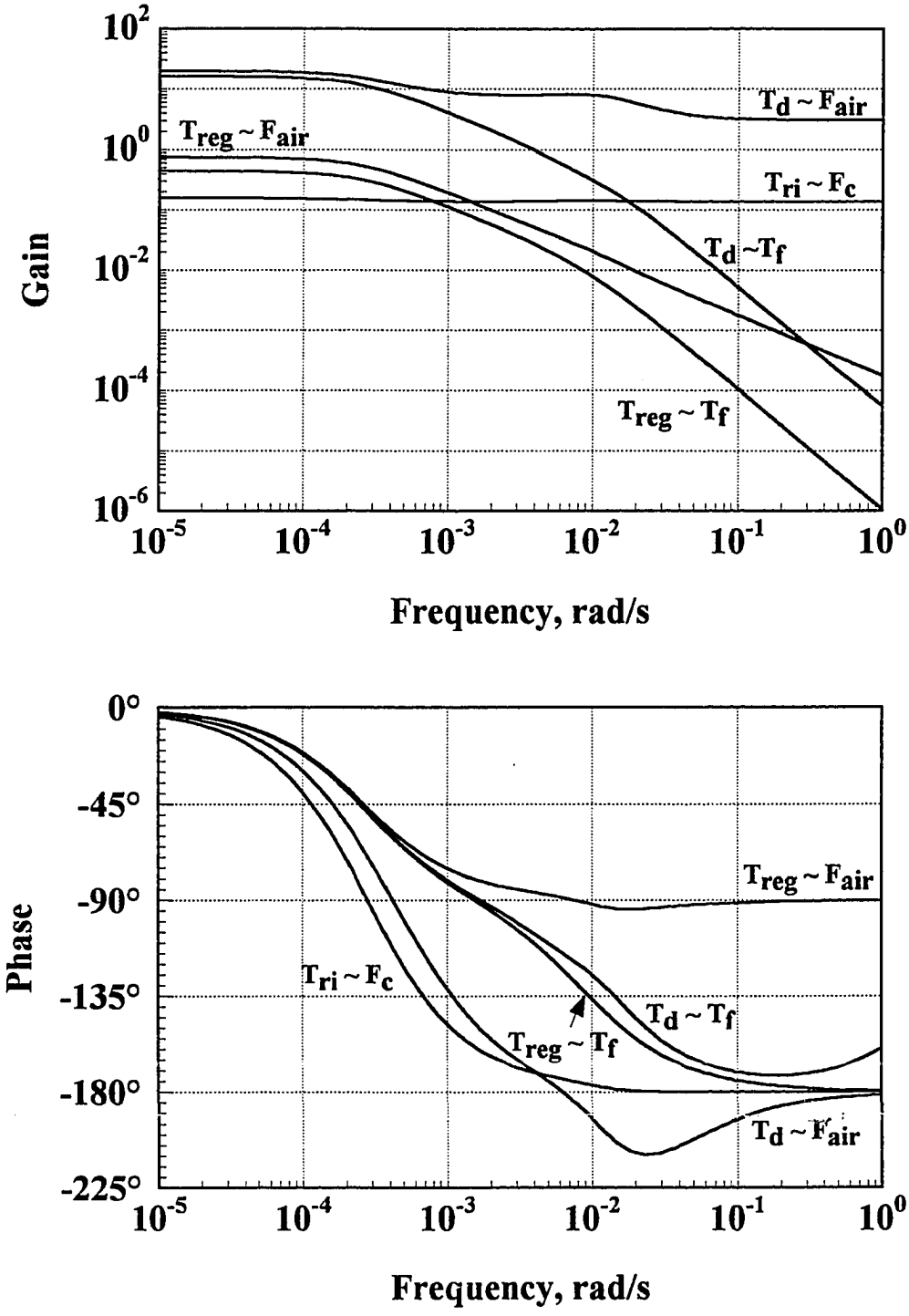

Figure 5-9. Frequency Responses at Steady-State Point ii

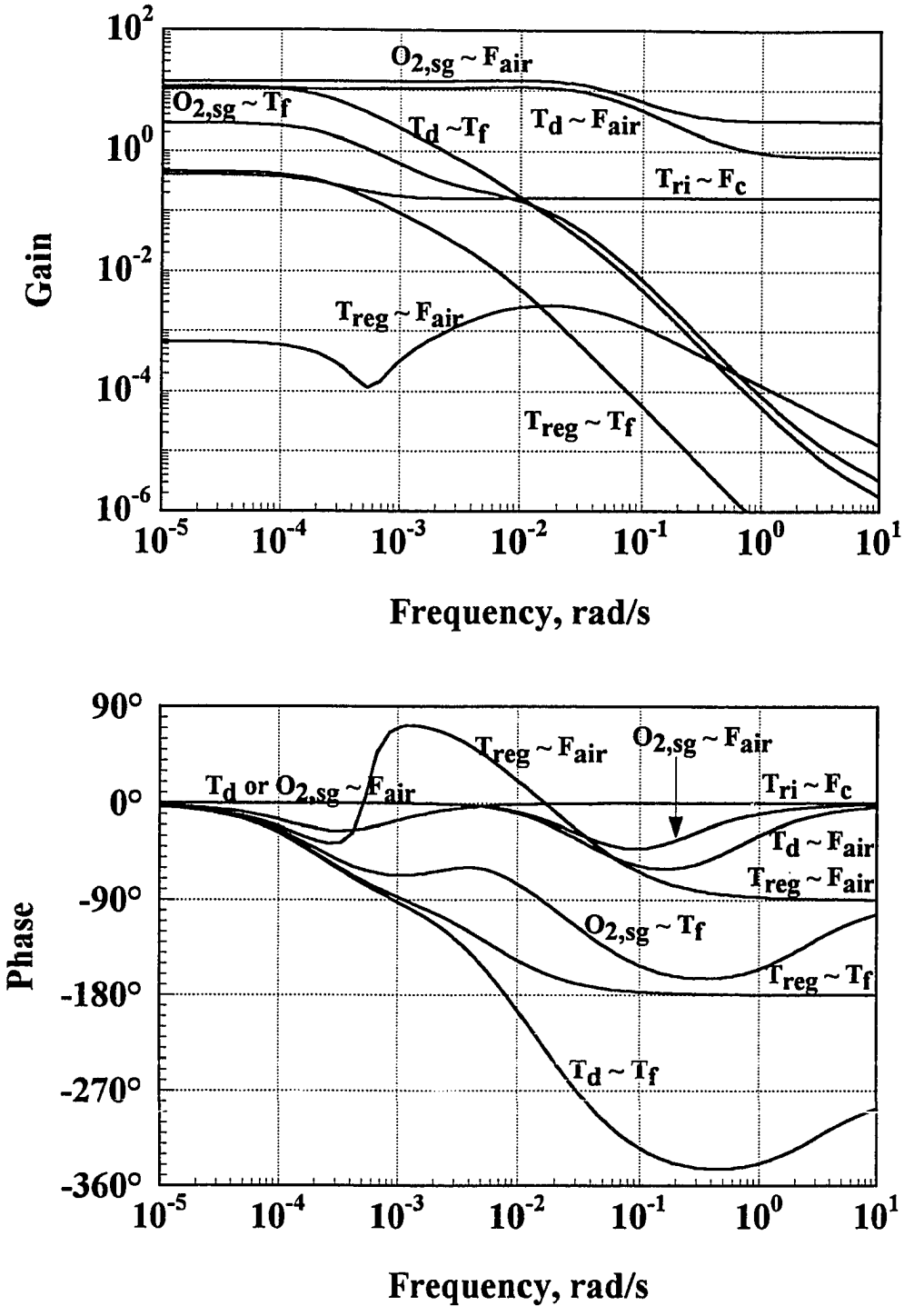

Figure 5-10. Frequency Responses at Steady-State Point iii

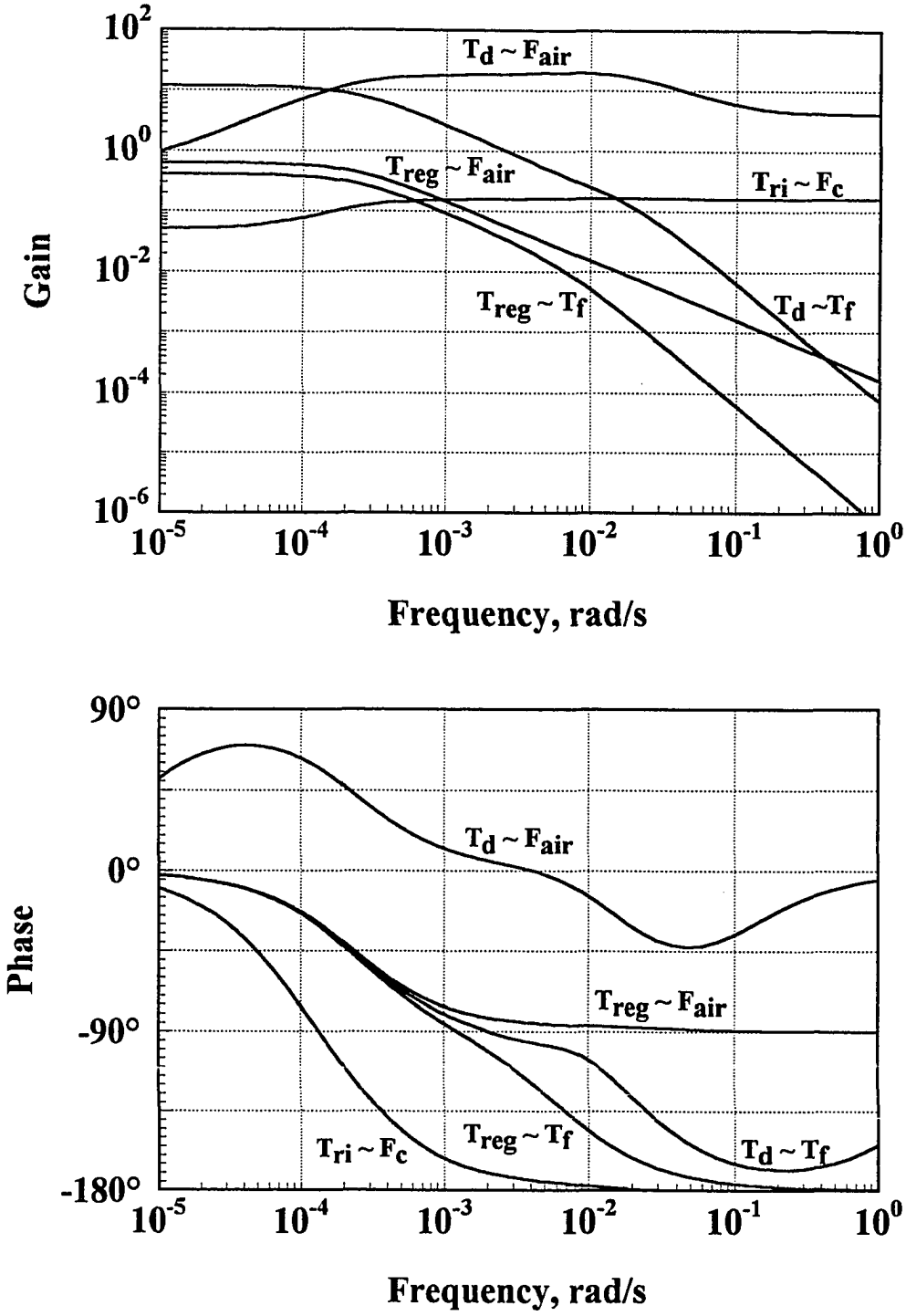

Figure 5-11. Frequency Responses at Steady-State Point iv

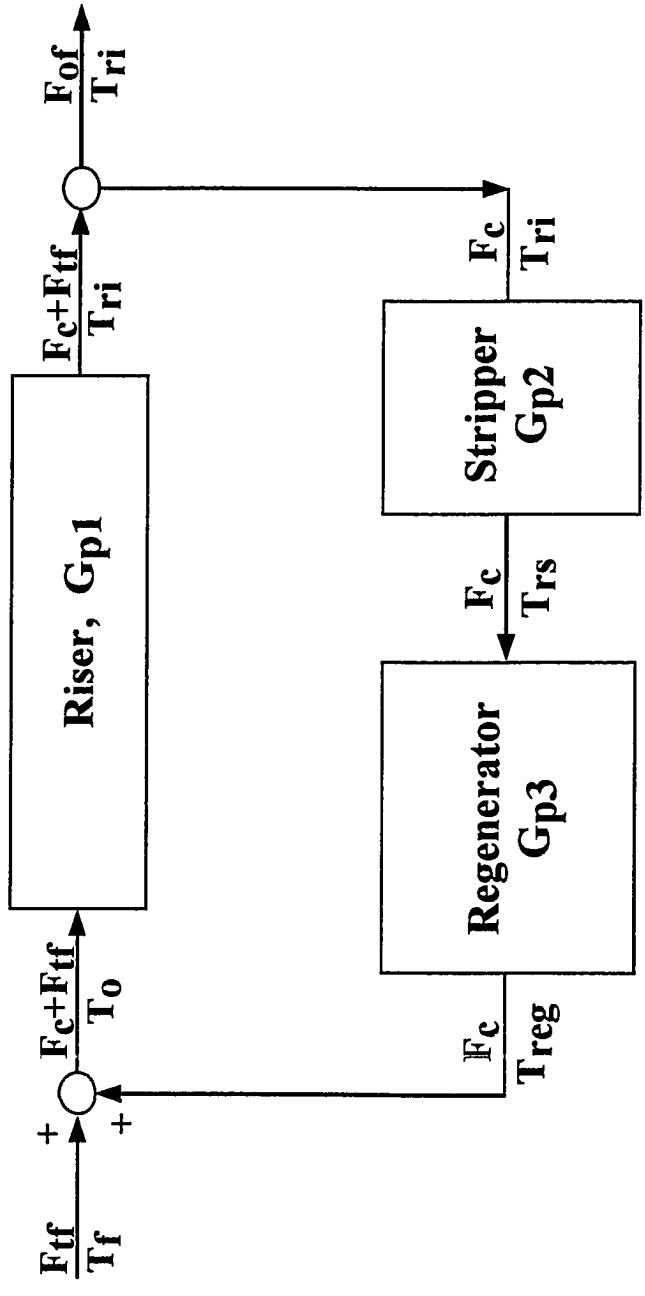

Figure 5-12. Flowsheet for the FCC Process with Recycle of Catalyst

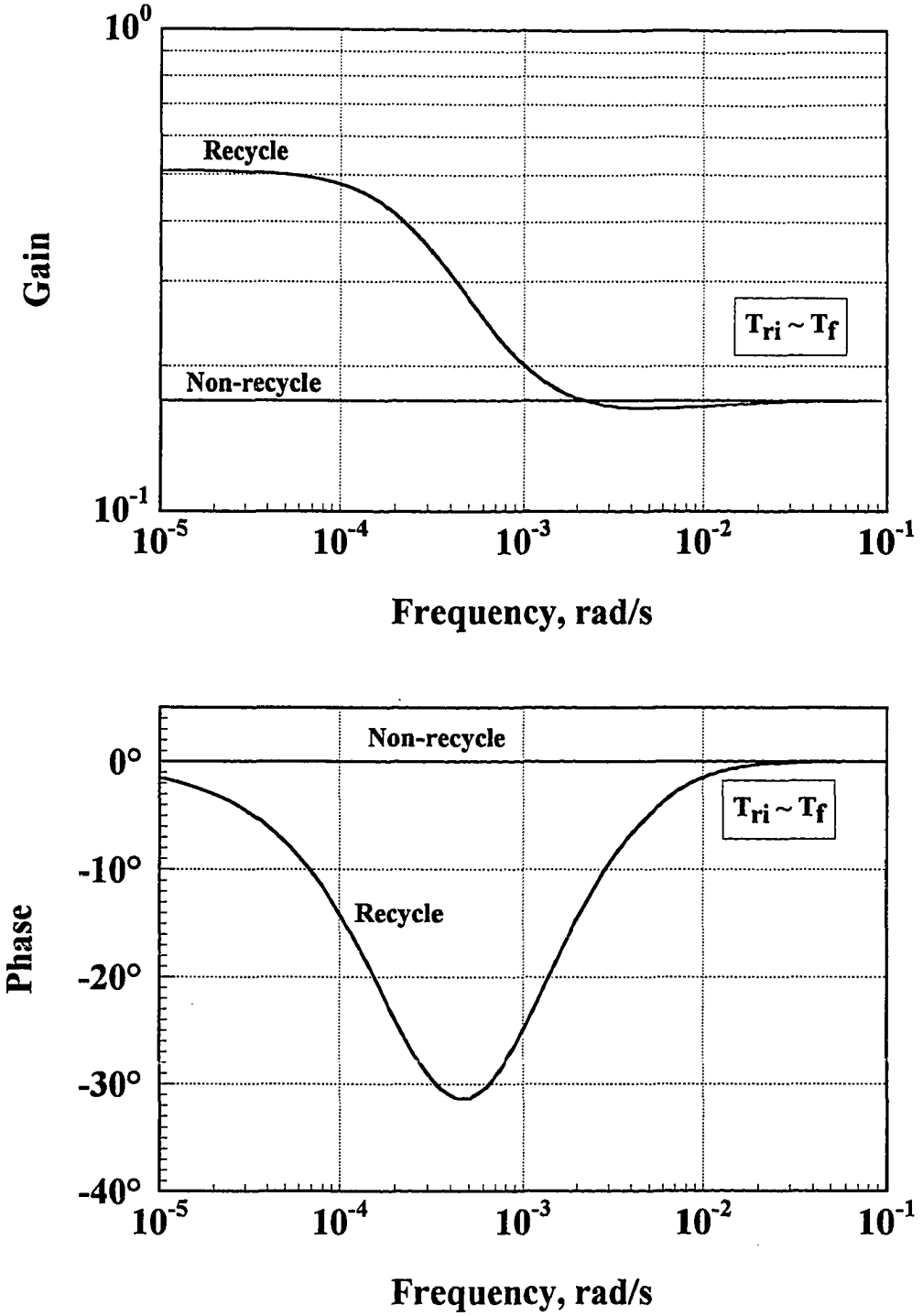

Figure 5-13. Bode Plot For Recycling FCC Dynamics

CHAPTER SIX

SUMMARY AND CONCLUSIONS

The FCC is the workhorse of the modern refinery throughout the world. Because of its complexity and profitability, control of the FCC has been a challenging task. Efficient control requires a detailed model. Many published papers have dealt with FCC modeling. However, evaluation of all of them has shown that they have severe limitations more or less. Present control studies are greatly hampered by that. Modeling of modern FCC therefore becomes essential.

A dynamic and steady-state model for modern FCC has been developed. The model has been tested to verify its validity by comparing it to actual industrial results. The main differences between our model and previous published models are:

(1) Proper description of the CO combustion kinetics both homogeneous and catalytic, which is especially important in the high temperature region. Earlier models either neglect it (e.g., Kurihara, 1967), use a correlation value of over a limited temperature range (Errazu, 1979) or in McFarlane's model (1993) use an unrealistic high value for catalytic combustion.

(2) A more realistic description of the reactor which in our case is a plug flow riser reactor with a ten-lumping kinetic model. Earlier models either use a three-lumping kinetic model (e.g., Lee and Groves, 1985) or neglect the details of the cracking reactions and use a stirred tank model for the riser (e.g., Kurihara, 1967; McFarlane et al., 1993) which was reasonable for old versions of FCC but not suitable for modern FCCUs.

The model was developed under the following basic assumptions:

Riser Model,

- Plug flow with negligible interparticle diffusion.
- Constant void fraction.
- Same linear velocities of the catalyst and the fluid, i.e., no velocity slip.
- Adiabatic operation.
- Same temperatures of the catalyst and the fluid at any position of the riser.
- Constant heat capacity and density of oil vapor.
- Quasi-steady-state process.

Stripper Model,

- Continuous stirred tank.
- No cracking reactions.
- Neglecting effects of steam and catalyst entrainment.
- Constant temperature drop in heat loss.

Regenerator Model,

- Plug flow in bubble phase and stirred tank in emulsion phase.
- Controlling rate being of the reaction rather than that of the mass transfer.
- Adiabatic operation.
- No catalyst particles at cyclone exit.
- Idea gas behavior.
- Constant heat capacities of all materials.
- Complete conversion of hydrogen presenting in the coke during combustion.

Our model is therefore available to other investigator. Because the FCC is a complex nonlinear

system, one can use the model to investigate most of the problems he faces in the control of complex processes.

Further work on the FCC model is still required which includes:

- a better description of product composition and properties containing the effects on octane and gas composition.
- a better care of nonlinear effects in the riser.
- application to different FCC designs using catalyst coolers or two stage regenerators.

Knowledge of the existence of multiple steady states and their stability is more important than its dynamic behavior in the control design of a complex system. In this work we have already tried to present a systematic approach in an FCC for understanding this issue.

If an FCC has only one stable steady state, it is inoperable as this state is trivial or cold. As present FCC's operate in a hot stable steady state, there are at least three steady states, two of which are stable. Not all the ranges of operating conditions are feasible. Only the range of three steady states is operable, and only the hot stable steady state is practical because the intermediate unstable steady state is of no interest even if it can be stabilized by control.

In commercial FCC operation the operator has to worry about the instabilities of the system due to the changes in feed properties or catalyst activity. In the FCC control design the major problem is also to understand the conditions at which the useful steady state disappears and therefore the units will wind down. From our work we showed that some changes in input conditions can make the system operate in an unstable steady state and/or let the system wind down. We have discussed systematically these impacts on stability limits. This should be a useful guide to control design.

The potential for more than three steady states has also been discussed. This is because the secondary homogeneous combustion rate of CO becomes much faster at regenerator temperature above 1270°F and heat release from CO to CO_2 is much larger than from carbon to CO. However, we have showed that while such steady states could be feasible, there was no experimental evidence for excess multiple steady states. To predict them was difficult for lack of the data. We also showed that based on the available data an open-loop unstable fourth steady state was unlikely at temperatures below 1270°F. Generally, units in partial combustion without the promoter do not operate above 1270°F. In full CO combustion this problem is irrelevant, as there can be no higher steady state.

The dynamic behavior of the FCC was also studied both on time domain and on frequency domain. This dynamic feature provides a good basis for the design of dynamic feedback control that keeps system being operated effectively at optimum points.

The system dynamic response time is dominated by the regenerator. It has an order of an hour. Generally, the FCC is designed to ensure a response slow enough to protect the system from wind-down.

FCC is a process with recycle of the catalyst. It has common features existed in any recycle process. The overall response in FCC shows that it has a higher steady-state gain and larger dominant time constant than the individual elements. The dynamic behavior seems equivalent to that of a system with a positive feedback controller.

APPENDIX A

DESCRIPTION OF A SIMPLIFIED FCC LINEARIZED MODEL

Here presents a simplified FCC linearized model. The model is developed from nonlinear FCC model in Chapter 3 under the conditions that pressures and catalyst inventories in regenerator and reactor are kept constant, and the assumption that the heat capacity of gas mixture in regenerator does not change very much and approximately equal to that of inlet air.

A.1 Simplified FCC Model

$$\frac{dT_{reg}}{dt} = \frac{1}{(W_{reg} + W_{sp})C_{pc} + M_I}\{F_{air}[C_{pair}(T_{air} - T_{sg}) + X_{CO,sg}\Delta H_1 + X_{CO_2,sg}\Delta H_2] + F_c(C_{sc} - C_{rgc})C_H\Delta H_H + F_c C_{pc}(T_{rs} - T_{reg}) - Q_e\} \tag{A.1}$$

$$\frac{dC_{rgc}}{dt} = \frac{1}{W_{reg}}\{(1 - C_H)F_c(C_{sc} - C_{rgc}) - M_c F_{air}(X_{CO,sg} + X_{CO_2,sg})\} \tag{A.2}$$

$$\frac{dT_{rs}}{dt} = \frac{F_c}{W_{rs}}(T_{ri} - T_{rs} - \Delta T_s) \tag{A.3}$$

$$\frac{dC_{sc}}{dt} = \frac{F_c}{W_{rs}}[(1 + \alpha)C_c|_{h=1} + C_{rgc} - C_{sc}] \tag{A.4}$$

where

$$C_c = C_c\,(T_{reg},\ C_{rgc},\ F_c,\ T_f) \tag{A.5}$$

$$T_{ri} = T_{ri}\,(T_{reg},\ C_{rgc},\ F_c,\ T_f) \tag{A.6}$$

In (A.5) and (A.6) feed flowrate is considered as constant.

$$X_{CO} = X_{CO}\,(T_{reg},\ C_{rgc},\ C_{sc},\ F_{air},\ F_c) \tag{A.7}$$

$$X_{CO2} = X_{CO2}\,(T_{reg},\ C_{rgc},\ C_{sc},\ F_{air},\ F_c) \tag{A.8}$$

$$T_d = T_d\,(T_{reg},\ C_{rgc},\ C_{sc},\ F_{air},\ F_c) \tag{A.9}$$

$$\Delta T_{sg} \doteq \Delta T_{reg} + \Delta T_d \tag{A.10}$$

For simplicity, in above and following equations we let

$$C_c = C_c\,|_{h=1} \tag{A.11}$$

$$X_{CO} = X_{CO,sg} \tag{A.12}$$

$$X_{CO2} = X_{CO2,sg} \tag{A.13}$$

A.2 Linearization of FCC Model

After linearization of (A.1), it is obtained that

$$\frac{d\Delta T_{reg}}{dt} = \frac{1}{(W_{reg} + W_{sp})C_{pc} + M_I}\{-[C_{pc}F_c + C_{pair}F_{air}(1 + \frac{\partial T_d}{\partial T_{reg}}) - F_{air}(\Delta H_1\frac{\partial X_{CO}}{\partial T_{reg}}$$

$$+ \Delta H_2\frac{\partial X_{CO_2}}{\partial T_{reg}})]_{ss}\Delta T_{reg} - [C_H\Delta H_H F_c + F_{air}(C_{pair}\frac{\partial T_d}{\partial C_{rgc}} - \Delta H_1\frac{\partial X_{CO}}{\partial C_{rgc}} -$$

$$\Delta H_2\frac{\partial X_{CO_2}}{\partial C_{rgc}})]_{ss}\Delta C_{rgc} + C_{pc}F_{c,ss}\Delta T_{rs} + [C_H\Delta H_H F_c + F_{air}(- C_{pair}\frac{\partial T_d}{\partial C_{sc}} +$$

$$\Delta H_1\frac{\partial X_{CO}}{\partial C_{sc}} + \Delta H_2\frac{\partial X_{CO_2}}{\partial C_{sc}})]_{ss}\Delta C_{sc} + [C_{pair}(T_{air} - T_{sg}) + X_{CO}\Delta H_1 +$$

$$X_{CO_2}\Delta H_2 + F_{air}(- C_{pair}\frac{\partial T_d}{\partial F_{air}} + \Delta H_1\frac{\partial X_{CO}}{\partial F_{air}} + \Delta H_2\frac{\partial X_{CO_2}}{\partial F_{air}})]_{ss}\Delta F_{air} +$$

$$[C_H\Delta H_H(C_{sc} - C_{rgc}) + C_{pc}(T_{rs} - T_{reg}) + F_{air}(- C_{pair}\frac{\partial T_d}{\partial F_c} + \Delta H_1\frac{\partial X_{CO}}{\partial F_c}$$

$$+ \Delta H_2\frac{\partial X_{CO_2}}{\partial F_c})]_{ss}\Delta F_c\} \qquad \text{(A.14)}$$

And,

$$\Delta W = \left.\frac{\partial W}{\partial T_{reg}}\right|_{ss}\Delta T_{reg} + \left.\frac{\partial W}{\partial C_{rgc}}\right|_{ss}\Delta C_{rgc} + \left.\frac{\partial W}{\partial F_c}\right|_{ss}\Delta F_c + \left.\frac{\partial W}{\partial T_f}\right|_{ss}\Delta T_f \qquad \text{(A.15)}$$

where, W = C_c or T_{ri}

$$\Delta V = \left.\frac{\partial V}{\partial T_{reg}}\right|_{ss} \Delta T_{reg} + \left.\frac{\partial V}{\partial C_{rgc}}\right|_{ss} \Delta C_{rgc} + \left.\frac{\partial V}{\partial C_{sc}}\right|_{ss} \Delta C_{sc} + \left.\frac{\partial V}{\partial F_{air}}\right|_{ss} \Delta F_{air} + \left.\frac{\partial V}{\partial F_c}\right|_{ss} \Delta F_c \tag{A.16}$$

where, V = X_{CO}, X_{CO2} or T_d.

Tatrai et al. (1994) have discussed the linearization of variables, W and V. From (A.2),

$$\frac{d\Delta C_{rgc}}{dt} = \frac{1}{W_{reg}}\{-[M_c F_{air}(\frac{\partial X_{CO}}{\partial T_{reg}} + \frac{\partial X_{CO_2}}{\partial T_{reg}})]_{ss}\Delta T_{reg} - [(1 - C_H)F_c + M_c F_{air}$$

$$(\frac{\partial X_{CO}}{\partial C_{rgc}} + \frac{\partial X_{CO_2}}{\partial C_{rgc}})]_{ss}\Delta C_{rgc} + [(1 - C_H)F_c - M_c F_{air}(\frac{\partial X_{CO}}{\partial C_{sc}} + \frac{\partial X_{CO_2}}{\partial C_{sc}})]_{ss}$$

$$\Delta C_{sc} - [M_c(X_{CO} + X_{CO_2}) + M_c F_{air}(\frac{\partial X_{CO}}{\partial F_{air}} + \frac{\partial X_{CO_2}}{\partial F_{air}})]_{ss}\Delta F_{air} + [(1 -$$

$$C_H)(C_{sc} - C_{rgc}) - M_c F_{air}(\frac{\partial X_{CO}}{\partial F_c} + \frac{\partial X_{CO_2}}{\partial F_c})]_{ss}\Delta F_c\} \tag{A.17}$$

From (A.3),

$$\frac{d\Delta T_{rs}}{dt} = \frac{F_{c,ss}}{W_{rs}}(\left.\frac{\partial T_{ri}}{\partial T_{reg}}\right|_{ss} \Delta T_{reg} + \left.\frac{\partial T_{ri}}{\partial C_{rgc}}\right|_{ss} \Delta C_{rgc} - \Delta T_{rs} + \left.\frac{\partial T_{ri}}{\partial F_c}\right|_{ss} \Delta F_c + \left.\frac{\partial T_{ri}}{\partial T_f}\right|_{ss} \Delta T_f) \tag{A.18}$$

From (A.4)

$$\frac{d\Delta C_{sc}}{dt} = \frac{1}{W_{rs}}\{(1+\alpha)(F_c\frac{\partial C_c}{\partial T_{reg}})_{ss}\Delta T_{reg} + [(1+\alpha)F_c\frac{\partial C_c}{\partial C_{rgc}} + 1]_{ss}\Delta C_{rgc}$$

$$- F_{c,ss}\Delta C_{sc} + (1+\alpha)(F_c\frac{\partial C_c}{\partial F_c})_{ss}\Delta F_c + (1+\alpha)(F_c\frac{\partial C_c}{\partial T_f})_{ss}\Delta T_f\} \quad (A.19)$$

A.3 State-Space Equation

The state-space matrix can be represented as the following form:

$$\frac{dX}{dt} = AX + BU \quad (A.20)$$

$$Y = CX + DU \quad (A.21)$$

where

$$X^T = [\ \frac{\Delta T_{reg}}{T_{reg,ss}} \quad \frac{\Delta C_{rgc}}{C_{rgc,ss}} \quad \frac{\Delta T_{rs}}{T_{rs,ss}} \quad \frac{\Delta C_{sc}}{C_{sc,ss}}\ ]\ ; \qquad U^T = [\ \frac{\Delta F_{air}}{F_{air,ss}} \quad \frac{\Delta F_c}{F_{c,ss}} \quad \frac{\Delta T_f}{T_{f,ss}}\ ]$$

$$Y^T = [\ \frac{\Delta T_d}{T_{d,ss}} \quad \frac{\Delta T_{ri}}{T_{ri,ss}}\ ] \ \text{or}\ Y^T = [\ \frac{\Delta T_{reg}}{T_{reg,ss}} \quad \frac{\Delta T_{ri}}{T_{ri,ss}}\ ] \ \text{or}\ Y^T = [\ \frac{\Delta X_{O_2}sg}{X_{O_2}sg,\ ss} \quad \frac{\Delta T_{ri}}{T_{ri,ss}}\ ]$$

Choice of y_1 depends on the operating conditions, and

$$\Delta X_{O_2} = 0.25C_H\left(\frac{F_c}{F_{air}}\right)_{ss}\left(\Delta C_{rgc} - \Delta C_{sc} + [C_{sc} - C_{rgc}]_{ss}\left[\frac{\Delta F_{air}}{F_{air,ss}} - \frac{\Delta F_c}{F_{c,ss}}\right]\right) - \Delta X_{CO_2} - 0.5\Delta X_{CO} \quad (A.22)$$

From equations (A.14), (A.17), (A.18) and (A.19), it is obtained that

$$\frac{dx_1}{dt} = \frac{1}{(W_{reg} + W_{sp})C_{pc} + M_I}\{-[C_{pc}F_c + C_{pair}F_{air}(1 + \frac{\partial T_d}{\partial T_{reg}}) - F_{air}(\Delta H_1\frac{\partial X_{CO}}{\partial T_{reg}} +$$

$$\Delta H_2\frac{\partial X_{CO_2}}{\partial T_{reg}})]_{ss}x_1 - \left(\frac{C_{rgc}}{T_{reg}}\right)_{ss}[C_H\Delta H_H F_c + F_{air}(C_{pair}\frac{\partial T_d}{\partial C_{rgc}} - \Delta H_1\frac{\partial X_{CO}}{\partial C_{rgc}} - \Delta H_2$$

$$\frac{\partial X_{CO_2}}{\partial C_{rgc}})]_{ss}x_2 + C_{pc}\left(\frac{F_c T_{rs}}{T_{reg}}\right)_{ss}x_3 + \left(\frac{C_{sc}}{T_{reg}}\right)_{ss}[C_H\Delta H_H F_c + F_{air}(- C_{pair}\frac{\partial T_d}{\partial C_{sc}} + \Delta H_1$$

$$\frac{\partial X_{CO}}{\partial C_{sc}} + \Delta H_2\frac{\partial X_{CO_2}}{\partial C_{sc}})]_{ss}x_4 + \left(\frac{F_{air}}{T_{reg}}\right)_{ss}[C_{pair}(T_{air} - T_{sg}) + X_{CO}\Delta H_1 + X_{CO_2}\Delta H_2 +$$

$$F_{air}(- C_{pair}\frac{\partial T_d}{\partial F_{air}} + \Delta H_1\frac{\partial X_{CO}}{\partial F_{air}} + \Delta H_2\frac{\partial X_{CO_2}}{\partial F_{air}})]_{ss}u_1 + \left(\frac{F_c}{T_{reg}}\right)_{ss}[C_H\Delta H_H(C_{sc} -$$

$$C_{rgc}) + C_{pc}(T_{rs} - T_{reg}) + F_{air}(- C_{pair}\frac{\partial T_d}{\partial F_c} + \Delta H_1\frac{\partial X_{CO}}{\partial F_c} + \Delta H_2\frac{\partial X_{CO_2}}{\partial F_c})]_{ss}u_2\} \quad (A.23)$$

$$\frac{dx_2}{dt} = \frac{1}{W_{reg}}\{-[\frac{M_c F_{air}T_{reg}}{C_{rgc}}(\frac{\partial X_{CO}}{\partial T_{reg}} + \frac{\partial X_{CO_2}}{\partial T_{reg}})]_{ss}x_1 - [(1 - C_H)F_c + M_c F_{air}(\frac{\partial X_{CO}}{\partial C_{rgc}}$$

$$+ \frac{\partial X_{CO_2}}{\partial C_{rgc}})]_{ss}x_2 + \left(\frac{C_{sc}}{C_{rgc}}\right)_{ss}[(1 - C_H)F_c - M_c F_{air}(\frac{\partial X_{CO}}{\partial C_{sc}} + \frac{\partial X_{CO_2}}{\partial C_{sc}})]_{ss}x_4 -$$

$$\left(\frac{F_{air}}{C_{rgc}}\right)_{ss}[M_c(X_{CO} + X_{CO_2}) + M_c F_{air}(\frac{\partial X_{CO}}{\partial F_{air}} + \frac{\partial X_{CO_2}}{\partial F_{air}})]_{ss}u_1 + \left(\frac{F_c}{C_{rgc}}\right)_{ss}[(1 -$$

$$C_H)(C_{sc} - C_{rgc}) - M_c F_{air}(\frac{\partial X_{CO}}{\partial F_c} + \frac{\partial X_{CO_2}}{\partial F_c})]_{ss}u_2\} \quad (A.24)$$

$$\frac{dx_3}{dt} = \frac{F_{c,ss}}{W_{rs}}\left[\left(\frac{T_{reg}}{T_{rs}}\frac{\partial T_{ri}}{\partial T_{reg}}\right)_{ss} x_1 + \left(\frac{C_{rgc}}{T_{rs}}\frac{\partial T_{ri}}{\partial C_{rgc}}\right)_{ss} x_2 - x_3 + \left(\frac{F_c}{T_{rs}}\frac{\partial T_{ri}}{\partial F_c}\right)_{ss} u_2 + \left(\frac{T_f}{T_{rs}}\frac{\partial T_{ri}}{\partial T_f}\right)_{ss} u_3\right] \tag{A.25}$$

$$\frac{dx_4}{dt} = \frac{F_{c,ss}}{W_{rs}}\{(1+\alpha)\left(\frac{T_{reg}}{C_{sc}}\frac{\partial C_c}{\partial T_{reg}}\right)_{ss} x_1 + \left(\frac{C_{rgc}}{F_c C_{sc}}\right)_{ss}[(1+\alpha)F_c\frac{\partial C_c}{\partial C_{rgc}} + 1]_{ss} x_2$$

$$- x_4 + (1+\alpha)\left(\frac{F_c}{C_{sc}}\frac{\partial C_c}{\partial F_c}\right)_{ss} u_2 + (1+\alpha)\left(\frac{T_f}{C_{sc}}\frac{\partial C_c}{\partial T_f}\right)_{ss} u_3\} \tag{A.26}$$

$$y_1 = \Delta T_{reg}/T_{reg,ss} = x_1 \tag{A.27}$$

or

$$y_1 = \frac{\Delta X_{O_2}}{X_{O_{2,ss}}} = \frac{1}{X_{O_{2,ss}}}\{-[T_{reg}(0.5\frac{\partial X_{CO}}{\partial T_{reg}} + \frac{\partial X_{CO_2}}{\partial T_{reg}})]_{ss} x_1 + [C_{rgc}(0.25 C_H \frac{F_c}{F_{air}} - 0.5\frac{\partial X_{CO}}{\partial C_{rgc}}$$

$$- \frac{\partial X_{CO_2}}{\partial C_{rgc}})]_{ss} x_2 - [C_{sc}(0.25 C_H \frac{F_c}{F_{air}} + 0.5\frac{\partial X_{CO}}{\partial C_{sc}} + \frac{\partial X_{CO_2}}{\partial C_{sc}})]_{ss} x_4 +$$

$$[0.25 C_H \frac{F_c}{F_{air}}(C_{sc} - C_{rgc}) - F_{air}(0.5\frac{\partial X_{CO}}{\partial F_{air}} + \frac{\partial X_{CO_2}}{\partial F_{air}})]_{ss} u_1 -$$

$$[F_c(0.25 C_H \frac{C_{sc} - C_{rgc}}{F_{air}} + 0.5\frac{\partial X_{CO}}{\partial F_c} + \frac{\partial X_{CO_2}}{\partial F_c})]_{ss} u_2\} \tag{A.28}$$

or,

$$y_1 = \frac{\Delta T_d}{T_{d,ss}} = \frac{1}{T_{d,ss}}\left[\left(T_{reg}\frac{\partial T_d}{\partial T_{reg}}\right)_{ss} x_1 + \left(C_{rgc}\frac{\partial T_d}{\partial C_{rgc}}\right)_{ss} x_2 + \left(C_{sc}\frac{\partial T_d}{\partial C_{sc}}\right)_{ss} x_4 + \left(F_{air}\frac{\partial T_d}{\partial F_{air}}\right)_{ss} u_1 + \left(F_c\frac{\partial T_d}{\partial F_c}\right)_{ss} u_2\right] \tag{A.29}$$

$$y_2 = \frac{1}{T_{ri,ss}}\left[\left(T_{reg}\frac{\partial T_{ri}}{\partial T_{reg}}\right)_{ss} x_1 + \left(C_{rgc}\frac{\partial T_{ri}}{\partial C_{rgc}}\right)_{ss} x_2 + \left(F_c\frac{\partial T_{ri}}{\partial F_c}\right)_{ss} u_2 + \left(T_f\frac{\partial T_{ri}}{\partial T_f}\right)_{ss} u_3\right] \tag{A.30}$$

NOMENCLATURE

A = dimensionless relative activity of catalyst

A_d = relative activity of catalyst, activity number/lb cat.

A_e = equilibrium catalyst relative activity, activity/lb cat.

A_h = weight fraction of aromatic substituent groups in HFO ($650°F^+$)

A_{h0} = weight fraction of aromatic substituent groups in HFO of charge

A_l = weight fraction of aromatic substituent groups in LFO (430° - 650°F)

A_{l0} = weight fraction of aromatic substituent groups in LFO of charge

A_m = average relative activity of catalyst, activity/lb cat.

A_n = relative activity of makeup catalyst, activity/lb cat.

A_{prgc} = area of slide valve port in regenerated line, ft^2

A_{psc} = area of slide valve port in spent line, ft^2

A_{reg} = cross sectional area of regenerator, ft^2 (590)

A_{ris} = cross sectional area of riser, ft^2 (6.4)

$A_{stripper}$ = cross sectional area of stripper, ft^2 (60)

A_0 = relative activity of startup catalyst, activity/lb cat.

a_{ik} = reaction stoichiometric coefficients of component i in reaction k,
negative values for reactants and positive values for products

b = performance parameter of cracking catalyst in coking reaction rate expression,
(1/3) (non-zeolite: 1/2, Y-type zeolite: 1/3~1/5)

b_i = coefficients in catalyst deactivation model by metal poison,
(1: -1.639×10^{-3}, 2: 1.539×10^{-7}, 3: -9.693×10^{-12})

C = C lum., H_2, H_2S, C_1 - C_4 + coke

CCR = Conradson carbon residue, lb/lb feed

C_c = catalytic coke concentration on catalyst in riser, lb coke/lb cat.

C_{cf} = coke concentration on catalyst at riser outlet, lb coke/lb cat.

C_{cr} = reference coke concentration in deactivation function expression, lb coke/lb cat. (0.01)

$C_{CO,sg}$ = concentration of carbon monoxide in stack gas, lbmol %

$C_{CO2,sg}$ = concentration of carbon dioxide in stack gas, lbmol %

C_H = weight fraction of hydrogen in coke, wt H/wt coke (0.075)

C_m = metal concentration on catalyst, ppm

$C_{O2,cyc}$ = concentration of oxygen at cyclone inlet, lbmol %

$C_{O2,sg}$ = concentration of oxygen in stack gas, lbmol %

C_p = heat capacity at constant pressure, Btu/lb°F

$C_p(z)$ = heat capacity in regenerator, Btu/lbmol°F

C_{pair} = heat capacity of air, Btu/lbmol°F (7.08)

C_{pc} = heat capacity of catalyst, Btu/lb°F (0.31)

C_{pCO} = heat capacity of carbon monoxide, Btu/lbmol°F (7.28)

C_{pCO2} = heat capacity of carbon dioxide, Btu/lbmol°F (11.0)

C_{pfl} = heat capacity of oil feed liquid, Btu/lb°F (0.82)

C_{pfv} = heat capacity of oil feed vapor, Btu/lb°F (0.81)

C_{pH2O} = heat capacity of steam, Btu/lbmol°F (8.62)

C_{pN2} = heat capacity of nitrogen, Btu/lbmol°F (7.22)

C_{pO2} = heat capacity of oxygen, Btu/lbmol°F (7.62)

C_{rgc} = coke concentration on regenerated catalyst, lb coke/lb cat.

C_{sc} = coke concentration on spent catalyst, lb coke/lb cat.

C_{sv} = flow coefficient (0.85)

C_v = heat capacity at constant volume, Btu/lb°F

c = coefficient in catalyst deactivation model by metal poison, (1.505×10^{-4})

c_i = coefficients in kinetic expression of CO catalytic burning,

(1: 204.8, 2: -7.164×10^3, 3: 8.4711×10^4)

c_{pt} = fitting constant in the expression of CO promoter impact, (2.549)

E_{base} = activation energy of base component in catalytic cracking reaction, Btu/lbmol

E_c = activation energy in coke burning, Btu/lbmol ($E_c/R=3.4\times10^4$ °F)

E_{cc} = activation energy of catalytic coke formation, Btu/lbmol (1×10^3)

E_d = activation energy of catalyst deactivation, Btu/lbmol ($E_d/R=1.8\times10^4$ °F)

E_j = activation energy of j^{th} lump, Btu/lbmol

E_β = activation energy in CO/CO2 expression, Btu/lbmol ($E_\beta/R=1.1232\times10^4$ °F)

E_{31} = activation energy for CO oxidation at homogeneous noncatalytic reaction,

Btu/lbmol ($E_{31}/R=6.4\times10^4$ °F)

E_{32} = activation energy for CO oxidation at heterogeneous catalytic reaction,

Btu/lbmol ($E_{32}/R=2.5\times10^4$ °F)

E_{33} = activation energy for CO oxidation at homogeneous free-radical reaction,

Btu/lbmol

F_{air} = air flow rate into regenerator, lbmol/s

F_c = flow rate of catalyst in riser, lb/s

F_{coke} = production of coke in riser, lb/s

F_H = burning rate of hydrogen, lb/s

F_l = loss rate of catalyst in FCC system, tons/day

F_{lg} = flow rate of light oil gas, lb/s

F_n = makeup rate of catalyst, tons/day

F_{of} = flow rate of oil gas at riser outlet, lb/s

F_{rgc} = flow rate of regenerated catalyst, lb/s

F_s = flow rate of steam in regenerator cooler, lb/s

F_{sc} = flow rate of spent catalyst, lb/s

F_{sg} = flow rate of stack gas, lbmol/s

F_{sp} = flow rate of catalyst into regenerator standpipe, lb/s

F_{ss} = flow rate of stripping steam in stripper, lb/s

F_{tf} = flow rate of oil feed, lb/s

F_{ush} = the amount of unstripped hydrocarbon in stripper, lb/s

F_v = flow rate of oil gas in riser, lb/s

F_w = withdrawal rate of catalyst, tons/day

F_{wg} = wet gas production in reactor, lbmol/s

G = G lump, gasoline (C_5 - 430°F), weight fraction of gasoline molecular

G_p = process transfer function

H = enthalpy of oil, Btu/lb

H_c = enthalpy of catalyst, Btu/lb

H_{coke} = enthalpy of coke, Btu/lb

h = dimensionless height of riser

h_f = formation enthalpy of oil, Btu/lb

h_{rgc} = height between bottoms of the standpipe and the riser, ft (60)

h_{ris} = height of riser, ft (120)

h_{sc} = height between bottoms of the stripper and the regenerator, ft (10)

K_c = proportional gain of controller

K_h = heavy aromatic ring adsorption coefficient, R_h^{-1} (12.8)

k_c = reaction rate constant for carbon reaction, $psia^{-1}.s^{-1}$

k_{cc} = reaction rate constant for catalytic coke formation, $(lb\ coke/lb\ cat)^{1/b}s^{-1}$

k_{cc0} = preexponential factor for catalytic coke formation, $(lb\ coke/lb\ cat)^{1/b}s^{-1}$ (2.251×10^{-10})

k_{c0} = preexponential factor for carbon reaction, $psia^{-1}.s^{-1}(1.698\times10^{7})$

k_d = deactivation rate constant of catalyst, $day^{-1}A^{-(n-1)}$

k_{d0} = preexponential factor for catalyst deactivation, $psia^{-1}day^{-1}A^{-(n-1)}$

k_j = kinetic constant of j^{th} lump in oil cracking, $(lb\ cat/ft^3)^{-1}s^{-1}$

k_0 = preexponential factor, $(lb\ cat/ft^3)^{-1}s^{-1}$

k_1 = reaction rate constant for reaction I, $psia^{-1}.s^{-1}$

k_2 = reaction rate constant for reaction II, psia^{-1}.s-1

k_3 = reaction rate constant for reaction III, $lbmol/ft^3.psia^2.s$

k_{31} = reaction rate constant for reaction III at homogeneous noncatalytic reaction, $lbmol/ft^3.psia^2.s$

k_{32} = reaction rate constant for reaction III at heterogeneous catalytic reaction, $lbmol/ft^3.psia^2.s$

k_{33} = reaction rate constant for reaction III at homogeneous free-radical reaction, $lbmol/ft^3.psia^2.s$

k_{310} = preexponential factor for CO oxidation at homogeneous noncatalytic reaction,

lbmol/ft^3.psia^2.s (5.110×10^{10})

k_{320} = preexponential factor for CO oxidation at heterogeneous catalytic reaction, lbmol/ft^3.psia^2.s (18.63)

k_{330} = preexponential factor for CO oxidation at homogeneous free-radical reaction, lbmol/ft^3.psia^2.s

M_c = molecular weight of carbon, lb/lbmol (12)

M_e = flowrate of entrained catalyst from dense bed into dilute phase, lb/s

M_g = average molecular weight of gasoline, lb/lbmol (100)

M_I = effective heat capacity of regenerator mass, Btu/°F (2×10^5)

M_{lg} = average molecular weight of light oil gas, lb/lbmol (44)

N_h = weight fraction of naphthenic molecules in HFO (650°F$^+$)

N_{h0} = weight fraction of naphthenic molecules in HFO charge

N_l = weight fraction of naphthenic molecules in LFO (430° to 650°F$^+$)

N_{l0} = weight fraction of naphthenic molecules in LFO charge

n = deactivation order of catalyst

P_{atm} = atmospheric pressure, psia (14.7)

P_{CO} = partial pressure of CO, psia

P_{H2O} = partial pressure of steam in regenerator, psia

P_h = weight fraction of paraffinic molecules in HFO (650°F$^+$)

P_{h0} = weight fraction of paraffinic molecules in HFO charge

P_l = weight fraction of paraffinic molecules in LFO (430° to 650°F$^+$)

P_{l0} = weight fraction of paraffinic molecules in LFO charge

P_{O2} = partial pressure of O_2, psia

P_{oil} = partial pressure of oil gas in riser, psia

P_r = reactor pressure, psia

P_{rb} = pressure at bottom of reactor riser, psia

P_{rg} = regenerator pressure, psia

P_{rgb} = pressure at bottom of regenerator, psia

Q_{air} = heat of incoming air, Btu/s

Q_c = total heat of burning carbon, Btu/s

Q_e = total heat loss in regenerator, Btu/s (2116)

Q_{fg} = heat of outgoing stack gas, Btu/s

Q_H = heat of incoming hydrogen, Btu/s

Q_{in} = heat into regenerator, Btu/s

Q_{loss} = heat loss in stripper, Btu/s

Q_{out} = heat out of regenerator, Btu/s

Q_{rgc} = heat of outgoing regenerated catalyst, Btu/s

Q_{rm} = removal heat of cooler in regenerator, Btu/s

Q_{sc} = heat of incoming spent catalyst, Btu/s

R = universal gas constant, ft^3.psi/lbmol.°R (10.73)

R_h = weight fraction of aromatic rings in HFO (650°F$^+$)

R_{h0} = weight fraction of aromatic rings in HFO charge

R_k = k^{th} reaction rate of oil, s^{-1}

R_l = weight fraction of aromatic rings in LFO (430° to 650°F$^+$)

R_{l0} = weight fraction of aromatic rings in LFO charge

R_{co} = catalyst to oil weight ratio

R_{coke} = production of coke per unit volume in riser, lb/ft^3.s

r_c = total carbon burning rate, lbmol/ft^3.s

r_k = kth reaction rate of oil per unit volume, lb/ft^3.s

r_{1c} = carbon burning rate according to reaction I, lbmol/ft^3.s

r_{2c} = carbon burning rate according to reaction II, lbmol/ft^3.s

r_{3CO} = CO oxidation rate according to reaction III, lbmol/ft^3.s

s = catalyst makeup rate as fraction of catalyst inventory

T = temperature of the riser, °F [T]

T_{air} = temperature of air entering regenerator, °F

T_{base} = base temperature, °F (1100)

T_{cyc} = regenerator cyclone inlet temperature, °F

T_d = temperature difference between regenerator cyclone inlet and outlet, °F

T_f = temperature of gas oil feed, °F

T_{reg} = temperature of regenerator dense bed, °F

T_{ri} = temperature of the riser outlet, °F

T_{rs} = temperature of reactor dense bed, °F

T_{sg} = temperature of stack gas at cyclone exit, °F

T_0 = temperature of mixture at riser inlet, °F

t = clock time, s

t_c = catalyst residence time, s

U = internal energy of oil, Btu/lb

U_c = internal energy of catalyst, Btu/lb

U_{coke} = internal energy of coke, Btu/lb

u_0 = linear velocity of gas oil at riser inlet, ft/s

u_c = linear velocity of catalyst, ft/s

u_v = linear velocity of oil at riser, ft/s

v_{ris} = volumetric flowrate in riser, ft^3/s

v_s = superficial velocity in regenerator, ft/s

W = catalyst inventory of FCC system, tons

WHSV = weight hourly space velocity, lb oil.hr^{-1}/lb cat.

W_{reg} = inventory of catalyst in regenerator, lb

W_{ris} = inventory of catalyst in riser, lb

W_{rs} = inventory of catalyst in reactor dense bed, lb

W_{sp} = inventory of catalyst in regenerator standpipe, lb

X = conversion of feedstocks, lb/lb feed

X_{CO} = molar ratio of CO to air

$X_{CO,sg}$ = molar ratio of CO to air in stack gas

X_{CO2} = molar ratio of CO_2 to air

$X_{CO2,sg}$ = molar ratio of CO_2 to air in stack gas

X_{H2O} = mole ratio of H_2O to air

X_{O2} = molar ratio of O_2 to air

$X_{O2,cyc}$ = molar ratio of O_2 to air at cyclone inlet

$X_{O2,sg}$ = molar ratio of O_2 to air in stack gas

X_{pt} = CO burning promoter in catalyst, lb/lb cat.

Y_g = yield of gasoline, lb/lb feed

Y_{wg} = yield of wet gas, lb/lb feed

y = weight fraction of oil, lb/lb feed

y_{oil} = mole fraction of oil gas in riser

z = height variable of the riser or regenerator, ft

z_{bed} = height of regenerator dense bed, ft

z_{cyc} = height of the cyclone inlet in regenerator, ft (45)

z_{top} = height of cyclone exit in the regenerator top, ft (49.5)

Greek Symbols

α = unstripped hydrocarbon content, lb/lb coke (0.1)

β = CO/CO_2 ratio at the catalyst site

β_0 = preexponential factor in CO/CO_2 ratio expression (2.512×10^3)

ΔH_{fv} = heat of gas oil feed vaporization, Btu/lb (75)

ΔH_r = heat of cracking reaction, Btu/lb

ΔH_H = heat of combustion of hydrogen, Btu/lb (60,960)

ΔH_s = latent heat of steam, Btu/lb

ΔH_1 = heat of formation of CO, Btu/lbmol (46,368)

ΔH_2 = heat of formation of CO_2, Btu/lbmol (169,080)

ΔP_{rgc} = pressure drop across the slide valve sides of regenerated cat. transported line, psia

ΔP_{RR} = differential pressure between reactor and regenerator, psia (3.4)

ΔP_{sc} = pressure drop across the slide valve sides of spent catalyst transported line, psia

ΔT_s = temperature drop across reactor stripper, °F (25)

ε = void fraction in riser

ε_e = effective void fraction in regenerator dense bed

ε_f = apparent void fraction in regenerator dense bed

η_m = mass transfer coefficient

η_q = heat transfer coefficient

λ_0, λ_1 = empirical parameters in deactivation function expression (6.709, 110)

ρ = density of oil, lb/ft^3

ρ_B = volume fraction of catalyst in regenerator

ρ_c = density of catalyst, lb/ft^3 (68)

$\rho_{c,dilute}$ = density of catalyst in the dilute phase, lb/ft^3

$\rho_{c,dense}$ = density of catalyst in the dense bed, lb/ft^3

ρ_{cs} = density of catalyst in circulation lines, lb/ft^3 (45)

ρ_g = density of exit gas, $lbmol/ft^3$

ρ_{ris} = average density of material in riser, lb/ft3

ρ_v = density of oil vapor in riser, lb/ft^3 (0.57)

ρ_0 = density of gas oil vapor at riser inlet, lb/ft^3

σ = CO_2/CO ratio in flue gas.

σ_B = CO_2/CO ratio without promoter in flue gas.

τ_i = integral time of controller, s

τ_r = average catalyst residence time, s

τ_{rr} = reference catalyst residence time in deactivation function expression, s (3.31)

Φ = catalyst deactivation function.

Ψ = coke formation function of gas oil feed

Subscript

ahal = reactions from A_h to A_l

ahc = reactions from A_h to C

ahg = reactions from A_h to G

ahrl = reactions from A_h to R_l

alc = reactions from A_l to C

alg = reactions from A_l to G

i, j = oil lumping component i, j

k = reaction k

nhc = reactions from N_h to C

nhg = reactions from N_h to G

nhnl = reactions from N_h to N_l

nlc = reactions from N_l to C

nlg = reactions from N_l to G

phc = reactions from P_h to C

phg = reactions from P_h to G

phpl = reactions from P_h to P_l

plc = reactions from P_l to C

plg = reactions from P_l to G

rhc = reactions from R_h to C

rhrl = reactions from R_h to R_l

rlc = reactions from R_l to C

sp = set point

ss = steady state

Abbreviation

C = carbon

CO = carbon monoxide

CO_2 = carbon dioxide

CO_2/CO = molar ratio of carbon dioxide to carbon monoxide

CSTR = continuous stirred tank reactor

FCC = Fluidized Catalytic Cracking (Cracker)

FCCU = Fluidized Catalytic Cracking Unit

HFO = Heavy Fuel Oil

H_2O = water

LFO = Light Fuel Oil

O_2 = oxygen

PFR = plug flow reactor

PI = proportional and integral

SS = steady state

REFERENCES

Allen, D. T., and Liguras, D., "Structural Models of Catalytic Cracking Chemistry: A Case Study of a Group Contribution Approach to Lumped Kinetic Modeling," *Mobil Workshop on Chemical Reaction in Complex Mixtures*, Van Nostrand Reinhold, New York, 101 (1991).

Arandes, J. M., and de Lasa, H. I., "Simulation and Multiplicity of Steady States in Fluidized FCCUs," *Chem. Eng. Sci.*, **47**, 2535 (1992).

Arkun, Y., and Stephanopoulos, G., "Studies in the Synthesis of Control Structures for Chemical Processes: Part IV. Design of Steady-State Optimizing Control Structures for Chemical Process Units," *AIChE J.*, **26**, 975 (1980).

Arkun, Y., and Ramakrishnan, R., "Structural Sensitivity Analysis in the Synthesis of Process Control Systems," *Chem. Eng. Sci.*, **39**, 1167 (1984).

Arthur, J. R., "Reactions Between Carbon and Oxygen," *Trans. Faraday Soc.*, **47**, 164 (1951).

Avidan, A. A., "Recent and Future Developments in FCC," *AKZO Cat. Symposium*, Fluid Catalytic Cracking, 43 (1991).

Avidan, A. A., Edwards, M. and Owen, H., "Innovative Improvements Highlight FCC's Past and Future," *Oil and Gas J.*, **88**, no. 1, 8 (1990).

Avidan, A. A., Edwards, M. and Owen, H., "Fluid Catalytic Cracking - Past and Future Challenges," *Reviews in Chem. Eng.*, **6**, no. 1, 1 (1990).

Avidan, A. A., and Shinnar, R., "Development of Catalytic Cracking Technology. A lesson in Chemical Reactor Design," *Ind. Eng. Chem. Res.*, **29**, 931 (1990).

Blanding, F. H., "Reaction Rates in Catalytic Cracking of Petroleum," *Ind. Eng. Chem.*, **45**, 1186 (1953).

Balchen, J. G., Ljungquist, D., and Strand, S., "State-Space Predictive Control," *Chem. Eng. Sci.*, **47**, 787 (1992)

Bozicevic, J., and Lukect, D., "Dynamic Mathematical Model of the Fluid Catalytic Cracking Process," *Trans. Inst. M. C.*, **9**, no. 1, 8 (1987).

Bromley, J. A., and Ward, T. J., "Fluidized Catalytic Cracker Control. A Structural Analysis Approach," *Ind. Eng. Chem. Process Des. Dev.*, **20**, 74 (1981).

Bulsara, P. U., Zenz, F. A., and Eckert, R. A., "Pressure and Additive Effects on Flow

of Bulk Solids," *Ind. Eng. Chem. Process Des. Dev.*, **3**, 348 (1964).

Chang, S., Wu, A., and Baron, K., "Application of Predictor Techniques to Fluid Catalytic Cracker Pilot Plant Control," *AIChE Ann. Meet.*, Chicago, Pap. 121e (1985).

Chester, A. W., Schwartz, A. B., Stover, W. A., and McWilliams, J. P., "Catalyzing the energy balance of Cat Cracking," *CHEMTECH*, **1**, 50 (1981).

Corella, J., and Frances, E., "A Model for the Riser of a FCC Unit Based on the Kinetics of Cracking and Deactivation from Lab Tests," *Prepr., Am. Chem. Soc., Div. Petro. Chem.*, **35**, 735 (1990)

Coxson, P. G., and Bischoff K. B.,"Lumping Strategy 1. Introductory Techniques and Applications of Cluster Analysis," *Ind. Eng. Chem. Res.*, **26**, 1239 (1987).

de Lasa, H. I., Errazu, A., Barreiro, E., and Solioz, S., "Analysis of Fluidized Bed Catalytic Cracking Regenerator Models in an Industrial Scale Unit," *Can. J. Chem. Eng.*, **59**, 549 (1981).

Denn, M. M., and Lavie, R., "Dynamics of Plants with Recycle," *Chem. Eng. J.*, **24**, 55 (1982).

Edwards, W. M., and Kim, H. N., "Multiple Steady States in FCC Unit Operations," *Chem. Eng. Sci.*, **43**, 1825 (1988).

Elnashaie, S. S., and Yates J. G., "Multiplicity of the Steady State in Fluidized Bed Reactors-I. Steady State Considerations," *Chem. Eng. Sci.*, **28**, 515 (1973).

Elnashaie, S. S. E. H., "Multiplicity of the Steady State in Fluidized Bed Reactors-III. Yield of the Consecutive Reaction A→B→C," *Chem. Eng. Sci.*, **32**, 295 (1977).

Elnashaie, S. S. E. H., and El-Hennawi, I. M., "Multiplicity of the Steady State in Fluidized Bed Reactors-IV. Fluid Catalytic Cracking (FCC)," *Chem. Eng. Sci.*, **34**, 1113 (1979).

Elnashaie, S. S. E. H., and Elshishini, S. S., "Digital Simulation of Industrial Fluid Catalytic Cracking Units - IV. Dynamic Behaviour," *Chem. Eng. Sci.*, **48**, 567 (1993).

Elshishini, S. S., and Elnashaie, S. S. E. H., "Digital Simulation of Industrial Fluid Catalytic Cracking Units: Bifurcation and Its Implications," *Chem. Eng. Sci.*, **45**, 553 (1990).

Elshishini, S. S., and Elnashaie, S. S. E. H., "Digital Simulation of Industrial Fluid Catalytic Cracking Units - II. Effect of Charge Stock Composition on Bifurcation and Gasoline Yield," *Chem. Eng. Sci.*, **45**, 2959 (1990).

Errazu, A. F., Delasa, H. I., and Sarti, F., "A Fluidized Bed Catalytic Cracking Regenerator Model, Grid Effects," *Can. J. Chem. Eng.*, **57**, 191 (1979).

Evangelista, J. J., Shinnar, R., and Katz, S., "The Effect of Imperfect Mixing on Stirred Combustion Reactor," *12th Symp. (Int.) Combust.*, Combust. Institute, Pittsburgh, PA, 901 (1969).

Ewell, R. B., and Gadmer, G., "Design Cat Crackers by Computer," *Hydrocarbon Processing*, **4**, 125 (1978).

Farag, H., Ng, S., and Lasa, H., "Kinetic Modeling of Catalytic Cracking of Gas Oils Using in Situ Traps (FCCT) To Prevent Metal Contaminant Effects," *Ind. Eng. Chem. Res.*, **32**, 1071 (1993).

Felipe, L. I., "Dynamic Modelling of an Industrial Fluid Catalytic Cracking Unit," *Computers Chem. Engng*, **16**, Suppl., S139 (1992).

Ford, W. D., Reineman, R. C., Vasalos, I. A., and Fahrig, R. J., "Modeling Catalytic Cracking Regenerators," *NPRA Ann. Meet.*, San Antonio, TX (1976).

Gates, B. C., Katzer, J. R., and Schuit, G. C. A., "Chemistry of Catalytic Processes," *McGraw-Hill*, Inc. (1979).

Georgakis, C., "On the Use of Extensive Variables in Process Dynamics and Control," *Chem. Eng. Sci.*, **41**, 1471 (1986).

Gould, L. A., Evans, L. B., and Kurihara, H., "Optimal Control of Fluid Catalytic Cracking Processes," *Automatica*, **6**, 695 (1970).

Grosdidier, P., Mason, A., Aitolahti, A., Heinonen, P., and Vanhamäki, V., "FCC Unit Reactor-Regenerator Control," *Computers Chem. Engng*, **17**, no. 2, 165 (1993)

Gross, B., Nace, D. M., and Voltz, S. E., "Application of a Kinetic Model for Comparison of Catalytic Cracking in a Fixed Bed Microreactor and a Fluidized Dense Bed," *Ind. Eng. Chem. Process Des. Dev.*, **13**, 199 (1974).

Gross, B., Jacob, S. M., Nace, D. M., and Voltz, S. E., "Simulation of Catalytic Cracking Process," *US Patent 3960707*, (1976).

Groves, F. R. Jr., "Optimizing Control of Fluidized Bed Catalytic Cracker-Regenerator," *Advance in Instrum. by ISA*, **40**, pt.1, 397 (1985).

Guigon, P., and Large, J. F., "Application of the Kunii-Levenspiel Model to a Multistage Baffled Catalytic Cracking Regenerator," *Chem. Eng. J.*, **28**, 131 (1984).

Hano, T., Nakashio, F., and Kusunoki, K., "The Burning Rate of Coke Deposited on

Zeolite Catalyst," *J. Chem. Eng. Jpn.*, **8**, 127 (1975).

Hovd, M. and Skogestad, S., "Procedure for Regulatory Control Structure Selection with Application to the FCC Process," *AIChE J.*, **39**, 1938 (1993).

Iscol, L., "The Dynamics and Stability of a Fluid Catalytic Cracker," *ASME 11th Jt. Automat. Contl. Conf. Amer. Automat. Contl. Council, Atlanta, Ga*, Pap. 23-B, 602 (1970).

Jacob, S. M., Gross B., Voltz, S. E., and Weekman, V. W. Jr., "A Lumping and Reaction Scheme for Catalytic Cracking," *AIChE J.*, **22**, 701 (1976).

Johnson, D. L., "A Catalyst Activity Model for the Mobil Olefins to Gasoline (MOG) Process," *AIChE Ann. Meet.*, Los Angeles (1991).

Kapoor, N., McAvoy, T. J., and Marlin, T. E., "Effect of Recycle Structure on Distillation Tower Time Constants," *AIChE J.*, **32**, 411 (1986).

Koppel, L. B., "Iuput Multiplicities in Nonlinear, Multivariable Control Systems," *AIChE J.*, **28**, 935 (1982).

Koppel, L. B., "Conditions Imposed by Process Statics on Multivariable Process Dynamics," *AIChE J.*, **31**, 70 (1985).

Krambeck, F. J., Katz, S., and Shinnar, R., "The Effects of Perturbation in Flow-Rate on a Stirred Combustor," *Combust. Sci. Tech.* **4**, 221 (1972).

Krambeck, F. J., "Continuous Mixtures in Fluid Catalytic Cracking and Extensions," *Mobil Workshop on Chemical Reaction in Complex Mixtures*, Van Nostrand Reinhold, New York, 42 (1991).

Krishna, A. S., and Parkin, E. S., "Modeling the Regenerator in Commercial Fluid Catalytic Cracking Units," *Chem. Eng. Prog.*, **81**, 4, 57 (1985).

Kunii, D. and Levenspiel, O., "Fluidization Engineering," *Wiley*, New York (1969).

Kurihara, H., "Optimal Control of Fluid Catalytic Cracking Processes," *PhD Diss.*, MIT (1967).

Larocca, M., Ng, S., and Lasa, H., "Fast Catalytic Cracking of Heavy Gas Oils: Modeling Coke Deactivation," *Ind Eng. Chem. Res.*, **29** 171 (1990).

Larocca, M., Farag, H., Ng, S., and Lasa, H., "Cracking Catalyst Deactivation by Nickel and Vanadium Contaminants" *Ind Eng. Chem. Res.*, **29** 2181 (1990).

Lee, E., and Groves, F. R. Jr., "Mathematical Model of the Fluidized Bed Catalytic

Cracking Plant," *Trans. Soc. Comput. Simulation*, **2**, 219 (1985).

Lee, L., Yu, S., and Cheng, C., "Fluidized-bed Catalyst Cracking Regenerator Modelling and Analysis," *Chem. Eng. J.*, **40**, 71 (1989).

Lee, L., Chen, Y., Huang, T., and Pan, W., "Four-Lump Kinetic Model for Fluid Catalytic Cracking Process," *Can. J. Chem. Eng.*, **67**, 615 (1989).

Lee, W., "Dynamic Optimization of Catalyst Make-Up Rate for Catalytic Cracking Systems," *Ind. Eng. Chem. Process Des. Dev.*, **9**, 154 (1970).

Lee, W., and Kugelman, A. M., "Number of Steady-State Operating Points and Local Stability of Open-Loop Fluid Catalytic Cracker," *Ind. Eng. Chem. Process Des. Dev.*, **12**, 197 (1973).

Lee, W., and Weekman, V. W., Jr., "Advanced Control Practice in the Chemical Process Industry: A View from Industry," *AIChE J.*, **22**, 27 (1976).

Liguras, D. K., and Allen, D. T., "Structural Models for Catalytic Cracking 1. Model Compound Reaction," *Ind. Eng. Chem. Res.*, **28**, 665 (1989).

Liguras, D. K., and Allen, D. T., "Structural Models for Catalytic Cracking 2. Reactions of Simulated Oil Mixtures," *Ind. Eng. Chem. Res.*, **28**, 674 (1989).

Ljungquist, D., "Online Estimation in Nonlinear State-Space Models with Application to Catalytic Cracking," *Dr. Ing. Thesis, ITK-Report no. 90-89-W*, Norwegian Institute of Technology (1990).

Longwell, J. P., and Weiss, M. A., "High Temperature Reaction Rates in Hydrocarbon Combustion," *Ind. Eng. Chem.*, **47** 1634 (1955).

Luyben, W. L., and Lamb, D. E., "Feedforward control of a Fluidized Catalytic Reactor-Regenerator System," *Chem. Eng. Prog. Symposium. Ser.*, **59**, no. 46 165 (1963).

Mandal, S., Das, A. K. and Ghosh, S., "Effect of Coke on Catalysts in Distillate FCC Unit Performance," *Ind. Eng. Chem. Res.*, **32**, 1018 (1993).

Martin, G. D., Mahoney, J. D., and Kliesch, H. C., "Rigorous Simulation Used to Determin FCC Computer Control Strategies," *6th Ann. FCC Symposium*, Munich, Germany (1985)

Mauleon, J. L., and Sigaud, J. B., "Mix Temperature Control Enhances FCC," *Oil and Gas J.*, **85**, no. 8, 52 (1987).

McDonald, G. W. G., and Harkins, B. L., "Maximizing FCC Profits by Process Optimization," *NPRA Ann. Meet.*, San Antonio, Texas (1987).

McFarlane, R. C., Bacon, D. W., "Adaptive Optimizing Control of Multivariable Constrained Chemical Processes. 2. Application Studies," *Ind. Eng. Chem. Res.*, **28**, 1834 (1989).

McFarlane, R. C., Reineman, R. C., Bartee, J. F., and Georgakis, C., "Dynamic Simulator for a Model IV Fluid Catalytic Cracking Unit," *Computers Chem. Engng*, **17**, no. 3, 275 (1993).

McGreavy, C. and Isles-Smith, P. C., "Modelling of a Fluid Catalytic Cracker," *Trans. Inst. M. C.*, **8**, no. 3, 130 (1986).

McPherson, M., Naire, I., Lee, P., and Horn, L. D. V., "Experience with FCCU Computer Control," *Natl Petrol. Refiner Assoc.*, (tech. paper) Washington, DC, Pap. cc-85-108 (1985).

Monge J. J. and Georgakis, C., "Multivariable Control of Catalytic Cracking Processes," *Chem. Eng. Commum.*, **61**, 197 (1987).

Morari, M., Arkun, Y., and Stephanopolous, G., "Studies in the Synthesis of Control Structures for Chemical processes, Part I, II and III," *AIChE J.*, **28**, 60 (1982).

Morari, M., "Robust Stability of Systems with Integral Control," *IEEE Trans. Automat. Contr.*, vol. **AC-30**, 574 (1985).

Morari, M., and Zafiriou, E., "Robust Process Control," *Prentice-Hall,* Engelwood Cliffs, NJ (1988).

Morley, K., and de Lasa, H. I., "On the Determination of Kinetic Parameters for the Regeneration of Cracking Catalyst," *Can. J. Chem. Eng.*, **65**, 773 (1987).

Morley, K., and de Lasa, H. I., "Regeneration of Cracking Catalyst Influence of the Homogeneous CO Postcombustion Reaction," *Can. J. Chem. Eng.*, **66**, 428 (1988).

Nace, D. M., Voltz, S. E., and Weekman, V. W. Jr., "Application of a Kinetic Model for Catalytic Cracking - Effects of Charge Stocks," *Ind. Eng. Chem. Process Des. Dev.*, **10**, 530 (1971).

Narendra, C. D., Gregory, J. D., and Pinky, U., "A Four-lump Kinetic Model for the Cracking/Coking of Recycled Heavy Oil," *Fuel*, **72**, 1331 (1993).

Otterstedt, J. A., and Upson, L. L., "Catalytic Cracking of Heavy Vacuum Gas Oils," Chapter 5 in *Handbook of Heat and Mass Transfer:* Catalysis, Kinetics, and Reactor Engineering, Cheremisinoff, N. P., Ed., **3**, 183, Gulf Publisher (1989).

Palazoglu, A., and Khambanonda, T., "Dynamic Operability Analysis of a Fluidized

Catalytic Cracker," *AIChE J.*, **33**, 1037 (1987).

Paraskos, J. A., Shah, Y. T., McKinney, J. D., and Carr, N. L., "A Kinematic Model for Catalytic Cracking in a Transfer Line Reactor," *Ind. Eng. Chem. Process Des. Dev.* **15**, 165 (1976).

Prater, C. D., Wei, J., Weekman, V. W., Jr., and Gross, B., "A Reaction Engineering Case History: Coke Burning in Thermofor Catalytic Cracking Regenerators," *advances in Chemical Engineering*, Wei, J., Ed., Academic Press, New York, **12**, 1 (1983).

Prett, D. M., and Gillette, R. D., "Optimization and Constrained Multivariable Control of a Catalytic Cracking Unit," *Proc. 1980 Joint Autom. Contl. Conf.*, 270 (1980).

Rhemann, H., Schwarz, G., Badgwell, T. A., Darby, M. L., and White, D. C.,"Application of Advanced Controls to a Refinery Fluid Catalytic Cracking Unit," *Proc. Amer. Contl. Conf.*, 2340 (1988).

Rinard, I. H., and Benjamin, B. W., "Control of Recycle Systems. Part 1. Continuous Control," *ACC*, (1982).

Ross, I. B., Patel, M. S., and Davidson, J. F., "The Temperature of Burning Carbon Particles in Fluidized Beds," *Trans. Inst. Chem. Eng.* **59**, 83 (1981).

Ross, I. B., and Davidson, J. F., "The Combustion of Carbon Particles in a Fluidized Bed," *Trans. Inst. Chem. Eng.* **60**, 108 (1982).

Sapre, A. V., Leib, T. M., and Anderson, D. H., "FCC Regenerator Flow Model," *Chem. Eng. Sci.*, **45**, 2203 (1990)

Sapre, A. V., and Leib, T. M., "Translation of Laboratory Fluid Cracking Catalyst Characterization Tests to Riser Reactors," *ACS Symposium Series 452*, Fluid Catalytic Cracking II-Concepts in Catalyst Design, Edited by M. L. Occelli, Chapter 9, 144 (1991).

Sapre, A. V., "Kinetic Modeling at Mobil: An Historical Perspective," *Mobil Workshop on Chemical Reaction in Complex Mixtures*, Van Nostrand Reinhold, New York, 222 (1991).

Schmit, C. and Biegler, L. T., "Application of Multistep Newton-Type Controller to Fluid Catalytic Cracking," *Proc. Amer. Contl. Conf.*, San Diego, California (1990).

Schult, S. B., and Smith, F. B., Jr., "An Application of Quadratic Performance Synthesis Techniques to a Fluid Cat Cracker," *Proc. 1971 Joint Autom. Contl. Conf.*, 270 (1971).

Seko, H., Tone, S., and Otake, T., "Operation and Control of a Fluid Catalytic Cracker,"

J. Chem. Eng. Jpn, **11**, 130 (1978).

Seko, H., Tone, S., and Otake, T., "Criterion for Stability of Steady States and its Prediction in a Fluid Catalytic Cracker," *J. Chem. Eng. Jpn*, **15**, 305 (1982).

Schuurmans, H. J. A., "Measurements in a Commercial Catalyst Cracking Unit," *Ind. Eng. Chem. Process Des. Dev.*, **19**, 267 (1980).

Sha, Y., Deng, X., Chen, X., Weng, H., Mao, X., and Wang, S., "Investigation and Application of the Lumped Kinetic Model for Catalytic Cracking," *Proc. Int. Conf. Pet. Refin. Petrochem. Process*, Hou, X., Ed., Int. Acad. Publ., Beijing, China, **3**, 1517 (1991).

Shah, Y. T., Huling, G. T. Paraskos, J. A., and Mckinney, J. D., "A Kinematic Model for an Adiabatic Transfer Line Catalytic Cracking Reactor," *Ind. Eng. Chem. Process Des. Dev.*, **16**, 89 (1977).

Shinnar, R., "Chemical Reactor Modelling for Purposes of Controller Design," *Chem. Eng. Commum.*, **9**, 73 (1981).

Shnaider, G. S., and Shnaider, A. G., "Kinetic Models of Catalytic Cracking of Oil Fractions in Single-stage and Multistage Reactors with Fluidized Beds and Interpretation of Experimental Data of Catalytic Cracking Performed in these Reactors," *Chem. Eng. J.*, **44**, 53 (1990).

Taiwo, O., "The Design of Robust Control Systems for Plants with Recycle," *Int. J. Contl.*, **43**, 671 (1986)

Tatrai, F. Z., Lant, P. A., Lee, P. L., Cameron, I. T., and Newell, R. B., "A Lumped Parameter Model for 'Model IV' Fluid Catalytic Cracking Units," *Computers Chem. Engng*, **18**, Suppl., S177 (1994).

Tatrai, F. Z., Lant, P. A., Lee, P. L., Cameron, I. T., and Newell, R. B., "Model Reduction for Regulatory Control: An FCCU Case Study," *Trans. Inst. Chem. Eng.*, **72**, Part A, 402 (1994).

Takatsuka, T., Sato, S., Morimoto, Y., and Hashimoto, H., "A Reaction Model for Fluidized-Bed Catalytic Cracking of Residual Oil," *Int. Chem. Eng.*, **27**, 107 (1987).

Theologos, K. N., and Markatos, N. C., "Modeling of Flow and Heat Transfer in Fluidized Catalytic Cracking Riser-Type Reactors," *Trans. Inst. Chem. Eng.*, **70**, Part A 239 (1992)

Theologos, K. N., and Markatos, N. C., "Advanced Modeling of Fluid Catalytic Cracking Riser-Type Reactors," *AIChE J.*, **39**, 1007 (1993)

Tomlins, A. H., and Thieme, T. R., "Application of Predictive Multivariable Control to a Fluid Catalytic Cracking Process," *Proc. ISA/89 Int. Conf. Exhib. Adv. Instrum. Contl. Publ by ISA Services Inc. Research Triangle Pk*, NC, 515 (1989).

Upson, L. L., Hemler, C. L. and Lomas, D. A., "Unit Design and Operational Control: Impact on Product Yields and Product Quality," Chapter 11 in Fluid Catalytic Cracking: Science and Technology, Magee, J. S., and Mitchell M. M., Jr., Ed., *Studies in Surf. Sci. Cat.*, **76** 385 (1993).

Venuto, P. B., and Habib E. T., Jr., "Fluid Catalytic Cracking with Zeolite Catalysts," *Marcel Dekker, Inc.*, New York (1979).

Viitanen, P. I., "Tracer Studies on a Riser Reactor of a Fluidized Catalyst Cracking Plant," *Ind. Eng. Chem. Res.*, **32**, 577 (1993).

Voltz, S. E., Nace, D. M., and Weekman, V. W. Jr., "Application of a Kinetic Model for Catalytic Cracking - Some Correlation of Rate Constants," *Ind. Eng. Chem. Process Des. Dev.*, **10**, 538 (1971).

Voorhies, A., "Carbon Formation in Catalytic Cracking," *Ind. Eng. Chem.*, **37**, 318 (1945).

Wang, G., Lin, S., and Yang, G., "The Kinetics and Mechanism of Elimination of Carbonaceous Deposits on Cracking Catalysts in Regeneration," *Proceedings of 32nd Chem. Eng. Conf.*, **2**, 807, Vancouver, Canada (1982).

Wang, G., Lin, S., Mo, W., Peng, C., and Yang, G., "Kinetics of Combustion of Carbon and Hydrogen in Carbonaceous Deposits on Zeolite-Type Cracking Catalysts," *Ind. Eng. Chem. Process Des. Dev.*, **25**, 627, (1986).

Wang, G., Lin, S., and Yang, G., "Properties and Kinetics of Zeolite-Type Cracking Catalysts," Chapter 2 in *Handbook of Heat and Mass Transfer:* Catalysis, Kinetics, and Reactor Engineering, Cheremisinoff, N. P., Ed., **3**, 63, Gulf Publisher (1989).

Weekman, V. W., Jr., and Nace, D. M., "Kinetics of Catalytic Cracking Selectivity in Fixed, Moving, and Fluid Bed Reactors," *AIChE J.*, **16**, 397 (1970).

Weekman, V. W., Jr., "Lumps, Models, and Kinetics in Practice," *AIChE Monograph Series*, 75 (1979).

Wei, F., Lin, S., and Yang, G., "Gas and Solids Mixing in a Commercial FCC Regenerator," *Chem. Eng. Technol.*, **16**, 109 (1993).

Wei, J., Lee, W., and Krambeck, F. J., "Catalyst Attrition and Deactivation in Fluid Catalytic Cracking System," *Chem. Eng. Sci.*, **32**, 1211 (1977).

Weisz, P. B., "Combustion of Carbonaceous Deposits within Porous Catalyst Particles,

III. The CO_2/CO Product Ratio," *J. Catal.*, **6**, 425 (1966).

Weisz, P. B., Goodwin, R. D., "Combustion of Carbonaceous Deposits within Porous Catalyst Particles, II. Intrinsic Burning Rate," *J. Catal.*, **6**, 227 (1966).

Wollaston, E. G., Haflin, W. J., and Ford, W. D., "What Influences Cat Cracking," *Hydrocarbon Processing*, **9**, 93 (1975).

Yen, L. C., Wrench, R. E., and Ong, A. S., "Reaction Kinetic Correlation Equation Predicts Fluid Catalytic Cracking Coke Yield," *Oil and Gas J.*, Jan. 11, 67 (1988).

Zhao, X., and Lu, Y., "Nonlinear Dynamic Model and Parameter Estimation for Fluidized Catalytic Cracking Unit," *IFAC Proceedings Series*, **2**, 1079 (1988).

Zheng, Y., "Dynamic Modeling and Simulation of a Catalytic Cracking Unit," *Computers Chem. Engng*, **18**, no. 1, 39 (1994).

Ziegler, J. G., and Nichols, N. B., "Optimum Settings for Automatic Controllers," *Trans. ASME*, **64**, 759 (1942)